Cell type-specific functions of neuropsychiatric disease-associated gene CYFIP1 in the brain

James Drew

Department of Neuroscience, Physiology and Pharmacology
University College London

This dissertation is submitted for the degree of
Doctor of Philosophy

February 2019

Declaration

I, James Drew, hereby declare that the work presented in this thesis is my own. Where information has been derived from other sources, I confirm that this has been indicated in the thesis.

James Drew
February 2019

Acknowledgements

In some ways I am worse off coming out of PhD than when I entered. I have spent four years more than most not contributing to the economy, and am no closer to paying off my student loan. I am thinning on top and am less physically active. I have spent more time than I would ever imagined thinking about this topic I stumbled into. I have also loved it and would do it all again without question.

I want to start by acknowledging Dr Richard Dorrell. His unwavering enthusiasm and wonder for cell biology was a major inspiration for me and I am now more in awe of that than ever. I am grateful for the MRC and, by extension, the taxpayer for giving me the opportunity to learn and contribute to a field that will always be close to my heart. The gift of being given the time to think about something deeply is one I have tried not to take for granted.

I am extremely thankful to the lab of Josef Kittler. To Josef for having the faith in me to follow what I was interested in, and for providing guidance, support and a questioning frown when it was needed. To the students I've supervised over the years - through sheer trial and error you made me a more competent person. And to all the colleagues in the lab; special mentions to Davor (for making every day in the lab infuriating and hilarious), Christian (for your endless supply of *interesting* facts), Jack (for bringing the North to me so I don't have to go to it) and Flavie (for being the best 432 partner I could ask for). Keep in touch and best of luck with everything.

Appreciation for Mum, Dad and my brother for laying the groundwork for this. Lastly to Ling, for sharing the last four years so closely with me. You know better than anyone how the experience has been and I attribute a significant amount of any success I've had to your support.

Abstract

The shape and connectivity of neurons underlies all higher brain functions and abnormalities in these features are a hallmark of many neuropsychiatric disorders. In the brain, functional neural networks arise through an interplay between intrinsic intracellular processes and interactions between neurons and other cell types, including glia. CYFIP1 is a neuropsychiatric disease-associated gene with established roles in actin remodeling and local protein translation. Previous studies have shown that altered expression of CYFIP1 regulates neuronal morphology, connectivity and synaptic plasticity, although it is currently unclear to what extent these represent cell-autonomous effects. Additionally, the embryonic lethality of CYFIP1 has precluded the study of complete CYFIP1 loss *in vivo*. This thesis aims to address some of these questions using transgenic mice harboring cell type-specific deletions of CYFIP1. Firstly, an excitatory neuron-specific CYFIP1 knockout was generated. Loss of neuronal CYFIP1 led to stunted dendrite growth *in vitro* and *in vivo* and to differential effects on axon growth. Migration of neuronal progenitor cells during embryogenesis was unaffected in this model. Investigation revealed normal synapse formation in cultured neurons lacking CYFIP1. However, several developmentally-dependent changes were observed *in vivo*, including immature spine morphology and an increase in post-synaptic inhibition in young adult mice. Lastly, a novel role for CYFIP1 in microglia was investigated. Using a live-imaging assay of acute slices, a role for CYFIP1-associated actin remodeling complexes in microglial motility was established. A microglia-specific CYFIP1 knockout mouse showed changes in microglial morphology and a specific defect in surveillance motility. These results provide evidence for novel functions of CYFIP1 in neurons and microglia that will inform our understanding of the cellular interactions underlying disorders such as autism and schizophrenia.

Table of contents

List of Figures and Tables

Impact Statement

The treatment of neuropsychiatric disorders requires an understanding of the biological processes underlying these conditions. Clinical genetics has, and will continue to, identify new etiological causes that must be matched by basic research to elucidate their biological impact. Work presented here falls under this endeavor. This study has focused on furthering understanding of the consequences of changes in levels of autism and schizophrenia associated gene CYFIP1 in the brain, with relevance for neuroscientists, cell biologists, clinicians and others. Dissemination of this work has/will be through presentations at local and international conferences and publications in peer-reviewed journals.

The production of this work has also led to communication of ideas and skills presented here to numerous people outside of the research community, including undergraduate Bachelor's and Master's students, and key stage 5 students through the In2Science scheme.

Chapter 1

Introduction

Understanding the context within which altered CYFIP1 function in the brain occurs requires an overview of how neurons develop and the relevant cellular and molecular processes involved. As remodelling of the cytoskeleton is a critical function of CYFIP1 and underlies many of it's associated functions, this introduction will begin with an overview of cytoskeletal dynamics, focused particularly on regulation of actin involved in establishing cell morphology and motility. This will form the basis for a discussion on neuronal development and synaptic transmission, with emphasis on the role of cytoskeletal dynamics and links with psychiatric disease. Finally, the known molecular functions and clinical associations of CYFIP1 will be covered in this context.

1.1 Control of cell shape and movement

1.1.1 Core components of the cytoskeleton

Cells adopt different shapes in order to perform specific functions efficiently. Often this means dynamically changing their shape over timescales varying from

milliseconds to days. The generation of specific morphologies is an active process for animal cells that requires intracellular protein 'scaffolds' to provide mechanical tension, rigidity and directed force to mold the shape of the plasma membrane. Together, the network of proteins that compose this intracellular scaffold and its regulators are known as the cytoskeleton.

The cytoskeleton is composed of three major filament types; actin filaments (microfilaments), microtubules and intermediate filaments. These three building blocks differ in their size, tensile strength and dynamics. However, they are all primarily composed on monomeric units that polymerise to form filamentous macromolecules. Alongside its role in cell shape and motility, the cytoskeleton is also critical for intracellular trafficking, cell adhesion and division.

1.1.1.1 Microtubules

Microtubules (MTs) are the largest element (by width) of the cytoskeleton. They have critical roles in cell division, intracellular trafficking of organelles and establishing cell shape and stability. MTs are composed of globular heterodimers of α-tubulin and β-tubulin monomers. These dimers assemble end-to-end into linear protofilaments, with β-subunits interacting with the α-subunit of the adjacent dimer (Fig 1.1). Protofilaments align laterally to form a tube-like filament that typically contains 13 protofilaments and is roughly 25 μm in diameter with a central lumen (Goodson and Jonasson, 2018). Due to this assembly pattern, MTs have inherent polarity; a fast growing plus end with β-tubulin exposed and more slowly growing minus end with exposed α-tubulin.

Both tubulin monomers bind guanosine triphosphate (GTP), and though α-tubulin GTP is stable, β-tubulin GTP can be hydrolysed once the dimer is integrated into a MT filament. This feature is critical for the cycles of MT extension and retraction known as 'dynamic instability'. Dynamic instability reflects the fact that the plus-end of MTs stably polymerise only when the rate of addition of GTP-bound

α/β-tubulin dimers is greater than the subsequent hydrolysis of GTP to GDP in those dimers. Should the addition rate slow such that the GTP-bound 'cap' of the plus is hydrolysed, the plus end will rapidly depolymerise in a process termed 'collapse'. In most metazoan cells, the minus end of MTs are stabilised in a microtubule-organising complex (MTOC), the most common being the centrosome that resides near the nucleus. Thus, the cycling of growth and collapse occurs mainly at the plus end and underpins the MT dynamics in the cell.

MT filaments can be stabilised in a number of ways. MTs are subject to a number of post-translational modifications (PTMs), the best characterised example of which is tyrosination of the carboxy-tail of β-tubulin (Janke and Bulinski, 2011). Due to the preferential activity for dimeric tubulin of the tyrosine ligase, TTL, new MT filaments are almost entirely tyrosinated. Over time, MTs are detyrosinated and become increasingly stable, in part due to reduced affinity of detyrosinated tubulin for depolymerising kinesin, KIF2A (Peris et al., 2009). Other PTMs include acetylation (which also increases MT stability), polyglutamylation and polyglycylation. Interestingly, many of these PTMs are specifically enriched in the brain; MTs in the axon are heavily detyrosinated, polyglutamylated and polyglycylated (Janke and Bulinski, 2011). Given the length and longevity of axons, this supports PTMs of axonal MTs as functionally relevant. Indeed, loss of TTL in neurons alters MT stability and axonal morphology (Peris et al., 2009).

Many proteins broadly termed microtubule binding proteins (MTBPs) interact directly with MTs. This diverse group can be split into two categories: motor and non-motor MTBPs. As mentioned, MTs are intracellular highways that coordinate long range trafficking within the cell. Motor proteins bind and track along MTs and, through concomitant binding to cargo, mediate intracellular trafficking of organelles and macrocomplexes. MT motor proteins can be split into kinesins and dyneins based on their preference to movement towards the plus end or minus end of MTs (Hirokawa et al., 2009). Another group (+TIPs) bind to the growing ends of MTs and either sway the balance of dynamic instability in favour of polymerisation

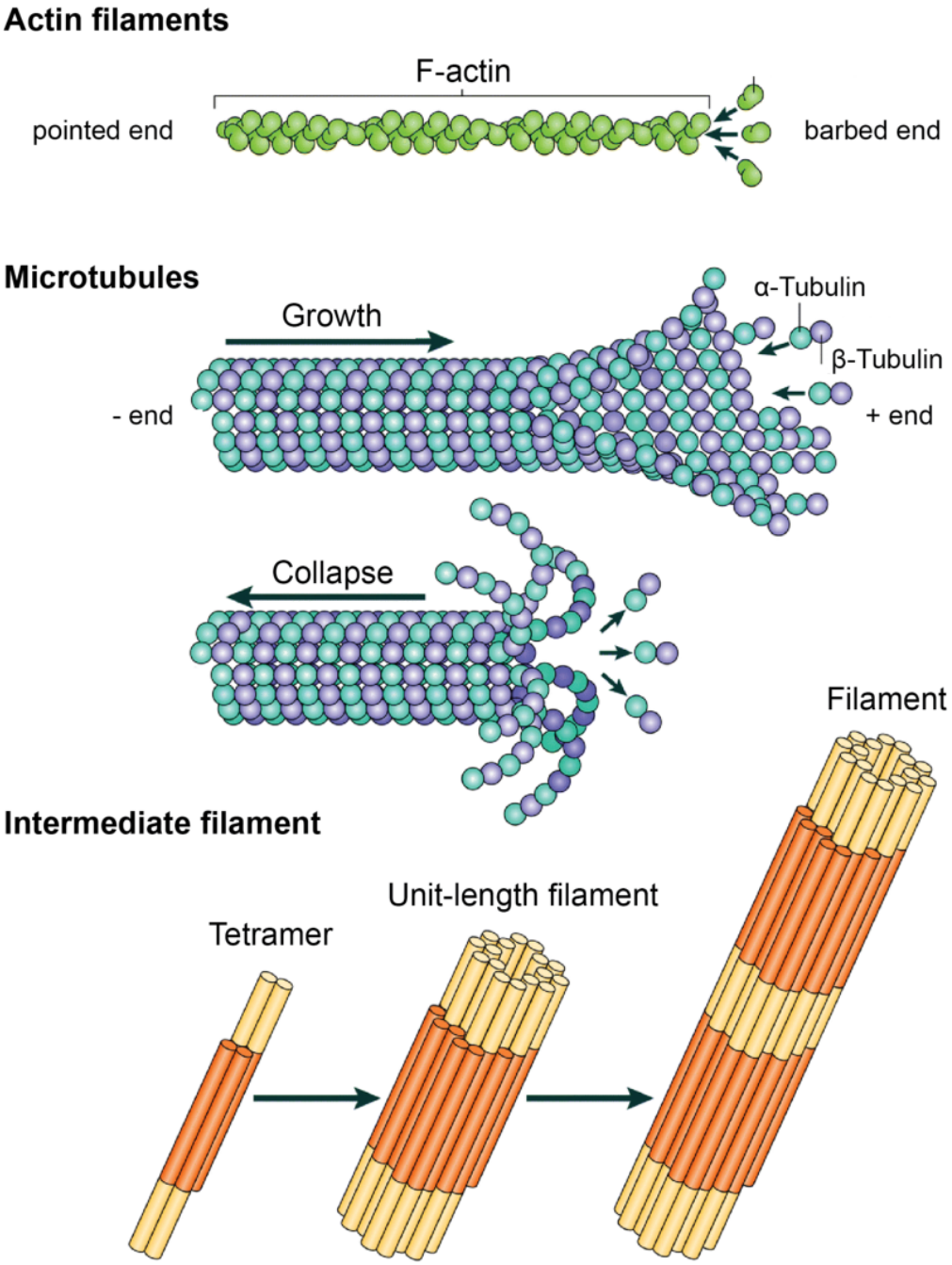

Fig. 1.1: Types of cytoskeletal filaments
Illustration of the three filamentous components of the cytoskeleton. Actin filaments and microtubules are formed from addition of actin and tubulin monomers to dynamic ends respectively. Intermediate filaments form from the lateral association of tetrameric subunits. From (Mostowy and Cossart, 2012).

(EB1, APC) or catastrophe (Stathmin, kinesin-13) (Goodson and Jonasson, 2018). Although +TIPs bind both plus and the minus end *in vitro*, in eukaryotes minus end MTs are more commonly associated with stabilising complexes, such as γ-TuRC. Finally, a large number of MT-associated proteins (MAPs) bind the body of MTs, where they have important roles in stabilising MTs via crosslinking of protofilaments or bundling of separate MT filaments. In neurons, a number of MAPs show spatially distinct distributions, such as tau and MAP2, which are localised to axon and dendritic compartments respectively.

It is worth stressing that these different systems do not work in isolation. MAPs and +TIPs compete with each other for binding to the lattice and ends of MTs respectively. Equally, MAPs have been shown to alter the association of motor proteins to MTs, and a subset of motor proteins are capable of actively depolymerising the plus end (Monroy et al., 2018). Finally, MAPs link the MT network to other cytoskeletal elements, including actin and intermediate filaments, which is critical for orchestrating cytoskeleton-wide remodelling events such as cell division.

1.1.1.2 Intermediate filaments

Intermediate filaments (IFs) are large and genetically diverse group of proteins, with humans having at least 65 IF genes (Herrmann et al., 2007). In contrast to the globular monomers of MTs, IF proteins share a conserved α-helical rod domain flanked by additional residues at N- and C-termini that are more structurally diverse. Another key difference to MTs is the lack of intrinsic polarity, which arises from the fact that IFs do not form from the addition of monomeric subunits to an extending filament. Instead, individual IF proteins form anti-parrallel homo- or heterodimers that associate laterally into tetrameric building blocks. Assembly of these tetrameric units together forms unit-length filaments that can subsequently anneal end-to-end to create mature filaments that have a width of 10 µm (Fig 1.1). The lack of polarity means that IFs are not used for intracellular trafficking by motor

proteins. Instead, IFs function by altering the mechanical properties of the cell, in part by modulating physical properties of actin filaments and MTs (Herrmann et al., 2007). The genetic diversity of IFs allows for tissue-specific and cell-type specific expression, for instance in neurons (neurofilaments) and glia (GFAP) in the brain. IFs also show spatial diversity within the cell; a class of IFs called lamins form the nuclear lamina that lines the inner nuclear membrane, whereas other IF classes (ketarins, vimentin-like) are cytoplasmic and have roles in linking cell-cell adhesions and extracellular matrix (ECM) interactions (via focal adhesions and hemidesmosomes) to the cytoskeleton.

1.1.1.3 Actin filaments

Actin filaments (AFs) are the smallest component of the cytoskeleton, roughly 8 μm in diameter, and also the most evolutionarily conserved. Actin genes are found in all forms of life of Earth, from bacteria to eukaryotes (Pollard and Cooper, 2009). Although some eukaryotes have only one actin gene (e.g. budding yeast), most have multiple copies generated via evolutionary duplication and divergence. Humans have 3 α-actin genes, a β-actin gene and 2 γ-actin genes which differ primarily in their expression in either muscle or non-muscle cells.

AFs are formed from the polymerisation of globular actin monomers (G-actin), which accounts for approximately 5% of total cell protein (Pollard and Cooper, 2009). Similar to MTs, G-actin binds phospho-nucleotides but these are adenosine-based (ATP/ADP). ATP-bound actin monomers assemble to form a helical structure held together by non-covalent bonds between subunits of the filament (Fig 1.1). Another shared feature of AFs and MTs is polarity, as revealed in electron microscopy (EM) studies of negatively stained filaments saturated with myosin heads (Ishikawa et al., 1969). This revealed a ‘barbed’ end and a ‘pointed’ end, named after the myosin-bound filament end looking like a pointed arrow head.

Polymerisation of actin can occur at both the pointed and barbed ends, though they have different kinetics. Addition of ATP-bound G-actin is roughly 10-fold faster at the barbed end, though it also dissociates more readily. Because of this difference, assembled actin monomers in a filament gradually move from the barbed end to the pointed end, a process known as treadmilling. Additionally, assembly into filamentous actin (F-actin) shifts the equilibrium in favour of hydrolysis of actin-bound ATP, meaning that over time F-actin becomes increasingly ADP-bound. Despite their dynamism, the polymerisation dynamics of AFs are far more measured than the all-or-nothing dynamic instability of MTs.

All else being equal, the concentration of free G-actin within the cytoplasm of cells (50-200 μM) would lead to the spontaneous incorporation of all monomers into AFs. In order for cells to regulate the incorporation of G-actin into filaments, a vast array of actin-binding proteins exist that modulate this equilibrium. Additionally, AFs in cells are not simply a selection of individual filaments but instead a complex array of different macro-structures, including branched actin, bundled parallel filaments and crosslinked filament webs. This diversity of the actin cytoskeleton exists due to a large group of actin-binding proteins (ABPs), an overview of which will be discussed presently.

1.1.2 Regulation of the actin cytoskeleton

1.1.2.1 Profilin, cofilin and capping

A number of actin-binding proteins (ABPs) control actin dynamics through controlling polymerisation rates. The majority of monomeric actin in eukaryotic cells exists in complex with profilin. Profilin binds the barbed end of actin, sterically inhibiting pointed end polymerisation but facilitating elongation at the barbed end (Pollard and Cooper, 2009). Elongation is further promoted by interaction of profilin with proline-rich domains (PRDs) present in formins and Ena/VaSP ABPs

(discussed later). Once incorporated into an AF the profilin-actin complex weakens, leading to dissociation of profilin and facilitating further addition of actin. Mammals have an additional ABP that binds monomeric actin called thymosin-β4, which competes with profilin G-actin. In contrast to profilin, thymosin-β4 binding sequesters G-actin preventing its incorporation into F-actin.

Cofilin is a small ABP that binds both G-actin and ADP-bound F-actin. Cofilin competes with profilin to sequestor the pool of G-actin, whereas its association with F-actin facilitates severing of existing filaments. Interestingly, cofilin activity is often associated with increased actin polymerisation, due to the generation of new barbed ends that filament severing generates. As a result, cofilin is required during formation of membrane protrusions in some instances (Bravo-Cordero et al., 2013). Regulation of severing activity by cofilin activity is quite varied; phosphotyidylinositol-4,5-bisphosphate (PIP_2) inhibits cofilin, as does phosphorylation by LIM kinase. A functionally related family of ABPs to cofilin are the Gelsolin family. These proteins have various related but different functions to that of cofilin, such as Glial maturation factor (GMF), which specifically severs branches from branched actin filaments (see Arp2/3) (Ydenberg et al., 2013).

The barbed-end tips of AFs are often 'capped' with the appropriately named capping protein. In antagonism with profilin, capping protein stabilises ends, limiting elongation and leading to depolymerisation as a consequence of actin treadmilling. However, capping protein function can be modulated, for instance by phosphatidylinositols (PIs), to allow for steady polymerisation (Pollard and Cooper, 2009). Pointed-end capping also occurs, for instance by the Arp2/3 complex after branch severing. Thus, the dynamics of AF elongation and depolymerisation are equisitely tuned by a variety of ABPs that act on monomeric actin, and both the tips and filament of F-actin.

1.1.2.2 Actin nucleation factors: Formins and Arp2/3

Profilin, cofilin and capping proteins all function by altering the polymerization and treadmilling activity of existing actin filaments. However, cells also need mechanisms to produce new actin filaments from G-actin *de novo*. There are two major classes of ABPs that perform this function, namely the formins and the Arp2/3 complex.

Formins were discovered in the 1990s as genes critical for cytokinesis, polarity, and tissue morphogenesis and have since been shown to nucleate new unbranched AFs (Breitsprecher and Goode, 2013; Mass et al., 1990). They are a homodimeric class of proteins that have 15 known members in mammalian cells and are characterized by the presence of two C-terminal domains, formin-homology 1 and 2 (FH1 and FH2 respectively) (Breitsprecher and Goode, 2013). These conserved FH1/FH2 domains mediate nucleation activity of formins, though precisely how this occurs is incompletely understood. FH2 can bind G-actin dimers to initiate nucleation *in vitro*, although this activity is largely absent with profilin-bound actin (Chesarone et al., 2010). The FH1 domain contains several proline-rich domains that can bind profilin-actin. Thus, it is currently thought that domains in the C-terminal domain (CTD) act cooperatively to bring profilin-actin monomers together and nucleate new filaments (Heimsath and Higgs, 2012). The diversity of formins arise from their divergent N-terminal domain (NTD) sequences, that guide protein-protein and protein-lipid interactions that localize formins to different intracellular structures including the plasma membrane, golgi and ER (Breitsprecher and Goode, 2013; Gorelik et al., 2011).

After nucleation, formins stay bound to the growing barbed end via interaction between FH2 and F-actin. This has dual roles in protecting the barded end from capping proteins and in sequestering new profilin-actin monomers for polymerization, facilitating AF formation (Breitsprecher and Goode, 2013). Formins differ in their processivity, with some (e.g. mDia1) orchestrating elongation of barbed ends for hundreds of actin monomers. In addition, many formins

(concretlely, Diaphanous-related formins) have Dia-inhibitory domain (DID) and Dia-autoregulatory domain (DAD) domains on their CTD and NTD respectively. These autoinhibit formin activity by preventing the CTD actin-binding activity, as revealed by X-ray crystallography experiments (Nezami et al., 2010). Often, binding of active small RhoGTPases can relieve this autoinhibition thus directing formin activity. Finally, growing evidence suggests formins alter microtubule targeting, association with AFs and stabilization via direct binding (Chesarone et al., 2010). Overexpression of mDia1 and 2 in fibroblasts increases the proportion of stable MTs that orient towards the cell periphery (Palazzo et al., 2001). Though the important of formins cooperative AF and MT binding has been difficult to untangle, it is likely an important point of cytoskeletal crosstalk.

Since the discovery of formins several other proteins with unbranched nucleation activity have been identified that do not structurally fit in the same family as the formins. These include Spire and JMY (Quinlan et al., 2005; Zuchero et al., 2009). These proteins utilise WASP homology (WH2) domains to bind G-actin/profilin-actin dimers to overcome the initial activation energy required for nucleation. Together with differing processivity of formins and balance between nucleation and elongation activity, these proteins represent the diverse ways in which actin filaments can be formed *de novo* in the cell.

Cells generate branched actin networks through the activity of the actin-related protein complex Arp2/3. First discovered nearly 25 years ago, the Arp2/3 complex was the first identified actin nucleator (Machesky et al., 1994). Arp2/3 is a heteromeric assembly of seven proteins, including Arp2 and 3, all of which are conserved in almost all eukaryotes. The complex is basally inactive, requiring activation by nucleation promoting factors (NPFs). Upon activation, the actin-related proteins Arp2 and Arp3 align to form a binding surface for the pointed end of actin monomers, thereby initiating nucleation of a new actin branch. EM micrographs of Arp2/3 and actin *in vitro* revealed that the Arp2/3 complex stay attached to branch point as long as it exists, and maintains the branch at a precise

70° angle from the mother filament (Rouiller et al., 2008). Additionally, when AF branches are severed (e.g. by the gelsolin protein GMF), the Arp2/3 complex remains attached to the pointed end were it limits depolymerization (Mullins et al., 1998).

1.1.2.3 Nucleation Promoting Factors

As discussed, the Arp2/3 complex is basally inactive and requires association with activated NPFs and ATP for branch nucleation. Arp2/3 NPFs are a class of NPF (type I) that are functionally distinct from type II NPFs (e.g. cortactin) that despite Arp2/3-binding do not activate the complex. Type I NPFs are all members of the Wiskott-Aldrich Syndrome (WAS) family of proteins, of which there are five identified members in mammalian systems; WASp, N-WASP, WAVE (isoforms 1-3), WHAMM, WASH and JMY. Despite their divergent structures, upstream activators and downstream effectors, these proteins all share a conserved mechanism for Arp2/3 activation (Fig 1.2). Concretely, all possess a C-terminal VCA/WCA (verprolin/WH2, central, acidic) domain that is required for actin binding and Arp2/3 activation. Binding of the WCA domain to Arp2/3 induces a conformational change that both brings Arp2 and 3 subunits together and increases the affinity of Arp2/3 to mother AFs. Simultaneously, the WH2 (W) component of the WCA domain recruits G-actin to the complex, providing a seed to initiate nucleation of a new branch. Adjacent to the WCA domain, WAS family proteins have a proline-rich domain (PRD) that binds profilin-actin to further promote elongation (Alekhina et al., 2017). An important general feature of WASP proteins in basal inhibition of WCA activity via intra- or intermolecular occlusion.

The diversity of WASP family function arises from their differential localisation, protein and lipid interactions and activation states within the cell. This has enabled WASP proteins to become functionally specialised in various critical intracellular processes that require actin remodelling (Fig 1.2). As such, WASP, WASH and

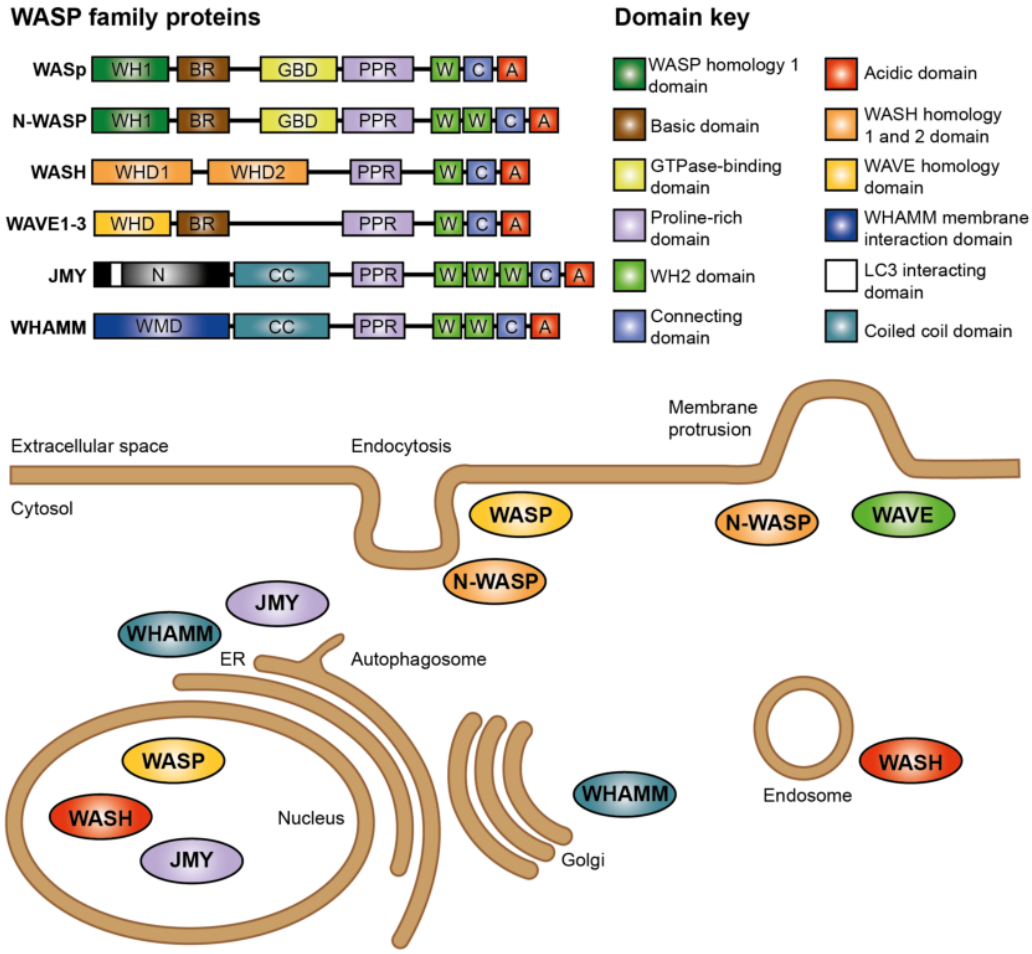

Fig. 1.2: Structural and functional diversity of WASP family proteins
Top panel: The major domain structure of the different WASP family members. All members have a conserved C-terminal WCA motif and PPR regions but divergent N-terminal domains. Notice the GDB binding domains of WASp and N-WASP that mediate cdc42-mediated activation of these proteins. Also the three WH2 domains of JMY that facilitate *de novo* actin nucleation. **Bottom panel:** Illustration of the subcellular localisations of WASP proteins. WASp, N-WASP and WAVE are primarily associated with the plasma membrane whereas others have roles in actin remodelling of intracellular organelles, such as endosomes (WASH), autophagosome formation (WHAMM, JMY) and ERGIC remodelling (WHAMM). WASp, WASH and JMY also have functions within the nucleus. From (Alekhina et al., 2017)

WAVE proteins are all evolutionarily ancient, whereas WHAMM and JMY proteins first arose in invertebrates (Veltman and Insall, 2010).

WAS family proteins are named after the first identified member, WASp, being the protein product of the gene mutated in the immune-deficiency disease Wiskott-Aldrich Syndrome (Derry et al., 1994). WASp is primarily expressed in haemopoietic systems, including the spleen, thymus and lymphocytes. In contrast, N-WASP is expressed more ubiquitously, and its deletion is embryonically lethal in mice (Snapper et al., 2001). WASp and N-WASP are structurally very similar, differing only in an extra WH2 domain in the WCA region of N-WASP (Fig1.2). Both proteins are autoinhibited by binding of central and acidic domains of the WCA to the GTPase-binding domain (GBD, also known as CRIB) region. This inactive conformation is further stabilized by WH1-interacting protein (WIP). Binding of the RhoGTPase cdc42 to a central GBD relieves autoinhibition of N-WASP and is a key activation signal. However, activity is also modulated by additional signals; PIP_2 binding to the basic region (BR), SH3-containing proteins binding to the proline-rich regions (PRR) (e.g. NCK1, ABI1), phosphorylation of tyrosine residues in the GDB (Campellone and Welch, 2010). Many of these interactions help localise WASp and N-WASP proteins to the plasma membrane, where they have critical functions in phagocytosis, endocytosis and cell motility. Interestingly, recent work has uncovered a role for WASP in the nucleaus where it recruits chromatin remodelling factors to the TBX21 promoter in T-cells to regulate autoimmune response (Sarkar et al., 2015).

The other important group of WASP proteins at the plasma membrane are WAVEs. WAVE proteins form heteromeric complexes in the cell and are inhibited by transmolecular interactions (Ismail et al., 2009). WAVE proteins (of which there are 3 mammalian isoforms) are active when isolated (Innocenti et al., 2004). However, in cells they exist exclusively as part of a heteropentameric complex consisting of NAP1, CYFIP, ABI and HSPC300 proteins that together is termed the WAVE regulatory complex (WRC). In this complex, the WCA region of WAVE is

buried and therefore inaccessible to either actin monomers or the Arp2/3 complex (Chen et al., 2010). This intermolecular inhibition is relieved by binding of another RhoGTPase, Rac1. The regulation of this complex is discussed in further detail in section 1.4. WAVE proteins have well-defined functions in cell motility and lamellipodia formation and, alongside N-WASP, directly regulate Arp2/3 activity at the plasma membrane.

Analogous to WAVEs, WASH proteins have unique N-terminal WASH homology domains (WHD1 and 2) that mediate interactions with proteins, including capping protein, FAM21, strumpellin and CCDC53 (Jia et al., 2010). It is thought these interactions form a complex similar to the WRC, that inhibits WASH activity under basal conditions, although the details of this are poorly understood. It is interesting to note that capping protein has independent roles in AF polymerisation and thus provides a way of coordinating different actin remodelling functions locally. Functionally, WASH is localised to endolysosomal compartments and is critical for actin remodelling during the formation and sorting of endosomes and lysosomes. Loss of the WASH results in collapse of the endolysosomal system and accumulation of cargo-filled membrane tubules (Gomez et al., 2012). In accordance with this critical role in organelle biogenesis, WASH knockout mice are embryonically lethal.

WHAMM is localised to the endoplasmic reticulum-Golgi intermediate compartment (ERGIC) where it facilitates vesicle formation important for intracellular trafficking of transmembrane proteins (Campellone et al., 2008). Additionally, WHAMM interacts with microtubules via the coiled-coil (CC) domain and this interaction masks its WCA domain, thus providing another novel mechanism of WASP protein inhibition. JMY is unique in its ability to nucleate AFs via two distinct mechanisms: 1) canonical activation of Arp2/3 via the it's WCA region and 2) *de novo* AF nucleation independent of Arp2/3 via binding of G-actin to three serial C-terminal WH2 domains (Zuchero et al., 2012). It also has unique roles as a transcriptional regulator; JMY translocates to the nucleus in a process

regulated my cytoplasmic monomeric actin levels, where it activates p53 during DNA damage response (Zuchero et al., 2012). Both JMY and WHAMM regulate autophagosome biogenesis at the ER through remodelling of the ER membrane (Kast et al., 2015). Thus, the variety of Arp2/3 NPFs facilitate a diverse array of functional nodes where Arp2/3 activity can be independently regulated.

1.1.2.4 RhoGTPases

The RhoGTPases are family of small GTPases within the larger Ras-related superfamily, with well-described roles in the regulation of cytoskeletal remodelling. As mentioned, several RhoGTPases are key upstream activators of NPFs. However, these proteins also interact, directly or indirectly, with the other ABP proteins discussed to orchestrate complex actin remodelling cascades. Thus, the function of RhoGTPases is critical to an understanding of cytoskeleton dynamics.

In humans, there are 22 known RhoGTPase proteins, that can be further subdivided based on sequence similarity. Though they have unique regulatory pathways, expression profiles and downstream effectors, they all function in a fundamentally similar way. GTPases can bind a single guanine nucleotide in either GDP or GTP form. The GTP-bound form switches on the RhoGTPase, enabling conformation-specific protein interactions with downstream effectors, whereas the GDP-bound form is inactive. Three subfamilies of the RhoGTPase family (termed classical RhoGTPases) have emerged as particularly critical for actin remodelling, namely Rac (1, 2 and 3), cdc42 and Rho (A,B,C). Over 50 unique protein interactions have been identified for Rac1 and cdc42 alone, highlighting their importance as hubs of intracellular signalling (Jaffe and Hall, 2005).

Regulation of this GTP switch is achieved by three classes of protein; guanine nucleotide exchange factors (GEFs), GTPase activating proteins (GAPs) and guanine nucleotide dissociation factors (GDIs). GEFs promote the exchange of GDP to GTP by stimulating GDP release and therefore promote activation of Rho

GTPases, whereas GAPs stimulate intrinsic GTPase activity of RhoGTPases leading to hydrolysis of GTP and deactivation (Jaffe and Hall, 2005). GDIs oppose the exchange of GDP for GTP, maintaining targets in an 'off' state and limiting spontaneous activation. Interestingly, the have also been shown to disrupt RhoGTPase association with membranes, something critical for many of their functions related to cytoskeleton dynamics (Heasman and Ridley, 2008). Together, these determine the activation state of the RhoGTPase to ensure correct spatial and temporal dynamics.

1.1.3 Important cytoskeletal structures in cell growth and motility

The mechanisms of motility and growth of eukaryotic cells is complex and diverse. However, studies across species have identified several highly evolutionarily conserved sub-cellular structures that are critical for these processes. The structures include filopodia, lamellipodia and focal adhesion sites (Ridley, 2011). These structures are present in higher organisms and form the basis of our understanding of development of the complex morphologies of neurons. Classical RhoGTPases are critical conductors of these large scale changes in actin remodelling, and are all capable of modulating the activity of multiple ABPs discussed previously. Interestingly, each classical RhoGTPase is associated with a specific structure; Rac1 for lamellipodia, cdc42 for filopodia and RhoA for stress fibres formation. In reality the situation is more complex and the spatial and temporal activation of different RhoGTPases simultaneously in the cell facilitates fine control over the balance of actin incorporation in these different structures.

1.1.3.1 Filapodia formation

Filopodia are thin, finger-like structures about 100-300 nm wide that protrude from the cell edge. They are formed from an actin-rich core of parallel bundles of unbranched actin fibers whose polymerization provides the mechanical force to drive membrane protrusion. Filopodia have well-established roles in sensing of the environment and in cell motility, and therefore are critical for a number of important processes during brain development, including axon extension and dendritic spine formation (discussed section 1.2.4.1). The tips of filipodia are often enriched in integrin and cadherin molecules that interact with the extracellular environment (Galbraith et al., 2007).

The formation of filopodia is well understood. Importantly, cdc42 has emerged as a master regulator of this process; activation of cdc42 induces the formation of filopodia and loss activity via overexpression (OE) of dominant negative cdc42 or knockdown leads to loss of filipodia in mouse embryonic fibroblasts (MEFs) and reductions in the growth cones of neurons (Korobova and Svitkina, 2008). This appears counter-intuitive given cdc42's canonical role in promoting acting branching via N-WASP. Arp2/3 activity may be required for initiation of filopodia formation by providing a branched network at the base of the filopodia that converge and elongate. This is supported by the observation that filopodia arise from lamellopodial actin network (Svitkina et al., 2003). Interestingly, although loss of N-WASP perturbs normal filipodia formation, it's activtion is not absolutely required to form filopodia, suggesting other cdc42 targets may be involved (Snapper et al., 2001).

One important cdc42 target is the adapter protein, IRSp53. IRSp53 was identified by yeast two-hybrid screens to bind both cdc42 and WAVE2 and interacts with Rac1 (Miki et al., 2000). It contains an I-BAR domain that can induce bends in the membrane to induce protrusions (Suetsugu et al., 2006). This appears critical for filopodia induction, as overexpression of IRSp53 dramatically increases filopodia formation in a cdc42-dependent manner (Lim et al., 2008). Membrane curvature

likely decreases the mechanical stress on actin fibers at the membrane, facilitating their elongation into parallel bundles.

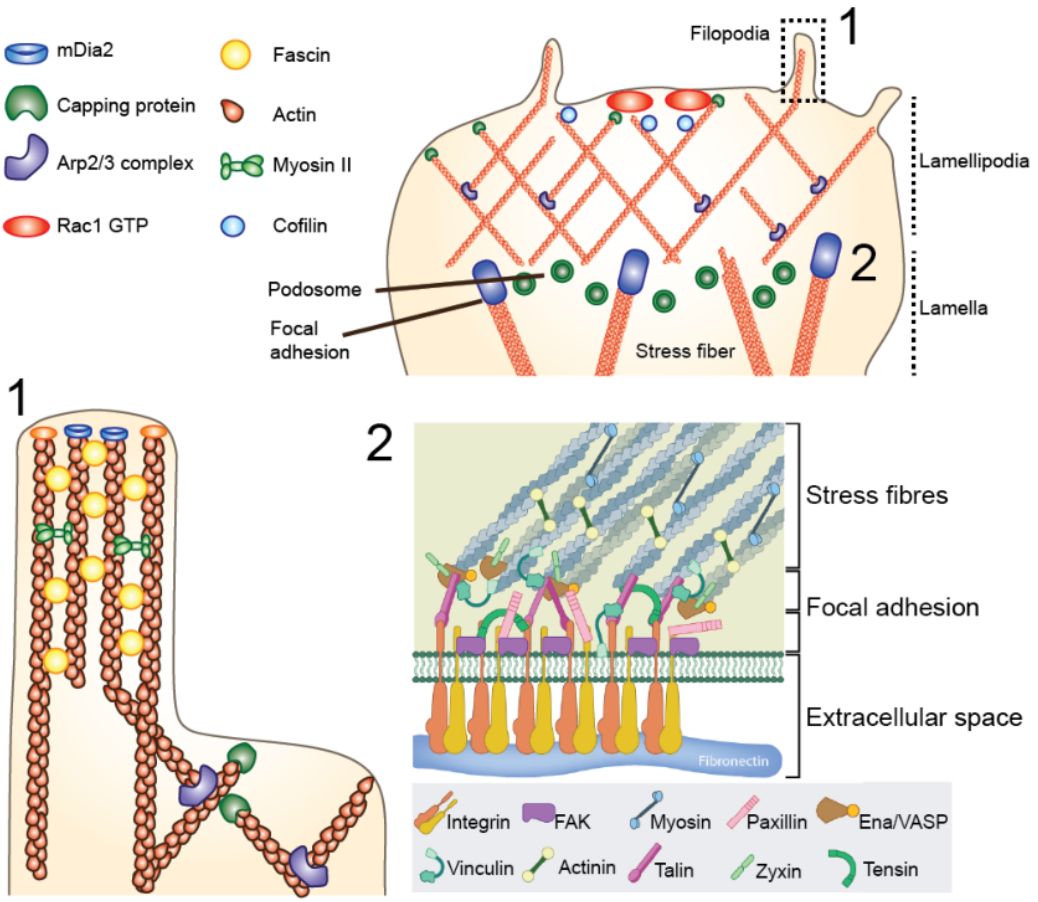

Fig. 1.3: Actin structure in lamellipodia, filopodia and focal adhesions
Graphical illustration of three important sub-cellular structures critical for cell growth and motility and the actin-binding proteins and transmembrane proteins involved. Lamellipodia are characterised by a dense network of branched, dendritic actin. Filopodia commonly form at the leading edge but have bundled parallel fibres. The lamella region is a more stable region containing stress fibres, focal adhesions and podosomes. From (Blanque et al., 2015)

Polymerisation of AFs in filopodia requires several other ABPs. Formins bind to the barbed end of elongating AFs in the nascent filopodia. In mammalian systems, mDia2 is particularly critical in this capacity and is found at the tips of filopodia (Peng et al., 2003). mDia2 is activated by cdc42. Mena/VASP proteins also interact with the barbed ends to protect them from capping proteins and thus promote polymerization. VASP also associates with the body of AFs where it 'bundles' adjacent AFs together, increasing their stability and reducing treadmilling (Schirenbeck et al., 2006). Fascin

is another AF-bundling protein that is important for generating stiff and tight F-actin structures. Interestingly, loss of fascin leads to collapse of actin bundles that buckle against the plasma membrane and thus are unable to form stable filopodia (Vignjevic et al., 2006).

Together, this highlights that filopodia formation is a highly complex and tightly regulated process that involves a range of different ABPs. Many of these are directly activated by cdc42, whilst other likely become associated with filopodia due to inherent features the structure (i.e. multiple parallel, stable AFs). It is worth mentioning that this is a generalized model of filopodia formation and that the importance of specific proteins differs on the cell type and conditions the filopodia is formed under. For example, Arp2/3 (which is activated by N-WASP) is not required for filopodia formation in MEFs whereas it is critical in in growth cones (Di Nardo et al., 2005; Korobova and Svitkina, 2008).

1.1.3.2 Lamellipodia formation

Many cells in culture display a characteristic sheet-like structure at the leading edge of the cell membrane during whole cell motility. Termed lamellipodia by Abercrombie et al. in the 1970s, these structures are critical for cells to extend their membrane to drive cell motility and are important cytoskeletal structures in cell migration during development and beyond.

Early EM imaging showed that lamellipodia were actin rich and lacking significant MTs (Svitkina and Borisy, 1999). Additionally, in contrast to the parallel fibers of filopodia, AFs formed a highly branched network of interconnected fibers. Imaging studies showed this region is highly dynamic, with actin polymerization driving the forwards movement of the plasma membrane (Krause and Gautreau, 2014). Behind this actin sheet lies a more stable region termed the lamella, which is characterized by myosin-based contractibility and adhesive contacts with extracellular substrates. Because of this, Arp2/3 activity has long thought to be

critical for lamellipodia formation. As such, inhibition of Arp2/3 with CK666 or knockout of a critical subunit both lead to complete loss of lamellipodia (Steffen et al., 2006; Wu et al., 2012). Further, severing of branched AFs by GMF is critical for retraction of lamellipodia (Goode et al., 2018). Thus the 'dendritic' actin network formed by Arp2/3 branching forms the basis of the lamellopodial sheet.

The Rac1-WAVE-Arp2/3 signalling pathway appears to be particularly important for lamellipodia formation. Inhibition of Rac1 inhibits lamellipodia and loss of various WRC components inhibit Rac1-induced lamellipodia (Oikawa et al., 2004; Steffen et al., 2004). Interaction with PIs in the plasma membrane, namely PIP_2 and PIP_3, play an important role in specific activation of Rac1 and WAVE (Oikawa et al., 2004). Disruption of Rac1 binding to IRSp53, which localises cdc42, Rac1 and WAVE2 to the plasma membrane (PM), inhibits lamellipodia formation (Roy et al., 2009). Interestingly, despite this the only study correlating Rac1, cdc42 and RhoA activity during lamellipodial protrusion show precise waves of activation of all three of these RhoGTPases with RhoA being active at the very edge of the PM whereas Rac1 and cdc42 showed more disperse activity (Machacek et al., 2009). To support this, active RhoA and cdc42 are required for lamellipodia in certain conditions (Kurokawa et al., 2004; Ridley, 2011). Thus Rac1 signalling may be required upstream of other RhoGTPase pathways aswell as directly activating ABPs.

More recent studies have unveiled novel roles for other ABPs in lamellipodia. Formins and Spire-family proteins, such as mDia1 and Courdon-Bleu, promote polymerization of barbed ends at the leading edge, and protect them from capping (Ridley, 2011). VASP protein stabilizes and brings together barbed ends. Indeed, the dogma of branched actin networks dominating lamellipodial structure has been questioned by recent EM studies showing very little 'dendritic actin', and more overlapping and crosslinked structures (Urban et al., 2010). In support of this, the AF severing protein cofilin promotes polymerization by creation of new barbed ends, and is important for directing lamellipodium growth during chemotaxis (Sidani et al., 2007). Importantly, activity of cofilin is regulated by Rac1 via LIM kinase

activation, with the effect of localising cofilin activity at the PM (Yang et al., 1998). Additionally, the type-II NPF cortactin is present at the lamellipodial front and regulates actin persistence, though probably via RhoGTPase activation rather than direct Arp2/3 binding (Lai et al., 2009).

Thus, lamellipodia formation involves a concerted activation of RhoGTPases at the membrane. Rac1-driven activation of WAVE-Arp2/3 remains critical for generating the dendritic actin network that forms the basis of the structure. However the stability and elongation of these branches are controlled by a host of other factors whose activity generate the emergent properties of the lamellipodia (protrusion speed, longevity, processivity etc). Importantly, this cytoskeletal activity is influenced by external factors such as cell-cell contact and substrate interactions. These are discussed next.

1.1.3.3 Focal adhesions and podosomes

There are many reasons why cells might need to physically interact with the external environment: coordination with other cells to form larger structures, attachment to an extracellular surface for stability, clearing a path for growth through tissue to name a few. Because they involve interactions outside of the cell, these interactions are mediated by proteins that span the plasma membrane.

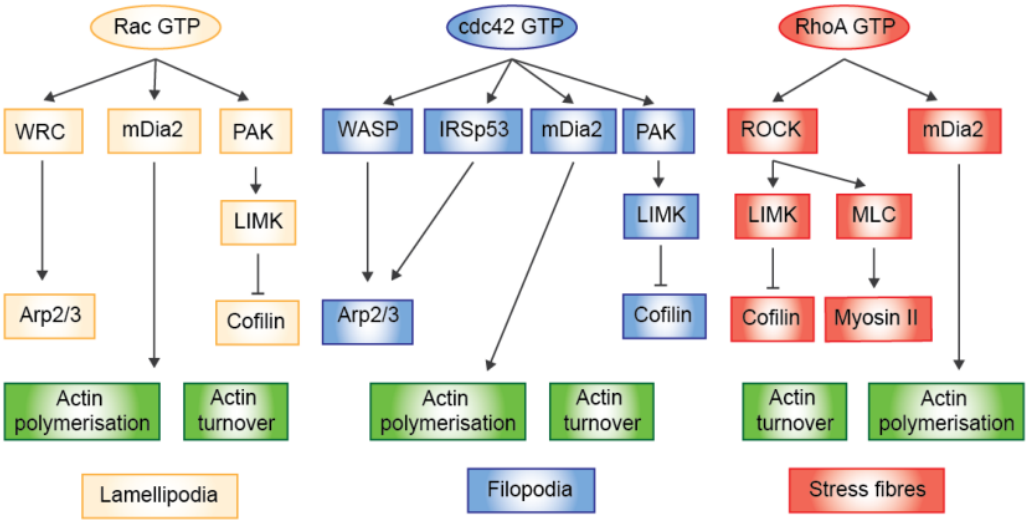

Fig. 1.4: Downstream effectors of RhoGTPases relating to actin remodelling
Illustration of three important sub-cellular structures critical for cell growth and motility and the actin-binding proteins and transmembrane proteins involved. From (Heasman and Ridley, 2008)

The best characterised group of proteins here are the integrins. Integrins are heteromeric dimers formed of an α and β subunit, of which 24 α and 9 β gene variants have been identified in mammals. Both subunits have a large extracellular NTD that interacts with binding partners outside of the cell and a small CTD tail that signals to the cytoskeleton. An important feature of integrins is the ability for bi-directional signalling; binding of extracellular targets can result in a conformation change in the CTD that activates intracellular downstream targets ('outside-in' signalling), but interactions and alterations to CTDs and transmembrane domains (TMDs) can also alter the affinity of integrins for extracellular ligands ('inside-out signalling') (Harburger and Calderwood, 2009). Although a growing body of research has identified a hundreds of integrin interactors, their roles in focal adhesions and podosomes remain some of the best understood.

Focal adhesions (FAs) are integrin-based macromolecular complexes that link the actin bundles to extracellular substrates to provide mechanical support for adhesion and migration; and transmit signalling cues to direct chemotaxis and other downstream pathways. FAs are observed *in vitro* and in a range of *in vivo* contexts, including in neuronal growth cones (Cypher and Letourneau, 1991). At their core, mature FAs are a complex joining ligand-bound integrins to bundled AF bundle, via talin, vinculin and α-actinin (Fig 1.3) (Case and Waterman, 2015). However, in addition to these core components, FAs have highly dynamic associations with scaffolding proteins, kinases and phosphatases that regulate their stability. One important kinase is Focal Adhesion Kinase (FAK). FAK associates with nascent FAs at the base of the lamellipodia, linking activated integrins to signalling adapters paxillin and Src, and phosphorylating these targets. These lammelipodial FAs are highly dynamic and turnover at a rate of 1 min^{-1} (Case and Waterman, 2015). Their stabilisation involves additional signalling that forms an important part of controlling the directionality and speed of membrane protrusion.

Maturation of FAs involves movement into the lamellum, which is rich in α-actinin bound AF bundles. Interestingly, an early characterisation of FAK KO

fibroblasts showed increased FA numbers (Ilić et al., 1995). Studies since have shown that FAK inhibits maturation of FAs via phosphorylation of N-WASP and α-actinin, which increases actin polymerisation (via Arp2/3 nucleation) and reduces bundling respectively. In mature FAs, FAK is inactivated itself by phosphorylation. Actomyosin contractility is also critical for FA maturation, and is mediated primarily by myosin-II (Choi et al., 2008). In line with myosin II involvement, RhoA is active at FAs where in promotes myosin contractility via ROCK-MLC phosphatase-MLCK pathway (Mitra et al., 2005).

Podosomes are another class of integrin-based adhesion that are important for matrix degradation needed during invasion through ECM. As such, they are found in invasive cell types such as macrophages and microglia (Vincent et al., 2012). They are closely related to a sister structure, invadopodia of carcinoma cells (Yamaguchi et al., 2005). Both podosomes and invadopodia have a two-domain doughnut-like structure, with an actin-rich core surrounded by an outer ring of adhesion molecules such as talin, vinculin and integrins (Murphy and Courtneidge, 2011). The central actin domain contains N-WASP, Arp2/3 and cortactin; in line with this, cdc42 and WASP activity is required for podosome formation (Linder, 2007). Further, the tyrosine kinase Src is highly enriched in podosomes and N-WASP and cortactin are both Src substrates. Interestingly, Rac1/2 are also required for podosome formation in primary macrophages (Wheeler et al., 2006). This may be due to interaction with PAK1 and βPIX, present in the outer ring. Finally, podosomes are stabilised by interaction with MTs, in part controlled by the MT-binding properties of the formin, mDia1.

Podosomes degrade extracellular material via the release of metalloproteinases into the extracellular space. Concretely, MT1-MMP, MMP-2 and MMP-9 are commonly found in podosomes of different cell types (Linder, 2007). These enzymes are directed to podosome via vesicular trafficking, which are likely to be directed to podosomes via stabilised MTs mentioned already. Metalloproteinases degrade a variety of ECM components, such as collagen.

Together, FAs and podosomes represent two important examples of how cytoskeletal machinery can be linked to signals outside of the cell. As the next section will illustrate, this is critical during neuronal development in the brain and disruption of these signalling cascades are implicated in many psychiatric disorders.

1.2 Neuronal development and synaptic transmission

1.2.1 Neuronal morphology

Neurons are the primary information transfer unit in the nervous system. As such, they are required to transmit information across vast distances from a cellular perspective; in humans, dorsal root ganglion neurons in the spinal cord can grow over a meter in length. This extremely polarised morphology facilitates the millisecond timescale of communication needed for animals to process external information and make suitable responses. Another interesting feature of neurons is the diversity of morphologies neurons adopt in different parts of the central nervous system (CNS). Control of this process is driven by a combination of unique transcriptional signatures, external signaling and inherent cellular processes.

1.2.2 Structure of the neuron

As units of information transmission, the structure of the neuron can be simplified based on its two primary functional roles; receiving and relaying signals. These two processes are physically separated to enable the cellular specialization required for these very different tasks. Information is received via a network of processes emerging from the cell soma, called dendrites (Fig 1.5). Inputs are received by dendrites either directly onto the dendritic shaft or onto small protrusions from the shaft called dendritic spines (discussed later). As hinted previously, the dendritic arbor of a neuron can differ greatly in size, shape and complexity. These parameters

establish the volume of parenchyma within which a neuron can receive signals from and thus to a large extend determines a neurons connectivity. The observation that, despite the huge potential for variety in this substructure, neurons of the same subtype in the brain have highly conserved dendritic morphology highlight the importance of establishing the correct structure.

Information is transmitted to other cells via a second cellular protrusion called the axon (Fig 1.5). In many ways axons are similar to dendrites in that they are long, tube-like protrusions from the cell soma that branch to contact up to thousands of other neurons. Like dendrites, these contact are dotted along the shaft of the axon at specific locations called presynaptic terminals or boutons. There are some unique feature of axons that pertain to their function. Firstly, the majority of axons are wrapped in a fatty coat called the myelin sheath. The sheath is produced by a specialist type of glial cell (Schwann cells in the peripheral nervous system, oligodendrocytes in the CNS) and helps isolate the electrical signals that pass through the axon to ensure efficient and rapid signal transduction. Secondly, in general axons tend to be a lot longer than dendrites, delivering signals across different part of the body to the brain and between regions of the brain.

Dendrites and axons possess very different protein compositions and organelles. The difference in cytoskeletal composition is a good illustration of this. The shafts of both axons and dendrites are characterised by dense bundles of microtubules that are required for structural stability and trafficking. However, many MAPs associated with MTs show distinct polarity. For instance, tau is localized exclusively to axonal MTs, whereas MAP2B is localized exclusively to dendrites (Dehmelt and Halpain, 2005). Additionally, axonal MTs are arranged in a unipolar fashion with the plus ends facing away from the cell soma whereas in dendrites MTs can be found in both orientations. This has important consequences for the roles of end-directed motor proteins like kinesins and dyneins in these different compartments. In contrast, F-actin structures are largely excluded from dendritic shafts but highly concentrated in dendritic spines (Konietzny et al., 2017). Recent studies have identified local actin

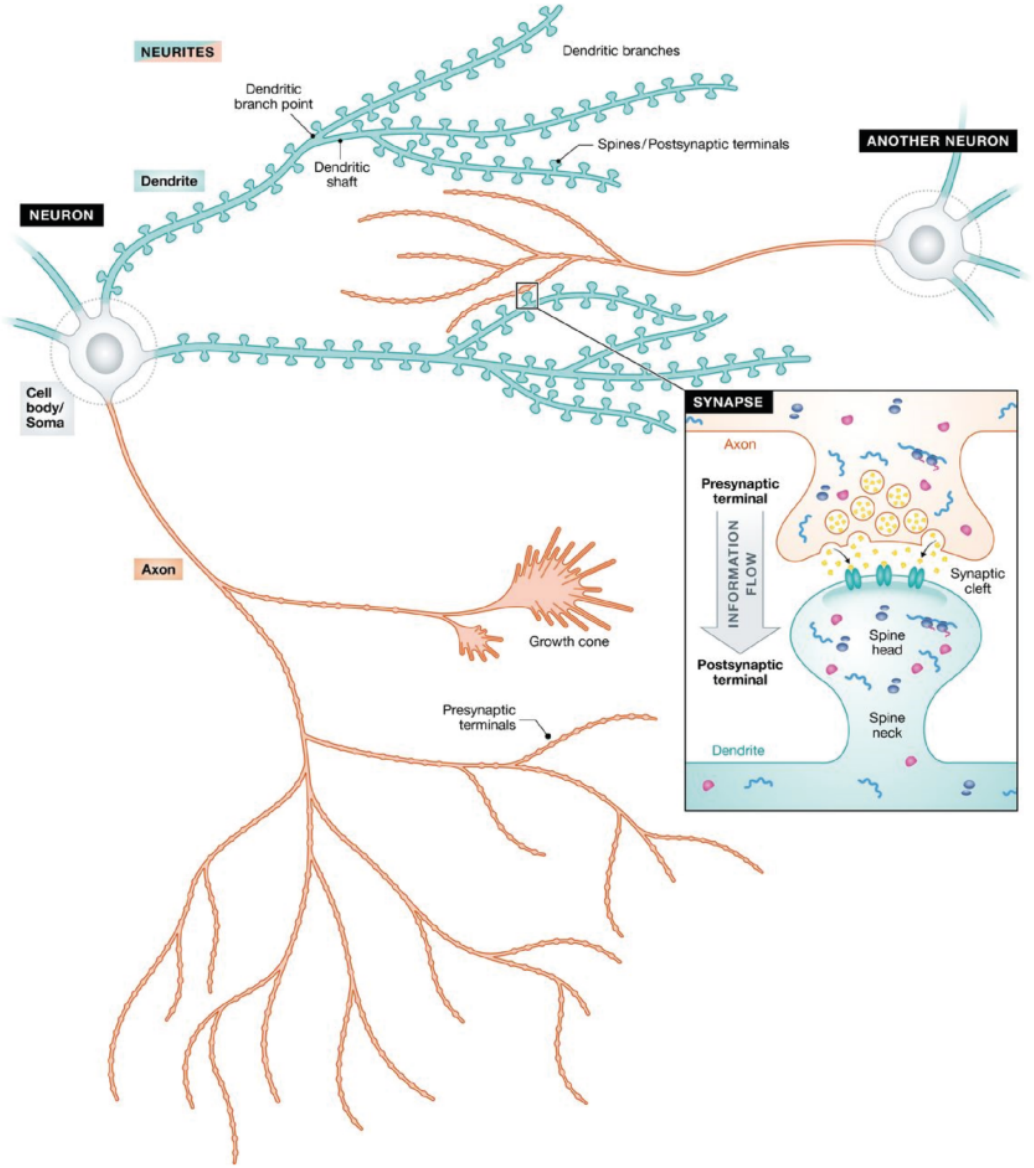

Fig. 1.5: Graphical illustration of a neuron
Neurons have two major process types that control information transfer. Dendrites (blue) receive excitatory inputs from other neurons at protrusions called dendritic spines (see zoom). Typically neurons have a single axon (orange) that is specialised for transmission of action potentials to presynaptic sites. From (Rangaraju et al., 2017).

structures in dendritic shafts, such as actin patches, longitudinal fibres and rings that associate with specific ABPs, including spectrins. Super-resolution imaging of axons has revealed that spectrin-associated actin rings are much more common in axons and occur at regular intervals. The function of these rings is incompletely understood but their distribution is coordinated with sodium channel distribution suggesting they have functional roles in action potential transduction (Xu et al., 2013). In addition, the leading process of both dendrites and axons (termed to growth cone) is a highly actin rich structure.

1.2.3 Mechanisms of dendritogenesis

Dendrites and axons arise concurrently during development and share a similar subcellular origin. A newly born neuron begins the process of cellular growth by generating numerous dynamic processes that emerge from the cell soma, called neurites. Very rapidly one of these neurites becomes established as the axon, taking on a unique molecular profile and different growth dynamics (Barnes and Polleux, 2009). In hippocampal culture, this occurs within two days of plating and represents a first step in neuronal maturation. Although the molecular signals underlying this specialization have been heavily studied, it is still incompletely understood. The PI kinase PI3K has emerged as a critical determinant for polarity; loss of PI3K prevents axon formation and OE produces multiple axons (Barnes and Polleux, 2009). Concurrently, many proteins involved in modulating PI3K activity or downstream of PIP3 signalling have been similarly implicated, including PTEN, AKT and GSK3β. Interestingly, GSK3β has a link to CYFIP1/WAVE localisation via phosphorylation of CRMP-2, evidence that actin remodelling dynamics likely play a role in axon specification (Inagaki et al., 2001). *In vivo*, the situation is more complex and conclusions made from *in vitro* experiments do not all transfer. One reason for this may be that neurons establish dendrite-axon polarity during migration with the leading and trailing processes of postmitotic neurons forming the basis for this segregation (Barnes and Polleux, 2009).

As mentioned, the development of dendritic arbor is determined by intrinsic and extrinsic factors. The intrinsic factors include transcription factors (TFs) that control the expression of the machinery for dendrite growth. Many of these TFs have been identified through genetic screens in Drosophila, including CUT. CUT determines the dendritic identity of certain neurons during larval development and its human homologs, the CUX genes (1+2) regulate arborisation of upper layer cortical neurons in mouse (Cubelos et al., 2010; Jan and Jan, 2010). Additional mammalian TFs such as neurogenin 2, NEUROD1 and CREB have also been identified, and add additional functionality such as the calcium-sensitive responses of CREB (Jan and Jan, 2010). Extrinsic signals augment these transcriptional profiles via transmembrane receptors on the plasma membrane. Binding of appropriate ligands to these receptors can either attract or repel dendritic growth and the balance of many of these signals determines local growth dynamics. Important receptors include the ROBO and Semaphorin (SEMA) classes. Signalling of growth factors such as NGF and BDNF via TrkB receptors are an important group of pro-growth signals; ablation of BDNF or its receptor both lead to dramatic reductions in dendritic complexity of cortical neurons *in vivo* (Xu et al., 2000).

Finally, adhesion molecules link growing dendrites with the ECM to stabilise nascent branches. A subset of the cadherin superfamily, called protocadherins (PCDHs), have emerged as particularly important for dendrite development. α- and γ-protocadherins are localised to dendrites and spines and knockout of either molecule impairs arborisation of cortical neurons (Keeler et al., 2015). Interestingly, in both these cases OE of constitutively active Rac1 can rescue these defects, suggesting that PCDHs signal upstream of Rac1. In addition, γ-PCDH leads to increased activation of FAK which may slow dendritic growth via affecting stabilisation of focal adhesions (Suo et al., 2012). In line with this, many of the upstream signalling pathways controlling dendritogenesis converge on the cytoskeleton remodelling. Rac1 and cdc42 have both been shown to positively regulate dendrite formation, whereas knockout of RhoA expands the dendritic arbor (Chen and Firestein, 2007; Jan and Jan, 2010). Stabilisation of MTs is an important downstream effect of activation of

these pathways; the negative impact of RhoA signalling is via downregulation of Cypin levels, a MT stabilisation protein (Chen and Firestein, 2007). These pathways also regulate actin polymerisation that occurs at growing tips and nascent branch points. A recent live-imaging paper showed that F-actin rich sites preempted branch formation (Nithianandam and Chien, 2018). Thus, dendritic growth is a dynamic process of actin-mediated protrusion followed by MT infiltration and stabilisation.

It is worth noting that many of the signaling pathways regulating dendritogenesis have parallel roles in synapse formation. Indeed, there is substantial evidence that neuronal activity itself is critical for regulating dendrite growth. Influx of calcium through NMDARs and mGluR activation during synaptic activity has direct impacts on dendritic growth, such as via activation of CaMKII and CREB signalling mentioned previously (Ghiretti and Paradis, 2014). As discussed in the next section, actin remodelling is critical for synapse formation and maturation. Thus, it is likely that defective actin dynamics have knock-on effects on dendrite stability via a changes at the synapse (Koleske, 2013).

1.2.4 The excitatory synapse

Synapses are the primary sites of information transmission between neurons. One could imagine many ways of organizing synapses in order to perform this function. However, in general synapses have a stereotypical basic structure that, whilst dynamic and specialised, is consistent throughout the CNS and across the animal kingdom. This consists of a clustering of postsynaptic ion channels whose gating is determined by extracellular molecules called neurotransmitters. On activation these receptors open, leading to a passive redistribution of ions across the plasma membrane, along electrochemical gradients. This has the overall effect of altering the polarization state of the cell, and thus its likelihood to fire an action potential. There are several important features of this model of information transmission. Firstly, information can be summed across many different synapses to converge on a single cellular parameter

(membrane potential). Indeed, the effect of activating any particular synapse will depend on its location in the dendritic arbor, the quantity and type of ions exchanged, and the activity of other synapses. Secondly, the fact that transmission occurs at precise locations in the cell makes it possible to extensively fine tune specific inputs into cells. The control of synapse strength (called synaptic plasticity) is a fundamental process during brain development, and in higher functions like learning and memory (Bliss et al., 2014).

Excitatory synapses are named after their ability to initiate a depolarizing current in the postsynaptic cells, 'exciting' the neuron by increasing the likelihood to reach its depolarizing threshold and fire an action potential. Although there are many types of excitatory synapse in the brain, by far the most common are those that respond to the neurotransmitter glutamate, termed glutamatergic synapses. There are three main classes of ion channel (ionotropic channels) sensitive to glutamate at these synapses: AMPA, Kainate and NMDA receptors, which are named after their sensitivity to these respective ligands. When activated by glutamate binding, these channels open allowing influx of cations (Na^+ or Ca^{2+}). Additionally, excitatory synapses also contain metabotropic glutamate receptors that are also activated by extracellular glutamate but switch on a diverse range of G-protein coupled intracellular signaling pathways to transmit information. The composition, ratios and stability of these receptors at the post-synapse shapes neuronal excitation. As shall be discussed, the form and function of excitatory synapses is a tightly regulated process.

1.2.4.1 Dendritic spine formation and actin dynamics

A key feature of excitatory synapses is that their preferentially localisation to specialized protrusions from the dendritic arbor called dendritic spines (spines from now on). First observed over 100 years ago by the elegant drawings of Ramon y Cajal, spines were shown by EM to be the location of the excitatory postsynaptic density (PSD) – the name given to the electron-dense postsynaptic clustering of neurotransmitter receptors and associated proteins (Dhawale and Bhalla, 2008; Gray,

1959). A single hippocampal neuron can contain thousands of spines across its dendritic arbor. The localisation of excitatory inputs at spines isolate these signals from the rest of the cell and enables exquisite control of synaptic transmission. Modern imaging has revealed spines to be highly dynamic, growing and shrinking in response to changing in network activity or single inputs. Despite this fluidity, during development spines undergo a gradual sterotyped change in both shape and stability that correlates with establishment of mature networks (Bourne and Harris, 2008). In addition, abnormal numbers or morphology of spines is a pervasive phenotype in neuropsychiatric diseases. Thus, spines have become a focus of attention for both basic and clinical neuroscience.

Substantial evidence suggests that dendritic spines form from the stabilisation of filopodia-like processes extending from the dendritic arbor. During early postnatal development, hippocampal neurons are dotted with a high number of dynamic, filopodial protrusions (Dailey and Smith, 1996). The molecular composition of dendritic filopodia (DF) are similar to that of the conventional filopodia, although there are some key differences. Fascin is absent in DFs whereas myosin-II and α-actinin seem to be the major actin bundling proteins in the shaft. Perhaps surprisingly, Arp2/3 are present within the shaft and the base of DFs where it seems to provide a base of branched actin from which unbranched AFs form (Korobova and Svitkina, 2010). Despite this, Arp2/3 is not required for DF formation and knockout of the complex actually leads to increased density of DFs early in development (Spence et al., 2016). The tips of filopodia are marked by the presence of mDia2 and capping protein, both of which promotes DF formation (Hotulainen et al., 2009; Korobova and Svitkina, 2010).

Interestingly, the number of DFs is regulated by neuronal activity; silencing synaptic transmission with TTX increases DF density and length, and local uncaging of glutamate is sufficient to induce DF formation (Hotulainen and Hoogenraad, 2010; Portera-Cailliau et al., 2003). It is currently poorly understood how extracellular glutamate is linked to DF formation. One important pathway is local intracellular

calcium signalling via NMDAR or mGluR activation, which can switch on actin remodelling via calcium-dependent phosphorylation of RhoGTPase GEFs and GAPs (Penzes et al., 2011).

Over the course of development dendrites undergo a morphological transition from unstable, filopodial spines to stable, mature spines. Stabilisation of spines requires both pre and postsynaptic elements but postsynaptic maturation is driven by changes in actin dynamics. EM images of spine heads show actin is highly branched, lamellipodia-like network and Arp2/3 is enriched in spine heads (Hotulainen et al., 2009; Korobova and Svitkina, 2010). Thus even though Arp2/3 knockout increases DF formation, inhibition or knockout of Arp2/3 or components of the WRC reduces the number of mature spines (de Rubeis et al., 2013; Soderling et al., 2007; Spence et al., 2016). Increased spine head size is also associated with an increase in F-actin/G-actin ratio, suggesting that Arp2/3 generation of new barbed ends leads to increased incorporation of monomeric actin in AFs (Okamoto et al., 2004). The redistribution of profilin to spine heads further promotes this elongation activity. Actin contractility also shapes spine head formation; myosin II relocates from the neck to the head during maturation and both activation and inhibition of myosin II alters spine morphology (Hotulainen and Hoogenraad, 2010; Tatavarty et al., 2012).

In addition to these familiar ABPs, proteins with specific functions in spines have been identified. These include AF binding proteins neurabin I, spinophilin and Drebrin A (Sala and Segal, 2014). Drebrin A is specifically localised to spine heads where it inhibits AF bindings of myosin II, α-actinin, and overexpression *in vitro* increases spine length and instability (Ivanov et al., 2009; Sala and Segal, 2014). Spines are also enriched in a host of GEFs and GAPs for Rac1, cdc42 and RhoA that link intracellular signalling cascades to actin remodelling.

Imaging studies of spines have converged on four main spine morphologies seen in the adult brain; filopodia-like, long/thin, mushroom and stubby (Fig 1.6). The former two are considered immature whereas mushroom and stubby spines are mature. There is substantial evidence that this maturity reflects increased

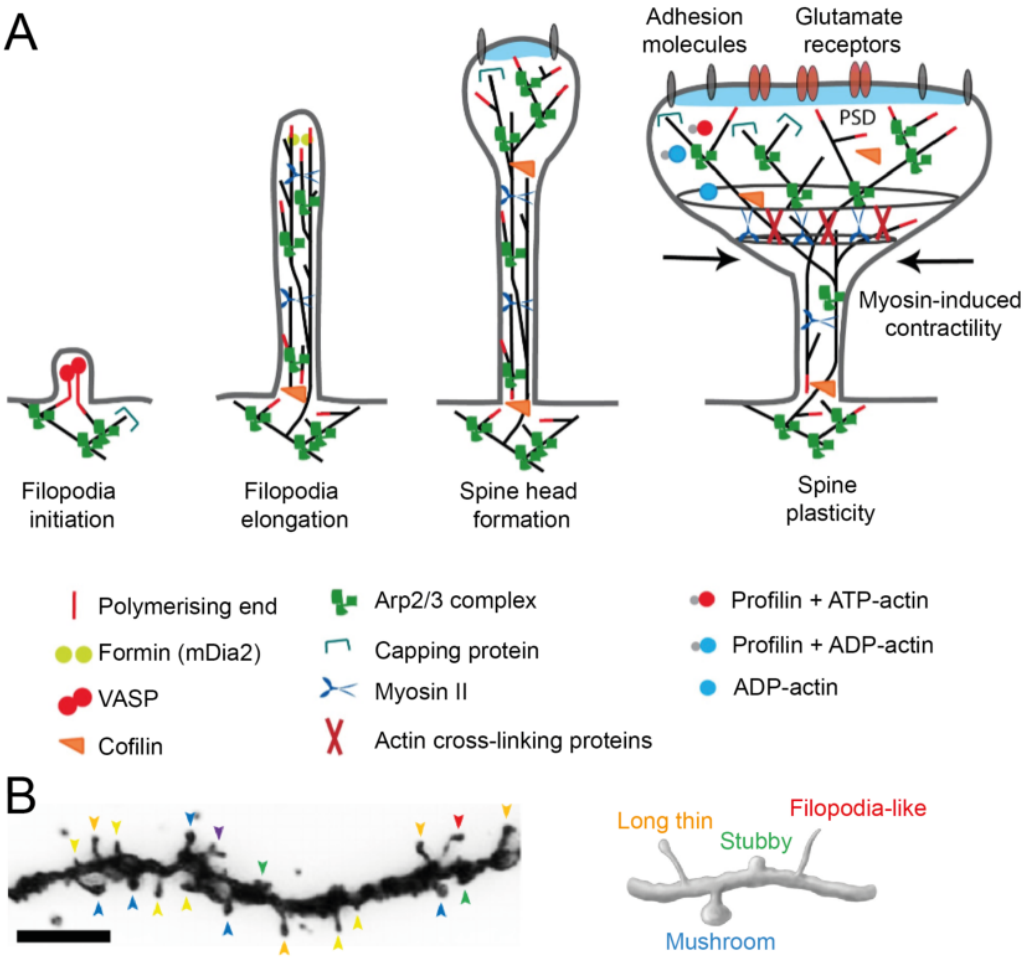

Fig. 1.6: The formation and morphology of dendritic spines
A: Actin dynamics underlying dendritic filopodia formation and spine maturation. Formins and barbed-end binding protins promote the formation of filopodia that are stabilised by actin bundling. Arp2/3 activity in the spine head drives expansion of a branched network that facilitates growth of the PSD. **B:** Left panel shows Golgi-Cox stained dendrite with spines of different morphologies dotted along the shaft. Right panel shows a graphical illustration of the stereotypical morphologies. From (Hotulainen and Hoogenraad, 2010; Risher et al., 2014).

functionality of synapses on these spines. Mature spines have increased in surface AMPA receptors in the spine head, sensitivity to glutamate and increased width of the PSD (Cingolani and Goda, 2008). Spine head size also correlates with synaptic efficacy changes induced during synaptic plasticity protocols such as LTD and LTP, which reduce and increase head size respectively. Further, spine growth has been shown to precede PSD formation supporting a causative link between the two (Knott et al., 2006). Actin dynamics regulate the process by 1) increasing the head width to facilitate more receptors 2) stabilising AMPA receptors at the PSD by linking to the cytoskeleton and 3) controlling the recycling and trafficking of AMPA receptors to and from the PSD (Cingolani and Goda, 2008). Although a consistent general rule, it is worth noting that exceptions have been identified. For instance, in the amygdala different spine types segregate the input from cortical or thalamic sources rather than determining synaptic efficacy *per se* (Humeau et al., 2005).

1.2.4.2 Composition and regulation of the PSD

The PSD is a dynamic macromolecular complex composed of hundreds of proteins, many of which have well-established roles in synaptic transmission. As mentioned, in addition to AMPARs the PSD contains NMDARs and mGluRs, specifically group I mGluR1 and 5. In fact, mGluRs act in part by regulating NMDAR activity and are colocalised at PSDs (Tu et al., 1999). These receptors are stabilised at the PSD by scaffolding proteins. The most common of these, indeed the most abundant PSD protein identified, is PSD95 (Chen et al., 2011). PSD95 binds both directly (e.g. via PDZ domains of NMDARs) or indirectly (e.g. via adapters proteins called TARPs for AMPARs) to receptors. Other important scaffold molecules include the Shank proteins (SHANK1-3), Homer (HOMER1-3) and GKAP. These proteins interact to form a complex that links receptors to one another, primarily via PDZ domains. As such, these proteins, in particular PSD95, have all been implicated in synaptic plasticity and stabilisation. Interestingly, overexpression of PSD95 occludes LTP but

enhances LTD, suggesting that scaffolds may prevent addition of new receptors but not loss of existing ones at the PSD (Stein et al., 2003).

Another important class of PSD proteins are adhesion molecules that mediate interaction between the PSD, the ECM and the presynaptic membrane. Adhesion proteins come in protein pairs that link to form trans-synaptic bridges. The best characterised of these are the neurexin-neuroligin family that are present on the pre- and postsynaptic membrane respectively. Humans and mice have four neuroligin (NLGN) genes and three neurexins (NRXN), though only 1 and 3 (partially) localise to excitatory synapses; NLGN2 is inhibitory and NLGN4 is primarily glycinergic (Südhof, 2008). NLGN-NRXN contacts have been suggested to be important for the stabilisation of dendritic filopodia apposed to presynaptic contacts, and NLGN-PSD clusters are seen in nascent spines prior to recruitment of AMPARs. However, although neuroligin 1-3 triple knockout mice die soon after birth of respiratory failure, brain stem respiratory centres show normal spine densities but impaired transmission suggesting that their primary function is in synapse maturation (Varoqueaux et al., 2006). Other classes of adhesion molecules include Synaptic Adhesion-Like Molecules (SALMs), EphB-Ephrins, N-cadherin and NCAMs (Sheng and Kim, 2011).

The dynamic nature of the PSD is driven largely by cytoplasmic signalling molecules; kinases, phosphatases and RhoGTPase-associated proteins make up around 20% of the PSD (Sheng and Kim, 2014). These have a range of functions in regulating receptor activity and localisation, actin remodelling, and others. The calcium-sensitive kinase αCaMKII is particularly abundant and is used for 1) linking NMDAR Ca2+ influx to AMPAR exocytosis and 2) recruitment of the proteasome to the PSD for protein turnover (Jarome et al. 2013). Rac1, cdc42 and RhoA are all implicated in spine morphogenesis and RhoGEFs have emerged as key regulators of their activity at the postsynapse (Tashiro and Yuste, 2004). Kalirin-7 is a GEF for all three classical RhoGTPases, binds to the PSD95, promotes spine formation and is linked to NMDAR-dependent plasticity via CaMKII phosphorylation (Sala

and Segal, 2014). αPIX, βPIX and Tiam1 are Rac1/cdc42-specific GEFs also implicated in NMDAR-dependent plasticity. BDNF-induced long term potentiation (LTP) activates Vav-dependent Rac1-GTP production downstream of TrkB receptors that is critical for spine head enlargement (Hale et al. 2011). Relevant RhoGAPs have also been identified, including SRGAP2 and RhoGAP2. Although a broad picture emerges that Rac1/cdc42 activity promotes spine growth and maturation, there are clearly context-dependent exceptions to this rule.

The relevant downstream effects of RhoGTPase activation at spines remains incompletely understood, but clearly involve actin remodelling. P21-activated kinases (PAKs) are also important. Interestingly, αPIX, PAK3 and the scaffold protein GIT1 form a functional complex in spines that regulates spine formation. Thus, signalling molecules link receptor activity to downstream cellular processes including actin remodelling, protein synthesis, and vesicular trafficking that are critical for the maturation and plasticity of spines.

1.2.4.3 Spine changes during development

The density and maturity of spines changes dramatically during development. Although the precise timings depend on lifespan, the pattern is consistent across mammalian species. Concretely, neonatal dendrites have few DFs that rapidly expand in number during early postnatal life. During adolescence and early adulthood these spines mature or are eliminated (or pruned) such that there is an overall reduction in spine density that plateaus in adulthood, when there is a low rate of matched formation and elimination of spines (Chen et al., 2014b). The cellular processes mediating this loss of synapses are complex and still being uncovered. In general, mature spines seem to be less vulnerable to elimination which has supported the theory that pruning involves the refinement of connections in the brain, strengthening established connections and removing weaker ones. In sensory areas, loss of external stimuli (e.g. by whisker trimming or ocular deprivation) limits elimination and spine maturation (Chen et al., 2014b). A recent study in primary

somatosensory cortex showed that adjacent synapses on a dendritic shaft compete for the local pool of β-catenin that was required for catenin-cadherin adhesions, stabilising synapses and protecting them from elimination (Bian et al., 2015).

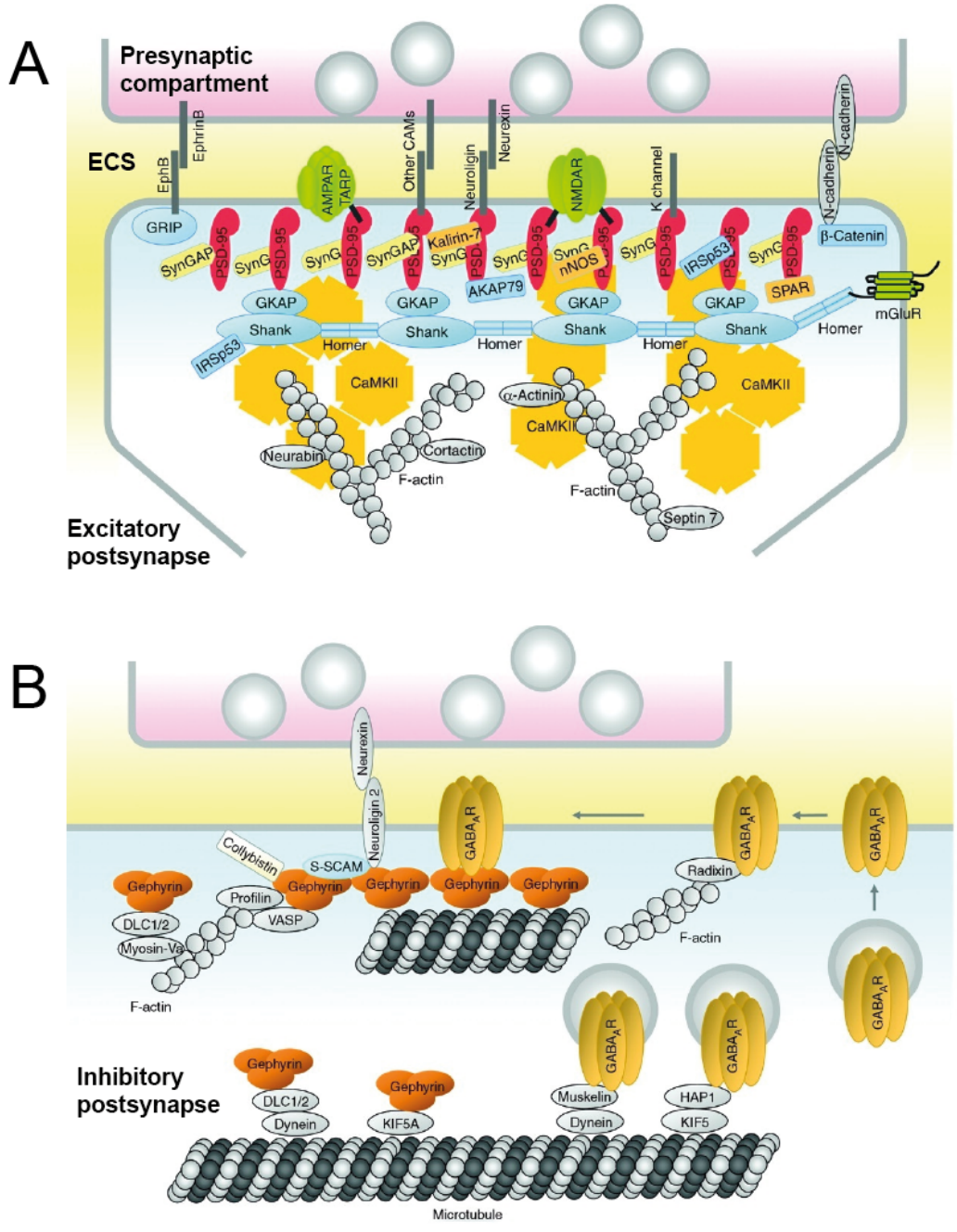

Fig. 1.7: Components of the excitatory and inhibitory postsynaptic density
A: The excitatory PSD. Scaffolding proteins like PSD95 link receptors to actin cytoskeleton via signalling molecules including CaMKII. Adhesion molecules from trans-synaptic stabilisation. **B:** The inhibitory PSD. The major scaffolding protein Gephyrin links GABA receptors to adhesion molecules and the cytoskeleton. From (Sheng and Kim, 2011).

Multiple lines of evidence suggest that as well as cell-autonomous loss of immature spines, glial cells play important roles in synaptic pruning during development and in adult learning. Astrocytes, the most numerous glial cells in the brain, release various molecules that regulate synaptic strength (Henneberger et al., 2010; Yu et al., 2013). In addition, astrocytes are capable of phagocytosing both axon inputs and spines. This has been best studied in visual system, where the astrocytic pruning of synapses is required for normal eye-segregation in the dorsal lateral geniculate nucleus (dLGN) (Neniskyte and Gross, 2017). Signalling proteins MEGF10 and APOE and the MERTK receptors are implicated in this process. Additionally, microglia have recently emerged as synpatic pruners. RGC synapses at P5 are decorated with complement cascade proteins C1q and C3 (Schafer et al., 2012). These proteins are classical opsins that are clearance signals to the innate immune system, and initiate the phagocytosis of these synapses. Microglia are also thought to phagocytose postsynaptic material in the adolescent hippocampus, and during synaptic loss associated with Alzheimer's disease (AD) (Hong and Stevens, 2016; Paolicelli et al., 2011). In addition, microglia also regulate adult spine plasticity during learning tasks, though this is through targeted release of BDNF (Parkhurst et al., 2013). Thus, spine changes during development involve an interplay between neurons and glia.

1.2.5 The inhibitory synapse

Inhibitory synapses hyperpolarise the postsynaptic cell, dampening down it's excitability and act in antagonism to excitatory inputs. The balance between excitation and inhibition (termed E/I balance) sets the overall activity output of neural networks, is critical for normal brain function and as such has been implicated in many neurodevelopmental and psychiatric disorders.

As discussed, inhibitory synapses share many core features of excitatory synapses. However, a key difference is that, rather from being isolated in dendritic spines,

inhibitory synapses preferentially form on the dendritic shaft and cell soma. This was recognised early via EM studies that identified 'symmetrical' synapses (type II), later confirmed to be sites of inhibition (Gray, 1959). The consequences for this include 1) inhibitory currents are less isolated and have a more direct impact of cellular membrane potential than via secondary messenger signalling and 2) the cytoskeletal structure of the inhibitory postsynapse is more simplistic. Whilst this has led to the general view that the inhibitory postsynapse is less intricate, it is emerging as a source of significant regulation and plasticity.

1.2.5.1 The iPSD; similarities and differences

The inhibitory postsynaptic density (iPSD) contain all the classes of protein seen at the PSD. The primary inhibitory neurotransmitter in the brain is γ-aminobutyric acid (GABA), itself a precursor to glutamate. Extracellular GABA is recognised by ionotropic and metabotropic receptors, grouped into the protein families $GABA_A$Rs and $GABA_B$Rs respectively. Activation of $GABA_A$Rs allow influx of chlorine ions when open that decreases membrane potential, whereas $GABA_B$Rs are coupled to Gi/Go signalling pathways. $GABA_A$Rs have 18 subunits in mammals, split into 8 subgroups that can combine in different combinations to generate functional diversity of channel dynamics. The majority of synaptic GABAaR subtypes are composed of two $\alpha 1$, $\alpha 2$ or $\alpha 3$ subunits, together with two $\beta 2$ or $\beta 3$ subunits and one $\gamma 2$ subunit. Indeed, the $\gamma 2$ subunit is required for postsynaptic clustering of these receptors (Essrich et al., 1998). In contrast, extracellular $GABA_A$Rs have different compositions and mediate tonic inhibition to neurons. In the spinal cord, brainstem and retina, glycinergic synapses containing chlorine-permissible glycine receptors are the major source of inhibition.

One scaffold protein, gephyrin, has emerged as a critical component of the iPSD. Gephyrin is a 93kDa protein that auto-aggregates under suitable conditions to form a lattice-like structure that forms the basis of the iPSD (Tyagarajan and Fritschy, 2014). GlyRs and, to a much lesser extent $GABA_A$Rs, interact with Gephyrin and

promotes their clustering at postsynaptic sites, though this doesn't occur via PDZ domains as is often the case in the excitatory PSD. Gephyrin also interacts with inhibitory adhesion molecules. Recognised inhibitory adhesion molecules include NLGN2, NLGN3 (which is also present at excitatory postsynapse), Slitrk3 and the glycosylphosphatidylinositol anchor proteins MDGA1 and MDGA2 (Takahashi et al., 2012; Tyagarajan and Fritschy, 2014). These proteins have all been implicated in inhibitory synapse formation or maintenance, though often have brain-region specific effects. Interestingly, although OE of NLGN2 increases inhibitory clusters, NLGN2 knockout still form functional GABAergic synapses, although inhibition is decreased in a subset of interneurons in the cerebral cortex (Gibson et al., 2009). A triple knockout of NLGN1-3 in mice leads to severe defects in GABAergic and glycinergic transmission (Varoqueaux et al., 2006).

Another key gephyrin interactor is the cdc42 GEF collybistin (encoded by Arhgef9). Collybistin helps localise Gephyrin to the plasma membrane and is present at the iPSD; loss of collybistin reduces the clustering of gephyrin and $GABA_A$Rs in the hippocampus and led to reduced inhibitory transmission and behavioural deficits such as social anxiety and impaired spatial learning (Papadopoulos et al., 2007). Mutations in Arhgef9 are a rare cause of X-linked mental retardation (XLMR), characterised by seizures, anxiety and aggressive behaviour (Harvey et al., 2004, 2008). Whether collybistin function is linked to cdc42-mediated regulation of actin is less clear. Indeed, it has been suggested that collybistin acts via PI3K-Akt-GSK3β to alter phosphorylation of Gephyrin, which has been shown to alter clustering (Tyagarajan and Fritschy, 2014). Gephyrin binds with several ABPs, including profilin, Mena and G-actin. However, blocking actin polymerisation of mature neuronal cultures did not effect Gephyrin clustering (Bausen et al., 2006). Thus, whether AFs play a role in stabilisation of the iPSD remain unclear.

One well-established aspect of iPSD function that relies on the cytoskeleton is intracellular trafficking of $GABA_A$Rs, which is important for basic GABAergic

transmission as well as synaptic plasticity. Newly synthesised $GABA_A$Rs are trafficked to the iPSD via the secretory pathway, in coordination with specific proteins such as BIG2, that facilitates exit of $GABA_A$Rs from the Golgi (Charych et al., 2004). MT-dependent trafficking is mediated by interactions with the kinesin motor KIF5A, which can interact with GABAaRs via adapters GABARAP and HAP1 (Nakajima et al., 2012; Twelvetrees et al., 2010). Once at the membrane, $GABA_A$Rs can move laterally in and out of synapses and be endocytosed for degradation to recycling to synapses (Arancibia-Cárcamo et al., 2009; Twelvetrees et al., 2010).

1.2.6 Neuropsychiatric diseases: convergent cellular and molecular pathways

The genetics of many neurodevelopmental and neuropsychiatric conditions, including autistic spectrum disorders (ASDs), schizophrenia (SCZ) and intellectual disabilities (IDs), are complex and involve small contributions from a many different genes. These genetic biases, in combination with environmental/lifestyle factors, combine to increase the likelihood of an individual presenting with clinical symptoms. Additionally, there are several different types of genetic lesion that can be associated with clinical conditions. These include: single nucleotide polymorphisms (SNPs), which can occur at high frequencies in the population; rare variant mutations, which are uncommon and can arise either de novo or through germline transmission; copy number variations (CNVs) of whole sections of chromosome (duplications or deletions) and affecting multiple genes. Further, at the protein level, these changes can lead to changes in expression, localisation, and loss or gain of function.

Despite this complexity, understanding the genetics of neuropsychiatric diseases is critical to improving our knowledge of the underlying cellular processes and molecular substrates that go awry. As shall be discussed, whilst different conditions

have unique characteristics, they often converge on common pathways that highlight their generalised importance in brain function. Three neuropsychiatric diseases particularly relevant to this thesis will be discussed presently.

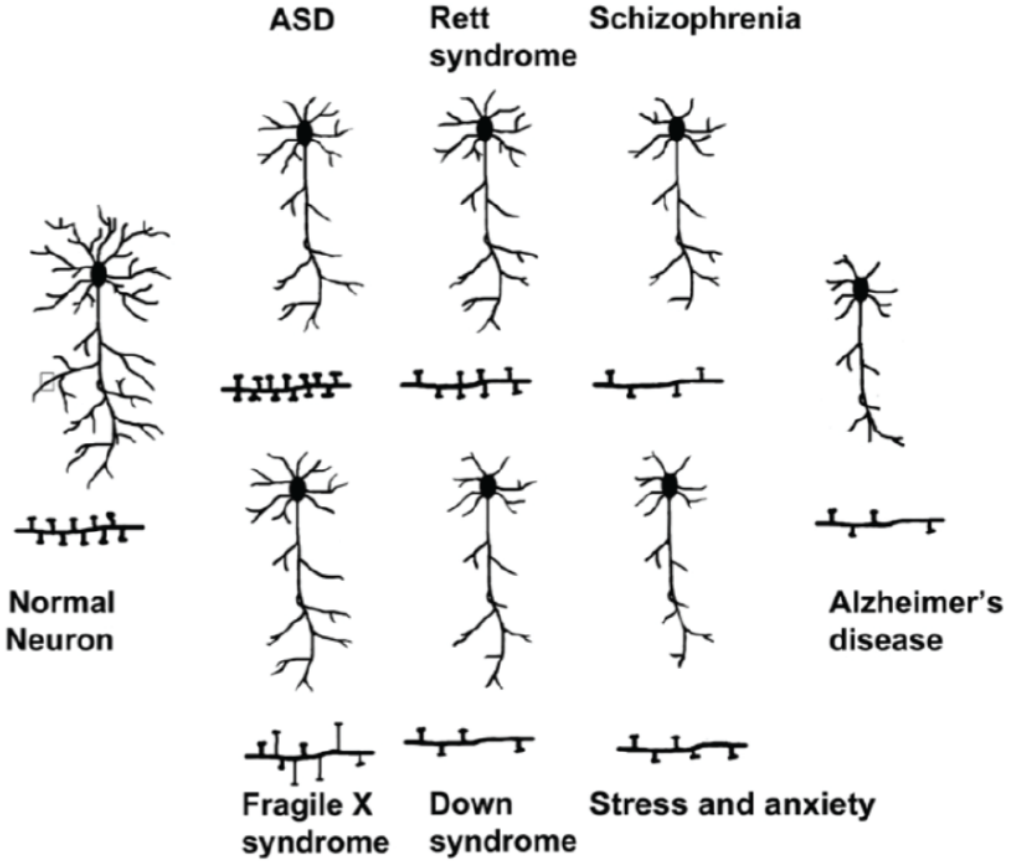

Fig. 1.8: Abnormalities in neuronal morphology associated with neuropsychiatric disease
Schematic representation of neuron depicting changes in dendrite morphology and spines patients with various neuropsychiatric disorders. Autism spectrum disorder (ASD): decreased dendrite branching and higher spine density than normal is observed. Rett syndrome: reduced dendrite branching. Schizophrenia: neurons have reduced dendritic arbor and spine density. Alzheimer's disease (AD): dramatic atrophy of the dendritic arbor and massive loss of synapses. Fragile X syndrome (FXS): Neurons in FXS patients have high densities of long, immature spines. Down syndrome (DS): reduction in dendrite branching and length and spine density is reported in adults with DS. Stress and anxiety: humans and animal models with chronic stress and anxiety have decreased dendrites and spine density have been observed in the hippocampus. From (Kulkarni and Firestein, 2012)

1.2.6.1 Fragile X Syndrome

Fragile X syndrome (FXS) is a monogenetic disorder caused by loss of functional expression of Fragile X Mental Retardation Protein (FMRP). In the majority of cases, this is caused by an expansion of a CGG repeat region (typically over 800 repeats) in the 5' untranslated regin (UTR) of the FMR1 gene that leads to hypermethylation of the region and transcriptional silencing of FMRP expression (Bagni and Greenough, 2005). Rare cases of point mutations in the FMR1 gene have also been identified, such as the I304N mutation, which also lead to severe FXS (Feng et al., 1997). FXS is of particular interest for two reasons: 1) it is the most frequent inherited form of mental retardation and is the single greatest risk factor for ASD currently known; 2) as a monogenetic disorder it provides researchers with an extremely useful model for which to understand both FXS and related disorders. Clinically, FXS is characterised by varying degrees of cognitive impairment, physical abnormalities, attention deficit, autistic behaviour and childhood seizures (Comery et al., 1997; Penagarikano et al., 2007). Post-mortem studies have identified major spine abnormalities in FXS brains; spine density is increased and spines have more immature morphologies, a phenotype also seen in the FXS mouse model (Comery et al., 1997; Hinton et al., 1991).

FMRP is an mRNA-binding protein that is widely expressed but particularly present in the brain. It's KH and RGC-box domains appear to be particularly important for RNA binding, and preferentially recognise G-quartet structures present of target mRNAs. However, FMRP is reported to bind almost 4% of the mRNAs present in the mammalian brain, suggesting that it associates fairly unselectively and disruption could impact of a large number of cellular processes (Bagni and Greenough, 2005). Binding of FMRP to mRNA has been implicated in mRNA trafficking, localisation and stability. However, the best characterised is as a repressor of translation. In models of FXS, FMRP target mRNAs are more associated with polyribosomes and protein expression levels are increased, including αCaMKII, MAP1B, PSD95, and Arc/Ar3.1 (Brown et al., 2004; Zalfa et al., 2003). Further, a large screen of proteins from purified synaptosomes in the FXS mouse revealed

altered expression in over 100 synaptic proteins (Darnell et al., 2011; Liao et al., 2008). Thus, the emerging picture is that loss of FMRP alters dendritic and synpatic mRNA localisation and translation, leading to synapse dysfunction. It is worth noting here that CYFIP1 is a key FMRP-interactor that facilitates translational repression via it's actions as a 4E-binding protein. This is discussed in more detail in section 1.4.

Further evidence for hypertranslation comes from the observation that mGluR-dependent long-term depression (LTD) is enhanced in FXS mice (Gantois et al., 2017). In wild-type, mGluR activation can initiate internalisation of AMPARs via initiating increased Arc expression. In contrast, FXS tissue has basally increased Arc expression and this appears to drive an enhanced response that does not require additional protein synthesis. Additional FMRP-binding proteins such as MAP1B and APP could also be affected similarly. However, there have also been reports of decreased protein expression in the FXS, including several $GABA_AR$ subunits (D'Hulst et al., 2006). Interestingly, the δ subunit was shown to be trafficked to the dendrite in response to mGluR activation in wildtype but not FMRP knockout neurons (Dictenberg et al., 2008). Thus, altered inhibition may also contribute to FXS pathology.

1.2.6.2 Autistic spectrum disorders

ASD is a term given to the broad spectrum of neurodevelopmental disorders characterised atypical social behaviors, impaired verbal and non-verbal communication and patterns of obsessive and repetitive behaviors that typically present before the age of 3 (Geschwind and Levitt, 2007). ASDs affect between 1-2% of the population, although they are found at much higher frequencies as comorbid with other conditions. Morphological studies found increased head size for autistic cases and specific enlargements of the hippocampus and amygdala have been reported (Kulkarni and Firestein, 2012). In addition, differential alterations in neuronal densities has been observed; increased density of cortical minicolumns,

decreased density of layer III neurons in the fusiform gyrus, aberrant organisation of the prefrontal cortex (Chen et al., 2015). At the cellular level, ASDs are associated with decreases in dendritic branching in the hippocampus and increased spine density in subregions of the hippocampus and layer II of cerebral cortex (Hutsler and Zhang, 2010; Raymond et al., 1996). Thus, a current theory of the cellular basis of ASDs involves a mismatch in connectivity that favours short-range communication at the expense of long range connectivity (Geschwind and Levitt, 2007).

In contrast to FXS, the phenotypic variability in ASDs is matched with equally varied and complex genetics. ASDs are highly heritable and a child has between 25-100 fold increased risk if a parent is autistic. As mentioned, autism is comorbid with several monogenetic conditions (termed 'syndromic autism'), including FXS (FMRP), Rett's syndrome (MECP2) and tuberous sclerosis complex disorders (TSC1/2) (Chen et al., 2015). Additionally, CNVs of multigene regions have been associated with ASDs. However, together these sources may represent up to 20% of total ASD cases, suggesting that a major genetic contribution to ASDs comes from a large number of nominally insignificant common variants, or SNPs. Due to their low penetrance, identification of these SNPs and their associated genes is extremely challenging and requires large cohort sizes. As a result, to date very few common variants have been identified that reach genome-wide significance. This has led to a focus on identifying inherited or *de novo* mutations that are extremely rare and therefore can be more easily identified as being enriched in ASD cases. This strategy has led to numerous risk genes being identified. Although the relevance of these genes and other are still being uncovered, there is a clear convergence onto a set of functional groups that include E/I balance (FMR1, CNTNAP2, NLGN3, SHANK3), synaptic function (NLGN3, NLGN4, SHANK3, GRIN2A/B, GRIK2/3, CYFIP1), cell adhesion (NLGN3, NLGN4, PCDH9, CNTN4/6) and transcriptional regulation (PTEN, TSC1/2, CYFIP1, MET, UBE3A).

1.2.6.3 Schizophrenia

Schizophrenia is a heterogenous condition characterised by altered perceptions of reality, cognition and thought that presents later in development than ASDs, typically in late adolescence and early adulthood. SCZ affects between 0.5-1% of the population and, like ASDs, showed significant heritability estimated at 80% (Hilker et al., 2018). The neuropathology of SCZ is better defined than ASDs. A defining feature is accelerated grey matter loss in the adolescent period in which synaptic connections are being refined (Moyer et al., 2015; Penzes et al., 2011). Indeed, numerous postmortem studies have shown that abnormal reductions in spine density across brain regions correlate with grey matter loss. The dorsolateral prefrontal cortex (DLPFC) and temporal lobe regions appear particularly affected, with significant spine loss and reduced functional activity observed in these areas (Penzes et al., 2011; Sweet et al., 2009; Yoshida et al., 2009). Further, spine defects are layer-specific, particularly affecting layer III, that undergo more extensive pruning that deeper layers during this period of development. This is supported by lack of evidence of change in cell numbers or gross axonal defects in SCZ (Selemon et al., 1998).

As expected from this pathology, research into the etiology of SCZ has identified genes that regulate synapse formation (NRXN1, NRG1, PCDH10, CACNB4), synapse maturity (DISC, NRXN1, NRG1, ErbB4) and dendritic morphology (DISC, GRIN2A) as risk genes (Penzes et al., 2011). There has been significant progress made by large cohort studies that have enabled common as well as rare variants to be identified, including GRIN2A and the trophic factor NRG1, which regulates spine formation through interactions with postsynaptic ErbB receptor tyrosine kinases (Mei and Xiong, 2008). Indeed, the largest genome-wide association study (GWAS) investigating any neuropsychiatric disease to date identified 83 novel risk alleles (Schizophrenia Working Group of the Psychiatric Genomics Consortium, 2014). Interestingly, disruptions to cytoskeletal-associated proteins have been another fruitful area of research. Hill et al. reported reduced mRNA expression levels of cdc42, Debrin A, Rac1 and kalirin-7 in DLPFC from SCZ patients (Hill

et al., 2006). In addition, rare coding variants for Kalarin-7 and IRSp53 are associated with SCZ (Moyer et al., 2015; Purcell et al., 2014; Russell et al., 2014). *In vitro* studies of mutant Rac1 GEF, kalirin-7, showed impaired activation of Rac1 and downstream increases in spine size and density (Russell et al., 2014). IRSp53 link NMDAR signalling to actin remodelling, particularly interesting given the importance of NMDAR dysfunction in SCZ (Kang et al., 2016).

Finally, there is accumulating evidence of immune dysfunction in SCZ. Two major genetic associations with SCZ, the major histocompatibility complex (MHC) and the complement cascade protein C4, are core immune genes (Rees et al., 2015; Sekar et al., 2016). The association with the complement cascade is particularly interesting given recent evidence for complement mediated synaptic pruning at developmental time windows relevant to SCZ (Paolicelli et al., 2011; Schafer et al., 2012). In addition, other SCZ-associated genes such as Dysbindin-1 have recently been shown to have roles in regulating immune activation in the brain (Al-Shammari et al., 2018). Despite significant variability in reports, there is growing evidence for altered cytokine levels in SCZ patients (Stuart et al., 2014). Common patterns include increased levels of CXCL8 and CCL2, whereas others such as CXCL12 are reduced.

1.3 Microglia and their emerging roles in brain development

Microglia are the brains resident immune cell population. In the adult brain they appear as small, highly ramified cells that occupy the parenchyma in distinct spatial niches. Importantly, they have recently emerged as an important cellular substrate for understanding brain development and dysfunction.

1.3.1 Origins and behaviours of microglia

Microglia are unique in comparison to other glia (and indeed neurons) in that they do not originate from the neuroectoderm, but instead from a distinct lineage of ethyromyeloid progenitors (EMPs) in the embryonic yolk sac. They infiltrate the primitive brain early on in development, at E9.5, and rapidly proliferate and migrate within the parenchyma to pattern the entire brain (Ginhoux et al., 2010; Kierdorf et al., 2013; Prinz and Priller, 2014; Tay et al., 2017). Once established, microglia still retain proliferative potential and turnover slowly with an average lifespan of a few weeks in mice and 9 years in humans, though this is a topic of continued debate (Réu et al., 2017; Tay et al., 2017). Although the signalling driving this turnover remains to be fully elucidated, certain factors (e.g. colony stimulating factor) are critical for microglial survival throughout their lifespan (Elmore et al., 2014).

For many decades, microglia have been viewed solely as the innate immune defence of the CNS that became 'active' in response to numerous cues, including viral infection and brain trauma (Streit et al., 1988). Upon activation, microglia undergo dramatic change from ramified to amoeboid morphology that is coupled with changes in their transcriptional profile (Sousa et al., 2018). These changes are critical for microglia to act as 'first responders' to damage, though there is growing evidence that they can also lead to deleterious affects on brain function and disease progression (Salter and Stevens, 2017).

Pioneering imaging studies in the early 2000s of microglia *in vivo* showed that 'resting' microglia (ramified) are incredibly motile, extending and retracting their processes into the surroundings to sample the entire parenchyma every few hours (Davalos et al., 2005; Nimmerjahn et al., 2005). The realisation that microglia are highly dynamic at rest has opened up new avenues of research over the last decade unveiling novel functions that microglia play outside of immune defence and damage response.

1.3.2 Microglia-neuron interactions

Microglia shape brain development in numerous ways. Depletion of microglia from the embryonic brain alters cellular composition of neocortex, with defects in interneuron migration and increases in apoptosis of layer V principle neurons reported (Squarzoni et al., 2014; Ueno et al., 2013). In the dentate gyrus, where neurogenesis continues into adolescence, microglia help regulate the number of neuronal progenitor cells (NPCs) via apoptosis-coupled phagocytosis (Sierra et al., 2010). Microglia also modulate long-distance connectivity; microglial-depletion leads to aberrant projections of dopaminergic axons into the striatum, and are required for normal fasciculation of axons in the corpus callosum (Pont-Lezica et al., 2014; Squarzoni et al., 2014).

One of their most intriguing behaviours is their ability to 'prune' synapses. Microglia engulf synaptic material in the developing hippocampus and disrupting this process increases spine density and excitatory transmission at critical periods during brain development (Paolicelli et al., 2011; Weinhard et al., 2018). To do this, microglia take advantage of the complement signalling cascade, an innate immune response pathway, to 'tag' synapses for pruning, as part of normal network refinement during development and disease states (Bialas and Stevens, 2013; Hong and Stevens, 2016; Presumey et al., 2017; Schafer et al., 2012). Recently, this signalling pathway has been expanded to include the 'don't eat me' signal, CD47-SIRPα, that protects synapses from pruning (Lehrman et al., 2018). Defective microglial pruning is associated with impaired functional connectivity and altered social behaviours (Kim et al., 2014; Zhang et al., 2014a).

Interestingly, as well as pruning synapses, microglia can induce synapse formation. Co-culture of neurons with microglia increases spine density and a microglial BDNF signalling is required for learning-dependent synapse formation in adult motor cortex (Lenz et al., 2013; Lim et al., 2013; Parkhurst et al., 2013). Additionally, physical contact of microglial processes can induce filopodia

formation on dendrites (Miyamoto et al., 2016). Thus, microglia help shape brain connectivity via a growing array of interactions with neurons.

1.3.3 Associations with neurological disorders

Dendritic spine abnormalities and altered network connectivity are hallmarks of many neuropsychiatric disorders, including autism and schizophrenia. The involvement of microglia in this process has ignited interest in the role they might play in the pathology of these conditions. Immune compromise has long been known to increase susceptibility to conditions including ASDs (Estes and McAllister, 2015). Further, peripheral levels of both pro- and anti-inflammatory cytokines are increased in ASD and SCZ patients, and transcriptomic analysis of postmortem brains shows increased cytokine expression (Radtke et al., 2017; Saetre et al., 2007). Thus immune compromise particularly during critical periods of development has long lasting effects on brain development that predisposes to neuropsychiatric conditions. Further, In mouse models of AD, where there is a dramatic loss of synaptic connectivity prior to clinical presentation, microglia have been shown to actively overprune complement-tagged synapses (Hong and Stevens, 2016).

Etiological studies have identified a number of immune-related genes as risk factors for these conditions. Early genetic studies found links between specific Human Leukocyte Antigen (HLA) haplotypes and risk of ASD (Careaga et al., 2010; Needleman and McAllister, 2012). A landmark GWAS study in 2016 identified the complement gene C4 as a risk factor for schizophrenia (Sekar et al., 2016). Given the established roles of the complement cascade in synaptic pruning by microglia, this hinted that these processes could underlie pathology in neuropsychiatric disorders. However, whether other known disease-associated genes have unidentified roles in regulating microglial function is largely unknown.

1.4 CYFIP proteins in health and disease

1.4.1 Evolutionary diversity of CYFIPs

CYFIP proteins are highly evolutionarily conserved, with homologs found across the eukaryotes including Arabodopsis, Drosophila, C.elegans, mouse and humans (Basu et al., 2004; Schenck et al., 2003, 2001). Non-vertebrate animals, such as Drosophila and C.elegans, have a single CYFIP gene identified as dCYFIP and GEX-2 respectively (Schenck et al., 2003; Soto et al., 2002). In contrast, model vertebrate systems, including humans, have two CYFIP paralogues; CYFIP1 and CYFIP2 (Pittman et al., 2010). Despite the lack of known structural domains, CYFIP sequence is fairly highly conserved throughout the tree of life. Human CYFIP1 and 2 share 98.7% and 99.9% sequence homology to their mouse orthologs, and both human CYFIP proteins are approximately 67% and 51% similar to fruit fly and worm orthologs (Schenck et al., 2001). Due to their independent discoveries in different species, CYFIP1/2 orthologs have been given a variety of names (CYFIP1: Sra1, GEX-2, KIAA0068; CYFIP2: PIR121, nev-2, KIAA1168). For clarity, these orthologs with be called CYFIP1 and 2 in the following discussion unless relevant, and CYFIP is used to refer to either protein interchangeably.

Comparing CYFIP paralogs shows they share 88% homology in humans. In the CNS, expression of CYFIPs is temporally regulated during development, with both CYFIPs increasing in expression in the mouse cortex between embyonic-adulthood (Bonaccorso et al., 2015). However, in the embryonic zebrafish retina CYFIP1 is expressed early on but rapidly decreases as CYFIP2 expression is turned on around 72 hours post fertilisation, suggesting that there could be local specificity in CYFIP expression (Cioni et al., 2018). To support this, cell-type transcriptomes show that brain cells tend to preferentially express one CYFIP (Zhang et al., 2014b). There is limited evidence for functional specificity at the molecular level between the

two proteins. This will be highlighted in the following discussion of the molecular functions of CYFIP.

1.4.2 Structure and molecular functions of CYFIP proteins

CYFIP proteins were first identified two decades ago through two independent protein binding screens searching for novel Rac1 and FMRP interactors (Kobayashi et al., 1998; Schenck et al., 2001). Amazingly, these two interactions still form the basis of our understanding of the molecular functions of CYFIPs. Research since then has shed light on the precise nature of CYFIP function within these different protein complexes, the inter-relationship between them, and what the wider implications are for the biology of the cell.

1.4.2.1 WAVE regulatory complex

As discussed in the previous section (see Arp2/3 and NPFs), the WAVE regulatory complex (WRC) is an important Arp2/3 NPF with critical roles in lammellipodia formation and cell migration. CYFIP is a constitutive member of the WRC, alongside WAVE, ABI, NAP and HPSC300. X-ray crystallography of a modified version of the WRC revealed that the full complex is formed from the binding of two subcomplexes composed of a CYFIP-NAP1 dimer and a WAVE-ABI-HSPC300 trimer, supporting protein pull-down experiments (Chen et al., 2010; Ismail et al., 2009). In its basal state, the WCA region of WAVE lines up against a concave surface formed between CYFIP and a 5-helices of WAVE, termed the ‘meander region’, that tightly binds the ‘W’ and ‘C’ domains, thus preventing actin or Arp2/3 binding.

CYFIP serves as the critical link between the WRC and it’s canonical activator, Rac1. Binding of Rac1-GTP to the WRC is CYFIP (and NAP1) dependent (Steffen et al., 2004). Although initial mutagenic studies suggested that Rac1 bound to a region adjacent to the CYFIP-meander region interface, a recent EM-crystallography

study of the Rac1-bound WRC infact revealed two binding sites for Rac1 (Chen et al., 2017, 2010). Both binding sites involve the CYFIP surface, one being the hypothesised site near the meander region (A-site) and the other on the other end of the rod-shaped CYFIP (D-site). Rac1 binds the D-site with approximately 40 times affinity of A-site, but both are capable of increasing Arp2/3 activity by the WRC. Both these interactions between Rac1 and CYFIP are predicted to disrupt the WCA binding pocket, thereby enabling WRC activation. This planar structure of CYFIP is supported by a FRET study showing that the N- and C-terminal domains of CYFIP are spatially separated in the WRC (de Rubeis et al., 2013).

It is worth noting that activation of the WRC requires additional signaling aside from Rac1-binding. WAVE proteins have a N-terminal WAVE-homology domain (WHD), followed by a basic region (BR) and proline-rich domain (PR), which is nearer the C-terminus (Mendoza, 2013). The BR of WAVE mediates binding to membrane phospholipids, primarily PIP_3 but also PIP_2 (Koronakis et al., 2011; Oikawa et al., 2004). $PIP_2/_3$-binding localises WRC to membranes and is required for lammelipodia-formation by WAVE (Lebensohn and Kirschner, 2009; Oikawa et al., 2004). Additionally, WAVE is phosphorylated at a number of key residues that modify WRC activation but do not affect the inherent ability of WAVE to activate Arp2/3 (Lebensohn and Kirschner, 2009). Tyr150 (Tyr151 on WAVE1 and 3) phosphorylation by Abl kinase disrupts the CYFIP-WAVE binding surface of WCA, helping to relieve WRC inhibition (Chen et al., 2010; Lebensohn and Kirschner, 2009). WAVE phosphorylation has also been shown via Src, cyclin-dependent kinases and ERK (Mendoza, 2013). Interestingly, the different WAVE paralogs do have unique phosphorylation sites and kinases; ABI1 is not required for Abl-mediated WAVE3 phosphorylation whereas it is for WAVE3 (Sossey-Alaoui et al., 2007). Alongside differential expression of WRC components, this level of regulation could support cell type-specific actin dynamics.

Additionally, WRC activity is localised and regulated by a growing number of protein interactions outside of the pentameric complex and Rac1. IRSp53 can bind

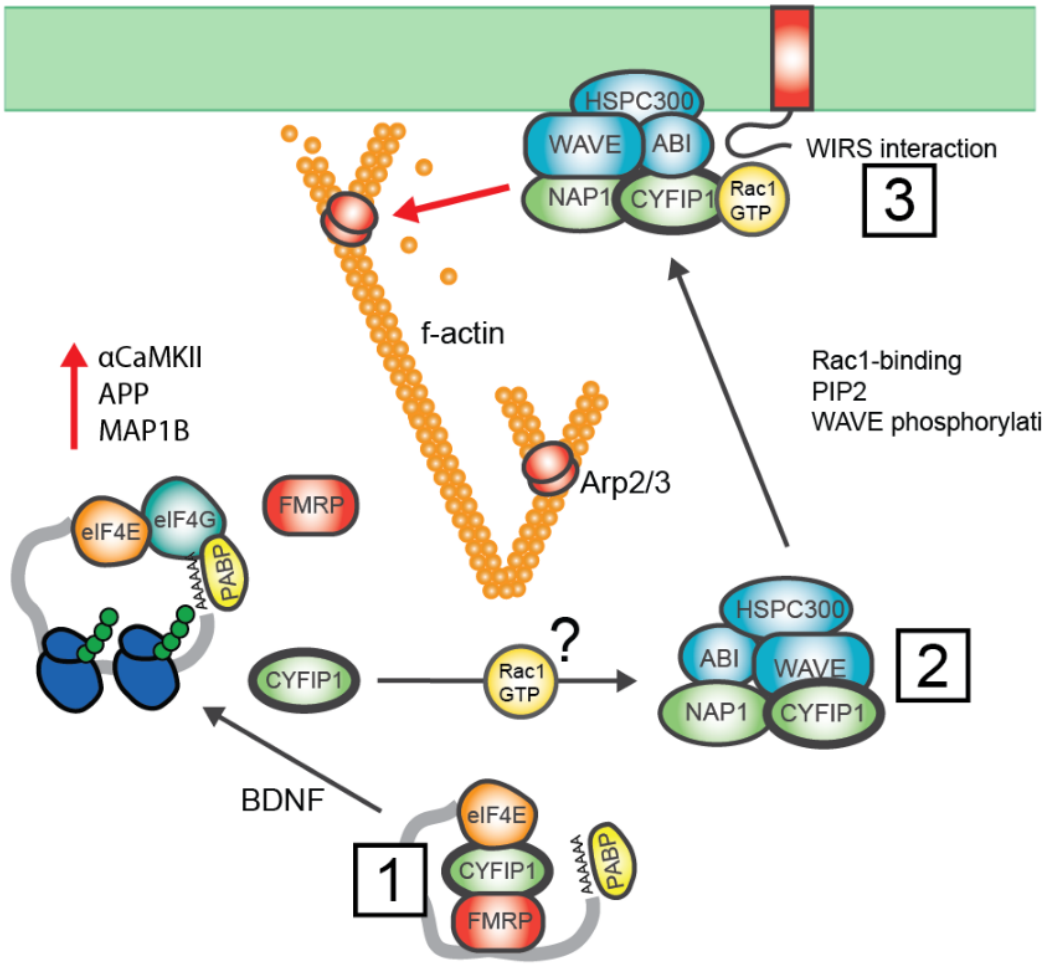

Fig. 1.9: The molecular functions of CYFIP1
CYFIP proteins exist in the cytoplasm as part of two complexes. (1) In association with FRMP, CYFIP1 represses translation of target mRNAs through disrupting the formation of the translational initiation complex. (2) CYFIP1 is a constitutive member of the WRC, a NPF for the actin branching complex Arp2/3. Transition between these complexes is mediated by Rac1-GTP, which also promotes activation of the WRC. (3) A binding surface between CYFIP1 and ABI interacts with various transmembrane receptors containing a WIRS motif.

to both WAVE (via SH3-PR domain interaction) and Rac1 (Miki et al., 2000). As mentioned prior, IRSp53 is activated by cdc42, thus representing a molecular bridge between Rac1 and cdc42 signalling pathways. Functionally, IRSp53 can regulate the formation of filopodia, lammellipodia (in multiple cell lines), but seems dispensable for phagocytosis and cell adhesion (Abou-Kheir et al., 2008; Miki et al., 2000; Suetsugu et al., 2006). Interestingly, IRSp53 is highly expressed by neurons in the brain and is associated with similar neuropsychiatric disorders to CYFIP, including schizophrenia and ASD (Kang et al., 2016). An immuno-EM study showed that IRSp53 is localised specifically to excitatory PSDs in the cortex, hippocampus and striatum, where it can interact with PSD proteins including Shank (Bockmann et al., 2002; Burette et al., 2014).

The pool of WRC-interactors has been greatly expanded by the identification of a WRC-binding motif that is present in a number of transmembrane proteins with diverse functions (Chen et al., 2014a). The loosely conserved motif named WIRS (F-x-T/S-F-X-X; F = preference for bulky hydrophobic residues; x = any residue; the X-X positions can accommodate single substitutions) binds a pocket in the WRC between CYFIP and ABI. The list of putative binding partners includes excitatory and inhibitory synapse receptors, synaptic scaffold proteins, ECM-binding proteins and others. Determining the relevance of these potential interactions could provide further insight into how local WRC activity regulates cellular function. Indeed, a recent study in Drosophila has shown that NLGN1-WRC interaction is required for actin remodeling at neuromuscular junctions (NMJs), and protocadherin-α interacts with the WRC via a WIRS motif to regulate cortical migration in mouse brain development (Fan et al., 2018; Xing et al., 2018). Thus, CYFIP is a core component of the WRC that plays a pivotal role in orchestrating the complexes interaction with other proteins, thereby determining the spatial and temporal dynamics of actin nucleation.

1.4.2.2 FMRP and translational repression

CYFIP proteins also interact strongly with Fragile X Mental Retardation Protein (FMRP) (Schenck et al., 2003, 2001). FMRP is an mRNA binding protein with roles in localization, stability and translation of target mRNAs (Bagni and Greenough, 2005). It is capable of binding to mRNA targets both via direct interaction or through RNA adaptors, such as BC1 (Zalfa et al., 2003). Screens for targets of FMRP have revealed that the protein binds a vast number of mRNAs that sum to roughly 4% of available mRNA pool (Ascano et al., 2012; Darnell et al., 2011). Although large in number, these targets are enriched in genes active at the pre- and postsynapse, and that have known associations with ASDs, ID and other neuropsychiatric conditions (Darnell et al., 2011). However, the precise functions and biological consequences of FMRP binding with mRNA is still incompletely understood.

A pioneering study by Napoli et al. revealed that CYFIP acts in coordination with FMRP to repress translation of FMRP-binding targets (Napoli et al., 2008). Cap-dependent translation involves the recruitment of eIF4A-eIF4G-eIF4E (eIF4F) complex to the 5' m7G cap (Richter and Sonenberg, 2005). When complexed with FMRP and mRNA, CYFIP interacts with eIF4E of the translational initiation complex. eIF4E-binding is a common and evolutionarily conserved mechanism of repressing translation, blocking the eIF4E-eIF4G interaction that is required for translational initiation (Richter and Sonenberg, 2005). Although most 4E-binding proteins (4E-BPs) controlling overall translational activity, others are tissue specific, such as Neuroguidin that is the only other known CNS 4E-BP (other than CYFIP) (Jung et al., 2006). Reduction in CYFIP1 expression in neurons increased expression of key FMRP targets, including αCAMKII, APP and ARC/Arg3.1 (Napoli et al., 2008). Further, a key synaptic pathology of FMRP loss, enhanced mGluR-dependent LTD, is also observed in haploinsufficient CYFIP1 mouse model (Bassell and Warren, 2008; Bozdagi et al., 2012). This effect is mediated via increased Arc-dependent AMPA receptor endocytosis via activation of the AP2-Clathrin pathway (Wall and

Corrêa, 2018). These studies point to a model where loss of either FMRP or CYFIP1 releives translational repression of key target mRNAs.

In neurons, the association of CYFIP with FMRP is activity-dependent. Treatment of cortical cultures with BDNF to stimulate the network leads to a decrease in association of CYFIP1 with eIF4E (Napoli et al., 2008). Interestingly, this seems to be mirrors by an increase in CYFIP1 integration into the WRC, and a structural change in CYFIP1 from a globular (FMRP-bound) to planar (WRC-bound) configuration (de Rubeis et al., 2013). This switch in CYFIP assembly appears to be dependent on Rac1 as NSC23766-treatment blocked this effect. In support of this, molecular dynamic modelling of the two CYFIP1 configurations suggests that Rac1 preferentially binds to the planar version (Di Marino et al., 2015). However, whether physical binding of Rac1 to CYFIP1 is responsible for this switch (in fact, molecular dynamics data argues against this) remains to be seen.

Interestingly, functional studies have provided evidence for CYFIP proteins and FRMP working in an antagonistic fashion. Early functional genetic experiments in flies showed that null mutants of dCYFIP had opposite effects on NMJ length than FMRP null mutants, whereas OE of dCYFIP1 phenocopied FMRP loss (Schenck et al., 2003). This study was recently expanded on, showing that double KO of dCYFIP and FMRP partially rescues NMJ length (Abekhoukh et al., 2017). As shall be discussed in the following section, FMRP and CYFIP also differentially effect mTOR signalling. A potential explanation for these interactions comes from another study of fly NMJ that looked at genetic interactions between CYFIP and WAVE (Zhao et al., 2013). Abnormal synaptic boutons in dCYFIP null flies could be partially rescued by reduced expression of WAVE, suggesting that loss of dCYFIP1 might have its effects via gain-of-function of a WAVE-dependent process. This is supported by the common observation that loss of CYFIP1 expression increases actin turnover in multiple systems (Pathania et al., 2014; Zhao et al., 2013).

1.4.2.3 mTOR signalling

The mechanistic target of rapamycin (mTOR) is a serine/threonine kinase which serves as a master regulator of cell metabolism, growth and survival. mTOR can exist as part of two distinct protein complexes, referred to as mTORC1 and mTORC2, which are rapamycin sensitive and insensitive respectively and also differ in the proteins they complex with (Jacinto et al., 2004). MTORC1 is the far better studied pathway; mTORC1 activity is dependent on GTP-bound Rheb, which is turn is regulated by TSC1/2 and Akt, themselves a source of regulation from a wide range of cellular cues (Crino, 2016). Key upstream signals include the PI3K/PIP_3/PDK1 pathway and ERK1/2 signalling. Activated mTORC1 leads to altered protein synthesis and mRNA handling via downstream effectors S6K and 4EBP1. In contrast, little is known about the activation of mTORC2, although PI3K activity has been implicated here as well (Thobe et al., 2017). Active mTORC2 regulates cytoskeletal dynamics through PKCα and Rac1 phosphorylation. Additionally, mTORC2 positively regulates mTORC1 activity via phosophorylation of Akt.

Altered mTOR signalling is perturbed in several neuropsychiatric disorders (Crino, 2016). mTOR phosphorylation is enhanced in the Fragile X mouse in coordination with dyregulation of various mTOR pathways components, cumulating in enhanced basal activity of the pathway (Sharma et al., 2010). The PI3K activator, PIKE-S, is an FMRP target and is the proposed mediator of this effect (Darnell et al., 2011). Supporting this, a study of patient FXS lymphocytes showed increased phosphorylation of S6K, eIF4E and Akt suggesting that protein translation could be upregulated (Hoeffer et al., 2012). Intriguingly, this study also found an increase in CYFIP2 but not CYFIP1 expression, as predicted by CYFIP2 mRNA as target of FMRP (Darnell et al., 2011). A recent study showed that metformin, which indirectly inhibits mTORC1 and ERK, could rescue many core behavioural and pathological hallmarks of FXS in FMR1 KO mice (Gantois et al., 2017).

Additionally, growing evidence suggests a link between ASDs and overactive mTOR signalling. Patients with PTEN mutations often present with ASD alongside ID (Varga et al., 2009). Tang et al. showed that levels of phosphorylated mTOR and S6K were increased in temporal lobes of ASD young adolescents (13-18yo) (Tang et al., 2014). Interestingly, this was correlated with increased spine density and decreased autophagic flux. This study went on to show that a Tsc heterozygous mouse model recapitulated many of these phenotypes and that these could be alleviated by inhibition of mTORC1 by rapamycin. This supports work in other 'overactive mTOR' mouse models that have shown ASD-like behaviours and neuronal pathologies (Tsai et al., 2012).

Two recent reports have suggested that CYFIP1 dosage effects mTOR signaliing. Overexpression of CYFIP1 in an in vivo mouse model led to altered gene expression of numerous mTOR pathway members (Oguro-Ando et al., 2015). Protein lysates from cultured neuronal progenitors OE CYFIP1 showed increased mTOR and reduced in PTEN levels, and rapamycin treatment reversed many effects of CYFIP1 OE, including increased cell size and branching. Further, protein samples from patient brains that carried a CYFIP1 duplication had increased pS6K levels, indicative of overactive mTOR. Conversely, knockdown of CYFIP1 has been shown by two independent groups to decrease mTOR expression (Abekhoukh et al., 2017; Oguro-Ando et al., 2015). Indeed, loss of CYFIP1 reverses the increase in pS6K seen in the FMRP KO cortical cultures (Abekhoukh et al., 2017). Thus, CYFIP1 dosage appears to regulate mTOR signaling in a dose-dependent manner, and in coordination with FMRP. However, the molecular basis for this is still unclear and not immediately intuitive given the coordinated role of CYFIP1 and FMRP in translational repression.

1.4.3 Pathological associations of CYFIP1

Since its association with FMRP, the link between CYFIP1 and neurodevelopmental and psychiatric disorders has been of interest. This etiological research has bore fruit and unveiled a host of genetic associations between CYFIP1 and various neurological conditions, characterised by altered CYFIP1 dosage (summarized in Table 1.10). Indeed, altered CYFIP1 expression has also been seen in a number of pathological conditions not caused by genetic lesions.

1.4.3.1 Prader-Willi and Angelman Syndromes

Human CYFIP1 is located on chromosome 15 in region q11.2 (roughly 1.2Mb) that also contains the genes TUBGCP5, NIPA1 and NIPA2 (Chai et al., 2003). TUBGCP5 encodes a tubulin gamma complex proteins, whereas NIPA1 and 2 are magnesium transporters with differential expression in the kidneys and brain respectively. 11.2 is at the proximal end of a larger region of chromosome 15 spanning q11-q13 that is associated with two related genetic disorders: Prader-Willi Syndrome (PWS) and Angelman Syndrome (AS). Both PWS and AS are severe neurodevelopmental disorders characterised by developmental delay (DD), ID and behavioral abnormalities (Cox and Butler, 2015).

The q11-q13 region contains three common breakpoints (BP1-3) due to recurrent low copy DNA repeats of pseudogenes, that allow for interstitial deletions and duplications between them. The q11.2 locus is contained within the region between BP1 and BP2, whereas a larger (roughly 5.3Mb) region is between BP2 and 3. PWS and AS can be caused by either deletion of the BP1-BP3 (Type I) or BP2-BP3 (Type II) regions. The clinical distinction between PWS and AS arises from the fact the genes within BP2-BP3 are differentially imprinted by epigenetic modifications specifically in the brain and thus the genes affected by deletion depend on the parental origin of the chromosome. Concretely, deletion of paternal origin leads to PWS with the snoRNA gene HMBII-85 thought to be the major causative gene (Ding et al.,

2008). Conversely, deletion in the maternal chromosome leads to AS and is due to loss of UBE3A function (Greer et al., 2010).

Although deletion of q11.2 is not required for PWS or AS, numerous studies have suggested type I deletions (that include the q11.2 locus) show more severe clinical phenotypes that those with Type II deletions. In PWS, type I patients have lower intelligence scores, delayed verbal speech acquisition and increased compulsive, self-injurious behaviours in PWS (Bittel et al., 2006; Varela et al., 2005). Interestingly, these behaviours correlate with expression of reduced expression of q11.2 genes, including CYFIP1 (Bittel et al., 2006). Similarly, type I AS patients have reduced verbal IQ and enhanced seizure susceptibility compared to type II (Milner et al., 2005; Valente et al., 2013). Finally, a recent prepublication study suggested a causative link between reduced CYFIP1 expression and hyperphasia and obestiy that is commonly seen in PWS (Babbs et al., 2018). In mice, haploinsufficiency of CYFIP1 led to increased compulsive behaviour and food intake, though increased food intake was more prevalent in mice with deletion of the paternally-inherited CYFIP1 allele. The parental origin effect is interesting considering that the q11.2 region is not known to be imprinted (Chai et al., 2003). Thus, CYFIP1 deletion in PWS and AS modifies various clinical outcomes including intellectual ability, epileptogenesis and behaviour.

1.4.3.2 Schizophrenia

Genetic instability at the q11.2 locus can also lead to microdeletions and microduplications of this region, separate from BP2-BP3. Indeed, CNV of q11.2 locus occurs in approximately 0.25% of the healthy population. Though CNV of q11.2 doesn't lead to either PWS or AS, duplications and deletions are found at higher frequencies (1.3% and 0.7% respectively) in patients with neurological conditions (Abdelmoity et al., 2012). A review of clinical phenotypes associated with q11.2 microdeletions in 200 such patients showed that the majority have delayed development, speech, writing and impaired memory (Cox and Butler, 2015).

Further, even though many occurrences of q11.2 CNV do not manifest with neuropsychiatric disorders, an Icelandic study showed these non-case examples have increased prevalance of dyslexia, dyscalculia and structural changes associated with first-episode psychosis in SCZ (Stefansson et al., 2014).

Table 1.10: Clinical associations between CYFIP1 and neuropsychiatric disorders

Disorder	Genetic variation	References
ASDs	15q11-13 duplication	(Pinto et al., 2014)
		(Depienne et al., 2009)
		(Nishimura et al., 2007)
	15q11.2 microduplication	(van der Zwaag et al., 2010)
		(Depienne et al., 2009)
	15q11.2 microdeletion	(Doornbos et al., 2009)
		(Depienne et al., 2009)
		(Leblond et al., 2012)
	SNP (non-synonymous coding)	(Waltes et al., 2014)
	SNP (eQTL/mRNA expression)	(Wang et al., 2015)
SCZ	15q11-13 duplication	(Ingason et al., 2011)
		(Isles et al., 2016)
	15q11.2 microduplication	(Kirov et al., 2012)
	15q11.2 microdeletion	(Kirov et al., 2012)
		(Tam et al., 2010)
		(Stefansson et al., 2008)
		(Zhao et al., 2013)
	rare variants	(Purcell et al., 2014)
	SNPs	(Zhao et al., 2013)
Epilepsy	15q11-13 duplication	(Marini et al., 2013)
	15q11.2 microdeletion	(de Kovel, Carolien G F et al., 2010)
		(Lal et al., 2015)

Numerous reports have shown an association between q11.2 CNV and SCZ. Several large scale GWAS have shown q11.2 deletion was over 2-fold enriched in SCZ cases over controls (Kirov et al., 2012; Rees et al., 2014; Stefansson et al., 2008; Tam et al., 2010; Zhao et al., 2013). Additionally, CNV gain has also been observed, though less frequently, in SCZ (Ingason et al., 2011; Rees et al., 2014). Though q11.2 CNVs involve changes in gene expression aside from CYFIP1, there is evidence for CYFIP1 playing a predominant role in SCZ association of this region. Firstly, neuronal progenitor cells (NPCs) carrying q11.2 deletion have reduced CYFIP1 expression and altered cell-adhesion signalling *in vitro* and *in vivo* (Yoon et al., 2014). Indeed, research into CYFIP1 has revealed a host of functions in brain development and connectivity that provides mechanistic link to SCZ (discussed in chapter 3 + 4). Finally, Zhao et al. have reported a putative association between a common SNP and SCZ in the Han Chinese population, though the functional relevance of this is unclear (Zhao et al., 2013).

1.4.3.3 ASDs and FXS

Altered CYFIP1 expression has also been associated with autism and ASDs. Both deletions and duplications of q11.2 are prevalent in ASD patients (Depienne et al., 2009; Leblond et al., 2012; van der Zwaag et al., 2010; Wiśniowiecka-Kowalnik et al., 2013). These can arise from either *de novo* genetic abnormalities or be inherited from either parent. Interestingly, Leblond et al. showed CYFIP1 deletion concurrent in patient with a SHANK2 deletion, suggesting that increased load of ASD-associated genetic mutations may affect susceptibility in an additive manner. Whole exome sequencing has revealed increased load of specific rare variants of CYFIP1 in ASD patients (Toma et al., 2014; Waltes et al., 2014). Interestingly, a subset of these ASD associated variants positively correlate with CYFIP1 mRNA levels in prefrontal cortex (Toma et al., 2014). How these variants alter mRNA levels is currently not known. However, a study of a CYFIP2 variant that diverged in two lineages of the CLB6 mouse line showed that one variant had reduced protein stability despite

normal interaction with WRC components (Kumar et al., 2013). Given the fact that deletions in q11.2 are also associated with ASDs, it would be interesting to know if any of these ASD-associated variants effect CYFIP1 stability.

ASD-associated rare variant mutations in the WRC component NCKAP1 have also been identified. A study looking for *de novo* mutations found a nonsense mutation in the C-terminal of NCKAP1 (Iossifov et al., 2012). This has been subsequently supported by other studies finding further *de novo* or inherited rare varients in NCKAP1 that are likely to be gene disruptive (de Rubeis et al., 2014; Wang et al., 2016). These findings suggest that WRC dysfunction may be a common thread linking multiple ASD-associated genes, including core WRC components but also upstream and downstream interactors, such as NLGN1 and 4 (Chen et al., 2014a).

These etiological studies suggest that altered CYFIP1 gene dosage is a risk factor for ASDs. However, given that q11.2 deletions or duplications are only found in a small percentage of cases (approximately 0.5%), it is important to know if CYFIP1 protein levels could be altered by indirect means. Evidence for this comes from a recent study examining CYFIP1/2 levels in ASD patients, not screened for genetic lesions at the q11.2 locus (Noroozi et al., 2018). They report increased levels of CYFIP1 and 2 mRNA in peripheral blood samples, suggesting that increased CYFIP1 expression could be a more generalized risk for ASD and even a biomarker. Although promising, the sample size in this study was small and larger cohorts will be needed to validate whether or not peripheral CYFIP1 levels are an accurate readout of ASD or a subset of these conditions.

Further indirect evidence for a CYFIP1-ASD association comes from the molecular interactions of CYFIP1 and FMRP. Autism is a common comorbidity in FXS. Although there is significant variability across studies, the prevalance of ASDs in FXS is roughly 50% (Abbeduto et al., 2014). Conversely, FXS accounts for between 1-6% of ASDs, making the loss of FMRP the strongest monogenetic risk factor identified to date (Muhle et al., 2004). Despite this clear association and

interest in the field to see FXS as a monogenetic model for ASD, there are important differences between FXS-ASD and non-syndromic ASDs (NS-ASD). For instance, FXS-ASD patients on average have greater ID and increased psychiatric problems (i.e. hyperactive behaviour and general anxiety) (Abbeduto et al., 2014). In addition, structural differences in brains of nonsyndromic-ASD patients are different from those seen in FXS-ASD patients (Meguid et al., 2010).

1.4.3.4 Cancer

Altered CYFIP1 expression has also been strongly associated with various cancers. Silva et al. first identified CYFIP1 as a putative tumor suppressor gene; finding that genetic deletion of CYFIP1 was a common occurrence in lung, breast and colon cancers (Silva et al., 2009). This study showed loss of CYFIP1 increased in malignancy of tumor cells via altering cell-cell and cell-ECM contacts. Concretely, WRC activity is required for epithelial morphogenesis, to form stable cadherin junctions between cells and focal adhesion sites between cells and ECM. Loss of CYFIP1 increases malignancy by reducing WRC activity, cell-cell/ECM contacts, thereby enhancing invasiveness of cells.

This study has been backed up by further research showing a similar reduction in CYFIP1 levels associated with tumor progression in skin cell carcinoma (SCC) (Dziunycz et al., 2017). Interestingly, in SSC CYFIP1 levels were controlled in part by activity of NOTCH1, a transcription factor critical during cell differentiation and that is deleted in many invasive epithelial cancers (Nicolas et al., 2003). In contrast, another study focusing on breast cancers suggested that CYFIP1, in coordination with NAP1 and WAVE3, was required for metastasis (Teng et al., 2016). This study focused on using synthetic peptides to interfere with the CYFIP1/NAP1-WAVE3 interaction but could have disrupted other interactions of WAVE3 or led to gain of function effects not seen in the previous CYFIP1 knockdown studies.

1.4.3.5 CYFIP2 disease associations

In comparison to CYFIP1, there has been limited evidence for clinical associations of CYFIP2. Two studies of interstitial deletions in the 5q33.3 region, where the CYFIP2 gene is located, reported clinical cases of varied degrees of mental retardation in a girl and boy (Lee et al., 2016; Spranger et al., 2000). However, a recent study identified four independent cases of a rare variant mutation in CYFIP2 at Arg87 that cause early-oncet epileptic encephalopathy (Nakashima et al., 2018). These mutations were all predicted to disrupt the CYFIP2-WAVE binding interface and possible disrupts Rac1 binding to CYFIP given the closeness of Arg87 to its binding site. Although no changes were seen in the expression of Rac1 or WAVE in lymphoblastoids derived from these patients, all Arg87 mutants had decreased binding to the VCA of WAVE1 (Nakashima et al., 2018). These variants represent the first identified disease-causing mutations in any CYFIP protein. The fact that these patients present with seizures and microcephaly provide the strongest evidence to date for the importance of CYFIP proteins in brain development. This study also highlighted that 10 CYFIP2 *de novo* variants have been recently reported in a cohort of patients with ASDs and development delay (C Yuen et al., 2017).

A recent study showed that CYFIP2 levels were decreased in brains of later stage AD patients, even after controlling for synaptic loss (Tiwari et al., 2016). Indeed, APP mRNA is a FMRP target and CYFIP2 heterozygous mice have increased APP in hippocampus. This same study showed that CYFIP1 levels were increased in the hippocampus of late-stage AD patients, possibly as a compensatory mechanism. The haemopoetic WRC component ABI3 was recently also identified as a AD risk gene, suggesting the WRC role of CYFIP may be important in the AD association (Satoh et al., 2017; Sims et al., 2017).

In mouse models, CYFIP2 mutations have been linked to clinically-relevant behaviours. In 2013, a study showed that the substrain of C57BL – 6N, had lower response to both cocaine and methanphetamine, reduced spine density in the nucleus

accumbens and reduced excitatory transmission (Kumar et al., 2013). Whole-genome sequence comparisons reveals a single missense mutation in CYFIP2 (S968F) between the two lines. Importantly, heterozygosity of the mutant allele was sufficient to restore acute and sensitised cocaine response, providing strong evidence for the CYFIP2 mutation being causative. This study was recently built upon by showing that a descendent of the 6N lineage also carrying the CYFIP2 mutation had increased palatable food intake used as a behavioral paradigm for binge-eating disorders (BEs) (Kirkpatrick et al., 2017). Although currently no genetic basis for BEs in humans has been uncovered, CYFIP2 appears a promising target.

1.4.4 Statement of aims

In summary, this introduction has provided an overview of the intracellular molecular machinery that regulates cell shape and motility. Whilst many of these signalling pathways are ubiquitous, it is clear that they play particularly important roles in cell types with either complex morphologies (e.g. neurons) or highly motile cells (e.g. microglia). It is also clear that disruption of this machinery is a common feature of various neuropsychiatric disorders.

As a core component of a major actin remodelling complex, CYFIP1 sits in the middle of many of the signalling pathways discussed. To date, there has been a significant research effort elucidating the function of CYFIP1 in cell lines and in establishing its etiological links with various clinical conditions. This has driven interest in the functions of CYFIP1 in neurons. However, given the broad expression of CYFIP1 within the brain, it is currently unclear how global alterations in CYFIP1 expression alter brain development. This thesis posits that CYFIP1 has cell-specific functions in different cell types in the brain that relate to their individual functional requirements. To test this overarching hypothesis, I aim to develop experimental systems that will facilitate the identification of these cell-specific functions of

CYFIP1, both *in vitro* and *in vivo*. I have focused on two cell types, principle neurons and microglia, which for reasons discussed are promising targets for this study.)

Chapter 2

Materials and methods

2.1 Animals

Animals were maintained under controlled conditions (temperature 20 ± 2°C; 12 hour light-dark cycle). Food and water were provided ad libitum. All breeding and experimental procedures were carried out in accordance with institutional animal welfare guidelines and licensed by the UK Home Office in accordance with the Animals (Scientific Procedures) Act 1986.

2.1.1 Mouse strains

The Cyfip1 KO mouse line (MGI:5002986; Allele: Cyfip1tm2a(EUCOMM)Wtsi) was obtained from the Wellcome Trust Sanger Institute as part of the International Knockout Mouse Consortium (IKMC). Cyfip1 'floxed' animals were generated by crossing with a Flipper mouse to generate tm1c (Conditional allele) mice, following the Knockout-First strategy on C57BL/6N Taconic USA background (Skarnes et al., 2011; White et al., 2013). The NEX^{Cre} line was obtained from The Jackson Laboratory (Neurod6tm1(cre)Kan) and has been previously described (Goebbels

et al., 2006). The CX3CR1^{CreERT2} line (B6.129P2(C)-Cx3cr1tm2.1(cre/ERT2)Jung/J) and IBA^{EGFP} line (Tg(Aif1-EGFP)1Kohs) were kindly gifted from the Attwell lab, UCL and have both been previously described (Hirasawa et al., 2005; Yona et al., 2013). All transgenic mice were bred on C57BL/6 Taconic USA background.

2.1.2 Tamoxifen administration

The Cre recombinase expressed by the CX3CR1^{CreERT2} line is fused to a mutant estrogen receptor (ER) ligand binding domain. ERT2-Hsp90 binding sequesters the Cre fusion in the cytoplasm, preventing recombination activity in the nucleus. To activate Cre, administration of estrogen receptor agonist tamoxifen leads to binding of 4-hydroxytamoxifen (4-OHT), the active metabolite produced from tamoxifen by the liver, to the ERT2 site, translocation of CreERT2 into the nucleus and enabling recombination activity between loxP sites. To deliver tamoxifen to adolescent/adult mice (P28 and older), mice were treated with 4 mg/100µl twice via oral gavage, 48 hours apart. Tamoxifen was dissolved in 40 mg/mL solution of 90% cornoil (Kolliphor EL, Sigma):10% ethanol by sonication.

2.1.3 *In utero* electroporation

At E14.5, pregnant mice were deeply anesthetized with isoflurane 5% in a mixture of 30%O_2/70%N_2O were maintained at 37 ± 0.5°C during all the procedure. Uterine horns were exposed via a midline abdominal incision and embryos carefully exposed using ring-forceps through the incision and placed on a humidified plastid surface. Plasmid DNA solution (0.3 µg/µL pCAG-GFP) mixed with Fast Green solution (2 mg/mL; Sigma, St Louis, MO, USA) was microinjected via a calibrated glass micropipette (Drummond Scientific, Broomall, PA, USA) and a microinjector (30 ms; 30 psi; Pico-Liter Injector PLI-10; Warner Instruments, Hamden, CT, USA) into

the lateral ventricle of each embryo. Immediately after DNA injection, the heads of the embryos were placed and held between 5 mm platinium electrodes with the anode directly toward the cortex and electronic pulses were applied (five 50 ms pulses of 35 V at 950 ms intervals) using an EM830 electroporator (BTX, Harvard Apparatus, Holliston, MA, USA). During the procedure, the embryos were constantly bathed with warm sterilised phosphate-buffered saline (PBS). Then, uterine horns were placed back in the abdominal cavity to allow embryos to continue normal development until the desired time of observation. Finally, the abdomen wall and skin were sutured using surgical needle and thread and mice placed in a heating chamber until anaethesia wore off. Pregnant mice were injected with buprenorphine (Vetalgesic, 0.09 mg/kg) prior to surgery and Marcain (Astra Zeneca, 0.05%) was administered locally after surgery. Carpofen (0.5 mg/mL) treated drinking water was administrated post-surgically for 48 h. All IUE surgeries were performed with Dr Flavie Lesept.

2.1.4 Transcardial perfusion

For all relevant experiments in Chapter 5, brains were fixed by transcardial perfusion (TCP) of 4% paraformaldehyde (PFA) (4% PFA, PBS). Animals were given terminal anaesthesia via intraperitoneal injection of 1 µl/g pentobarbital solution. When fully anaesthetised, the chest cavity is opened and diaphragm cut to reveal the heart. A 21-guage needle is inserted into the posterior end of the left ventricle and clamped in place. In quick succession, a cut in the right atrium is made and the PFA perfusion pump is started. After 10-15 ml of ice-cold 4% PFA has circulated, perfusion is stopped, the animal decapitated and brain dissected and placed in ice-cold 4% PFA overnight. Certain protocols required TCP of PBS to remove all blood from the brain. In these cases, the protocol above was used except that ice-cold PBS was perfused.

Table 2.1: PCR reaction cycle

Step	Temperature (∘C)	Time	
Melting	95°C	2m	
Melting	95°C	30s	
Annealing	58°C	30s	Repeat 35X
Extension	72°C	40s	
Hold	4°C	∞	

2.1.5 Genotyping

DNA was extracted from ear biopsies or tail biopsies using the Hot Shot method (Truett et al., 2000). Genotyping PCR (polymerisation chain reaction) was carried out using a standard PCR reaction (table) using the appropriate primers (table), to a final volume of 20 µl per reaction containing: 0.8 µl forward and reverse primers, 0.125 µL Taq Polymerase (NEB), 5 µl Taq buffer (4X) and 122.75 µl ddH20. 10 µl of the PCR product was ran on a 1.5% agarose gel (1.5 g Agarose, 100 mL TAE) to determine the size of the PCR products.

To genotype mice younger than P10, a small tissue sample (<1mm) of tail was taken using an unused, flat blade. Local cryo-analgesia was applied using an ethylene chloride-soaked cotton bud. To identify animals post-genotyping, pups were tattooed using the Aramis Micro Tattoo Kit (Ketchum) on foot pads.

2.2 Cell culture and biochemistry

2.2.1 Primary neuronal culture

Cortical and hippocampal neurons were cultured from E16 mouse embryos as previously described (Gordon et al., 2013). Briefly, time pregnant mice were killed by cervical dislocation and decapitation and embryos removed and placed onto ice cold HBSS. Individually, brains were extracted, meninges were removed and hippocampi

and cortices were dissected. Dissected tissue was incubated in 0.125% trypsin diluted in HBSS for 15 minutes at 37°C. Tissue was washed twice with attachment media (Minimal Essential Media (GIBCO), 10% horse serum, 1 mM sodium pyruvate, 0.6% glucose) and triturated to a single cell suspension in 1 ml of attachment media. For hippocampal neurons, 650 µl of the cell suspension (approximately 350,000 cells) was plated in a 6 cm dish containing pre-prepared poly-L-lysine (PLL) coated 13 mm glass coverslips. For cortical cultures, 250 µl of cell suspension was added to PLL coated 6 cm dishes. PLL was incubated for a minimum of 3 hours with coverslips and plates at 500 µg/ml and 50 µg/ml respectively. Cells were incubated at 37°C in 5% CO_2 humidified atmosphere. Attachment media was changed 4-6 hours later to maintenance media (Neurobasal Media (GIBCO), 2% B27 (GIBCO), 1% glutaMAX (GIBCO), 33 mM glucose).

2.2.2 Lipofection

Neurons were transfected at the required age using Lipofectamine 2000 (Invitrogen). For 8-9 coverslips in a 6cm dish, 3 µg DNA was combined with 400 µl unsupplemented Neurobasal (NB) and 6 µl Lipofectamine with 400 µl NB in separate falcon tubes. Following 5 minutes incubation at RT, the Lipofectamine solution was combined with the DNA and incubated for 20 minutes at RT. 1.2 ml pre-warmed NB + 0.6% glucose was added to the DNA + Lipofectamine solution, gently mixed and added to the culture dish. Following a 2 hour incubation at 37°C, transfection media was replaced with pre-warmed conditioned maintenance media. Volumes were scaled as required for different dish sizes.

2.2.3 Preparation of brain lysates

Mice were killed using a Schedule 1 method and brains placed in ice-cold HBSS. Cortex, hippocampi and cerebella were dissected and placed in 500 µl, 250 µl and

300 µl ice-cold HEPES buffer respectively (50 mM HEPES pH 7.5, 0.5% Triton X-100, 150 mM NaCl, 1 mM EDTA, 1 mM PMSF, 10 µg/ml antipain, pepstatin and leupeptin) and kept on ice. Tissue was solubilised by sonication, centrifuged at 14000 rpm for 15 minutes and the supernatant collected. Protein concentration was quantified using the Bradford assay following the manufacturer's protocol (BioRad). Western blot samples were generated from these lysates by adding 1/3 volume of Sample Buffer (3X) and boiling samples for 5 minutes. Samples were stored at -80°C until use.

2.2.4 Adult microglia isolation

To generate Western blotting samples of enriched adult microglia from transgenic mice, a percoll-based isolation method was used as described previously (Lee and Tansey 2013). Briefly, 3 mice per experimental condition were transcardially perfused with PBS, brains extracted and finely minced using a flat scalpel blade in 3 ml HBSS. Tissue was enzymatically digested in a dispase-papain-DNAase solution and triturated into a single cell suspension. This suspension was loaded into a 70%:37%:30% percoll gradient. After centrifugation without brakes, myelin debris migrated to the 30%:37% interface and microglial cells were enriched in the 70%:37% interface. The microglia fraction was extracted, washed and lysed in sample buffer to generate western blot samples.

2.2.5 Western blotting

Protein samples were loaded into a stacking gel and separated on an 8% agarose gel by gel electrophoresis (XCell SureLock, Invitrogen) for 90 minutes at 120 V. Protein was then transferred from gel to a nitrocellulose membrane at either 350 A or 30 V for 2 hours. Nitrocellulose membrane was stained with Ponceau (0.5% Ponceau S, 1% acetic acid) and blocked for 1 hour in milk (4% dried milk powder, 0.1%

Tween, PBS). Membrane was cut and the appropriate areas inclubated with primary antibodies diluted in milk at 4°C overnight. Membrane was washed 3X in PBST (0.1% Tween, PBS) for 30 minutes prior to HRP secondary antibody incubation diluted in milk for 45 minutes. Membrane was washed 3X in PBST and horse radish peroxidase (HRP) substrate (Pierce ECM substrate, Thermofisher) added to the dry membrane for 2 minutes. Chemiluminescence was measured using a CCD imager. Quantifications of western blots were performed within ImageJ and Microsoft Excel. All protein levels were normalised to a loading control (either β-Tubulin III, actin or NADPH) and to the averaged value of normalised control samples. All quantifications were from a single representative western blot that contained at least 3 experimental replicates per condition.

2.3 Immunofluorescence and bright-field staining

2.3.1 Antibodies

Secondary antibodies for western blots were anti-rabbit and anti-mouse HRP-conjugated secondaries from Jackson ImmunoResearch (WB: 1:10000). Secondary antibodies for fluorescent imaging were AlexaFluor conjugated 488, 555, 568, 647 (1:1000, Molecular Probes). DAPI 405 dye was used 1:1000.

2.3.2 Immunocytochemistry and immunohistochemistry

Hippocampal cultures on glass coverslips were fixed in 4% PFA (4% paraformaldehyde, 4% sucrose, PBS, pH 7) for 7 minutes prior to blocking and permeabilization in blocking solution (10% horse serum, 0.5% BSA, 0.2% Triton X-100, PBS). Coverslips were incubated in primary antibody for 1 hour, washed 5x in PBS+0.2% Triton X-100, then incubated for 1 hour in secondary antibody. Antibody solutions both diluted in blocking solution. Coverslips were mounted with

Prolong Gold antifade mountant (Invitrogen). If coverslips were not stained immediately after fixation, they were stored at -20°C in cryoprotect solution (30% ethylene glycol, 30% glycerol, 40% PBS).

For slice staining, mouse brains from litter matched pairs were fixed in 4% PFA overnight, after cervical dislocation and decapitation. For experiments performed using the CX3CR1^{CreERT2} line, brains were fixed initially by TCP (see Transcardial perfusion) prior to fixation overnight. Brains were transferred to 30% sucrose/PBS solution prior to long term storage at -80°C. For cryoslices, samples were embedding in OCT (Optimal Control Temperature) and 30 µm sections made using a Cryostat (Bright Instruments, Luton, UK). Slices were stored at -20°C either as free-floating slices in cryoprotect solution (postnatal) or on frosted slides (embryonic). For 100 µm slices, brains were stored in PBS after fixation and sliced using a vibratome (Leica Microsystems, Heerbrugg, Switzerland).

For immunohistochemistry, free floating sections were washed in PBS before permeabilization in blocking solution (10% horse serum, 0.5% BSA, 0.2% Triton X-100, PBS) for 2-4 hours then incubated with primary antibody diluted in block solution overnight at 4°C. For mouse primary antibodies, slices were first incubated overnight at 4°C with mouse Fab fragment (1:50 with block solution; 115007-003, Jackson ImmunoResearch, West Grove, PA, USA). Slices were washed 4-5X in PBS for 2 hours then incubated for 3-4 hours with secondary antibody at RT. Slices were then washed 4-5X in PBS for 2 hours and mounted onto glass slides using Mowiol mounting medium. For antigen retrieval, slices were incubated in sodium citrate solution at 80°C for 40 mins and then washed 3X in PBS prior to blocking.

FluoroNissl and FluoroMyelin dyes were used as per the manufacturer's instructions (Sigma Invitrogen). Briefly, cryoslices were washed in PBS+0.2% Triton X-100 and incubated with the FluoroNissl or FluoroMyelin (1:100 and 1:300 respectively, diluted in PBS) for 2 hours prior to washing and mounting.

Table 2.2: List of primary antibodies

Antigen	Species	Company	Product code	Western blot	ICC	IHC
Actin	Rabbit	-	-	1:1000	-	-
β-PIX	Rabbit	Upstate	07-1450	1:1000	-	-
β-Tubulin	Mouse	Sigma	M4863-T5293	1:1000	-	-
CYFIP1	Rabbit	Upstate	07-531	1:1000	-	-
CYFIP1	Rabbit	Millipore	AB6046	-	-	1:500
FMRP	Mouse	-	-	1:500	-	-
$GABA_A\beta 2/3$	Mouse	Neuromab	MAB341	1:500	-	-
GAPDH	-	-	-	1:2000	-	-
Gephyrin	Mouse	Synaptic systems	147 001	1:500	1:1000	1:500
GFP	Rat	Nacalai-Tesque	04404-84	-	1:2000	1:1000
GIT1	Mouse	Neuromab	N39/B8	1:500	-	-
Homer	Rabbit	Synaptic systems	160 002	1:500	1:1000	1:500
Neuroligin-2	Rabbit	Synaptic systems	129 202	1:500	-	-
Neuroligin-3	Mouse	Neuromab	N110/29	1:100	-	-
PanShank	Mouse	Neuromab	73-089	1:500	-	-
PSD95	Mouse	Neuromab	K28/N43	1:1000	1:500	-
VGAT	Rabbit	Synaptic systems	131003	1:1000	1:500	-
VGLUT1	Guinea pig	Synaptic systems	135304	1:1000	1:500	1:500
WAVE1	Rabbit	-	-	1:1000	1:500	-

2.3.3 Golgi-Cox preparation

Dendritic and spine morphology in P30 mice was analysed using the FD Rapid Golgi Stain kit (FD NeuroTechnologies, Baltimore, MD, USA) and Neurolucida (MBF Bioscience, Williston, VT, USA). Experimental animals were culled by cervical dislocation, brains removed and placed immediately in staining solution for 2 weeks. After transfer to solution C, Golgi-impregnated brains were sliced at 100 µm using a vibratome (Leica Microsystems, Heerbrugg, Switzerland) and air dried on gelatin-coated slides for 24-48 hours. Slices were stained as per the manufacturer's instructions and mounted with Permount. Slides were stored in darkness at room temperature (RT).

2.4 Electrophysiology

2.4.1 Acute slice preparation

To prepare acute hippocampal slices, male and female mice aged postnatal day 28-34 were used. Immediately after decapitation, the brain was removed and kept in ice-cold dissecting solution. Transverse hippocampal slices (300 µm) were obtained using a vibratome (Leica, VT–1200S). Slices were stored at 35°C for 30min after slicing and then at 22°C. For the dissection and storage of slices, the solution contained (in mM): 87 NaCl, 25 $NaHCO_3$, 10 glucose, 75 sucrose, 2.5KCl, 1.25NaH_2PO 4, 0.5$CaCl_2$ and 7 $MgCl_2$ saturated with 95%O_2/5% CO_2.

2.4.2 Electrophysiology of acute slices

For patch-clamp experiments, CA1 pyramidal neurons were identified under infrared-differential interference contrast (DIC) imaging with a water-immersion 60X objective (Olympus) and whole-cell recordings were performed. Neurons were

held at -70 mV. Patch electrodes (4-5 MΩ) were filled with an internal solution containing (in mM): 120 CsCl, 5 QX314Br, 8 NaCl, 0.2 $MgCl_2$, 10 HEPES, 2 EGTA, 2 MgATP and 0.3 Na_3GTP. The osmolarity and pH were adjusted to 300 mOsm/L and 7.2 respectively. The external artificial cerebro-spinal fluid (ACSF) solution consisted of the following (in mM): 125 NaCl, 25 $NaHCO_3$, 2.5 KCl, 2 $MgCl_2$, 1.25 NaH_2PO_4, 2 $CaCl_2$, and 25 glucose saturated with 95%O_2/5% CO_2 (pH 7.4, 320 mOsm). This solution was supplemented with CNQX (20 µM), APV (50 µM) and TTX (1 µM) to isolate mIPSCs or with bicuculline (20 µM) and TTX (1 µM) for mEPSCs recording. All recordings were performed at room temperatures (22-25°C). The access resistance, monitored throughout the experiments, was <20 MΩ and results were discarded if it changed by more than 20%. Miniature events and their kinetics were analysed using template-based event detection in Clampfit (Molecular Devices, Sunnyvale, CA, USA). Total charge transfer was calculated as described by Peden and colleagues (Peden et al., 2008).

2.5 Imaging and analysis

2.5.1 Neuronal and microglial reconstructions

2D reconstructions of dendritic and axonal morphology *in vitro* were made semi-manually from maximum intensity projections of single cells at 40X using NeuronStudio software (Wearne et al. 2005). Branch points and branch points sholl analysis was performed using in-built tools in NeuronStudio, whereas total process length and intersection sholl analysis was performed using a custom MATLAB script. For spine morphology analysis of cultured neurons, confocal image stacks were acquired. Spines were manually identified on 100-200 µm long dendritic filaments and analysed in Imaris software (Bitplane, Zurich, Switzerland). For spine subtype classification custom parameters were used. Classification was entirely automated until the final step where blatant errors in classification were removed.

Dendritic and spine morphology in P30 mice was analysed using the FD Rapid Golgi Stain kit (FD NeuroTechnologies, Baltimore, MD, USA) and Neurolucida (MBF Bioscience, Williston, VT, USA). Golgi-impregnated brains were sliced at 100 µm using a vibratome (Leica Microsystems, Heerbrugg, Switzerland). Well-isolated hippocampal CA1 neurons were imaged at 20X using the Neurolucida software system and an upright light microscope with a motorized stage (MBF Bioscience). The entire dendritic tree (apical and basal) was traced and reconstructed. 3-dimensional Sholl analysis of reconstructions was performed using a custom MATLAB script. For spine analysis of Golgi-Cox sections, 50 µm z-stacks of 2 µm step size were imaged at 40X using a ZEISS Axio Scan system and sections of basal dendrite were randomly selected for analysis. Spine length and head width were manually traced in ImageJ and the data analysed using a custom EXCEL macro.

For reconstructing 3D microglial morphology imaged via two-photon or confocal microscopy, automatic traces were generated using the open source software Vaa3D (Peng et al. 2014). Input z-stack images were pre-processed using a custom ImageJ macro to subtract background, remove noise using median filtering, and improve contrast. Generated reconstructions were manually checked, and any clear abnormalities corrected. Reconstructions were subsequently analysed as described.

2.5.2 Synaptic clusters

For synaptic localisation and cluster analysis experiments in hippocampal cultures, a single plane reference image of each cell was taken at 0.5X zoom with a 63X objective. From this, three regions of primary or secondary dendrite approximately 100 µm from the soma were imaged using a 3.5X zoom. For brain sections from fixed slices treated by IHC, two reference field of views (FOVs) containing the three CA1 strata were imaged. From these, three regions of each strata were imaged using

a 2X zoom. Antibody concentrations, acquisition settings and laser power were kept constant within all experiments.

For synaptic clusters analysis of cultured neurons, the length of dendrite was traced to generate a region of interest (ROI) that was used as a mask for all other channels. A user-defined threshold was applied to each synaptic marker channel and cluster ROIs generated from thesholded area. Number and total area of clusters were quantified. Clusters smaller than 0.01 μm^2 were excluded from the analysis. Synaptic staining from IHC of brain slices was analysed using the Synapse Counter plugin for ImageJ (NIH, Bethesda, MD, USA), using the following parameters: background subtraction, 10px; maximum filtering, 1px. Clusters between 0.05 μm^2 - 5 μm^2 were considered for analysis.

2.5.3 Microglial motility analysis

Acute slices of IBA^{eGFP+} animals (plus additional transgenic modifications) were stored and imaged in HEPES-buffered ACSF (in mM): 140 NaCl, 10 glucose, 10 HEPES, 2.5 KCl, 1 $MgCl_2$, 2 $CaCl_2$, 1 NaH_2PO_4, saturated with 100%O_2 (pH 7.4). Slices were imaged between 30 minutes to 4 hours after slicing. Slices were imaged using by two-photon microscopy (Zeiss LSM 7 MP system, Mai Tai SpectraPhysics lasers). Hippocampus was found using brightfield illumination and regions containing well-labelled, unactivated microglia between 50-150 µm from the slice surface were used for live imaging analysis. For surveillance measurements, z-stacks of 52 µm (26 stacks, 2 µm interval, 512x512px) were taken every 30s for 10 minutes, except for cytochalasin D treatment which was taken every 60s for 10 minutes. CK666 and NSC23766 drug treatments were imaged at 1.5X zoom and CYFIP1 cKO at 2X zoom. For chemotaxis measurements, a circular ROI of 15 µm diameter was selected in an area surrounding by labelled microglia. High-powered laser excitation (90% power) within the ROI was used to create a lesion in the slice, using the bleaching plugin in Zen 2010 (12 iterations, 2 speed). Immediately after

lesion, 3D movies were taken using the same imaging parameters as for surveillance (2X zoom).

For chemotaxis analysis, MIPs of raw images were pre-processed using a custom ImageJ macro that involved: XY registration, background subtraction (50px), maximum filtering (2px). As part of preprocessing, single z-planes at the extremes of the stack were sometimes removed. Preprocessed MIPs were manually thresholded and analysed using a custom MATLAB script written by Dr. Renuad Jolivet (as used in (Madry et al., 2018a)). For surveillance analysis, regions containing single cells were cropped from raw images. Crops were pre-processed using a separate ImageJ macro that involved: XYZ registration, background substraction (50px), maximum filtering (2px), 3D-bleach correction. Finally, GFP signal from surrounding cells was cleared to isolate motility of a single cell. MIPs from these processed images were thresholded and inputted into a MATLAB script written by Renaud Jolivet and published in Madry et al. 2018.

2.5.4 Statistics

All data were obtained using cells from at least three independent preparations or litter-matched experimental pairs. Repeats for experiments are given in the figure legends as N numbers and refer to number of cells unless otherwise stated. All statistical analysis was carried out using GraphPad Prism (GraphPad Software, CA, USA). Data was tested for normal distribution with D'Agostino and Person to determine the use of parametric (student's unpaired t-test, one-way ANOVA, two-way ANOVA) or non-parametric (Mann-Whitney, Kruskal-Wallis) tests. For posthoc analyses of two-way ANOVA, Bonferroni posthoc tests were carried out unless stated otherwise in figure legends. Data are shown as mean ± standard error of the mean (SEM).

Chapter 3

Generation of an *in vivo* excitatory neuron-specific model of CYFIP1 loss

3.1 Introduction

Schizophrenia (SCZ) and Autistic Spectrum Disorders (ASDs) have a significant genetic component to their etiology, with numerous studies identifying copy number variations (CNVs) and rare variant mutations increasing susceptibility. Understanding the effects of these genetic abnormalities and the functions of the proteins affected is critical to improving our understanding of these conditions.

Altered morphology of neurons is a common pathology in neuropsychiatric conditions (Forrest et al., 2018; Kulkarni and Firestein, 2012). Together with dendritic spines, the architecture of the dendritic arbor determines a neuron's synaptic field and is therefore intrinsically linked to network connectivity. Though rare, studies of post-mortem brains of both ASD and SCZ patients have shown reductions in complexity of dendritic arbor in hippocampus and prefrontal cortical regions (Broadbelt et al., 2002; Kolomeets et al., 2005; Mukaetova-Ladinska et al., 2004; Raymond et al., 1996). This is supported by studies of human-derived

induced pluripotent stem cell (IPSC) neurons; conditional heterozygosity of ASD-associated SHANK3 in human IPSCs had decreased dendrite length and branching, and hIPSCs-derived neurons from SCZ patients have been shown to have reduced dendrite numbers (Brennand et al., 2011; Yi et al., 2016).

Axonal morphology is much harder to study in human tissue due to their complex and extensive arborization in the brain. However, white matter abnormalities have been found in both SCZ and ASDs patients (Aoki et al., 2017; Bopp et al., 2017; Vogan et al., 2016). Additionally, genes associated with these conditions have been shown to have important functions in axon extension and guidance, including CNTNAP2, ZDHHC8 and ROBO proteins (Anitha et al., 2008; Canali et al., 2018; Mukai et al., 2015; Potkin et al., 2009). As the sites of presynapses, defects in axonal development are often correlated with altered synaptic transmission and network connectivity (Mukai et al., 2015). Thus, changes in gross neuronal morphology are commonly associated with neuropsychiatric disorders.

As discussed, CYFIP1 is implicated in neuropsychiatric conditions through various clinical associations. In humans the gene is present in c15q11.2, an area prone to microdeletions and duplications (Cox and Butler, 2015; Zhao et al., 2013). 15q11.2 CNV loss is found in schizophrenic patients (Marshall et al., 2017; Rees et al., 2014; Stefansson et al., 2008), and both 15q11.2 duplications and deletions have been reported in individuals with ASDs (Doornbos et al., 2009; Picinelli et al., 2016; Pinto et al., 2014; van der Zwaag et al., 2010), intellectual disability and epilepsy (de Kovel et al., 2010; Nebel et al., 2016; Vanlerberghe et al., 2015). Additionally, rare variant mutations in *CYFIP1* have also been linked to ASD (Toma et al., 2014; Wang et al., 2015) and schizophrenia (Tam et al., 2010; Yoon et al., 2014). Thus, altered *CYFIP1* gene dosage is associated with various psychiatric disorders.

There is a wealth of evidence implicating CYFIP1 in regulating neuronal morphology. Early studies on neuronal CYFIP1 focused on abnormalities in axon growth and pathfinding. The Giangrande lab first showed that CYFIP1 is highly

enriched in CNS axons of Drosophila embryos and that axons of CYFIP1 null flies display abnormal midline crossing and stalled growth (Schenck et al., 2003). In murine neuronal cultures, CYFIP1 is transported to the axon growth cone in a CRMP-2 dependent manner and loss of this interaction impairs axonal extension (Kawano et al., 2005). A role for CYFIP1 in regulating presynaptic release in perinatal mice has also been established (Hsiao et al., 2016). An elegant study in zebrafish and Xenopus by the Holt lab showed that CYFIP1 was involved in early axonal extension in zebrafish retinal ganglion cells (Cioni et al., 2018). Interestingly, this paper also suggested that CYFIP1 and 2 had non-redundant functions in regulating axon extension and axon-axon interaction respectively to drive pathfinding behaviors. Though they show that dorso-ventral axon sorting was not affected by CYFIP1 deletion, expression analysis suggested that endogenous CYFIP1 was not expressed in retinal ganglion axons when axonal sorting occurred, thus leaving open the possibility of CYFIP1 function in axon sorting in other systems.

CYFIP1 has also been implicated in establishing dendritic morphology. Overexpression (OE) of CYFIP1 (and CYFIP2) increases dendritic length and branching of mouse neurons *in vitro* (Pathania et al., 2014). An *in vivo* CYFIP1 OE mouse also reported increased dendritic branching, though found decreased neurite length in layer II/III cortical neurons (Oguro-Ando et al., 2015). Reductions in CYFIP1 expression have been shown to have an opposite effect on dendrite development, with heterozygosity leading to reduced dendritic length and branching *in vitro* and *in vivo* (Pathania et al., 2014). Thus, CYFIP1 appears to have a dose-dependent effect on dendritogenesis, with increased CYFIP1 increasing arborization.

The known molecular functions of CYFIP1 suggest many possible mechanisms for alterations in neuronal morphology. As a constitutive member of the WAVE-regulatory complex (WRC), CYFIP1 could alter WRC-dependent actin branching by Arp2/3 (Kunda et al., 2003; Steffen et al., 2004). Loss of other members of the

WRC in Drosophila leads to collapse of the WRC and phenocopies CYFIP1 null defects in axonal midline crossing and synapse formation, and WAVE1 knockdown in mammalian neurons have dendritic abnormalities (Bogdan et al., 2004; Schenck et al., 2004; Xu et al., 2016). Further, Rac1 knockout mice have reduced axon extension in cerebellar granule neurons *in vitro* and *in vivo* (Luo et al., 1996; Tahirovic et al., 2010). This is caused in part by reduced localization of WRC components, including CYFIP1, to the growth cone. Cioni et al. showed that the CYFIP1 paralogue, CYFIP2, colocalised with WAVE1 in filopodia of axon growth cones (Cioni et al., 2018). Exactly how the Rac1-CYFIP1-Arp2/3 signalling axis influences growth dynamics is incompletely understood. Activity of the WRC is thought to promote neurite growth through the formation of lamellipodia. However, other roles such as endocytosis of surface receptors, stabilization of cell adhesion sites and scaffolding of transmembrane proteins could also be involved (Chen et al., 2014a; Xu et al., 2016; Yoon et al., 2014). In addition, CYFIP1 acts via the WRC to link surface receptors with established links to dendritic and axonal development, such as β-catenin, to the actin cytoskeleton (Chen et al., 2014a; Yu and Malenka, 2003).

CYFIP1 null mice die early on in embryogenesis, with failure in developmental patterning occurring soon after E8.5 (Pathania et al., 2014). As a result of this lethality, much of our understanding of CYFIP1 in the brain has come from the haploinsufficient mouse, which develops normally and is fertile (Babbs et al., 2018; Bozdagi et al., 2012; Hsiao et al., 2016). Whilst informative, there are important limitations in the use of this model. Firstly, the global loss of CYFIP1 precludes the ability to easily identify cell-autonomous effects. Multiple transcriptomic datasets have shown that CYFIP1 is expressed in many non-neuronal cell types in the brain, including astrocytes, microglia and oligodendrocyte precursors (Zeisel et al., 2018; Zhang et al., 2014a). It is well-established that altered function of glia can alter neuronal morphology and synaptic function (Barres, 2008). Thus, whilst some papers have utilized *in vitro* experiments or *in vivo* rescues to prove cell autonomous effects, precisely how loss of neuronal CYFIP1 contributes to defects observed in

the haploinsufficient mouse is largely unknown (Pathania et al., 2014; Pittman et al., 2010; Schenck et al., 2003).

The embryonic lethality of CYFIP1 null mice has also precluded the study of complete loss of CYFIP1 from neurons *in vivo*. Similarly, strategies for silencing expression, that have been used extensively in the CYFIP1 literature, will not completely abolish CYFIP1 expression (Hsiao et al., 2016; Xu et al., 2016; Yoon et al., 2014). The residual pool of CYFIP1 could well be sufficient to maintain important CYFIP1-dependent functions, as is the case for many other genes (Paolicelli et al., 2014). Given the dosage-dependent effects of CYFIP1 observed previously, the complete loss of CYFIP1 could be hypothesised to have more extreme defects compared to the haploinsufficient model.

In this chapter, a novel mouse model is developed in which the *Cyfip1* gene is conditionally knocked out from principle cells in the hippocampus and neocortex and the effects on gross neuronal morphology are investigated *in vitro* and *in vivo*. The model leads to efficient reduction of CYFIP1 expression though levels of CYFIP1-associated proteins remain unchanged. Loss of neuronal CYFIP1 is shown to cause mild decreases in complexity of hippocampal dendritic arbors. Surprisingly, an increase in extension is seen in cKO axons *in vitro*, though this cannot be validated *in vivo*. These data provide a deeper understanding of the specific effects of loss of neuronal CYFIP1 on cell morphology and form the basis for further investigation.

3.2 Results

3.2.1 Generation of neuron-specific CYFIP1 knockout

In order to investigate the effects of complete loss of CYFIP1 in neurons *in vitro* and *in vivo*, a conditional knockout mouse line was generated using the Cre-loxP system (Fig 3.1A) (Sauer, 1998). Briefly, a knockout-first strategy was used to

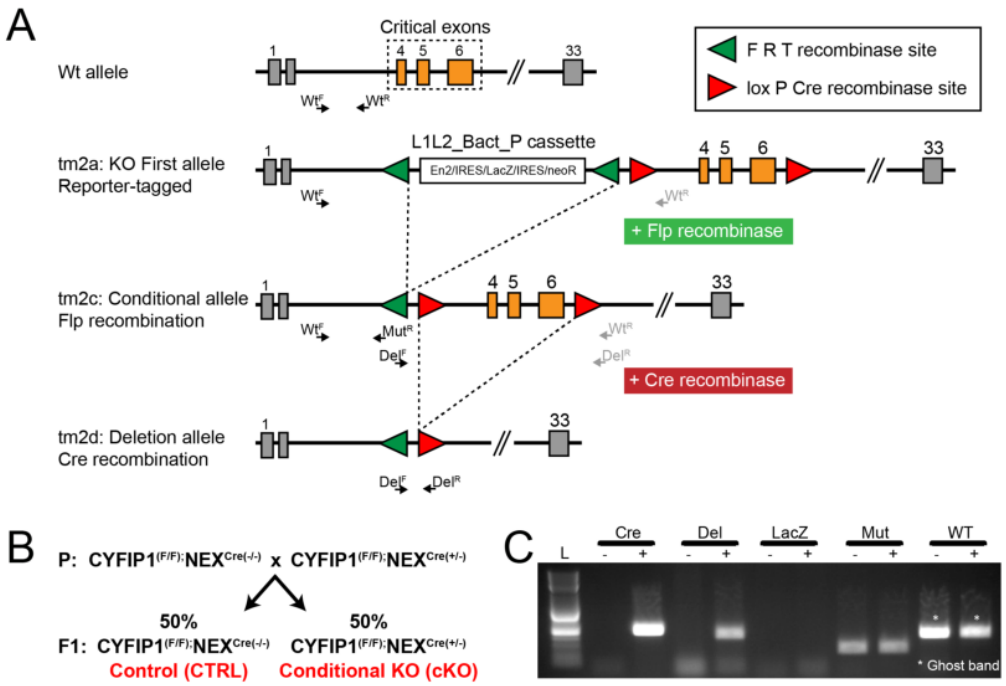

Fig. 3.1: Generation of CYFIP1 conditional knockout mouse model
(A) Schematic showing the knockout (KO)-first strategy for generating the *Cyfip1* conditional allele. The tm2a cassette inserted into the endogenous *Cyfip1* gene between exons 3 and 4 renders the gene non-expressing. tm2a contains LacZ and neomycin reporters flanked by FRT sites and critical exons 4-6 are flanked by loxP sites. To generate conditional allele, tm2a cassette is crossed with a pan-Flp recombinase mouse. Crossing tm2c with a Cre recombinase mouse excises critical exons 4-6, leading to loss of functional CYFIP1. **(B)** Diagram showing genetic cross used to produce experimental CTRL and cKO animals. **(C)** PCR analysis of tissue samples from CTRL and cKO animals confirm deletion of critical exons in the presence of Cre recombinase. Both samples are homozygous for the tm2c allele but differ in the presence of a NEX promoter-driven Cre recombinase. The deletion product (DEL), only produced in the tm2d allele, is only seen in the cKO sample as expected. Both samples lack LacZ, are positive for the CYFIP1 cassette (Mut), and lack a band at the expected size for the endogenous CYFIP1 gene (WT).

insert a reporter-tagged cassette within the endogenous *Cyfip1* gene that included a pair of loxP sites flanking exons 4-6, critical to the expression of CYFIP1 (Skarnes et al., 2011). These mice were generated by the Welcome Trust Sanger Institute. Conditional alleles were produced by crossing this line with a 'flipper mouse' to remove a reporter cassette flanked by FRT sites. To induce excision of critical exons of *Cyfip1* specifically in principle neurons in the animal, exogenous Cre recombinase expression was driven using the NEX promoter (Goebbels et al., 2006). This promoter has been shown to be active in principle neurons of the hippocampus and neocortex from early in embryogenesis, at approx. E11.5, whereas expression is absent in both granule cells of the cerebellum and in inhibitory neurons throughout the brain (Agarwal et al., 2012).

To generate experimental animals, a male and female that carried two copies (homozygous) for the conditional allele (tm2c) were crossed. Additionally, one of these animals (male or female used interchangeably) carried a single allele of the NEX^{Cre} cassette. Thus, litters from this cross were one of two genotypes; homozygous for the floxed *Cyfip1* allele with the absence or presence of a single allele of the NEX^{Cre} cassette (Fig 3.1B). These animals are denoted control ('CTRL') or conditional knockout ('cKO') respectively. Confirmation of genotype by PCR shows that both CTRL and cKO brain tissue have a band for the cassette ('Mut') but no band at the correct base pair length for the endogenous CYFIP1 gene ('WT') (Fig 3.1C). cKO tissue is positive for Cre recombinase ('Cre') and for a PCR product that detects deleted form of the CYFIP1 cassette ('Del').

Western blots generated from brain region lysates and probed using an antibody against CYFIP1 showed roughly 50% and 30% reductions in the protein level of CYFIP1 P30 hippocampus and cortex respectively (Fig 3.2A) (hippocampus: CTRL 100 ± 5.72%, cKO 53.21 ± 4.79%, $p<0.01$; cortex: CTRL 100 ± 15.38%, cKO 71.42 ± 5.21%). Levels in the cerebellum were unchanged, fitting with the expression pattern of the NEX^{Cre} driver (CTRL 100 ± 13.41%, cKO 107.5 ± 10.92%). It has previously been reported that reductions in CYFIP1 levels can destablise other WRC

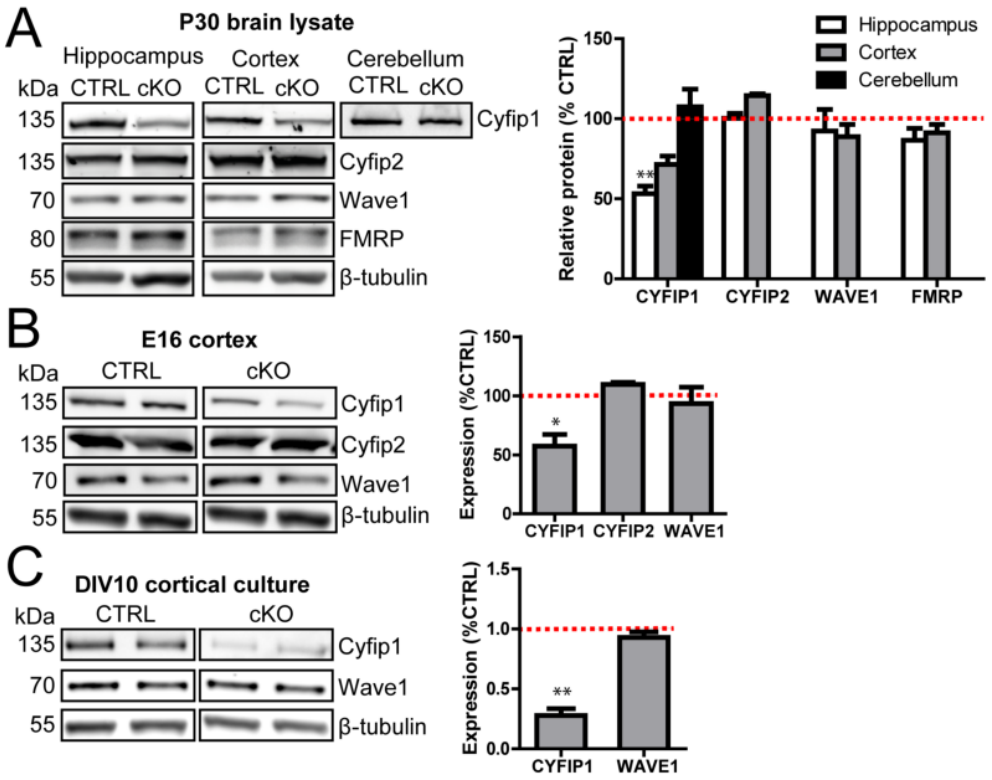

Fig. 3.2: Protein expression of CYFIP1 and CYFIP1-associated proteins in cKO
(A) Western blots of brain region lysates from P30 CTRL and cKO animals. CYFIP1 expression is reduced in the hippocampus and cortex, but not in the cerebellum. Levels of CYFIP1-associated proteins CYFIP2, WAVE1 and FMRP remain unchanged. **(B)** Western blots of cortical lysate from E16 CTRL and cKO embryos showing reduced CYFIP1 expression but unaltered CYFIP2 and WAVE1 expression. **(C)** Western blots of DIV10 cortical cultures show enhanced loss of CYFIP1 expression in neuronally-enriched cultures. N=3 individually prepared lysates per condition, Student's unpaired t-tests.

components (Bogdan et al., 2004; Yoon et al., 2014). To test if loss of neuronal CYFIP1 effected expression of key CYFIP1-associated proteins, hippocampal lysates were also probed for CYFIP2, WAVE1 and FMRP (Fig 3.2A). No changes were observed in levels of any of these proteins (CYFIP2: CTRL 100 ± 11.59%, cKO 100.2 ± 3.14%; WAVE1: CTRL 100 ± 8.14%, cKO 92.29 ± 13.47%; FMRP: CTRL 100 ± 7.72%, cKO 86.55 ± 7.42%).

The fact that the Cre-driver NEX is active in post-mitotic neurons from E11.5 means that this system should allow generation of cKO neuronal cultures from mouse embryos at E16.5. To confirm that loss of CYFIP1 occurs early on in neurogenesis, cortical lysates from E16.5 embryos were probed for CYFIP1, CYFIP2 and WAVE1 (Fig 3.2B). These results mirror that of the P30 lysates, with decrease in CYFIP1 but other levels unchanged (CYFIP1: CTRL 100 ± 8.58%, cKO 57.37 ± 9.98%, $p<0.05$; WAVE1: CTRL 100 ± 13.28%, cKO 93.31 ± 13.94%). To show this facilitates the generation of cultures lacking CYFIP1, western blot samples from cortical neuron cultures were generated from E16 embryos, which also showed a significant reduction in CYFIP1 expression, but no change in WAVE1 (Fig 3.2C) (CYFIP1: CTRL 100 ± 7.09%, cKO 27.82 ± 5.66%, $p<0.01$; WAVE1: CTRL 100 ± 4.65%, cKO 92.91 ± 4.49%). Thus, the NEX^{Cre} model appears to be a suitable system to investigate the loss of CYFIP1 from excitatory cells in the hippocampal and cortical circuits, both *in vitro* and *in vivo*.

3.2.2 Normal gross brain morphology and neuronal migration in cKO

cKO animals appear to develop normally, are fertile, and were indistinguishable from CTRL littermates. In order to see if gross brain morphology was altered, cryoslices from P30 animals were stained with FluoroNissl and FluoroMyelin to label neuronal somata and major axon tracts respectively (Fig 3.3A-B). No gross abnormalities in brain structure were observed, with normal hippocampal morphology, cortical

thickness and ventricle formation in cKO slices (Fig 3.3A). Cortico-cortical and thalamocortical axon tracts also appeared normal (Fig 3.3B). No overt differences were apparent in the size of brains between CTRL and cKO (data not shown). Thus, loss of neuronal CYFIP1 does not cause large-scale changes in brain morphology.

Previous research has shown that loss of CYFIP1 from radial glial cells (RGCs), the progenitors of principle neurons in the cortex, leads to impaired migration of neuronal progenitors (NPCs) that could underlie impact on neuronal development (Yoon et al., 2014). To test if early loss of CYFIP1 from postmitotic neurons impacts on migration of these cells, an *in utero* electroporation assay was established. Embryos from timed-pregnant mothers were electroporated with pCAG-eGFP at E14.5 and harvested four days later, at E18.5 (Fig 3.4A). This protocol targets radial glia in the subventricular zone (SVZ) that divide to generate NPCs that migrate from the SVZ through the cortical plate (CP) to reach their final destination in the upper layers of the CP (Fig 3.4B). NPCs from cKO embryos appeared to reach the upper CP normally (Fig 3.4C). Quantification of migration by counting the number of cells within distinct bins of the CP revealed no difference in the distribution of GFP+ve cells (Fig 3.4D). Additionally, cryoslices were stained for Pax6 to label RGCs in the SVZ (Fig 3.4E). Density and distribution of Pax6+ve cells appeared normal in cKO animals, in line with the assumption that the NEX^{Cre} system does not disrupt RGC function. Thus, loss of CYFIP1 in post-mitotic neurons during development does not alter migration of newly-generated neurons in the CP.

3.2.3 Loss of neuronal CYFIP1 alters neuronal morphology

Given previous research showing reductions in CYFIP1 expression impairing the formation of dendritic arbors, we hypothesized that dendritic development would be affected in the NEX^{Cre} model. To investigate this, CTRL or cKO hippocampal neurons were cultured, transfected with eGFP, fixed and imaged to reconstruct their morphology (Fig 3.5A). Analysis of reconstructions reveals a decrease in total

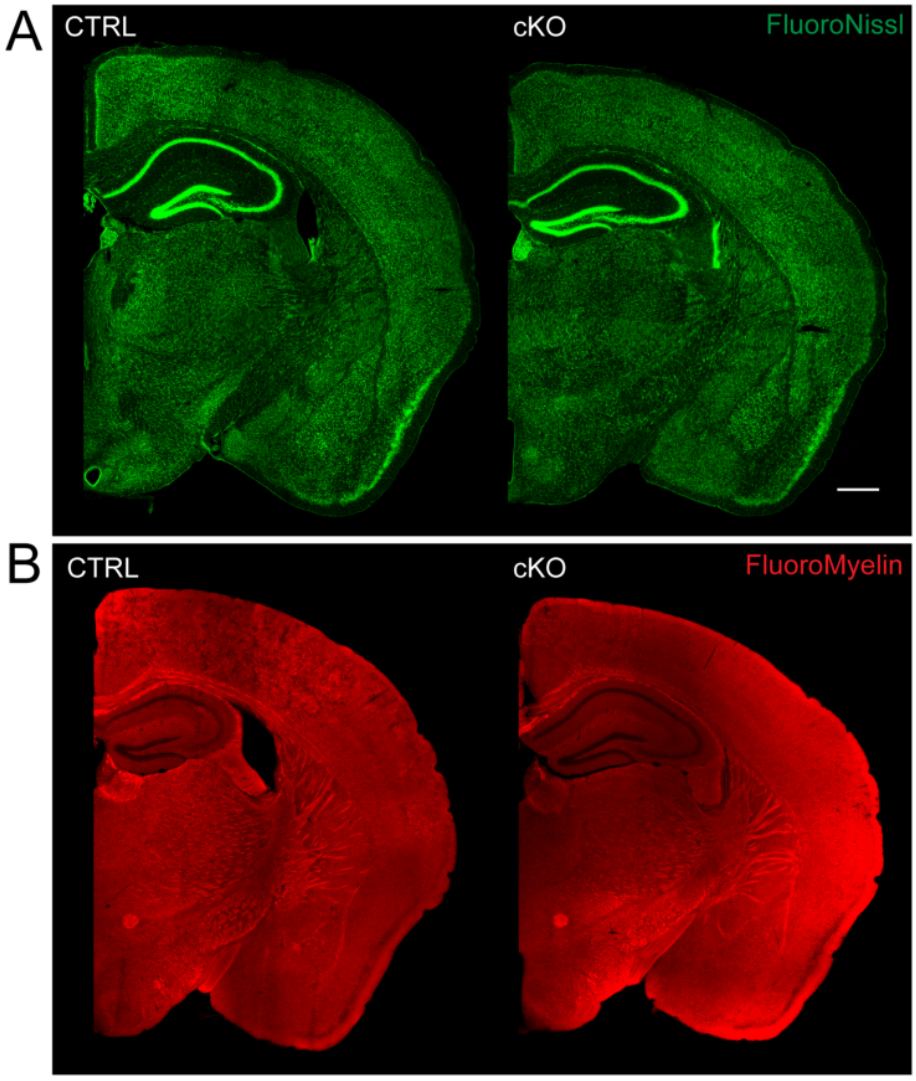

Fig. 3.3: Normal gross brain morphology in cKO
(A) Coronal section of P30 brain slices from CTRL and cKO mice. Slices stained with FluorNissl to visualise gross morphology and cell density. Regional morphology appear unchanged in cKO. **(B)** Slices stained with FluoroMyelin to visualise axonal tracts. Major callosal and thalamocortical tracts appear normal. Scale bar: 500 µm

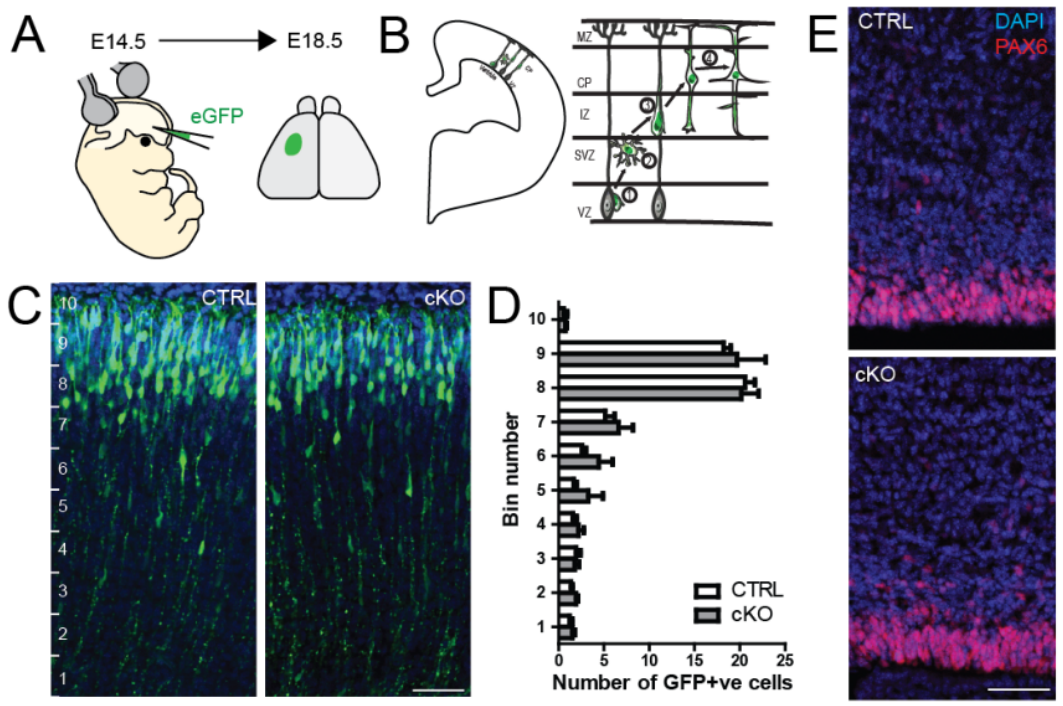

Fig. 3.4: Normal cortical migration of neuronal progenitors in cKO embryos
(A) Illustration of *in utero* electroporation procedure. Embryos are injected with eGFP plasmid into the lateral ventricle and electroporated to transfect radial glia in the subventricular zone (SVZ) at E14.5. Embryos harvested at E18.5. **(B)** Illustration of cortical migration of transfected NPCs from SVZ to the cortical plate. **(C)** Representative images of cryoslices from E18.5 embryos stained for GFP and DAPI, showing migration of cells from the intermediate zone (bin 1) to the upper cortical plate (bins 8-9). Scale bar: 50 µm. **(D)** Quantification of cell counts within each binned area of the cortical plate. No change observed between CTRL and cKO (Two-way ANOVA RM). N=3 averaged values from 3 embryos across 2 separate electroporation experiments. **(E)** IHC of DAPI and Pax6, showing normal distribution of Pax6+ve cells in the SVZ region. Scale bar: 50 µm

dendritic length (CTRL: 3148 ± 102.3 µm, cKO 2775 ± 112.5 µm, $p<0.05$) but no change in branch number (CTRL 64.28 ± 3.06, cKO 59.36 ± 2.97) in cKO neurons (Fig 3.5B. Sholl analysis to reveal changes in dendritic distribution showed no significant differences in either intersections or branches across the arbor (Fig 3.5C-D) (two-way RM ANOVA).

To see if similar alterations in dendritic morphology also occur *in vivo*, P30 brains from control and cKO animals were prepared for Golgi-Cox staining, which sparsely labels cells in the brain with silver chromate depositions to allow for visualization of morphology (Fig 3.6A). CA1 pyramidal cells were manually traced from these sections and analysed as before (Fig 3.6B). Interestingly, although total dendritic length and branching are unchanged (length: CTRL 2850 ± 162.7 µm, cKO 2708 ± 104.6 µm; branch points: CTRL 32.22 ± 3.29, cKO 32.08 ± 1.26), splitting the dendritic arbor into basal dendrites that project into the stratum oriens and apical dendrites that extend into the stratum radiatum reveal selective differences. Concretely, sholl analysis of intersections reveals a decrease in complexity across the basal arbor, whereas apical dendrites appear normal (Fig 3.6C, two-way RM ANOVA, basal: $p<0.05$, apical: NS). Total length of basal dendrites in the cKO is reduced (length: CTRL 1360 ± 65.85 µm, cKO 1099 ± 70.54 µm, $p<0.05$) whereas branch points are unaffected (Fig 3.6D-E) (CTRL 14.67 ± 1.57, cKO 13.00 ± 1.02). Length and branching of the apical arbor was unaffected (length: CTRL 1490 ± 153.5 µm, cKO 1609 ± 77.98 µm; branch points: CTRL: 17.56 ± 1.96, cKO: 19.08 ± 1.13). In conclusion, loss of CYFIP1 in neurons both *in vitro* and *in vivo* appears to cause mild changes in dendritic arbor, characterized by reduced length of dendrites.

CYFIP1 also has established roles in axon growth and pathfinding, although studies in mammalian systems have been limited. Given that NEX^{Cre} is active prior to axon formation in this model, it is a useful system for investigating early axon growth. To investigate this *in vitro*, hippocampal neurons were cultured to DIV4 and transfected with eGFP. In contrast to the reduced extension in dendrites, loss of CYFIP1 induced extended axon growth in comparison to CTRL (Fig 3.7A). Axon

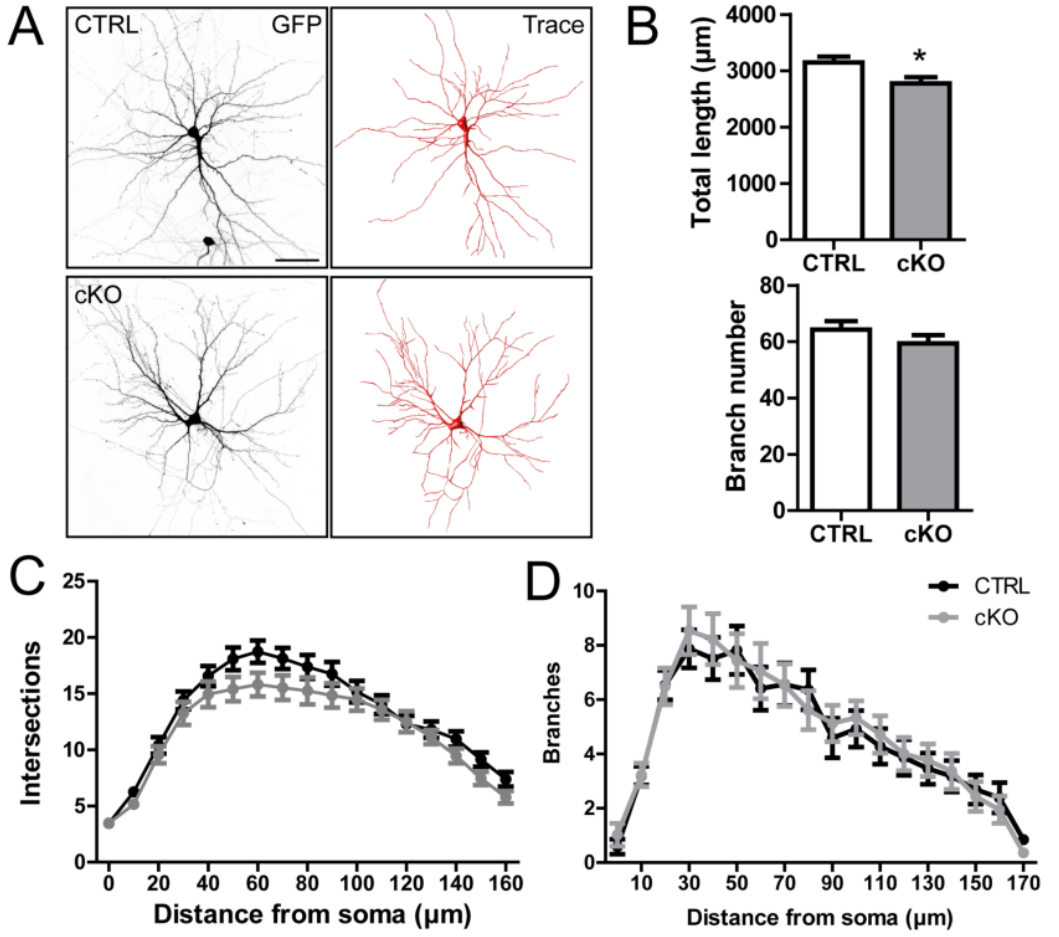

Fig. 3.5: cKO effects dendritic morphology *in vitro*
(A) Representative images of GFP-transfected hippocampal neurons at DIV14 from CTRL and cKO embryos. Reconstructions were generated from transfected cells (right). Scale bar: 50 µm. **(B)** Decreased total dendritic length ($p<0.05$, student's t-test) but normal branch number in cKO neurons. **(C)** Sholl analysis showed no significant change in dendritic complexity across the arbor by either intersection (left) or branching (right) (two-way RM ANOVA). N=39 cells from 4 separate litters.

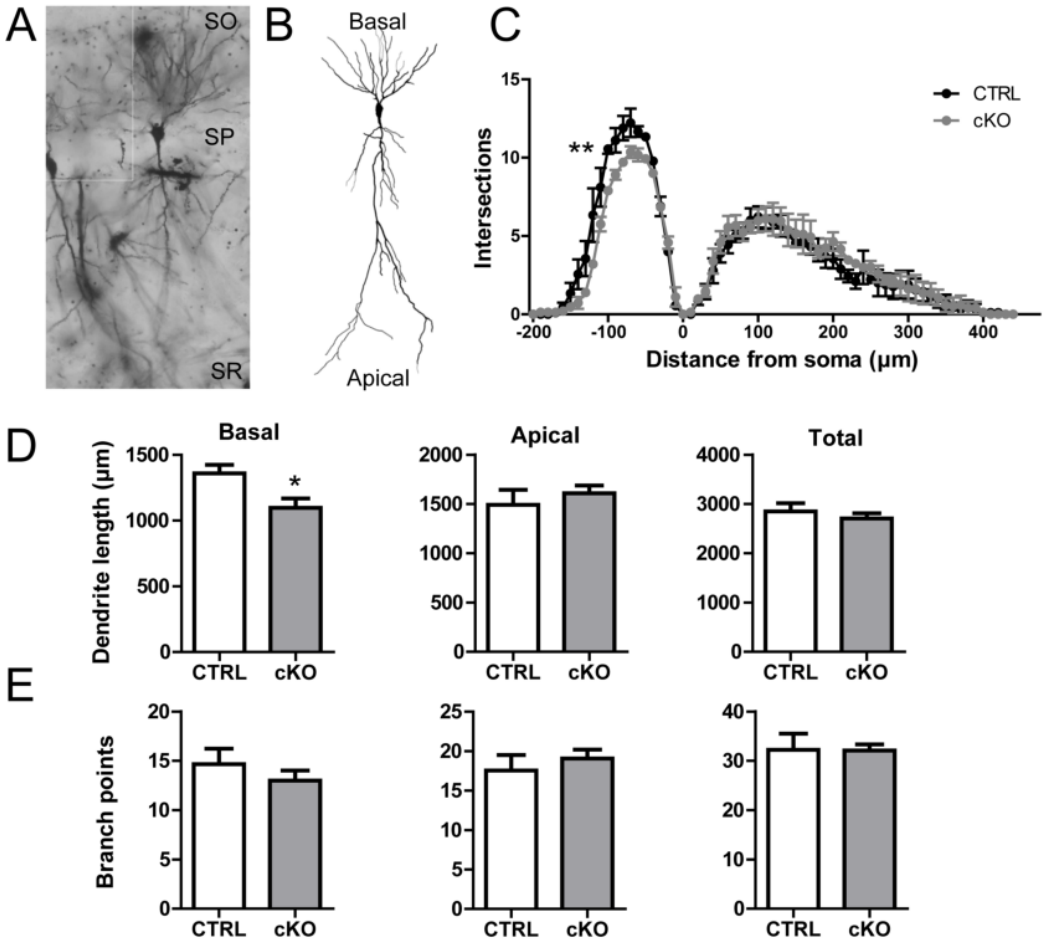

Fig. 3.6: cKO CA1 pyramidal neurons have decreased dendritic complexity
(A) Single plane from z-stack of brain slice stained using the Golgi-Cox method to sparsely label neurons, showing a single CA1 pyramidal neuron. **(B)** Example reconstruction from CTRL brain highlighting different morphology of basal and apical dendrites. **(C)** Sholl analysis of dendritic arbor showing a specific decrease in basal complexity ($p<0.01$, two-way RM ANOVA) whereas the apical arbor is unaffected. **(D)** Decrease in length of basal ($p<0.05$, student's t-test) but not apical dendrites. **(E)** Branch numbers in basal or apical dendrites are unaffected in cKO brains. N=9-13 neurons from 3 animals per condition.

length was increased by approximately 50% (Fig 3.7B) (CTRL 655.0 ± 54.63 μm, cKO 1010 ± 83 μm, $p<0.01$), with axonal branch points also increasing (Fig 3.7C) (CTRL 7.65 ± 1.04;, cKO: 11.91 ± 1.29, $p<0.05$). The number of branches per 100 μm of axon was similar between conditions, suggesting that the increase in branching was a direct consequence of the longer axon and not from intrinsically more branching (Fig 3.7D) (CTRL 1.23 ± 0.15 100 μm^{-1}, cKO: 1.24 ± 0.12 μm^{-1}).

At E18.5, cortical projection neurons labelled by IUE at E14.5 have begun sending axonal projections to the contralateral cortical hemisphere via the corpus callosum (Rashid et al., 2017). These axons are GFP-filled and thus can be visualised as they project from the ipsilateral hemisphere towards and across the midline. Given that a striking axonal extension phenotype was observed in cKO cultures, it was hypothesised that a similar phenotype could be observed *in vivo*. To assess axon crossing, the number of axons projecting towards the contralateral hemisphere were counting at two places, on entry into the midline (Fig 3.8A-B;1,3) and at the midline (Fig 3.8A-B;2,4). No differences in axon number were observed at either of these locations between CTRL and cKO embryos (Fig 3.8C-D) (entry: CTRL 11.92 ± 0.96, cKO: 9.67 ± 1.54; midline: CTRL 7.42 ± 1.54, cKO 5.75 ± 3.71). It was noted however that the variability in axon counts between embryos differed significantly within conditions, making the interpretation of these data difficult.

3.3 Discussion

In this chapter, a conditional knockout mouse line was generated in which CYFIP1 was absent from excitatory neurons in the hippocampus and neocortex. The system provides a novel and elegant basis to answer some of the outstanding questions presented by the existing CYFIP1 literature.

In validating the model, it was shown that whilst brain lysates from cKO animals had reduced levels of Cyfip1 there was still a substantial level of residual expression,

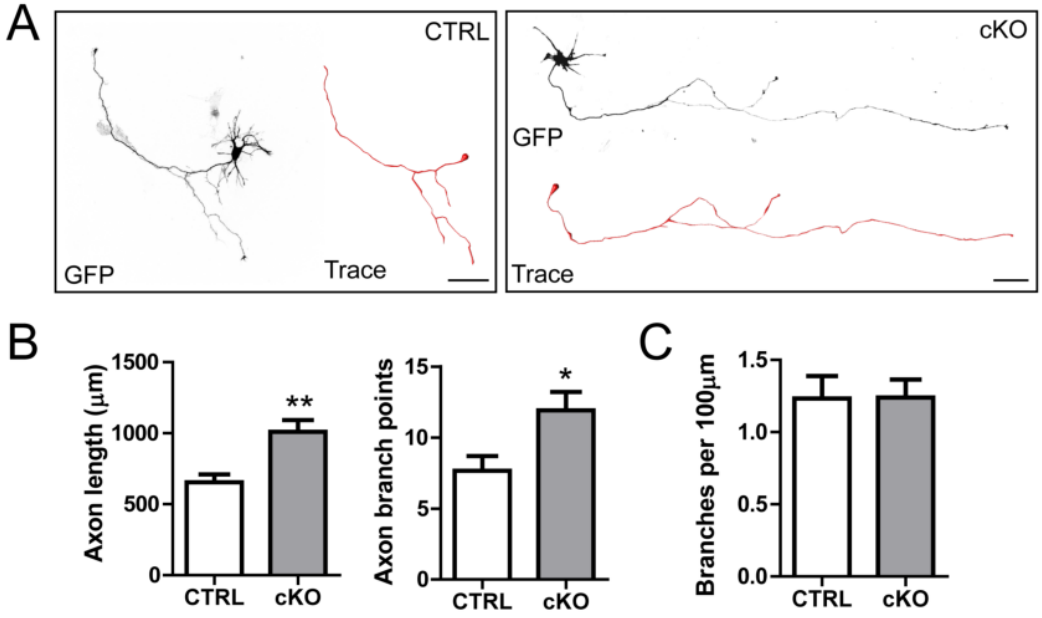

Fig. 3.7: cKO neurons have increased axon extension in vitro
(A) Illustrative images of GFP-transfected hippocampal neurons at DIV4 from CTRL and cKO embryos. Axonal reconstructions (trace) were generated by tracing the longest process extending from the soma. Scale bar: 50 µm. **(B)** Increase in total length ($p<0.01$, student's unpaired t-test) and branch number ($p<0.05$, student's unpaired t-test) of cKO axons. **(C)** Relative branch number was unchanged in cKO axons. N=22-23 neurons from 3 separate preps.

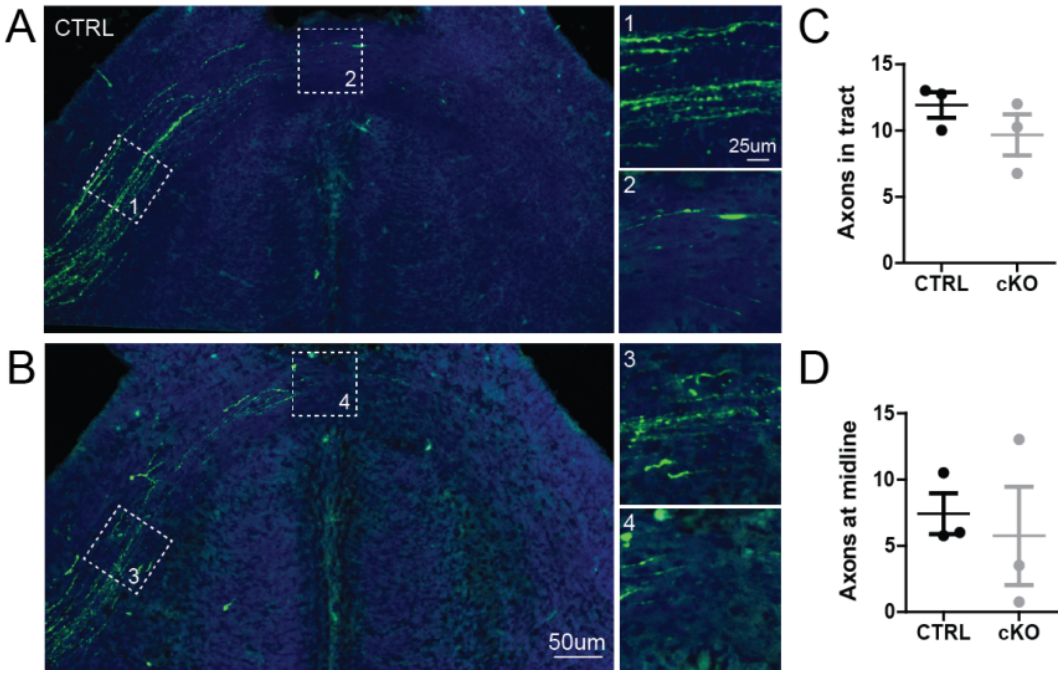

Fig. 3.8: cKO neurons have increased axon extension in vivo
(A-B) Representative images of coronal sections from E18.5 brains of CTRL and cKO showing cortical axonal projections from transfected neurons crossing the callosal commissure. Boxes show zooms of axons entering the tract (1+3) and those that reach the midline (2+4). **(C-D)** Counts of axons show no difference in number of axons either entering the tract or extending past the midline. N=3 averaged values from 3 embryos across 2 separate electroporation experiments.

suggesting that CYFIP1 is expressed by cells types aside from principle neurons in the brain. Data from recent RNAseq resources hints that many glial cell types in the brain highly express CYFIP1, including microglia, astrocytes and OPCs (Zeisel et al., 2018; Zhang et al., 2014a). The fact that CYFIP1 is reduced by approximately 50% in E16 cortex compared to 30% in 1 month old animals further supports this, given that the E16.5 brain contains relatively more neurons, being prior to the peak of gliogenesis. Given this, the presence of some residual CYFIP1 expression in neuronal cultures from cKO embryos is not unexpected, as these cultures contain significant astrocyte and OPC numbers (Hui et al., 2016).

Loss of CYFIP1 did not alter levels of WAVE1 or FMRP. In Drosophila, loss of dCYFIP1 resulted in collapse of the WRC and reduced expression of other constituents, and reduced CYFIP1 levels reduces WAVE expression in primitive neural precursor cells (Bogdan et al., 2004; Nebel et al., 2016; Schenck et al., 2004; Yoon et al., 2014). However, heterozygous CYFIP2 mice have reduced WAVE1 expression in cortex but not hippocampus, and silencing of CYFIP1 does not reduce WAVE1 signal in neuronal cultures (Bozdagi et al., 2012; Han et al., 2015; Hsiao et al., 2016). Thus, reduced CYFIP1 has differential effects on WRC stability, depending on the cell types and organism.

The discrepancies observed in the studies mentioned above alongside data presented here could be explained by differential expression of CYFIP proteins in these different systems. Investigation of available transcriptomic data of different cell types suggests that the composition of the WRC, based on expression of constituent paralogs, is cell-type specific. For instance, astrocytes and microglia almost exclusively express CYFIP1, whereas Oligodendrite Precursor Cells (OPCs) express both paralogues and neurons preferentially express CYFIP2. Concretely, WRC stability would be more affected in cell types in which CYFIP1 is the primary CYFIP protein, whereas cell types/lines with high CYFIP2 levels may be able to compensate efficiently for this loss. One might expect to observe an increase in expression of opposing paralog in this case, though this was not observed in these

data or in the heterozygous model (Hsiao et al., 2016). This could mean that basal levels of neuronal CYFIP2 are high enough to compensate for loss of CYFIP1, at least in terms of WRC stabilisation.

A previous study used silencing of CYFIP1 in RGCs to show defects in neuronal migration due to disrupted adheren junctions (Yoon et al., 2014). An outstanding question from this study was whether this delay was solely due to impaired RGC function or whether loss of CYFIP1 in NPCs could play an additional role. The NEX^{Cre} driver provides an elegant way to answer this as CYFIP1 is lost only in post-mitotic neurons and not RGCs, and has been used to show neuron-specific migration defects in NPCs (Rashid et al., 2017). No change in migration of neurons is observed in the cKO embryos, suggesting that neuronal CYFIP1 is not required for migration of NPCs across the cortical plate, but is important for RGC adhesion. These data are consistent with the observation that cKO animals show no overt changes in layering of the neocortex and brain morphology appears normal.

A number of experiments were undertaken aimed at understanding the effects of CYFIP1 loss in determining gross neuronal morphology. Prior research has identified CYFIP1 as a key regulator of dendritic morphology, and suggested a dose-dependence of protein expression on complexity of the dendritic arbor (Oguro-Ando et al., 2015; Pathania et al., 2014). Given this, it is surprising that complete loss of CYFIP1 in the cKO model has a relatively mild effect on dendritogenesis, with a consistent but minor reduction in total dendritic length observed in both hippocampal cultures and in basal arbor of CA1 pyramidal neurons *in vivo*. Indeed, the scale of this effect is similar to what has been observed previously in haploinsufficient mice (Pathania et al., 2014). A likely explanation for this is functional compensation by neuronal CYFIP2. In support of this, Xu et al. showed that silencing of both CYFIP1 and 2 had a much greater impact on neurite outgrowth than knockdown of individual CYFIP proteins (Xu et al., 2016). Additionally, overexpression of CYFIP1 and 2 have identical effects on dendrite growth, supporting their functional redundancy in dendrite development (Pathania et al., 2014). Given this, the silencing of CYFIP2

in this cKO model would be predicted to cause much more extreme defects than presented here. In combination with the *in utero* eletroporation technique described here, this would enable the first study of *in vivo* effect of loss of both CYFIP proteins in mammalian systems and would provide an interesting comparison to the Drosophila literature.

If CYFIP2 is able to efficiently compensate for CYFIP1 function in neurons, it raises the question of why there are any defects observed in CYFIP1-depleted systems. In 2014, the Rosen lab identified a binding surface on the WRC formed by the interaction between Sra1 (CYFIP1) and Abi2 (Chen et al., 2014a). Though its role in dendrite development has not been established, many of the surface receptors containing the WIRS-motif have established roles in dendritogenesis, such as the protocadherins (Keeler et al., 2015; Molumby et al., 2017, 2016). It is possible that this binding surface is altered or absent in the CYFIP2-containing WRC and thus these interactions between surface receptors and the actin cytoskeleton would be disrupted. It would be interesting to test if these defects could be replicated by inhibition of the WIRS interaction using a published peptide sequence (Chen et al., 2014a). Alternatively, overreliance on CYFIP2 could lead to gain-of-function effects from known CYFIP2-specific functions, such as interaction with FXR1P/2P (Schenck et al., 2001). Indeed, loss of FXR2P decreases dendritic complexity of granule cells in the dentate gyrus, providing a potential mechanism by which this could occur (Guo et al., 2015; Schenck et al., 2001).

The increase in axon length observed in cultured cKO neurons is surprising given published literature suggesting reduced CYFIP1 causing impaired axonal extension (Cioni et al., 2018; Kawano et al., 2005; Schenck et al., 2003). A potential explanation for this derives from studies on the effects on Arp2/3 inhibition on axon extension. Whilst the literature is divided, a number of studies have reported inhibition of Arp2/3 activity leading to increased axon extension and pathfinding defects (Pinyol et al., 2007; Strasser et al., 2004). Arp2/3 is located predominantly in the central regions of the growth cone rather than the periphery and isn't required for

filapodia formation. Rather, Arp2/3 may help dampen microtubule-driven extension through competitive dynamics between actin and microtubules in the central growth cone. Loss of CYFIP1 could mirror inhibition of the Arp2/3 complex via reduced activation by the WRC. Indeed, Strasser et al. report similar effects on axon growth upon expression of the VCA domain of WAVE1 to inhibit Arp2/3.

It is worth mentioning that effects of Arp2/3 inhibition on axon extension and pathfinding are substrate-dependent, with Arp2/3 activity being required for axon turning on L1 but not laminin (San Miguel-Ruiz and Letourneau, 2014). Interestingly, both studies reporting increased axon extension on Arp2/3 inhibition used poly-lysine (PLL) as a substrate, as used in the data presented here (Pinyol et al., 2007; Strasser et al., 2004). This could explain the discrepancies between these data and *in vivo* effects of CYFIP1 loss.

Investigation of midline crossing of axons from cortical neurons labelled via *in utero* electroporation did not replicate the *in vitro* findings of axonal hyperextension. There are several important caveats to this. Firstly, the *in vitro* effect was seen in hippocampal, not cortical neurons, and there may be differences in the role of axonal CYFIP1 between these. Secondly, it is worth mentioning that getting an accurate representation of the distance travelled by axons was difficult, as there was a lot of variability within conditions due to subtle differences in cutting angle and location of labelled cells. As a result, the experiment was likely to be underpowered. To test this hypothesis more robustly, clearing embryonic brains and imaging the whole callosal tract using light-sheet microscopy would solve the issue of slice sample error. Alternatively, analysing contralateral axonal arborisation at a postnatal timepoint is possible, where the more extensive arborisation is easier to track, and has been used previously to show defective axonal development (Mukai et al., 2015). Two recent pre-publication reports have both reported white matter abnormalities in rodent CYFIP1 haploinsufficient models, including thinning of the corpus callosum and reduced myelination of callosal axons (Dominguez-Iturza et al., 2018; Silva et al.,

2018). Interestingly, the two reports draw different conclusions about the cellular origins of these effects, highlighting the need for cell-specific models.

The axonal hyperextension observed *in vitro* is interesting in the context of a recent study showing increased VGLUT1 clusters and presynaptic release in haploinsufficient mice (Hsiao et al., 2016). This study posits a mechanism based on an increased ready releasable vesicle pool. However, the haploinsufficient phenotype could equally be explained by increased axon growth leading to more presynaptic terminal formation. Further, the timing of the recovery of this effect aligns with a period of axonal pruning in the hippocampus that would provide an explanation for recovery later in development described by Hsaio et al. (Faulkner et al., 2007).

Taken together, these data suggest that neuronal CYFIP1 does indeed have a role in controlling hippocampal neuron morphology both *in vitro* and *in vivo*. Surprisingly, complete loss of CYFIP1 does not have a more severe effect on dendritic arborisation than haploinsufficiency. Additionally, a novel role for CYFIP1 as a potential inhibitor of axon extension is reported. These data provide clarification of the cell-autonomy of known CYFIP1-depletion phenotypes and provide insight into the precise importance of CYFIP1 to these processes.

Chapter 4

Impact of loss of neuronal CYFIP1 on synaptic form and function

4.1 Introduction

In the previous chapter, a novel mouse model was developed in which the CYFIP1 gene was conditionally knocked out in principle neurons of the hippocampus and neocortex. This model was used to investigate how loss affected dendritic and axonal development. However, CYFIP1 has also been strongly associated with changes in network connectivity and function at the level of the synapse. Improving our understanding of how CYFIP1 is involved in regulating synapse formation, stability and functionality remains a key topic in gaining insight into its association with neuropsychiatric disorders.

Dendritic spines are the major postsynaptic site for excitatory transmission in principle neurons (Berry and Nedivi, 2017). The shape of spines is modulated throughout development and changes in spine morphology are also associated with experience-dependent plasticity (Holtmaat and Svoboda, 2009). In line with their central role in information transmission in the brain, alterations in the density and

shape of dendritic spines are a hallmark of many neuropsychiatric disorders, including SCZ and ASDs (Hutsler and Zhang, 2010; Moyer et al., 2015; Penzes et al., 2011). Similar changes have also been observed in conditions comorbid with psychiatric disorders, such as epilepsy and ID, suggesting that dendritic spines are an important point of convergence (Kaufmann and Moser, 2000; Swann et al., 2000). Imaging studies have shown that both haploinsufficiency and overexpression of CYFIP1 leads to a shift towards immature spine phenotypes and altered synaptic receptor stability (de Rubeis et al., 2013; Oguro-Ando et al., 2015; Pathania et al., 2014). Whilst haploinsufficiency of CYFIP1 doesn't alter spine density in the hippocampus, Oguro-Ando et al. reported overexpression leading to an increase in spine density in layer II/III pyramidal neurons.

The increased density of immature spines is reminiscent of spine pathology observed in both patients and FMR1 KO mouse model of Fragile X Syndrome (FXS) (Comery et al., 1997; Hinton et al., 1991). Indeed, CYFIP1 reduction recapitulates many physiological changes seen in FXS models, including enhanced mGluR-dependent LTD, increased expression of FMRP-targets and impaired avoidance behaviours (Bozdagi et al., 2012; Dölen et al., 2007; Napoli et al., 2008). Thus, correct CYFIP1 dosage is required for normal form and function of the excitatory postsynapse.

Studies of CYFIP1-deficient systems have also uncovered roles at the presynapse. The known roles of CYFIP1 in axon extension and pathfinding, discussed previously, are also associated with impaired synapse formation; dCYFIP null Drosophila have severely shortened neuromuscular junctions with immature features termed supernumerary buds (Abekhoukh et al., 2017; Schenck et al., 2003). Further, a role for CYFIP1 in regulating presynaptic release was recently established in the haploinsufficient mouse. Juvenile CYFIP1 haploinsufficient mice have increased presynaptic terminal size and vesicle release probability, that leads to increased frequency of mEPSCs in hippocampal recordings at P10 (Hsiao et al., 2016). Interestingly, this effect is lost by P21.

A number of the outstanding questions raised previously about the interpretation of models involving global changes in CYFIP1 levels exist for the synaptic literature. Whilst the focus of mammalian CYFIP1 research has been almost solely on principle cells of the CA1 (hippocampus) and layer II/III (neocortex), whether observations arise solely from changes in this subset of neurons is unclear. Firstly. the balance between excitation and inhibition in the brain is tightly regulated by processes such as synaptic scaling and homeostatic plasticity (Turrigiano, 2012, 2008). Thus, changes in activity of pyramidal cells can be caused by indirect changes in inhibitory interneurons or long-distance projection neurons, neither of which have been studied in the haploinsufficient model. Additionally, glial cells play a critical in establishing, maintaining and refining synaptic connections. Given the data presented in the previous chapter suggesting high CYFIP1 expression in certain glia, it is possible that some of these effects could have a non-neuronal origin. Interestingly, key dendritic spine phenotypes associated with FXS can be recapitulated in an astrocyte-specific knockout of FMRP, suggesting that interpretation of global genetic models may not be as straight forward as previously assumed (Higashimori et al., 2013, 2016). Thus, a neuronal conditional knockout model enables distinctions to be made between cell-autonomous and non-autonomous effects of CYFIP1 in relation to synapse form and function.

Altered inhibitory signalling and balance between excitation and inhibition (E/I balance) is a common feature of many neuropsychiatric disorders, as illustrated by the close clinical association between ASDs and epilepsy (Bolton et al., 2011). Synaptic inhibition is mediated by $GABA_A$ receptors, whose localisation and stabilisation at the postsynapse is regulated by a diverse array of transmembrane proteins, cytoskeletal anchors and intracellular signalling molecules (Davenport et al., 2018; Smith et al., 2014; Südhof, 2008). Interestingly, several members of the inhibitory postsynaptic density (iPSD) are associated with schizophrenia and ASDs, including NLGN3 and Shank-2, directly implicating the inhibitory postsynapse in disease (Leblond et al., 2012; Peykov et al., 2015; Rothwell et al., 2014).

To date, a role for CYFIP1 at the inhibitory postsynapse has not been described. However, the actin remodelling and translational repression functions of CYFIP1 suggest possible relevance. The iPSD is integrally linked to the actin cytoskeleton, primarily via interactions between Gephyrin and and actin-regulatory proteins (Bausen et al., 2006; Luscher et al., 2011). Indeed, many of these actin signalling pathways are shared between excitatory and inhibitory synapses; a postsynaptic signalling complex involving Rac1 and the Rac1 GEF, βPIX, first identified as modulating excitatory spine morphogenesis has since been shown to be critical for stabilization of inhibitory $GABA_A$ receptors (Smith et al., 2014; Zhang et al., 2005). Additionally, a number of mRNA targets of FMRP-CYFIP1 complex screens are members of the iPSD with known associations with psychiatric disorders, including $GABA_A$Rs, $GABA_B$Rs and neuroligins (Ascano et al., 2012; Darnell et al., 2011). Thus, it could be hypothesised that many of the described roles for CYFIP1 at the excitatory synapse could apply to the inhibitory postsynapse.

In this chapter, the NEX^{Cre} model is used to investigate the effect of loss of neuronal CYFIP1 to both excitatory and inhibitory synapse form and function. Surprisingly, we see no effect of CYFIP1 on dendritic spines or synapse formation *in vitro*. However, *in vivo* we report hippocampal hyperexcitability in pups that is recovered in young adults. Additionally, we find a novel role for CYFIP1 in restraining postsynaptic inhibition. Synaptic staining, protein expression and functional recordings all point to enhanced inhibitory transmission in cKO young adult mice. As excitatory transmission is normal in these animals, this enhanced inhibition represents a shift in the balance of excitation and inhibition. Given the close clinical relevance of altered inhibition and E/I balance to neuropsychiatric disorders, this novel role of CYFIP1 in regulating the inhibitory postsynapse suggests a new mechanistic link between CYFIP1 and these conditions.

4.2 Results

4.2.1 Normal synapse formation in cKO neurons *in vitro*

To investigate the effect of CYFIP1 loss on dendritic spine formation, hippocampal neurons were cultured to DIV18, when the *in vitro* network is mature, and transfected with eGFP to visualise spines (Fig 4.1A). Counting of spines along secondary processes showed no difference in the density of spines, although the mean density was roughly 10% higher in cKO over control (Fig 4.1C) (CTRL: 0.64 ± 0.03 μm^{-1}, cKO: 0.71 ± 0.04 μm^{-1}). Dendritic spines are morphologically diverse, and a range of spine lengths and head widths were observable (see arrows). To assess spine morphology, a 3D estimation of key morphological parameters was undertaken (Fig 4.1D-E). No significant differences in the average length or width of spines were observed (length: CTRL 1.39 ± 0.04 µm, cKO 1.41 ± 0.03 µm; width: CTRL 0.92 ± 0.02 µm, cKO 0.89 ± 0.01 µm). In line with this, the spine length-head width ratio (LWR), which has been used as a readout of spine maturity, was unchanged in cKO (Forrest et al., 2018) (CTRL 0.88 ± 0.03, cKO 0.85 ± 0.03). Thus, loss of neuronal CYFIP1 does not alter either the density or morphology of dendritic spines *in vitro*.

It is possible that functional changes in excitatory synapses can occur without overt changes in dendritic spines. To investigate this, DIV18 hippocampal neuron cultures were stained by ICC for core components of the excitatory pre- and post-synapse, using VGLUT1 and Homer, respectively (Fig 4.2A). Clear punctate clusters of both proteins were observable that were often juxtaposed to one another (white arrows). Cluster analysis showed no change in the number and area of either VGLUT and Homer clusters in cKO cultures (Fig 4.2B-C) (VGLUT1 number: CTRL 29.22 ± 2.04, cKO 29.90 ± 2.43; VGLUT1 area: CTRL 6.20 ± 0.61 μm^2, cKO 7.41 ± 1.08 μm^2; HOMER number: CTRL 34.82 ± 1.53, cKO 32.36 ± 2.96; HOMER area: CTRL 7.644 ± 0.64 μm^2, cKO 7.19 ± 0.82 μm^2).

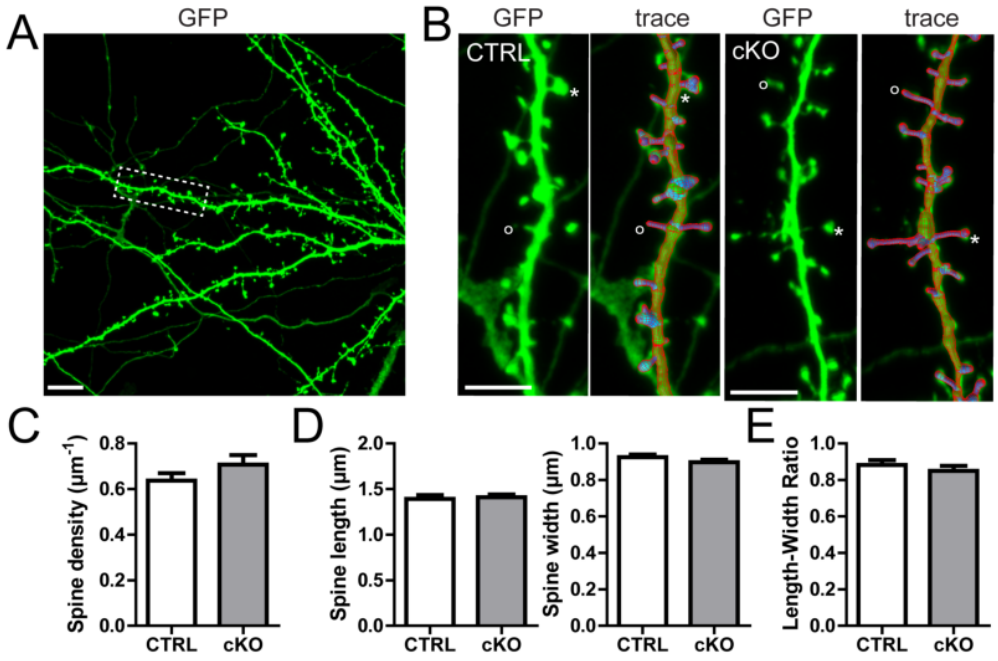

Fig. 4.1: Dendritic spines *in vitro* are normal in cKO
(A) Image of GFP transfected DIV18 hippocampal neuron showing region of secondary dendrite selected for spine analysis. Scale bar: 10 µm. **(B)** Images of dendritic spines from DIV18 neurons from CTRL (left) or cKO (right) cultures. Right panels show surface rendered reconstructions of dendritic shaft and spines. Scale bar: 5 µm. **(C)** No change in density of spines in cKO. **(D-E)** Morphological characteristics of spines are normal, with no change in length, width or length-width ratio in cKO. N=22 cells from 3 separate litters.

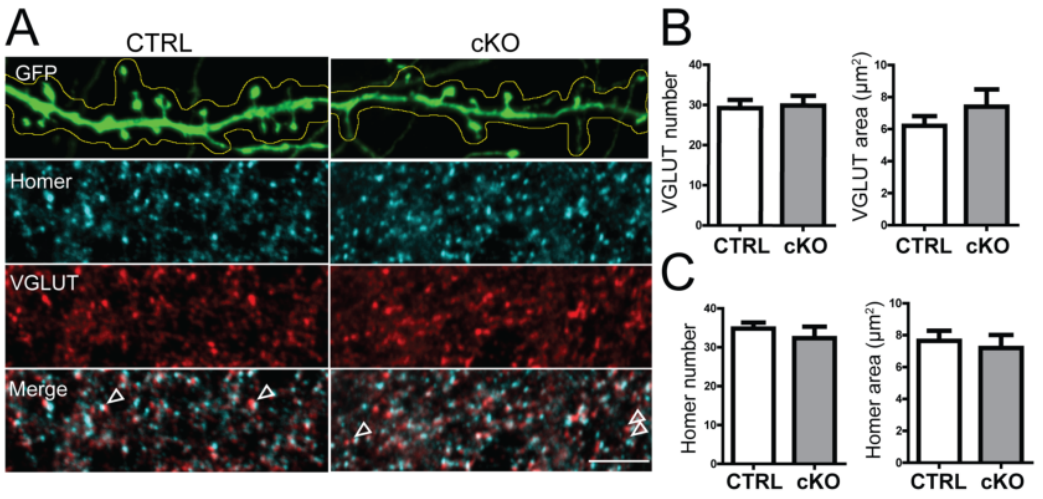

Fig. 4.2: Excitatory synapse formation in cKO is normal *in vitro*
(A) GFP-filled DIV18 neuronal cultures stained for VGLUT1 and HOMER to label excitatory pre- and postsynaptic compartments respectively. Representative regions from CTRL (left) and cKO (right) cultures. Superimposing images (bottom panels) shows VGLUT and Homer puncta apposed to one another (white arrows). Scale bar: 5 µm. **(B)** Analysis of VGLUT1 clusters shows no change in number or total area. **(C)** Analysis of Homer clusters shows no change in number or total area.

Hippocampal cultures contain approximately 6% inhibitory interneurons and by DIV18 have well-established inhibitory connectivity (Benson et al., 1994). Previous results in the lab suggested that CYFIP1 was present at inhibitory synapses. To confirm this, DIV18 neurons were stained for CYFIP1 and Gephyrin, to label the inhibitory postsynapse (Fig 4.3A). CYFIP1 staining was punctate in the processes (white outline), and regularly seen in association with Gephyrin punta. High magnifications showed CYFIP1 signal both colocalised with Gephyrin (Fig 4.3A, right) and forming ring-like structures around punta. As the vast majority of CYFIP1 is present in complexes, it was hypothesised that other components of the WRC would show the similar localisation. ICC staining for WAVE1 showed very similar associations to Gephyrin structures as CYFIP1 (Fig 4.3B). Specifically, ring-like WAVE1 signal was regularly observed surrounding Gephyrin. Thus, CYFIP1 is localised at the inhibitory postsynapse, and is likely complexed in the WRC.

To see if loss of CYFIP1 in principle neurons altered the development of inhibitory synapses, the same DIV18 neurons were stained for VGAT and Gephyrin to label inhibitory pre and postsynaptic compartments (Fig 4.4A). Inhibitory synapses were sparser and preferentially formed on the dendritic shaft rather than spines (dotted line). Comparing CTRL and cKO cultures, no changes in either VGAT or Gephyrin cluster number or area were observed (Fig 4.4B-C) (VGAT number: CTRL 13.60 ± 1.40, cKO 12.52 ± 1.62; VGAT area: CTRL 2.61 ± 0.6 μm^2, cKO 1.99 ± 0.30 μm^2; Gephyrin number: CTRL 13.27 ± 1.50, cKO 11.94 ± 1.11; Gephyrin area: CTRL 2.71 ± 0.39 μm^2, cKO 2.55 ± 0.39 μm^2). Together, these data suggest that loss of CYFIP1 in principle cells does not alter the formation of excitatory or inhibitory synapses *in vitro*.

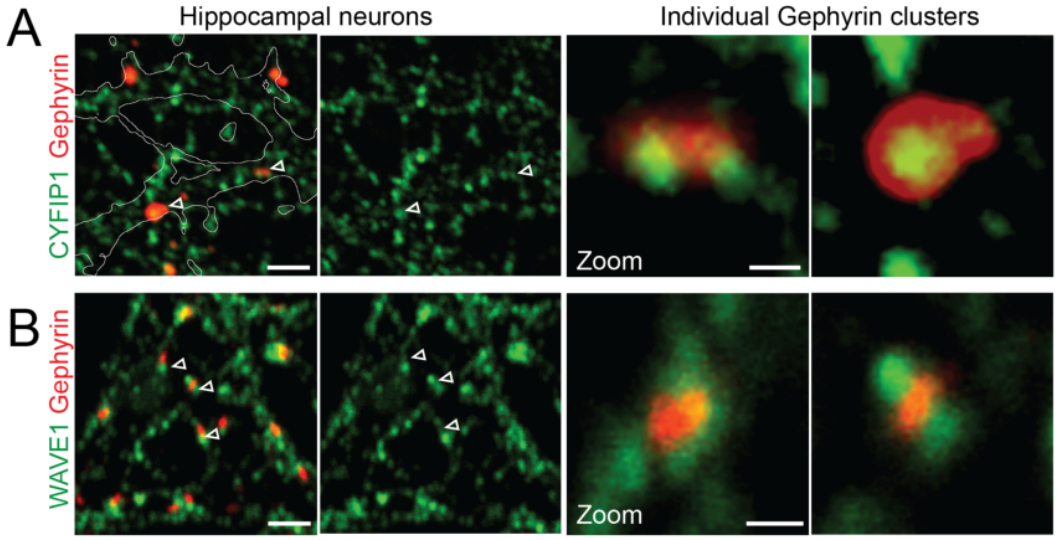

Fig. 4.3: CYFIP1 and the WAVE regulatory complex are present at inhibitory synapses **(A)** DIV18 neuronal cultures stained for CYFIP1 and Gephyrin. Left: CYFIP1 puncta are often found in association with Gephyrin clusters (white arrows). Right: High magnification images showing different interactions, including apposition (left) and colocalisation (right). Scale bars: 2 µm (left), 0.5 µm (right). **(B)** Immunocytochemical staining for WAVE1 and Gephyrin. Left: WAVE1 puncta are often found in association with Gephyrin clusters (white arrows). Right: Zoomed images showing WAVE1 encapsulating Gephyrin puncta. Scale bars: 2 µm (left), 0.5 µm (right).

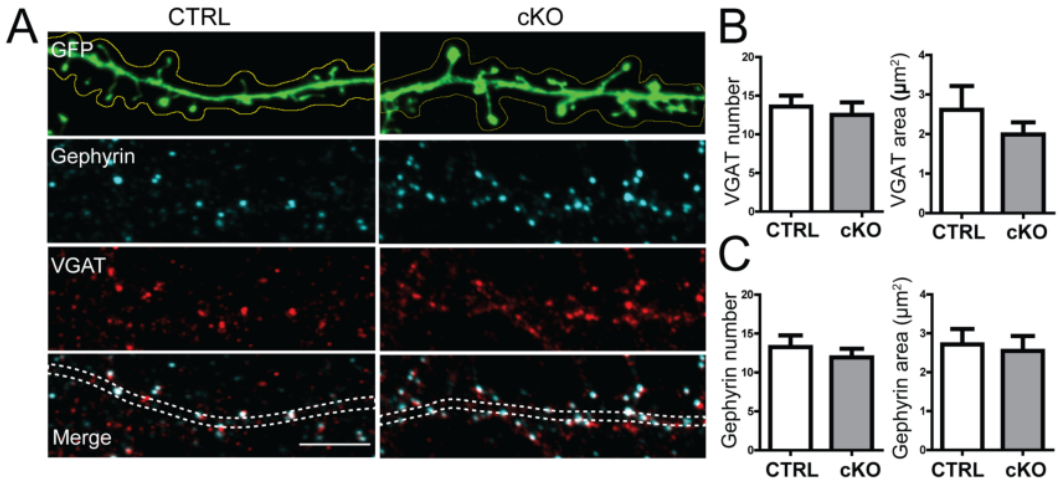

Fig. 4.4: Inhibitory synapse formation in cKO is normal *in vitro*
(A) GFP-filled DIV18 neuronal cultures stained for VGAT and Gephyrin to label inhibitory pre- and postsynaptic compartments respectively. Representative regions from CTRL (left) and cKO (right) cultures. Superimposing images (bottom panels) shows VGAT and Gephyrin puncta apposed to one another. Scale bar: 5 µm. **(B)** Analysis of VGAT clusters shows no change in number or area. **(C)** Analysis of Gephyrin clusters shows no change in number or area. N=16-18 cells from 3 separate litters.

4.2.2 Changes in dendritic spines and excitatory synapse form and function *in vivo*

Having observed the surprising lack of effects of CYFIP1 loss on network connectivity *in vitro*, it was hypothesised that CYFIP1 loss may have differing effects *in vivo*. Hsaio et al. reported an increase in VGLUT cluster numbers and area at P10 in CYFIP1 haploinsufficient mice (Hsiao et al., 2016). To see if this effect is observed in our cKO model, P10 cryoslices from CTRL and cKO brains were stained for VGLUT1 and Homer by IHC. Fluorescence imaging showed dense staining in the stratum oriens and stratum radiatum layers of the CA1, with very little signal in the pyramidale layers (Fig 4.5A). This is consistent with the fact that the majority of excitatory inputs onto CA1 pyramidal neurons are onto dendrites rather than cell somas. Cluster analysis showed an increase in the total area of VGLUT1 staining in the radiatum (Fig 4.5D) (oriens: CTRL 358.7 ± 12.54 μm^2, cKO 358.4 ± 12.89 μm^2; radiatum: CTRL 336.5 ± 7.89 μm^2, cKO 370.6 ± 12.68 μm^2, $p<0.05$). No change in Homer cluster area is seen (oriens: CTRL 349.6 ± 3.84 μm^2, cKO 332.8 ± 8.13 μm^2; radiatum: CTRL 336.0 ± 5.62 μm^2, cKO 318.7 ± 6.64 μm^2).

In support of this, mEPSCs recorded from CA1 pyramidal cells in P10-11 acute slices of CTRL and cKO animals by Dr Blanka Sculz have found an increase in the frequency of mEPSCs (frequency: CTRL: 0.54 ± 0.16Hz, cKO: 1.21 ± 0.24Hz, $p<0.05$, student's unpaired t-test; amplitude: CTRL: -18.03 ± 1.38pA, cKO: -17.29 ± 0.73pA). The original observation of enhanced VGLUT1 clustering at P10 was limited to the CA1. To see if this change also occurred in the neocortex, regions of layer II/III somatosensory cortex were analysed (Fig 4.6A). In contrast to CA1, no change in VLGUT1 cluster area was observed (Fig 4.6B) (CTRL 225.0 ± 9.23 μm^2, cKO 216.8 ± 5.95 μm^2). Together, these data reveal a specific increase in excitatory transmission in the hippocampus of cKO pups.

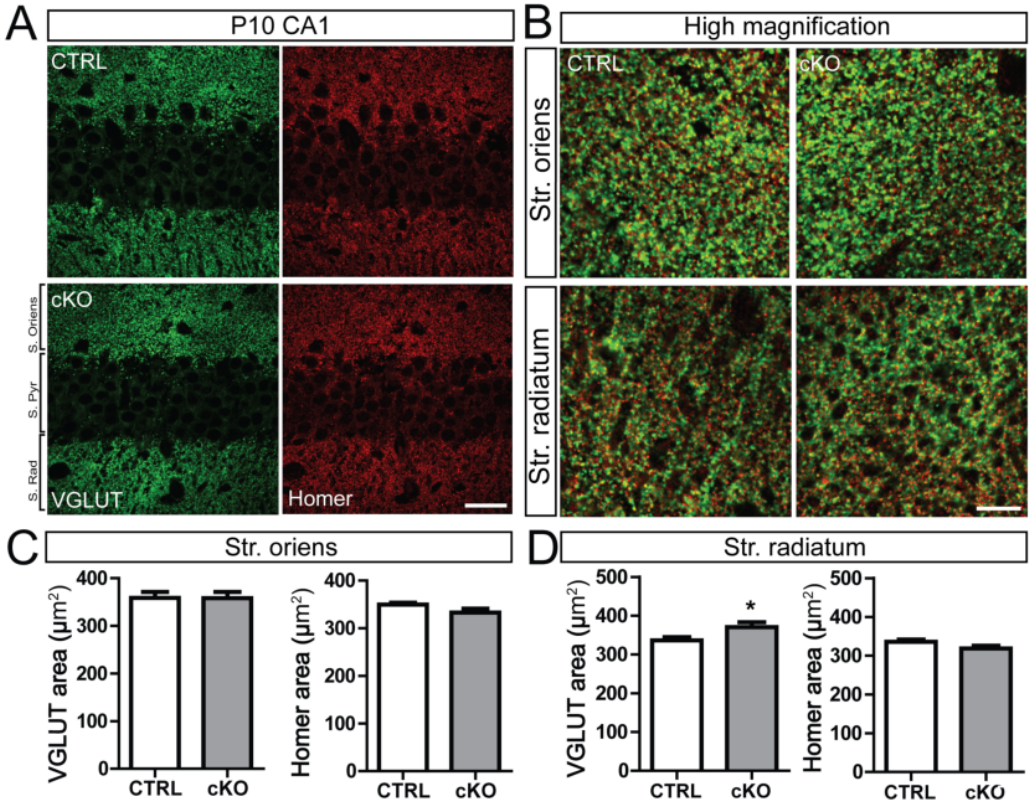

Fig. 4.5: Increased excitatory presynaptic clusters in early postnatal cKO animals **(A-B)** Immunohistochemistry of excitatory pre and postsynaptic markers (VGLUT1 and Homer respectively) in the CA1 region of the hippocampus at P10-11. Scale bar, 25 µm. **(B)** High magnification of the stratum oriens (top) and stratum radiatum (bottom). Scale bar, 10 µm. **(C)** Cluster analysis shows no change in excitatory synapses in the oriens. **(D)** Increased VGLUT1 puncta area in the radiatum ($p<0.05$, student's unpaired t-test). N=18 fields of view from 3 animals per condition.

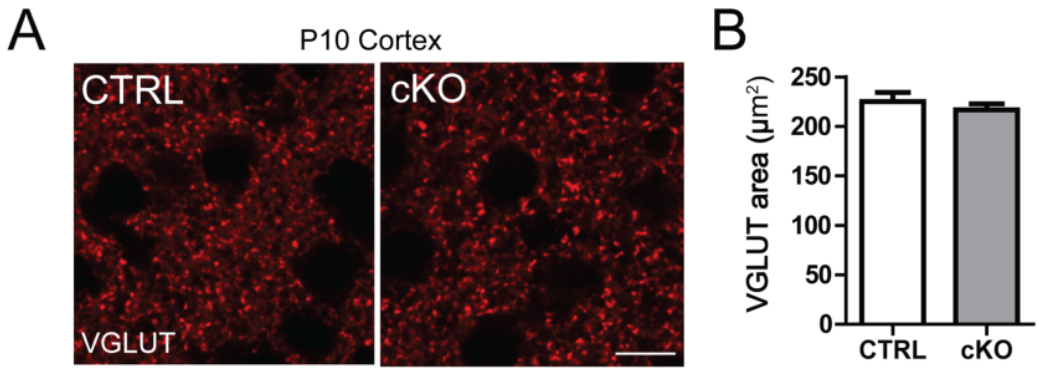

Fig. 4.6: Increased excitation in early postnatal cKO animals is region specific
(A) VGLUT1 immunohistochemistry in cryoslices of somatosensory cortex from P10-11 mice. Scale bar: 10 µm. **(B)** Cluster analysis showed no change in area between CTRL and cKO slices. N=18 fields of view from 3 animals per condition.

Next, cryoslices from P30 animals were stained as already described to see if the changes seen in excitatory synapse clusters in pups are sustained in young adult mice, when mild changes in dendritic arborisation and spine morphology were observed (Fig 4.7A). No changes in VGLUT1 cluster area were observed in either the oriens or radiatum layers of CA1 (Fig 4.7B) (oriens: CTRL 343.9 ± 20.61 μm^2, cKO 325.8 ± 18.12 μm^2; radiatum: CTRL 368.1 ± 15.52 μm^2, cKO 364.4 ± 11.91 μm^2). Interestingly, a small but significant decrease in area of Homer clusters was observed in the radiatum, whilst oriens clusters remained unchanged (Fig 4.7C) (oriens: CTRL 410.5 ± 9.51 μm^2, cKO 415.7 ± 9.16 μm^2; radiatum: CTRL 425.7 ± 4.96 μm^2, cKO 392.5 ± 11.87 μm^2, $p<0.05$). Thus, there appears to be an age-dependent increase in excitatory presynaptic puncta in mice lacking neuronal CYFIP1 that is recovered by 1 month of age.

To test if dendritic spines from the basal dendrites of CA1 pyramidal cells of the hippocampus were altered, brains from P30 mice were treated with Golgi-Cox staining to sparsely label neuronal morphology and enable the visualization of spines (Fig 4.8A). As in culture, a range of spine morphologies were observable, including long spines with no head to those with more mushroom-like shape (green and red arrows respectively). Assessment of numbers showed no overall change in spine density between CTRL and cKO (Fig 4.8B) (CTRL 1.17 ± 0.09 spines/μm^{-1}, cKO 1.19 ± 0.07 spines/μm^{-1}). However, analysis of spine morphology revealed an increase in average spine length (Fig 4.8C) (CTRL 1.65 ± 0.07 µm, cKO 1.94 ± 0.08 µm, $p<0.01$, student's unpaired t-test). Spine head diameter remained unchanged (CTRL 0.42 ± 0.02 µm, cKO 0.39 ± 0.02 µm). Following, when plotted as a ratio of length-head width for each spine, an increase in this ratio was observed (CTRL: 8.85 ± 0.67, cKO: 10.81 ± 0.72, $p<0.05$, student's unpaired t-test), indicative of immature spine morphology. Thus, loss of CYFIP1 from CA1 pyramidal neurons leads to specific spine morphology abnormalities but no change in the density of connections.

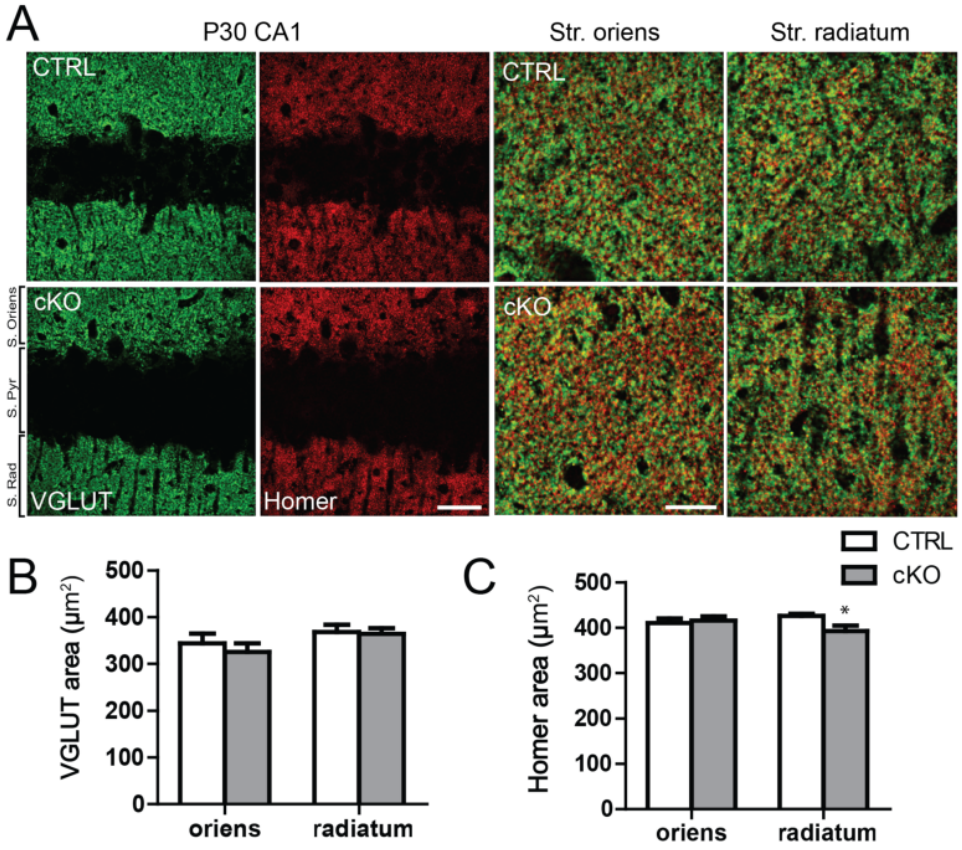

Fig. 4.7: Excitatory synapse staining cKO hippocampus of young adults
(A-A') Immunohistochemistry of excitatory pre and postsynaptic markers (VGLUT and Homer respectively) in the CA1 region of the hippocampus at P30. Scale bar, 25 µm. (A') High magnification of the stratum oriens (left) and stratum radiatum (right). Scale bar, 10 µm. **(B)** Cluster analysis shows no change in area of VGLUT1 but a selective increase in Homer in the stratum radiatum ($p<0.05$, student's unpaired t-test). N=18 fields of view from 3 animals per condition.

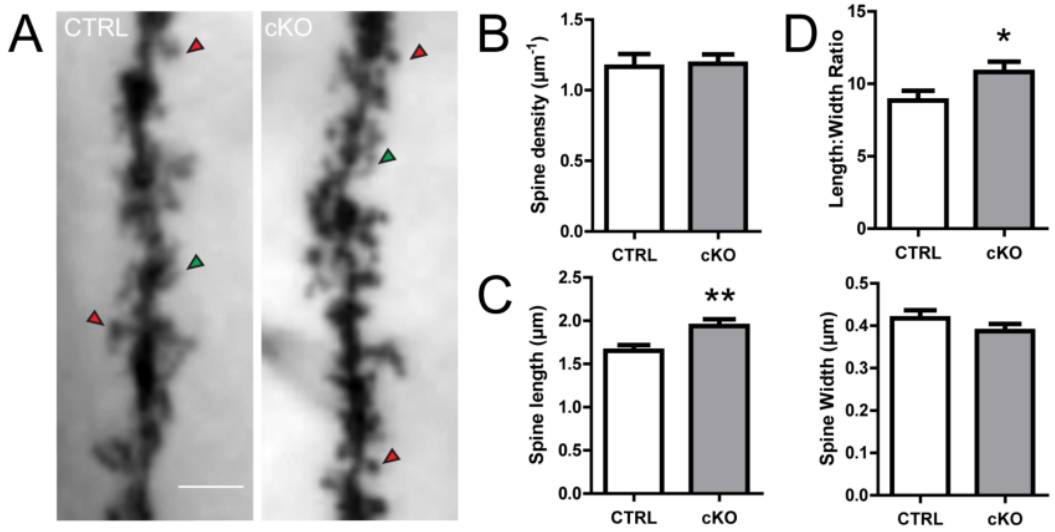

Fig. 4.8: Normal density but abnormal morphology of cKO spines *in vivo*
(A) Representative images of dendritic spines from basal arbor of CA1 pyramidal cells from 1 month old CTRL or cKO brains, stained using Golgi-Cox. Scale bar, 5 µm. **(B)** No change in density of spines in cKO. **(C-D)** Morphological characteristics of spines. Spine length is increased in cKO ($p<0.01$, student's unpaired t-test) but width is unchanged. Length-width ratio is increased in cKO ($p<0.05$, student's unpaired t-test). N=45 dendritic sections from 3 animals per condition.

4.2.3 Enhanced inhibition in cKO young adult mice

Given that CYFIP1 is present at inhibitory post-synapses of hippocampal neurons *in vitro*, it was hypothesised that loss of CYFIP1 may effect inhibitory synapse function *in vivo*. To investigate this, P30 slices were stained for inhibitory pre and postsynaptic markers, VGAT and Gephyrin (Fig 4.9A). Staining showed clear clusters that were concentrated in the stratum pyramidale layer, consistent with the majority of inhibition being directed onto somas of principle cells. Comparing CTRL and cKO, VGAT staining was unchanged between conditions (Fig 4.9B) (CTRL 100 ± 2.18%, cKO: 92.84 ± 5.39%). However, a clear increase in Gephyrin staining was apparent, reflected in the increase in Gephyrin area in cKO (CTRL 100 ± 6.92%, cKO 119.5 ± 6.08%, $p<0.05$).

To see if the observed changes in inhibitory synapse clusters reflected a more general increase in expression of proteins associated with the inhibitory synapse, P30 hippocampal lysates were probed with antibodies against various synapse-associated proteins (Fig 4.10A-B). A number of excitatory postsynaptic proteins were probed (Homer, PSD95, GluA2, GluA1, PanShank), none of which showed any altered expression aside from CYFIP1 (CTRL 100 ± 5.73%, cKO 53.21 ± 4.79%, $p<0.01$). Next, a series of inhibitory postsynaptic receptors ($GABA_AR\beta 2/3$), transmembrane proteins (NLGN2, NLGN3), synaptic scaffolds (Gephyrin, GIT1) and signaling molecules (βPIX) were probed. Interestingly, an increase in expression of the $GABA_A$ receptor subunits 2 and 3 and NLGN3 was observed ($GABA_AR\beta 2/3$: CTRL 100 ± 5.36%, cKO 141 ± 1.07%, $p<0.01$; NLGN3: CTRL 100 ± 2.21%, cKO 135.1 ± 10.24%, $p<0.05$). No changes were observed in other inhibitory synapse proteins. These data lend further support to a specific increase in inhibitory synaptic transmission in young adult cKO animals.

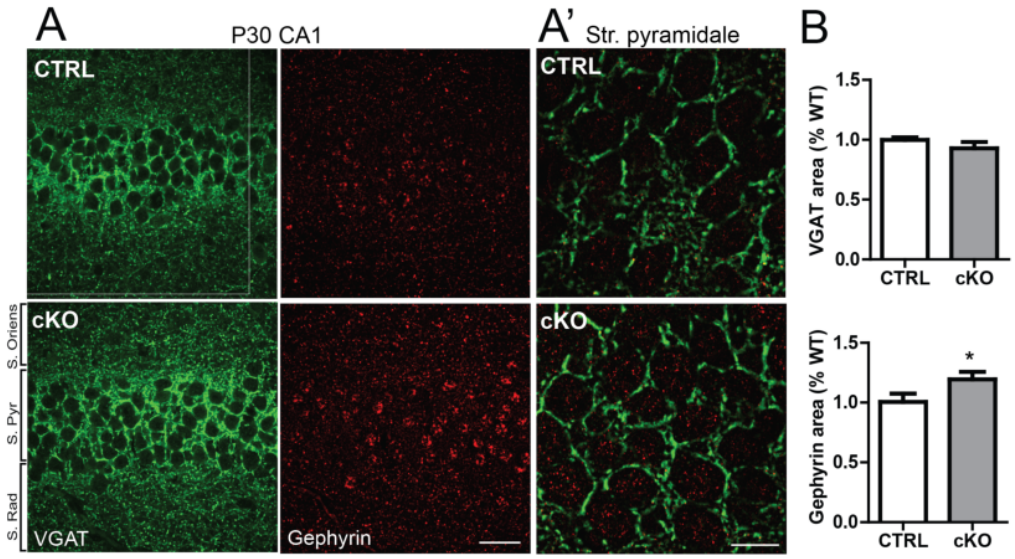

Fig. 4.9: Enhanced Gephyrin staining in cKO hippocampus of young adults
(A-A') Immunohistochemistry of inhibitory pre and postsynaptic markers (VGAT and Gephryin respectively) in the CA1 region of the hippocampus at P30. Scale bar, 25 µm. (A') High magnification of the stratum pyramidale. Scale bar, 10 µm. **(B)** Cluster analysis shows no change in VGAT but increased Gephyrin area in cKO ($p<0.05$, student's unpaired t-test). N=18 fields of view from 3 animals per condition.

Although synaptic staining and protein expression are useful metrics for comparing changes in connectivity, they do not provide a functional readout of neuronal activity. To investigate if the changes in inhibition observed correlate with functional effects, acute slices from P30 animals were prepared and basal excitatory and inhibitory activity was measured by patch-clamp electrophysiological recordings, performed by Dr Blanka Szulc (Fig 4.11A,C). Miniature excitatory post-synaptic currents (mEPSCs) from CA1 PCs showed no change in either frequency or amplitude of mEPSCs, in agreement with the normal excitatory staining data (Fig 4.11C-D) (amplitude: CTRL 19.2 ± 1.4 –pA, cKO 18 ± 1.4 -pA; frequency: CTRL 1.5 ± 0.2 Hz, cKO 1.3 ± 0.2 Hz). However, isolating inhibitory post-synaptic currents (mIPSCs) revealed an increase in amplitude but not frequency (Fig 4.11A-B) (amplitude: CTRL 23.8 ± 1.8 –pA, cKO 30.3 ± 2.2 -pA, $p<0.05$; frequency: CTRL 3.3 ± 0.3 Hz, cKO 3.7 ± 0.3 Hz). The increase in amplitude led to an increase in the total charge transfer of mIPSCs, whereas total charge transfer of mEPSCs was unchanged (Fig 4.11E-F) (mEPSCs: CTRL 0.31 ± 0.07 pC, cKO: 0.28 ± 0.03 pC; mIPSCs: CTRL 0.98 ± 0.11 pC,cKO: 1.68 ± 0.21 pC). Taken together, these data show a selective increase in postsynaptic inhibition in CA1 PCs lacking CYFIP1, whereas excitatory transmission remains normal.

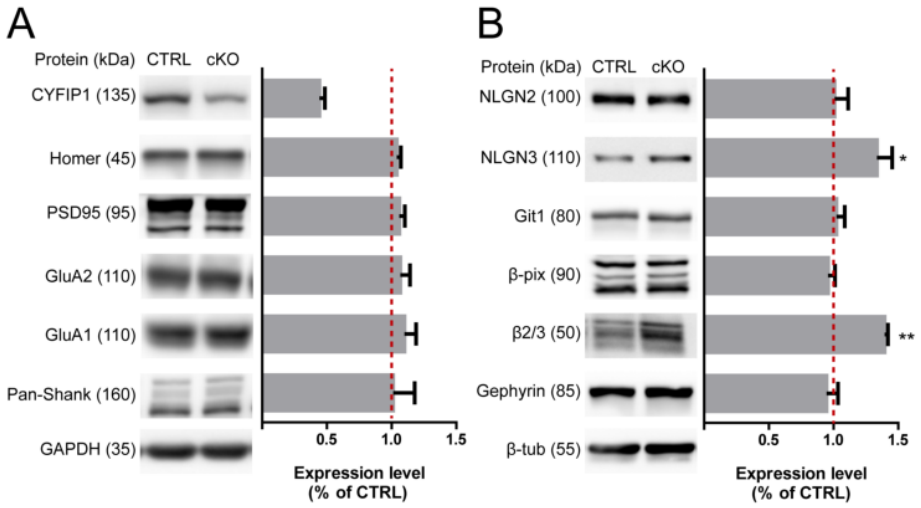

Fig. 4.10: Increased expression of inhibitory postsynaptic proteins in cKO hippocampus

(A) P30 hippocampal protein lysates probed for CYFIP1 and various excitatory postsynaptic proteins. No changes observed in expression of Homer, PSD95, GluA1 or A2, or Pan-Shank **(B)** P30 hippocampal protein lysates probed for various inhibitory postsynaptic proteins. Increased expression of NLGN3 ($p<0.05$, student's unpaired t-test) and $GABA_AR\beta 2/3$ ($p<0.01$, student's unpaired t-test). N = 3 animals per condition

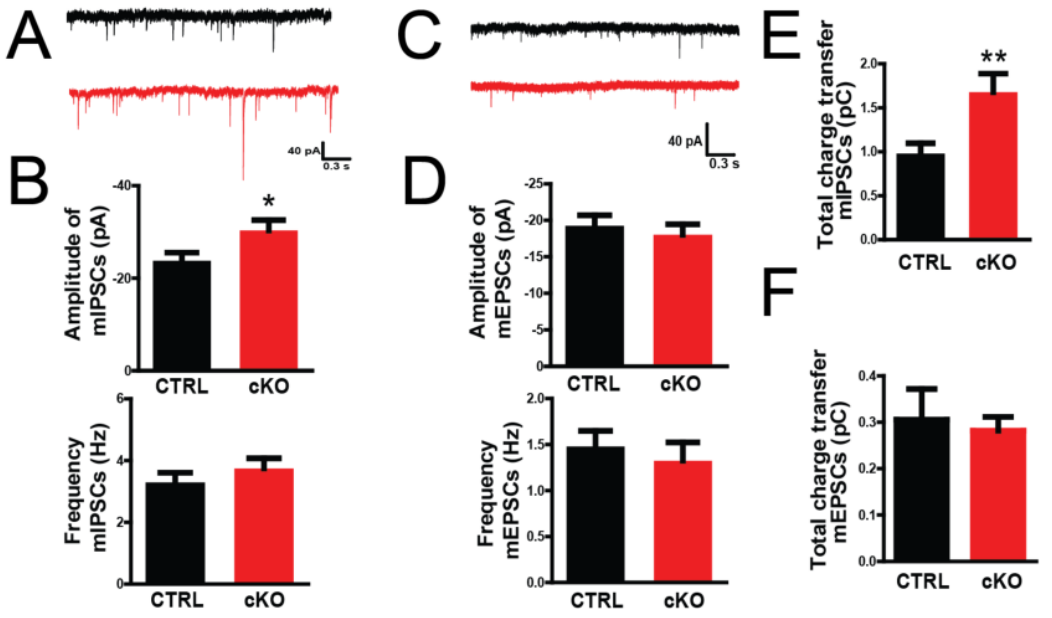

Fig. 4.11: Enhanced inhibitory synaptic transmission in cKO hippocampus
(A,C) Representative recordings of miniature inhibitory postsynaptic currents (mIPSCs, left) and miniature excitatory postsynaptic currents (mEPSCs, right) in CA1 pyramidal cells from CTRL and cKO acute slices. **(B)** Increased mIPSC mean amplitude in cKO ($p<0.05$, student's unpaired t-test) but normal frequency. **(D)** No change in mEPSC mean amplitude and frequency between CTRL and cKO. **(E-F)** No change in total charge transfer in mEPSCs but increased total charge transfer in mIPSCs ($p<0.01$, student's unpaired t-test). N=13-15 cells for inhibitory recordings and 18-22 cells for excitatory recordings across 3 animals per condition. All recordings performed by Dr Blanka Szulc.

4.3 Discussion

This chapter furthered the characterisation of the NEX^{Cre} conditional CYFIP1 knockout, focusing on changes in synaptic form and function. Whilst *in vitro* effects of loss of CYFIP1 appear non-existent, several interesting effects were observed in the hippocampus of cKO animals across development.

Differential effects on dendritic spines in cKO

The increase in spine length of dendritic spines of cKO CA1 pyramidal cells without altered density is highly reminiscent of defects reported in the haploinsufficient mouse (de Rubeis et al., 2013; Pathania et al., 2014). This strongly supports the cell-autonomous origin of this effect *in vivo*, in line with rescue experiments in neuronal cultures (de Rubeis et al., 2013). Thus, endogenous CYFIP1 appears to have a role in regulating spine form and function rather than formation. It is possible that regional differences in this exist. Indeed, haploinsufficiency of the CYFIP1 paralogue CYFIP2 has no impact of hippocampal spines but increases the density and length of cortical spines (Han et al., 2015).

It is worth noting that these spine defects were observed in the basal arbor of CA1 pyramidal cells, where altered dendritic morphology was observed in the previous chapter. Together, these data hint at highly altered connectivity in this region. The stratum oriens receives input from Schaffer collateral fibres from the hippocampus CA3, a circuit which is implicated in working memory formation (Teixeira et al., 2018). It would be interesting to see if the cKO mouse displays any defects in memory tasks that have been observed in other models of neurological conditions, including FXS (Bozdagi et al., 2012; Thomas et al., 2011).

The mechanism underlying these effects are currently unclear. Increased spine density and immaturity are a hallmark of FMRP KO mice, suggesting that dysregulated protein translation could underlie this effect (Irwin et al., 2000).

Indeed, haploinsuffient CYFIP1 mice have enhanced mGluR-dependant LTD and learning deficits similar to FMRP KO, strongly supporting FMRP-related dysfunction of the postsynapse in CYFIP1 deficiency (Bozdagi et al., 2012; Penagarikano et al., 2007). However, actin remodelling via the WRC is also critical for dendritic spine formation. Genetic studies have shown that knockdown of other WRC components WAVE1/2 and Abi1/2 leads to decreased spine density and immature spines (Grove et al., 2004; Ito et al., 2010; Kim et al., 2006; Soderling et al., 2007). Loss of Rac1, the RhoGTPase upstream activator of WRC that acts via CYFIP1, decreases spine density in numerous systems, and Rac1 activity is required for spine plasticity during cocaine response (Dietz et al., 2012; Tashiro and Yuste, 2004). Rac1 has been suggested to act as a mediator of the balance between WRC- and FMRP-complex association of CYFIP1, and CYFIP1 binds GTP-bound Rac1 (de Rubeis et al., 2013; Kobayashi et al., 1998). Thus, loss of CYFIP1 could also perturb Rac1 signalling in spines. Further, CYFIP1 haploinsufficient neurons have increased mobile fraction of actin in spine heads that correlates with enhanced NMDA receptor motility (Pathania et al., 2014).

It is entirely possible that spine defects observed here, and in other CYFIP1 CNV models, arise from a complex interaction between disruptions in these distinct functions. Mutant rescue studies of spine morphology after knockdown of CYFIP1, using CYFIP1 constructs that preserved only WRC or eIF4E complex formation, suggested that both functions are required for normal spine formation (de Rubeis et al., 2013). Further, a genetic interaction study showed that knockdown of CYFIP1 can rescue increased spine density of FMRP KO, although knockdown also caused reductions in WRC component mRNA levels, suggesting that altered activity of one complex could rescue phenotypes of the other (Abekhoukh et al., 2017).

Enhanced presynaptic release in young pups of cKO

Through VGLUT1 staining and mEPSC recordings from P10-11 cKO pups, we report a hyperexcitability phenotype that has been previously observed in haploinsufficient mice. The fact that we see this effect in our model strongly supports a cell-autonomous origin (Hsiao et al., 2016). Interestingly, the scale of the mEPSC frequency increase is around two-fold that reported for the haploinsufficient, suggesting that CYFIP1 levels could have a dose-dependent effect on presynaptic release. The synaptic staining suggests that the increase in presynaptic puncta is occuring in the radiatum rather than the oriens. It is possible that this area specific increase is related to the difference in inputs received. Although both apical and basal arbors receive input from CA3, the inputs onto proximal apical dendrites in the radiatum, where images were taken, are specifically from Schaffer collateral projections from CA3, whereas apical tufts receives input from the entorhinal cortex and the thalamic nucleus reuniens (Griffin, 2015). Given that the NEX^{Cre} is active in CA3, the ratio of inputs from cKO neurons may be higher in the proximal apical compared to the basal arbor.

The region specificity of this effect is also of interest; CYFIP1 is expressed in both cortical and hippocampal neurons, as revealed by the reduction in expression in both cortical and hippocampal lysates in chapter 3. CYFIP2 haploinsufficient mice have a specific increase in spine density in layer II/III principle cells, whereas CA1 pyramidal cells were normal (Han et al., 2015). These data suggest differential expression of CYFIP proteins that could explain these differences. A similar concept has been reported in CYFIP proteins role in retinal ganglion cell axon development, where temporal instead of spatial expression differences between CYFIP1 and 2 governed their knockout phenotypes (Cioni et al., 2018). It would be interesting to see if other neuronal cell types with predicted high CYFIP1/CYFIP2 expression, such as granule cells of the dentate gyrus, had more severe phenotypes (Zeisel et al., 2018).

As with the haploinsufficient model, the hyperexcitability in young pups is recovered by P30 with VGLUT1 staining and frequency of mEPSCs equal to control. Interestingly, synaptic staining of excitatory postsynapse showed a mild but significant decrease in Homer cluster area at this timepoint. This could represent a homeostatic response of the hippocampal network to limit excitatory input, although this was not observed at P10, when the increase in VGLUT1 was seen.

CYFIP1 at the inhibitory postsynapse

A role for CYFIP1 in the formation or regulation of inhibitory synapses has not been studied to date. Previous work in the lab has shown that CYFIP1 is also present at inhibitory synapses *in vitro*. This was confirmed here through colocalisation with Gephyrin to label the inhibitory postsynapse. Endogenous CYFIP1 staining showed that CYFIP1 had a close association to gephyrin clusters, either overlapping or directly adjacent. This proximity reflects that reported of other inhibitory synapse-associated proteins (Woo et al., 2013). It is currently unknown in what complex CYFIP1 exists at the inhibitory synapse. Hints from the literature suggest that both FMRP and WRC could be present at the iPSD. A recent study using a biotin-capture assay to label proteins of the inhibitory postsynaptic density showed that WAVE1 and the Arp2/3 complex were present in the iPSD (Uezu et al., 2016). The upstream signalling GTPase Rac1 has well-established roles in $GABA_A$ receptor stabilisation and endocytosis, and so would be predicted to be present to interact with WRC (Smith et al., 2014; Wang et al., 2017). Indeed, we observe colocalisation of gephyrin and WAVE1 in neuronal cultures, further supporting the presence of the WRC at the inhibitory postsynapse. Whilst FMRP hasn't been shown to localise to the inhibitory postsynapse, many FMRP mRNA targets are members of the iPSD, including $GABA_B$ receptors and neuroligins, and FMRP is localised throughout dendritic arbor (Darnell et al., 2011). Thus, it is feasible for CYFIP1 to be present at inhibitory synapses through various complexes.

As CYFIP1 is lost only in excitatory neurons in hippocampus and neocortex, the cKO model offered an ideal system in which to see if CYFIP1 has any specific role in regulation of the inhibitory postsynapse, and the presynapse would not be effected by the conditional knockout. Indeed, the increase in gephyrin clustering, mIPSC amplitude and expression of postsynaptic proteins observed in the chapter are all consistent with a postsynaptic effect. Whilst it is not possible to entirely rule out an indirect presynaptic effect through altered excitatory input onto inhibitory interneurons, it is very unlikely. No changes in VGAT staining or mIPSC frequency (indicator of presynaptic release probability) were observed at P30. Further, recordings of excitatory currents at this age suggested no change in excitatory drive of inhibitory interneurons. Additionally, the altered gephyrin clustering and increase in amplitude of inhibitory currents are reminiscent of known postsynaptic changes in other studies (Tabuchi et al., 2007).

Western blots showed specific increases in neuroligin-3 (NLGN3) and $GABA_A\beta$ receptor subunits. As the major ionotropic receptors of the inhibitory synapse in the CNS, alongside glycine receptors, $GABA_A$ receptors generate inhibitory current. Thus, the increase in expression provides a simple explanation for the enhanced amplitude of inhibitory currents observed at P30. NLGN3 is a member of the neuroligin family of transmembrane postsynaptic cell adhesion molecules that bind presynaptic neurexins to control synapse formation and stability (Südhof, 2008). Both missense and nonsense mutations of NLGN3 have been found in ASD patients and mouse models have shown ASD-like behavioural phenotypes (Jamain et al., 2003; Radyushkin et al., 2009; Rothwell et al., 2014). The neuroligins exhibit synapse specificity, with NLGN1 and 2 being associated with excitatory and inhibitory synapses respectively. Interestingly, NLGN3 is present at both excitatory and inhibitory synapses where it complexes with either NLGN1 or 2 (Budreck and Scheiffele, 2007). Given this dual localisation, it is curious that increased expression in cKO brains is associated with a specific increase in inhibition in this model. A study of a NLGN3 mutant mouse model has shown specific changes to inhibitory transmission (Chanda et al., 2017; Tabuchi et al., 2007). Additionally, overexpression

of NLGN3 has no effect of excitatory transmission in neuronal cultures, in contrast to the increase seen in NLGN1 overexpression (Chanda et al., 2017). The correlation between increased NLGN3 expression with enhanced inhibitory but not excitatory transmission supports the hypothesis that altered NLGN3 dosage preferentially alters inhibition.

A simplistic explanation of these effects is that loss of CYFIP1 leads reduced post-transcriptional repression of inhibitory synapse mRNAs of NLGN3 and GABAAβ2/3 receptor subunits. NLGN3 has been identified as a target by a comprehensive study of 842 FMRP-regulated mRNAs, alongside $GABA_BR$, and overexpression of CYFIP1 caused a decrease in NGLN3 mRNA levels *in vivo* (Darnell et al., 2011; Oguro-Ando et al., 2015). Additionally, differential expression of $GABA_AR$s mRNAs has been observed in FMRP KO mice (Braat et al., 2015). A combination of increased $GABA_AR$ expression and increased surface NLGN3 could stabilise $GABA_AR\beta$ receptor subunits, which in turn could explain the enhanced inhibitory transmission strength observed.

FMRP targets represent a significant proportion of components of both excitatory and inhibitory postsynapse, for many of which we observe no changes in expression in cKO. As a result, it is an outstanding question as to how and why only specific protein levels appear changed in the cKO. One explanation is that change requires combined dysfunction of both FMRP and WRC-related functions of CYFIP1. NLGN3 also contains a WIRS motif, enabling it to interact with the intact WRC via CYFIP1 (Chen et al., 2014a). In contrast, NLGN1 is not a known FMRP target and NLGN2 does not contain a WIRS motif. Thus, the selective increases in expression of NLGN3 observed in the cKO could be due to the interplay between relieved translational repression and anchoring at the iPSD. It would be interesting to see if other proteins that fit this pattern have altered expression, such as SHANK2, β-catenin, protocadherin-10 and ankyrins 2 and 3.

Overexpressed CYFIP2 is present at inhibitory synapses (unpublished observations). However, whether endogenous CYFIP2 localised similarly is

unknown. Thus, it is possible that endogenous CYFIP proteins have preferential synaptic localisation. Although the altered spine morphology seen in cKO argues against this, it is possible that CYFIP1 is playing fundamentally different roles at excitatory and inhibitory synapses based on their different architecture and PSD components.

Altered balance of excitation and inhibition in cKO

The specific impact on inhibitory transmission suggests changes in excitation/inhibition balance in the cKO model. Altered E/I balance is a common feature of numerous psychiatric disorders, although this has typically related to increased in E/I ratio. Decreased levels of GABA synthesising enzymes and GABA receptor subunits have been seen in ASD brains, and reductions in inhibitory neuron markers seen in SCZ (Selten et al., 2018). Additionally, there is significant comorbidity between ASD and epilepsy, with prevalence being approximately 25% in ASD patients (Bolton et al., 2011). If the effect of CYFIP1 loss on inhibition represents a dosage-dependent effect, then increased expression of CYFIP1 would be predicted to an increase in E/I balance. Indeed, increased CYFIP1 expression has been seen in patients and models of temporal lobe epilepsy (Huang, 2015; Sayad et al., 2018).

Studies of human mutations in known disease-associated genes have reported increases in inhibition (Tabuchi et al., 2007). Increased inhibition also contributes to models of intellectual disability, including Down's syndrome (Rudolph and Möhler, 2014). As this current study focused on principle neurons, it is unknown whether CYFIP1 loss could be having a similar effect on inhibitory interneurons. Interestingly, a human NLGN3 mutation has been shown to increase inhibition by CCK basket cells onto pyramidal neurons (Földy et al., 2013).

Together, the data in this chapter further our understanding of CYFIP1's role in synaptic function. The use of a cell-specific cKO enabled the cell-autonomous origin

of a number of effects previously reported in the haploinsufficient model to be shown, including spine immaturity and perinatal hyperexcitability. Further, a novel role for CYFIP1 in regulating the strength of inhibitory transmission is revealed, via altering expression of key proteins of the inhibitory postsynapse and gephyrin clustering. These data open new avenues to explore CYFIP1 function and add mechanistic insight into the genes associations with neuropsychiatric disorders.

Chapter 5

Investigating actin remodelling during microglial motility

5.1 Introduction

The development of functional neuronal networks require a vast array of interactions between neurons and glia. Glia, which make up to 90% of the cells in the mouse brain, have a diverse array of functions including in neurogenesis, neuronal migration, synaptogenesis, myelination and plasticity (Barres, 2008). Given their critical importance to neuronal function, it is unsurprising that many neurological disorders are either directly caused by changes in glial function or involve glial changes that shape disease progression. Recently, microglia have become a focus of attention due to their growing repertoire of interactions with neurons and links to brain pathology (Lehrman et al., 2018).

Many microglia-neuron interactions rely fundamentally on the motility of the complex, ramified processes of microglia. Local induction of LTP increases ramification of microglia (Pfeiffer et al., 2016). Interestingly, CX3CR1 knockout microglia have impaired migration *in vitro* and altered process motility in retinal

explants (Liang et al., 2009; Paolicelli et al., 2014). CX3CR1 knockout microglia are also morphologically less complex, suggesting that neuronal abnormalities reported in fractalkine knockout mice could be due to altered microglial motility as well as disrupted receptor signalling (Pagani et al., 2015). Thus, dynamics shape and movement of microglia are critical to their function.

The study of microglial motility has focused on two behavioural paradigms; surveillance and chemotaxis. During baseline surveillance, microglia extend and retract processes apparently randomly into the volume covered by a single cells domain. In contrast, in response to release of ATP via localised injury or microinjection, nearby microglia extend processes towards the ATP source and retract those away from it. The signalling pathways underlying these two behaviours are incompletely understood, though they are clearly distinct from each other. Chemotaxis is driven by ATP-sensing by the microglial P2Y12 receptor, as pharmacological inhibition or genetic ablation of P2Y12 inhibits chemotaxis (Haynes et al., 2006; Ohsawa et al., 2007). Additionally, P2Y12 is highly expressed at the tips of processes during chemotaxis. However, *in situ* ATP sensing leads to a rapid expansion of signalling via the degradation of ATP to ADP, AMP and other derivates by enzymes expressed by microglia. Additionally, chemotactic response can also be initiated by other molecules including fibrinogen and nitric oxide that do not require P2Y12 for process motility (Davalos et al., 2012; Dibaj et al., 2010).

The molecular basis of baseline surveillance are less well understood. ATP has been shown to modulate surveillance, and quenching of basal ATP levels reduces surveillance, suggesting that extracellular ATP could set the basal motility rate (Abiega et al., 2016; Dissing-Olesen et al., 2014). Further, astrocytes have been implicated in propagating ATP signalling to microglia via hemichannels as inhibition of these impairs microglial surveillance. NMDA signalling also seems to be an important regulatory cue, as bath application and local NMDAR activation drives process motility, though this is also dependent on ATP signalling (Dissing-Olesen et al., 2014; Eyo et al., 2014; Pfeiffer et al., 2016). However, a recent study showed

that the effects of apyrase, an ecto-ATPase used to hydrolyse ATP in many of these studies, actually alters microglial morphology and surveillance through intracellular depolarisation unrelated to puriginergic signalling (Madry et al., 2018a). This is supported by the fact that P2Y12 KO microglia survey normally (Haynes et al., 2006). Thus, how extracellular signals establish basal motility remains largely unknown.

Even less is known about the intracellular signalling cascades underlying microglial process motility. All forms of motility appear critically dependent on actin cytoskeleton remodelling, as block of actin polymerisation inhibits both surveillance and chemotactic motility (Hines et al., 2009). Indeed, EM phalloidin staining suggests that microglia are highly actin dense and actin clusters have been observed in situ (Barcia et al., 2012; Capani et al., 2001). During chemotaxis, P2Y12 activation leads to phosphorylation of Akt by PLC and PI3K and β-integrin levels are increased on P2Y12 activation in cultured microglia (Ohsawa et al., 2007, 2010). Akt and integrins are integral to cytoskeletal remodelling pathways, but act through a diverse array of signalling pathways in different cell types and scenarios, including mTORC and the RhoGTPases (Harburger and Calderwood, 2009; Xue and Hemmings, 2013). An *in vivo* study in zebrafish used FRET imaging to show active Rac1 localised to leading microglial processes in response to glutamate uncaging (Li et al., 2012). Thus, the identity of signalling pathways involved in actin cytoskeleton remodelling during microglial motility remain poorly understood.

Insight into pathways governing microglial motility comes from the macrophage literature, where cytoskeletal dynamics have been well-studied (Rougerie et al., 2013). Although distinct, macrophages and microglia share similar transcriptional profiles and many distinct behaviours, including phagocytosis and chemotaxis (Zhang et al., 2014a). A study of Arp2 knockout macrophages showed disrupted actin assembly and membrane protrusions, although interesting this led to enhanced motility of macrophages *in vitro* and *in vivo* (Rotty et al., 2017). Phagocytosis assays showed a specific impairment in CR3-mediated phagocytosis, particularly interesting given the established role of complement signalling in synaptic pruning by microglia. The

importance of Rac and NPF signalling upstream of Arp2/3 is highlighted by a number immune-deficiencies caused by mutations in WASP (Wiscott-Aldrich Syndome) and Rac2 (Thrasher and Burns, 2010; Williams et al., 2000). Activation of Arp2/3 by the WAVE Regulatory Complex (WRC) is required for lamellipodia formation and migration to specific cues in macrophages (Kheir et al., 2005). Additionally, the haemopoetic lineage-specific component of the WRC, HEM-1 (NCKAP1L), is critical for actin remodelling downstream of Rac1 in neutropils during chemotaxis and phagocytosis (Park et al., 2010). Thus, the RAC1-WAVE-ARP2/3 pathway plays an important role in actin remodelling of macrophages.

To date, the impact of altered CYFIP function has not been directly studied in any macrophage or microglial lineage. However, numerous microglial transcriptomes (bulk and single cell) have shown that CYFIP1 is highly expressed in microglia (Hammond et al., 2018; Saunders et al., 2018; Zeisel et al., 2018; Zhang et al., 2014b). Of note, expression of CYFIP2 in microglia is negligible, suggesting that CYFIP1 is the principle CYFIP protein these cells. Given the shared clinical associations of CYFIP1 and microglia, and the importance of microglial morphology and motility to their function, the role of CYFIP1 in microglia could be a promising new avenue of research.

In this chapter, a combination of pharmacological treatments and genetic systems are used to gain insight into the actin dynamics underlying microglial motility. Actin polymerisation is shown to be critical for microglial motility. Inhibition of Arp2/3 complex leads to altered microglial morphology, reduced baseline surveillance and slowed chemotaxis. Rac1 inhibition also impairs surveillance behaviour and results in characteristic changes in process formation. In order to investigate a role for CYFIP1 in regulating microglial shape and motility, a conditional mouse model was generated to study the loss of microglial CYFIP1 *in vivo*. CYFIP1 KO microglia have reduced morphological complexity and specifically impaired surveillance motility, whilst chemotaxis is unaffected.

5.2 Results

5.2.1 Setting up a live imaging assay for quantifying microglial motility

In order to better understand the importance of actin remodelling to microglial motility, microglia in situ were visualised in acute hippocampal slices from transgenic mice containing a IBA^{eGFP} reporter cassette (Hirasawa et al., 2005). Imaging acute slices by two-photon laser scanning microscopy (2P-LSM) showed bright labelling of microglia across all brain regions checked (cortex, hippocampus, midbrain; data not shown) (Fig 5.1A). As reported previously, microglia occupied distinct non-overlapping domains of 3D space, though patterning of tissue was not always uniform suggesting that the IBA^{eGFP} reporter does not label all microglia.

Two imaging paradigms were established to study microglial motility. The first, called 'surveillance', measured the rate at which individual microglia sampled their respective volumetric domains at rest (Fig 5.1A-C). 3-dimensional images were taken every 30 s over a 10 minute period to generate a time series of microglial movement. Superimposing maximum intensity projections (MIPs) of these 3D stacks between adjacent timepoints captures a number of core features of surveillance (Fig 5.1B). Firstly, the cell body and major processes of the cell are stable over this time period (yellow areas, merge panel). Second, that higher order processes are highly dynamic, either extending (red areas, merge panel) or retracting (green areas, merge panel). To quantify these movements, MIPs were thresholded and the new or absent binarised pixels were measured across time series, using a analysis script published recently (Madry et al., 2018b) (Fig 5.1C). This metric, termed Surveillance Index (SI), was seen to be fairly stable over time, and suggested that approximately 10% of the microglial area was motile between 30 s timepoints.

The second imaging paradigm aimed to quantify microglia response to a laser-induced lesion, termed 'chemotaxis'. Briefly, a small region void of microglia

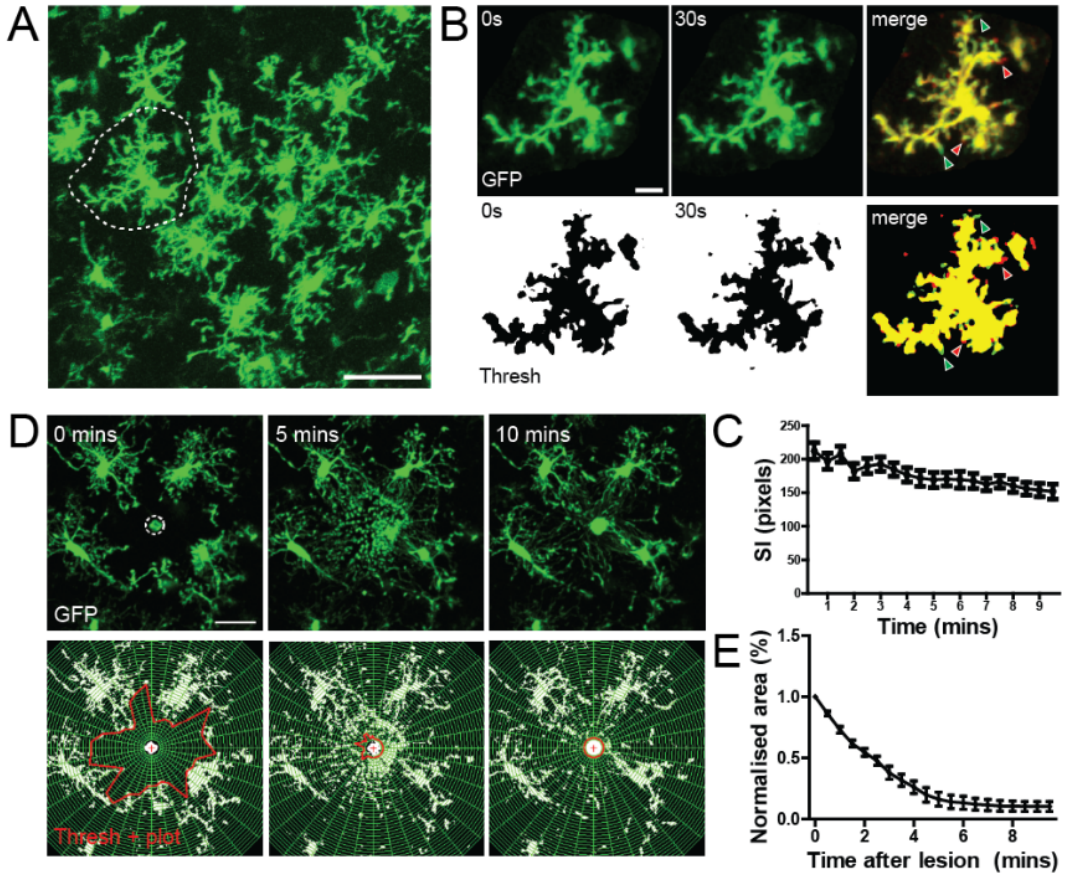

Fig. 5.1: Establishing live imaging paradigms for quantifying microglia movement
(A) Field of view image of GFP+ microglia in acute hippocampal slice. Microglia occupy distinct domains, allowing single cells to be selected for analysis of surveillance motility (dotted area). Scale bar: 50 µm **(B)** Top panel: max projection (MIP) of z-stacks from two adjacent timepoints. Merged image reveals retractions (green) and extension (red) and the stable area (yellow) in the 30s frame. Bottom panel: Threshold of MIP. Pixel counts of red and green areas are used as a read out of surveillance motility. Scale bar: 10 µm **(C)** Quantification of surveillance index (SI) over 10 minute time period. **(D-E)** Chemotaxis assay. **(D)** Top panel: Max projection showing microglia surrounding laser lesion (dotted line) in slice that nearby microglial processes converge to over 10 minutes. Bottom panel: Analysis of process convergence by tracking area of process front (red polygon). Scale bar: 10 µm. **(E)** Quantification of reduced area over time as processes converge on lesion.

(Fig 5.1D, dotted circle) was exposed to high laser power, creating a localised lesion that could be visualised by the autofluorescent signal emanating from the lesion. In response to this, nearby microglia rapidly extended their processes in a directed manner towards the lesion as has been reported previously (Davalos et al., 2005; Haynes et al., 2006). To quantify this movement, the area of GFP-free space surrounding the lesion was measured (red polygon) and tracked over time (Fig 5.1E). Interestingly, in our hands microglial processes converged on the lesion site within 10 minutes, in contrast to the much longer times reported elsewhere (Davalos et al., 2005). These two imaging and analysis workflows provide a way of quantifying two important and distinct behaviours of microglia.

5.2.2 Roles of key actin remodelling molecules in microglial motility

Little is known about the intracellular signalling pathways governing actin remodelling in microglia during surveillance or chemotaxis. In order to interrogate this, microglial motility was assessed during pharmacological inhibition of a number of key actin processes and signalling molecules. Firstly, the effect of actin polymerisation inhibition was investigated by treatment of slices with 10 μM cytochalasin D, a potent inhibitor of polymerisation of F-actin. Strikingly, cytochalasin D completely abolished microglial motility (Fig 5.2A). Surveillance index (SI) was reduced to approximately 20% of control in treated microglia (Fig 5.2B; Untreated 755.4 ± 105.9 px, cytochalasin D 145.3 ± 15.34 px, $p<0.001$). Given that observation showed that these microglia showed no process motility, this residual SI is a useful readout of the noise generated from the analysis. This is promisingly low, suggesting that SI analysis is a capable measure of surveillance. Cytochalasin D-treatment also abolished chemotactic response to laser damage, as can be seen in the lack of process convergence in treated slices (Fig 5.2C-D) ($p<0.001$, two-way RM ANOVA). Thus, actin polymerisation is critical for both microglial surveillance and chemotaxis.

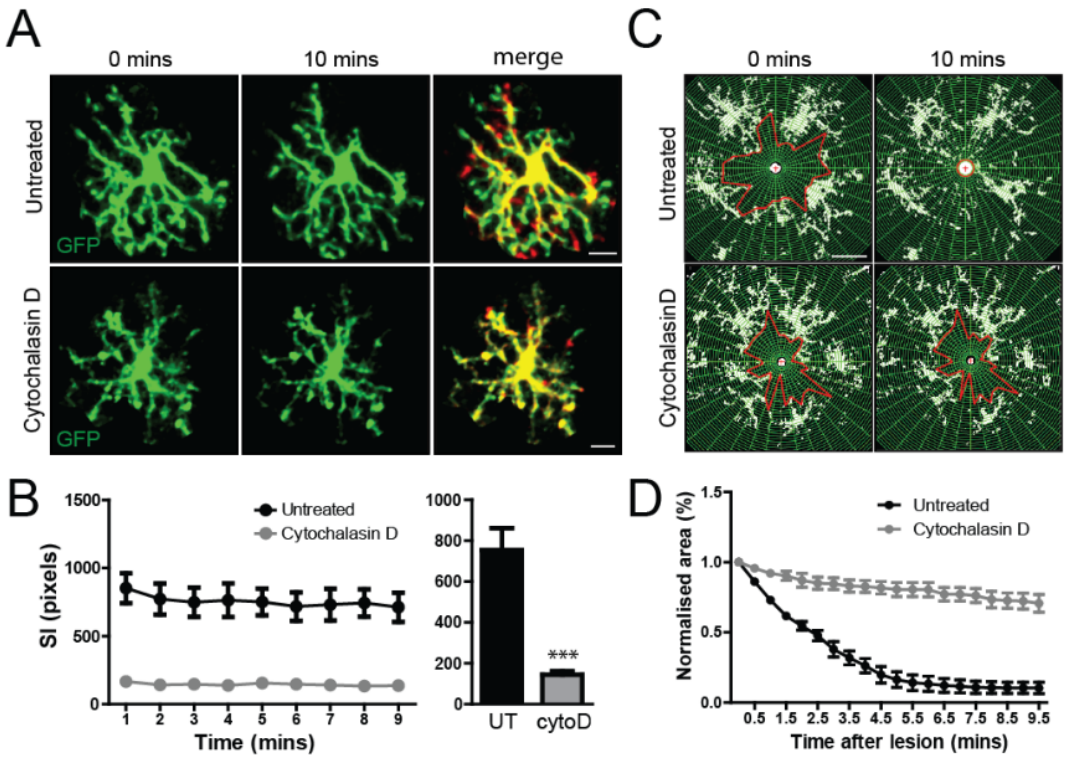

Fig. 5.2: Microglial motility is critically dependent of actin polymerisation
(A) Representative cells from untreated acute slices (top panel) or those pretreated with 10 µM cytochalasin D for 20 minutes (bot panel). Scale bar: 10 µm. **(B)** Surveillance Index (SI) of microglia over 10 minutes with 1 minute framerate (left) and averaged SI value over this period (right) shows a significant decrease in baseline surveillance in cytochalasin-treated slices ($p<0.001$, student's unpaired t-test, N=14-15 cells). **(C-D)** Abolished chemotactic response in cytochalasin D treated slices, quantified as a lack of process convergence onto lesion site ($P<0.001$, 2-way RM ANOVA, N=6 lesions).

The Arp2/3 complex is required for cells to generate new branches of F-actin and is a critical part of actin remodelling machinery. To test if actin branching is required for normal microglial motility, acute slices were treated for 30 minutes with selective Arp2/3 inhibitor CK666 (200 μM) prior to and during imaging (Hetrick et al., 2013). Inhibition of Arp2/3 had a dramatic effect on the morphology of microglia, characterised by retraction of secondary and tertiary processes (Fig 5.3A). 3D reconstructions of DMSO and CK666-treated microglia showed a dramatic loss of process complexity as seen by Sholl analysis of intersections (Fig 5.3A,B) ($p<0.001$, two-way RM ANOVA). The number of branches in CK666-treated cells was reduced, though total process length was not significantly different (Fig 5.3C) (branches: DMSO 14.40 ± 1.07, CK666 7.97 ± 0.92, $P<0.0001$; length: DMSO 651.4 ± 28.65 μm, CK666 550.2 ± 42.70 μm, $p=0.053$). Additionally, primary processes often appeared swollen, with large aberrant membrane blebbing seen (Fig 5.3D). Approximately 60% of CK666-treated cells showed blebbing, a 6-fold increase over control (Fig 5.3E) (DMSO: 9.68 ± 2.76%, CK666: 60.66 ± 5.53%, $P<0.0001$). Closer observation of CK666-treated slices showed highly dynamic, unstable filipodia often seen rapidly forming and disappearing from the enlarged primary processes (Fig 5.3D). Thus, Arp2/3 inhibition dramatically disrupts microglial morphology.

To investigate how these changes impacted motility, surveillance and chemotaxis behaviour was assessed. Arp2/3 inhibition reduced surveillance by approximately 50% compared to DMSO-treated cells (Fig 5.4B) (DMSO 185.3 ± 9.15 px, CK666 87.82 ± 6.92 px, $P<0.0001$). Surprisingly, the effect of Arp2/3 inhibition on chemotaxis was comparatively mild. CK666-treated microglia showed a remarkably robust chemotactic response (Fig 5.4C-D; NS, two-way RM ANOVA). Tracking the movement of individual processes revealed a slight decrease in process speed (Fig 5.4E) (DMSO 3.84 ± 0.13 μm/min^{-1}, CK666 3.48 ± 0.11 μm/min^{-1}, $p<0.05$). In agreement with the observations from the surveillance assay, tips of microglial processes were often abnormally swollen in comparison to the thin process and bulbous process head of control microglia. Thus, Arp2/3 activity is critical for surveillance motility but largely dispensable for lesion-induced chemotaxis *in situ*.

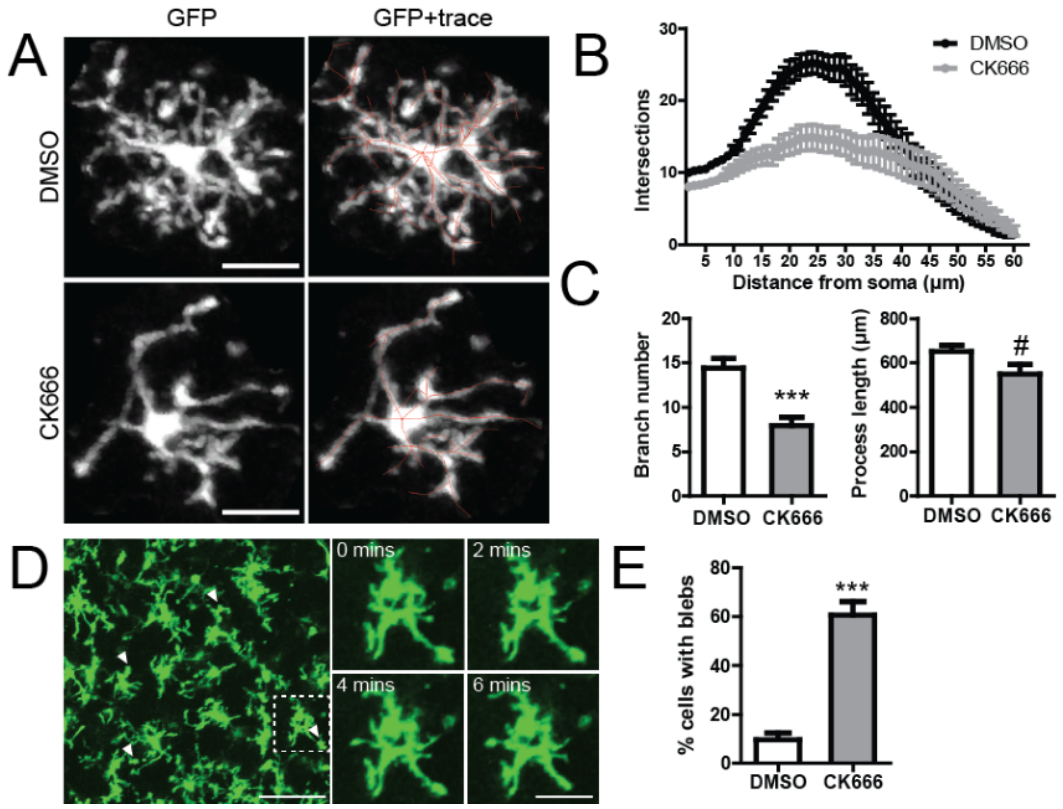

Fig. 5.3: Inhibition of Arp2/3 activity dramatically alters microglial morphology
(A) Representative cells from slices treated with DMSO (top) or 200 µM CK666 (bottom), showing loss of higher order processors. Left panel: MIP of GFP fluorescence. Right panel: GFP signal superimposed with 3D reconstruction of cell morphology (red skeleton). Scale bar: 20 µm. **(B)** Sholl analysis of intersections from 3D reconstructions ($p<0.001$, two-way RM ANOVA). **(C)** Summary of other morphological characteristics; decrease in branching (left, $p<0.0001$, student's unpaired t-test) whilst total process length is not significantly altered (right, $p=0.053$, student's unpaired t-test).) **(D)** CK666-treated microglia often seen with enlarged cellular protrusions. Left: Field of view of CK666-treated slice highlighting blebs (white arrows). Right: Timelapse showing retraction into primary process and filopodial extensions. Scale bar: 20 µm. **(E)** Quantification of proportion of microglia with blebs ($p<0.0001$, student's unpaired t-test, N=132-154 cells).

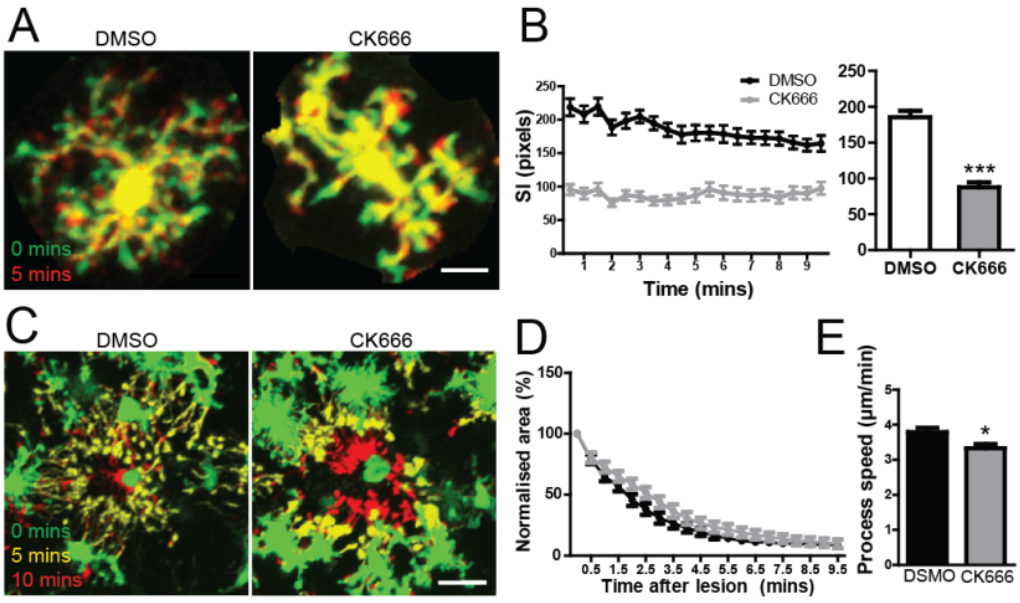

Fig. 5.4: Inhibition of Arp2/3 impairs microglial surveillance and chemotaxis
(A) Superimposed timelapse images of representative cells from DMSO (left) or CK666 (right) treated slices, showing extensions (red), retractions (green) and stable regions (yellow) over 5 minutes. Scale bar: 20 µm. **(B)** Quantification of SI from 10 minute, 30 second frame movies. SI of CK666-treated cells decreased to 47% of DMSO controls ($p<0.0001$, student's t-test, N=38-39 cells). **(C-E)** Delayed chemotaxis during Arp2/3 inhibition. **(C)** Superimposed timelapse showing process chemotaxis in DMSO (left) and CK666 (right) treated slices. Scale bar: 10 µm. **(D)** Slowed reduction in process convergence seen as right-shift (NS, two-way RM ANOVA). **(E)** Single process tracking shows reduction in speed of CK666-treated processes ($p<0.05$, N=31 processes).

Given the significant effect that Arp2/3 inhibition had on microglial morphology and surveillance behaviour, the signalling pathways feeding into this complex were further investigated. Rac1 is a key upstream activator of Arp2/3, acting via the WRC. Thus, it was hypothesised that Rac1 inhibition would have a similar effect to Arp2/3 inhibition. Acute slices were pretreated for 30 minutes with 100 μM NSC23766, a concentration which has been used previously to inhibit Rac1 in acute slices (Hou et al., 2014). The effects on morphology had similarities and difference compared to Arp2/3 inhibition (Fig 5.5). Abnormal blebbing of processes was also observed, though less often than seen with CK666 treatment (Fig 5.5A,C) (DMSO 9.68 ± 2.76%, NSC23766 35.39 ± 6.69%, $P<0.01$). Surprisingly, Sholl analysis suggested that microglia were similarly complex (Fig 5.5B,D) (two-way RM ANOVA). Branching and total process length were both unaffected (Fig 5.5E) (branches: DMSO 12.15 ± 1.06, CK666 12.21 ± 1.27; length: DMSO 608.3 ± 31 μm, CK666 632.7 ± 39.95 μm). Looking at surveillance, NSC23766-treated microglia showed a 30% reduced in SI (Fig 5.5F-G) (DMSO 200.5 ± 16.08 px, CK666 140.5 ± 11.70 px, $P<0.01$). Thus, Rac1 inhibition causes microglial blebbing and impairs surveillance.

Together, these data suggest that actin remodelling plays a critical role in regulating microglial shape and motility in situ. Concretely, actin polymerisation is critical for process movement. F-actin branching via Arp2/3 is required for the stability of microglial processes, though microglia are still capable of chemotaxis. As Rac1-inhibitied microglia share many similarities to those lacking Arp2/3 activity, it is likely that Rac1 activity modulates microglial actin remodelling via Arp2/3.

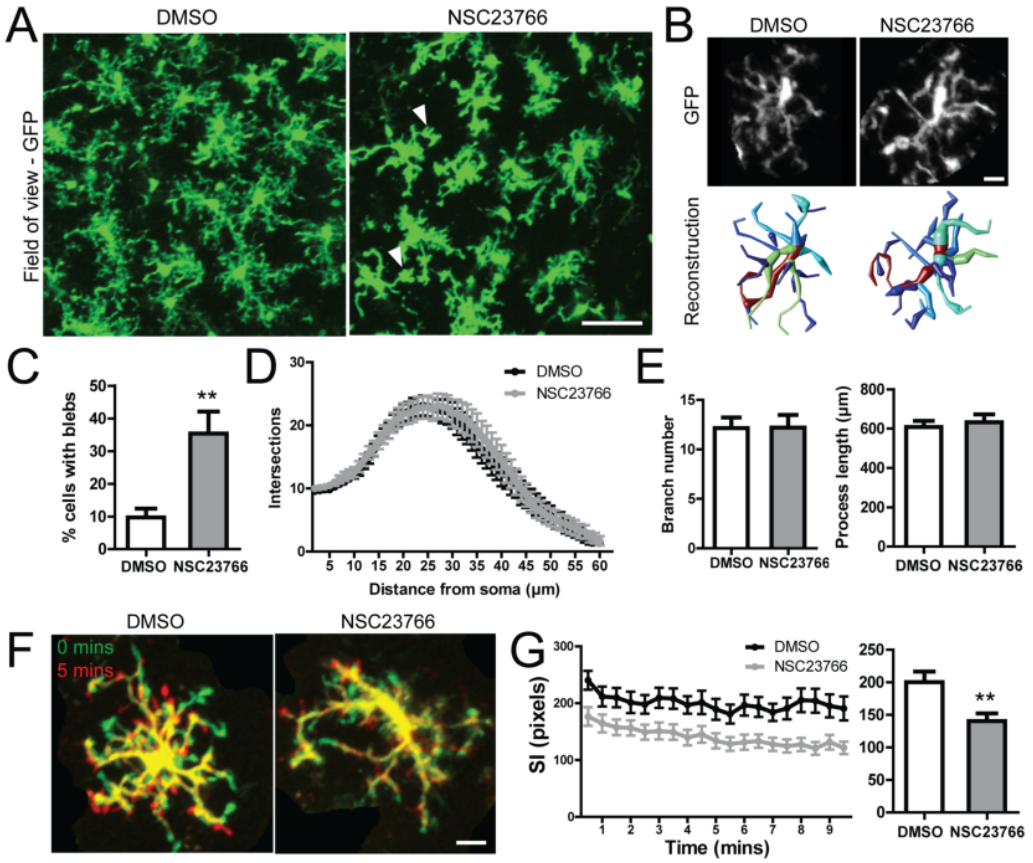

Fig. 5.5: Inhibition of Rac1 alters microglial morphology and surveillance motility
(A) FOV of DMSO and NC237666 treated slices showing clear morphological change and presence of blebs (white arrows). Scale bar: 25 µm. **(B)** Representative examples of 3D reconstructions of single cells, DMSO (left) and NSC23766 (right). **(C)** Quantification of proportion of microglia with blebs ($p<0.01$, N=132-154 cells). **(D)** Sholl analysis of intersections from 3D reconstructions (two-way RM ANOVA). **(E)** Summary of other morphological characteristics; no change in branching (left) or total process length (right), N=48-52 cells per condition. **(F)** Superimposed timelapse images of microglia from DMSO (left) or CK666 (right) treated slices, showing extensions (red), retractions (green) and stable regions (yellow) over 5 minutes. Scale bar: 10 µm. **(G)** Quantification of SI from 10 minute, 30 second frame movies. SI of CK666-treated cells decreased to 47% of DMSO controls ($p<0.01$, student's unpaired t-test, N=29-34 cells).

5.2.3 Generation of an inducible condition mouse model to study loss of microglial CYFIP1

The WAVE regulatory complex is the primary link between Rac1 and Arp2/3 activity; Rac1-binding to CYFIP1 to relieve intra-complex inhibition and lead to Arp2/3 activation (Chen et al., 2017). As discussed, multiple transcriptomic studies have shown that microglia highly express CYFIP1, whereas CYFIP2 expression is very low (Fig 5.6A) (CYFIP1: mouse 62.37 ± 7.30 FPKM, human 61.2 ± 16.24 FPKM; CYFIP2: mouse 2.35 ± 0.01 FPKM, human 0.54 ± 0.16 FPKM) (Zeisel et al., 2018; Zhang et al., 2014a). Thus, it was hypothesised that CYFIP1 loss could alter microglial dynamic behaviours.

In order to study loss of CYFIP1 in microglia *in vivo*, a conditional knockout mouse model was generated using a Cre-loxP recombination strategy of a knock-in floxed cassette of the endogenous CYFIP1 gene, as in Chapter 2 (Fig 5.6B). To target recombination specifically to microglia, the floxed CYFIP1 line was crossed with a Cre recombinase expressed under the CX3CR1 promoter (Yona et al., 2013). Additionally, the recombinase in this system is fused to a fragment of the estrogen receptor transporter (ERT), preventing access to the nucleus under basal conditions (Fig 5.6C). This is useful because, as well as microglia, the CX3CR1 promoter is active in peripheral monocytes. Constitive Cre activity would lead to a knockout of CYFIP1 in these cells that may have undesired consequences on animal viability and brain function. However, due to the relatively slow turnover of microglia in the brain compared to peripheral monocytes, acute activation of $CX3^{CreERT2}$ leads to stable recombination only in the microglial population and not in other cell types (Goldmann et al., 2013).

Activation of the Cre requires the presence of oestrogen-receptor agonist tamoxifen that binds to the ERT (in its active form 4-OHT) and facilitates the translocation of Cre into the nucleus where it can recombine the floxed cassette (Fig 5.6C). Thus, 4 mg tamoxifen was administered by oral gavage to adult mice twice

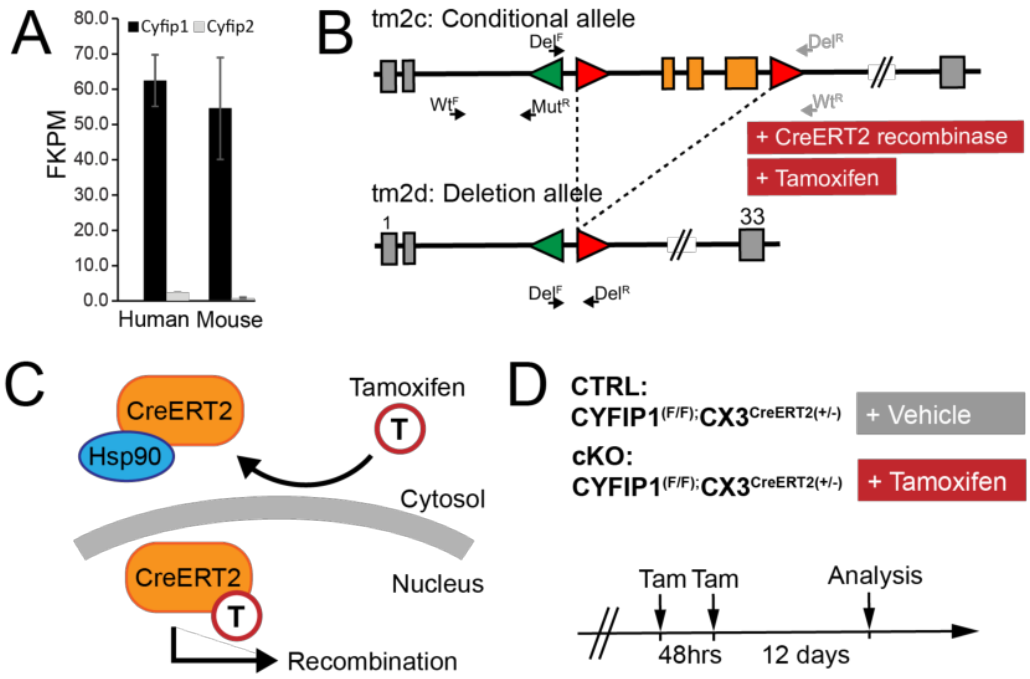

Fig. 5.6: Generation of a microglia-specific Cyfip1 conditional knockout mouse model **(A)** RNA levels of CYFIP1 and CYFIP2 in human and mouse microglia, adapted from Zhang et al. (2014). CYFIP1 is highly expressed whereas CYFIP2 is almost absent in both species. **(B)** Schematic showing generation of conditional CYFIP1 deletion in microglia using the CreERT2 driven from the microglia-specific CX3CR1 promoter. **(C)** CreERT2 is kept inactive under basal conditions by interaction between the estrogen receptor (ERT2) domain and Hsp90, preventing Cre entry into the nucleus. Tamoxifen (precisely, the tamoxifen-derivative 4-OHT) releases this interaction, leading to the entry into the nucleus and initiation of recombination events by Cre recombinase. **(D)** Treatment regime to generate experimental pairs. Control (CTRL) and conditional knockout (cKO) animals were both homozygous for the CYFIP1 floxed allele and carried a single $CX3^{CreERT2}$ allele. To activate the CreERT2, cKO animals were given two 4 mg/100 µL doses of tamoxifen via oral gavage, 48 hours apart. CTRL animals were dosed with an equal volume of vehicle. Animals were between P28-30 at start of treatment, unless stated otherwise.

48 hours apart, which has been used previously to induce efficient activation of the CX3CR1^{CreERT2} (Goldmann et al., 2013; Parkhurst et al., 2013). Animals were then left for 2 weeks after initial treatments prior to experiments to allow for the knockout of CYFIP1 to take effect. This time period also enables recovery of peripheral cell populations from recombination, as discussed (Goldmann et al., 2013).

In order to visualise the recombination efficiency of this tamoxifen regime, the CX3CR1^{CreERT2} line was crossed with a stop-floxed MitoDendra reporter line (Fig 5.7A). Using IHC staining against IBA1 to visualise all microglia in slices prepared from these animals, a percentage recombination could be calculated. Control slices (treated with vehicle) showed a very low rate of basal recombination (hippocampus: 1.16 ± 0.79%, cortex: 2.55 ± 1.07%, cerebellum: 2.11 ± 0.86%). This confirms that basal Cre is efficiently kept out of the nucleus and therefore unable to remove the mitoDendra stop codon (Fig 5.7B). In contrast, tamoxifen treatment led to the vast majority of IBA+ve cells expressing MitoDendra, with over 90% dual expression in both the hippocampus, cortex and cerebellum (Fig 5.7B; hippocampus: 89.57 ± 1.56%, cortex: 89.4 ± 0.48%, cerebellum: 90.57 ± 1.68%). Importantly, no ectopic expression of mitoDendra was observed in any non-IBA+ve cells, suggesting that the Cre was only activated in microglial cells, as expected (Fig 5.7B, zoom panels). These data suggest that this system enables specific and highly efficient recombination in microglia.

Recombination of the CYFIP1 cassette was confirmed by PCR for the deleted cassette (Del), present only in tamoxifen-treated animals (Fig 5.8A). To confirm that CYFIP1 was lost in microglia at the protein level, lysates from CTRL and cKO brains were generated. Whole brain region lysates did not show any loss of CYFIP1 at the protein level, which could be expected given that microglia only represent 10-15% of the total cells in the brain (data not shown). Thus, a percoll gradient isolation protocol was used to isolate an enriched microglia fraction from single cell suspensions of whole brain (Fig 5.8B) (Lee and Tansey, 2013). Enriched microglial lysates showed a significant decrease in CYFIP1 expression of approximately 50% (Fig 5.8C) (CTRL

1 ± 0.15, cKO 0.48 ± 0.06, P<0.05). Whilst there was still CYFIP1 signal present, this fraction is only enriched for microglia, and likely contained significant levels of peripheral macrophages and other cell types that would have retained CYFIP1 expression.

Finally, loss of microglial CYFIP1 was shown on the single cell level by IHC of slices stained with an antibody against CYFIP1 (Fig 5.8D). In control slices, CYFIP1 staining could seen seen as punctate signal concentrated in the cell soma but also seen within microglial processes (Fig 5.8D, zooms 1+2). In contrast, this signal was absent or significantly reduced from microglia from cKO slices (Fig 5.8D, zooms 3+4). Quantification of somal CYFIP1 signal showed significant reduction in cKO (Fig 5.8E; CTRL: 867.7 ± 132 IntDen, cKO: 410.2 ± 30.85 IntDen, p<0.01). Together, these data show that this model leads to efficient loss of microglial CYFIP1 expression *in vivo*, facilitating future study.

5.2.4 Alterations in microglial morphology and motility in CYFIP1 cKO

As CYFIP1 reduction leads to changes in neuronal morphology, and pharmacological inhibition of CYFIP1-associated proteins (Arp2/3 and Rac1) altered microglial morphology, it was hypothesised that cKO microglia might have altered morphology. To investigate this, control and cKO brains were PFA fixed and 75 µm - 100 µm slices were cut and stained to amplify the GFP signal. No gross abnormalities in microglial morphology were observable; cKO microglia had clearly ramified secondary and tertiary processes (Fig 5.9A). In order to get an accurate representation of the 3D structure of microglia, individual cells were reconstructed semi-automatically from 50 µm z-stacks using the open-source software platform Vaa3D (Fig 5.9A) (Peng et al., 2014). Interestingly, Sholl analysis of these reconstructions revealed a decrease in complexity of microglial processes that appeared consistent across the whole arbor (Fig 5.9B; two-way RM ANOVA, P<0.05). Concretely, total branch number, tip

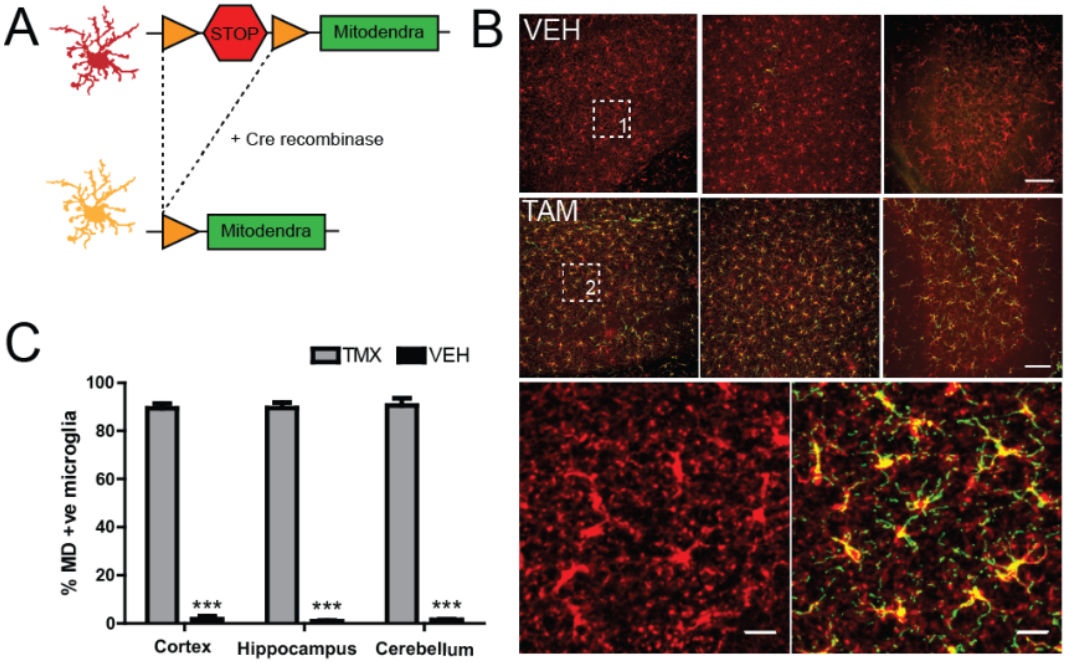

Fig. 5.7: Highly efficient recombination by CX3^{CreERT2} using MitoDendra reporter line

(A) Graphical illustration of genetic recombination of MitoDendra (MD) reporter cassette in presence of Cre recombinase. A premature stop codon (STOP), flanked by loxP sites (floxed), prevents MD expression basally. Presence of Cre removed the stop codon via recombination between loxP sites, leading to expression of MD. **(B)** IHC of CX3CR1^{CreERT2}(+/-);MD(+/-) mice treated with vehicle (top) or tamoxifen (bottom). Staining for IBA1 (red) and MD (green) showing very low levels of MD+ IBA+ cells in vehicle controls, whereas most IBA+ cells are MD+ in the tamoxifen-treatment. No MD+ IBA- cells were observed in either condition. Scale bar: 100 µm (top) and 25 µm (bottom). **(C)** Quantification of percentage of IBA+ cells that were MD+ across different brain regions. All regions showed equivalent fractions of MD+ cells (hippocampus: $p<0.0001$, cortex: $p<0.0001$, cerebellum: $p<0.0001$, two-way ANOVA).

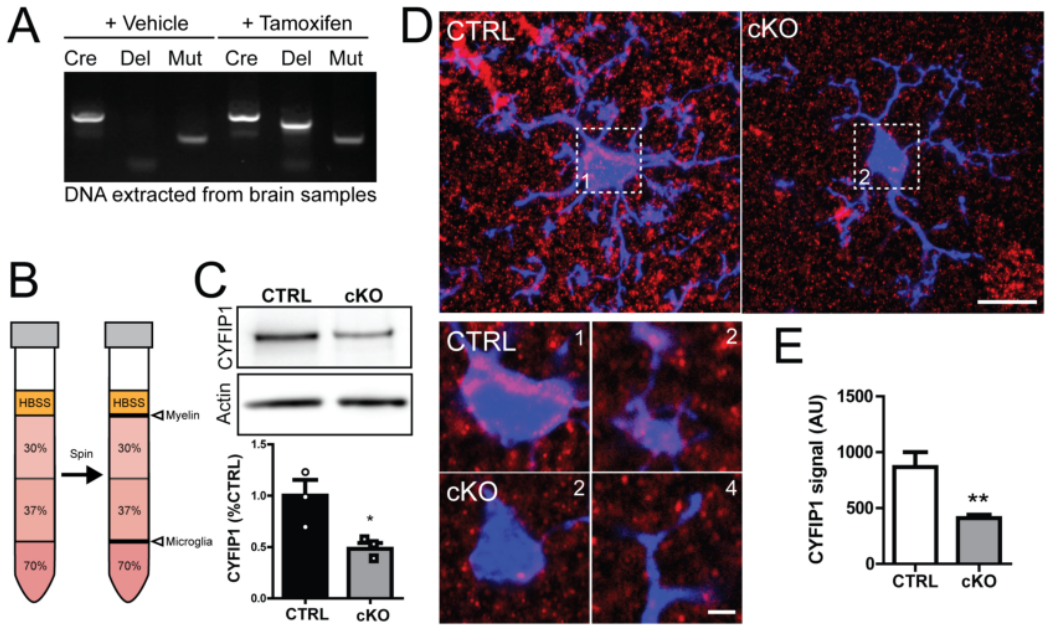

Fig. 5.8: Reduced CYFIP1 expression in enriched microglial brain lysate from cKO animals

(A) PCR for the deletion product (DEL) from brain tissue. DEL band only present in cKO. **(B)** Illustration of Percoll gradient used to extract enriched microglial fraction from single cell suspension of homogenized brain tissue. After centrifugation (see methods), microglia concentrate in the 70%:37% interphase. **(C)** Western blot of enriched microglial lysate from CTRL and cKO brains shows significant reduction in CYFIP1 levels in cKO ($p<0.05$, student's unpaired t-test, N=3 experimental pairs). **(D)** IHC of sections of CTRL and cKO brains from IBA^{eGFP+} animals, labelled for CYFIP1 and GFP. Left panels: max projections of z-stacks of representative microglia. Scale bar: 10 µm (large), 2 µm (zoom). Right panels: single planes of zoomed regions from these cells; CYFIP1 visible in both the soma and processes of CTRL cells, whereas this is reduced in cKO cells. **(E)** Quantification of CYFIP1 signal in microglial somas, showing reduction in cKO ($p<0.01$, student's unpaired t-test, N=25 cells from 3 experimental pairs).

number and process length were all significantly reduced (Fig 5.9C) (branches: CTRL 56.44 ± 4.85, cKO 41.31 ± 4.22, $p<0.05$; tips: CTRL 67.38 ± 5.28, cKO 50.89 ± 4.33, $p<0.05$; total process length: CTRL 1206 ± 63.30 µm, cKO 992.6 ± 74.47 µm, $p<0.05$). Thus, loss of CYFIP1 leads to a loss of microglial complexity.

This change in microglial morphology suggests that CYFIP1 may indeed be playing a role in remodelling actin within microglia. Given the previous association between morphology and impaired surveillance discussed previously, it was hypothesised that loss of CYFIP1 would alter microglia surveillance. To investigate this, acute slices of CTRL and cKO animals were imaged using the two assays of microglial motility established previously (Fig 5.10A,D). Quantifying surveillance of cKO microglia compared to control showed a significant reduction in SI (Fig 5.10B) (CTRL 612.5 ± 37.64 px, cKO 449.8 ± 32.67 px, $p<0.01$). Interestingly, loss of CYFIP1 had no effect on chemotactic response to laser-induced lesion with control and cKO microglia responding with equal process convergence (Fig 5.10C-D) (2-way ANOVA RM). In agreement with this, tracking individual processes showed no change in speed between conditions (Fig 5.10E) (CTRL 3.77 ± 0.14 µm/min^{-1}, cKO 3.90 ± 0.10 µm/min^{-1}). Taken together, these data suggest that loss of microglial CYFIP1 differentially effects microglial behaviours, causing a specific impairment in surveillance whilst chemotaxis is unaffected.

5.3 Discussion

In this chapter, the importance of actin remodelling to dynamic behaviours of microglia was interrogated, using both pharmacological and genetic interventions. These experiments unveiled novel roles for Arp2/3, Rac1 and WRC component CYFIP1 in establishment of microglial morphology and motility.

Despite the rapid expansion of literature on the functional roles microglial surveillance and chemotaxis play in both healthy brain development and disease

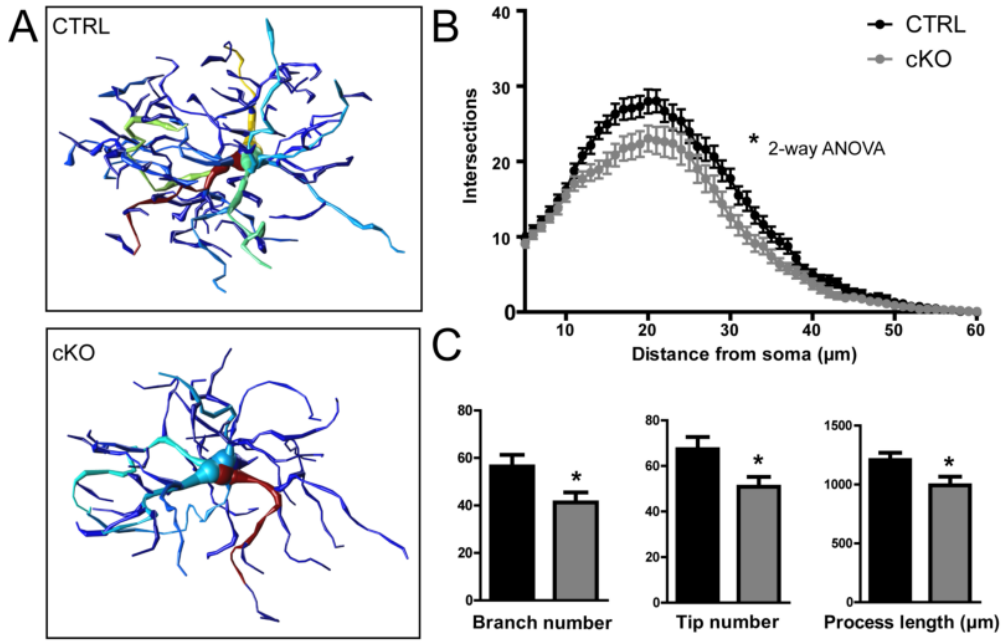

Fig. 5.9: Decreased morphological complexity of cKO microglia
(A) Representative 3D reconstructions of microglia taken from fixed slices of CTRL and cKO brains, showing reduced complexity of arborisations. **(B)** Sholl analysis of reconstructions reveal a decrease in the number of intersections across the arbor (two-way RM ANOVA, $p<0.05$). **(C)** Summary of morphological characteristics of microglia; reduced number of branches (left, $p<0.05$, student's unpaired t-test), tips (middle, $p<0.05$, student's unpaired t-test) and total process length (right, $p<0.05$, student's unpaired t-test). N=34-35 cells from 3 experimental pairs

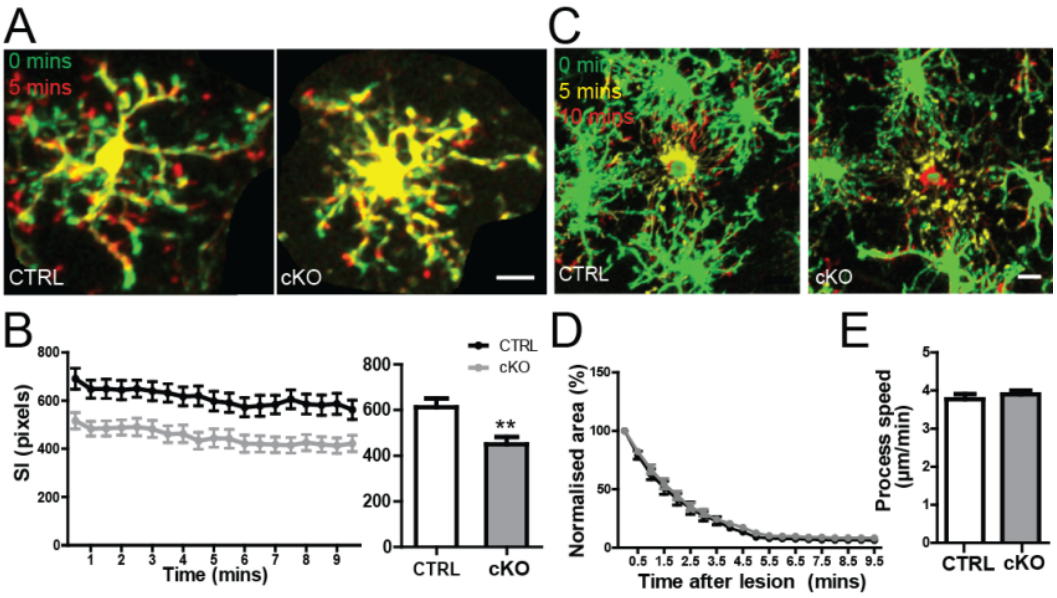

Fig. 5.10: Specific impairment in surveillance motility in cKO microglia
(A) Superimposed timelapse images of microglia from CTRL (left) or cKO (right) brain slices, showing extensions (red), retractions (green) and stable regions (yellow) over 5 minutes. Scale bar: 10 µm. **(B)** Quantification of SI from 10 minute, 30 s frame movies. SI of cKO microglia decreased to 47% of DMSO controls ($p<0.01$, student's unpaired t-test, N=52-56 cells from 3 experimental pairs). **(C-E)** Normal chemotaxis by cKO microglia. **(C)** Superimposed timelapse showing process chemotaxis in CTRL (left) and cKO (right) brain slices. Scale bar: 10 µm. **(D)** No change in process convergence (two-way RM ANOVA). **(E)** Single process tracking shows normal extension speed, N=48-59 processes from 3 experimental pairs.

models, the intracellular signalling underlying these processes is poorly understood (Colonna and Butovsky, 2017; Madry and Attwell, 2015). As actin remodelling is a critical driver of cell motility, it was hypothesised that it also played a key role in microglial dynamics, as had been suggested previously (Hines et al., 2009). In agreement with this, inhibition of actin polymerisation completely abolished both surveillance and chemotaxis of microglia. Interestingly, cytochalasin D-treated microglia still maintained a branched structure, but processes were undynamic and irresponsive. This is possibly due to short treatment time prior to imaging (10 minutes) that did not allow morphological changes to take place. Given this, it would be interesting to see if microglia maintained their complex morphology during more prolonged treatment. Alternatively, although microtubule density is thought to be low in microglia, acetylated and detyrosinated microtubules have been observed in microglial processes *in situ* (Fanarraga et al., 2009; Ilschner and Brandt, 1996). Thus, in the absence of actin dynamics, microtubules may stabilise microglial morphology.

Alterations in microglial morphology

To better understand the role of actin remodelling in microglia *in situ*, drug treatments were used to inhibit core remodelling complexes. Inhibiting Arp2/3 activity led to a dramatic change in microglial morphology, characterised by a loss of secondary and tertiary processes and a swelling of primary processes (blebs). One interpretation of this is that Arp2/3 is required for the stability of more dynamic processes. Loss of Arp2/3 in cultured macrophages prevents lamellipodia formation, but also disrupted focal adhesion (FA) rosettes and integrin-based haptotaxis (Rotty et al., 2017). Further, Arp2/3 is a critical component of podosomes in cultured microglia (Siddiqui et al., 2012; Vincent et al., 2012). Podosome and FAs link the actin cytoskeleton to the extracellular matrix (ECM) via transmembrane receptors and are required for cells to maintain stable adhesion. Thus, disrupted ECM association could underlie the loss of secondary higher-order processes. According to this interpretation, the

swelling of primary processes could be a consequence of extra plasma membrane collapsing in from unstable processes.

Alternatively, these membrane expansions are highly reminiscent of cellular structures termed blebs, that have well-characterised roles in cell migration (Paluch and Raz, 2013). Initially discovered during apoptosis, blebs are formed by hydrostatic pressure generated within the cytoplasm in response to actomyosin contraction and disruption of the membrane-actin cortex association. Interestingly, EM imaging of Arp2 knockout macrophages by Rotty et al. showed replacement of lamellipodia with blebs. Inhibition of Arp2/3 has also been shown to favour blebbing over lamellipodia in carcinoma cells and C. elegans embryos (Bergert et al., 2012; Bovellan et al., 2014; Roh-Johnson and Goldstein, 2009). Further, increased myosin contractibility was reported in Arp2c knockout macrophages which is also capable of driving bleb formation (Bergert et al., 2012; Rotty et al., 2017). Bleb-like protrustions were also seen in NSC23766-treated microglia in this chapter, despite a less dramatic change in cell morphology. Active Rac1 triggers switching from bleb to lamellipodia formation via activation of Arp2/3, and bleb formation is enhanced by activation of the alternative RhoGTPase signalling pathway RhoA/ROCK (Bergert et al., 2012; Lawson and Ridley, 2018). Further, SRA1 (fly CYFIP1 homologue) and other WRC components associate closely with cortical actin and could therefore play a role in membrane-cortex stability (Korobova and Svitkina, 2008). Thus, Rac1 inhibition could lead to bleb formation via both reduced Arp2/3 activation and comparatively increased RhoA/ROCK signalling.

If the protrusions seen in Arp2/3 and Rac1 inhibited microglia are indeed blebs, it is interesting to speculate on their potential function. Given the known roles for blebs in cellular migration, it is feasible that microglia may utilise blebs to migrate into the brain during embryogenesis. To date there have been few live imaging studies observing early microglial migration *in vivo*. Time-lapse movies of microglial precursors entering the larval zebrafish midbrain show cells with bleb-like processes, suggesting that blebbing could play a role (Xu et al., 2016). Though

pharmacological inhibition is an unphysiological condition, the de-ramification of microglia on Arp2/3 and Rac1 inhibition is reminiscent of activated microglia seen in early development and various disease-states (Hong and Stevens, 2016; Squarzoni et al., 2014). It would be interesting to see if localisation of active Rac1 and/or Arp2/3 was altered in microglia in these states, for instance using a FRET-based approach (Li et al., 2012).

Loss of CYFIP1 reduced morphological complexity of microglial processes, with reduced branching and total process length. Given the previously data on Rac1 and Arp2/3 inhibition, it is likely that this effect is due to disrupted Arp2/3 activation by the WRC upstream of Rac1. Interaction between the WRC and surface receptors containing a WIRS-motif could also be involved. Indeed, the P-selectin ligand, SELPLG, is highly expressed in microglia, contains a WIRS motif and has established roles in migration and chemotaxis in (Ali et al., 2015; Chen et al., 2014a). Membrane-actin links could control local Arp2/3 activity to guide process formation and stablisation. Whilst it cannot be ruled out, an FMRP-based mechanism is unlikely, given that expression in microglia is low, and the timescales of process dynamics (seconds) are too fast for a significant influence of local protein translation (Gholizadeh et al., 2015).

Interestingly, microglial blebs were not observed in CYFIP1 cKO microglia. This is perhaps surprisingly given that CYFIP1 sits in the middle of the Rac1-WRC-Arp2/3 signalling pathway. Rac1 has several downstream targets relating to actin remodelling aside from the WRC, including the formin mDia2 and LIMK-cofilin signalling (Lammers et al., 2008; Yang et al., 1998). Equally, the Arp2/3 complex is regulated by N-WASP and WASP via cdc42. These other interactions may explain the disparity between these pharmacological treatments and CYFIP1 loss. Inhibition of the WRC would be a useful comparison point for this question, although the current lack of specific pharmacological inhibitors of the WRC makes this difficult.

Surveillance and chemotaxis; divergent behaviours?

Altered morphology of microglia upon Arp2/3 and Rac1 inhibition was coincident with impaired surveillance of the microglial domain. Broadly, there are two ways this could occur; reduced movement of processes or reduced numbers of processes. Given the previous discussion, it is clear that the latter is contributing to the surveillance defect. No obvious defects in motility of cKO microglial processes were observed suggesting that the reduced SI was due to reduced complexity. Arp2/3 inhibited microglia did show altered process motility, with slow retraction of normally stable primary processes and blebbed structures in place of semi-stable secondary processes as discussed. To address this, tracking of individual processes to quantify motility in real terms (μm/min) would be required. In summary, the surveillance defects observed reflect a mix of altered cell morphology and process dynamics, depending on the intervention.

These experiments reveal an interesting discrepancy between effects on surveillance and chemotaxis. Although Arp2/3 inhibition did slow chemotactic response, it was surprisingly robust and process extension was far more similar to control than during surveillance. This raises the possibility that distinct actin remodelling pathways underlie these two different behaviours. It has previously been established that the surface receptors governing surveillance and chemotaxis in situ are different; P2Y12 being critical for chemotaxis but dispensable for surveillance, whereas the two-pore potassium channel THIK-1 regulates surveillance by controlling microglial membrane potential (Haynes et al., 2006; Madry et al., 2018a; Sipe et al., 2016). P2Y12 activation is associated with a number of actin regulators, including phosphorylation of Akt and ERK1/2 (Irino et al., 2008; Lee et al., 2012; Ohsawa et al., 2007, 2010). Importantly, Arp2/3 is not a typical downstream target of Akt or ERK1/2; which are associated with RhoA/ROCK/myosin-II and paxillin FAs respectively (Lee et al., 2012). Additionally, Rac1 is required for C5q but not ATP chemotaxis (Miller and Stella, 2009). Thus, data presented here alongside existing literature suggest that Arp2/3

activation is not necessary for ATP chemotaxis. It is worth noting that most of these studies used microglial cultures and studied whole cell migration towards a chemotactic stimuli. Whilst informative, it will be important to confirm that these signalling pathways are activated similarly *in situ*.

The intracellular signalling controlling Arp2/3 activity during surveillance is less clear. Rac1 activity is seen at the leading edge of microglial processes in response to glutamate uncaging (Li et al., 2012). It would be interesting to see if Arp2/3 activity is disrupted in THIK-1 KO microglia, for instance by using CK666 to investigate in THIK-1 and Arp2/3 were acting in the same pathway to control surveillance. An outstanding issue with the this model is that THIK-1 controls whole cell potential, whereas process motility requires localised activation of actin remodelling pathways. Although calcium transients do occur in microglia, they are too slow to be driving surveillance (Pozner et al., 2015). More likely is that surveillance motility is driven by outside-in signalling from ECM components to the cytoskeleton.

Consequences of defective surveillance in CYFIP1 cKO

The effects of loss of CYFIP1 on microglial morphology and surveillance open up a number of intriguing possibilities for the CYFIP1 field. Microglial surveillance has many important functions, including sensing dead or damaged cells to phagocytose, contacting dendritic spines to regulate neuronal activity, and pruning synapses (Li et al., 2012; Schafer et al., 2012; Sierra et al., 2010). In theory, reduced baseline surveillance could impair the ability of microglia to sense these important events in their respective domains. This could have important consequences for network connectivity, E/I balance and behavioural traits including social interaction and memory formation. This is of particular interest given CYFIP1s well-established association with neuropsychiatric disorders. Indeed, many of the developmental abnormalities that have been discovered when microglial function is disrupted are

reminiscent of common pathologies on these conditions. Thus, these data suggest a new cellular substrate by which CYFIP1 CNVs can cause altered brain function.

The presence of filopodia-like, immature spines is a perineal feature of mouse models of CYFIP1 CNV (de Rubeis et al., 2013; Oguro-Ando et al., 2015; Pathania et al., 2014). Data presented in chapter 4 suggests that in hippocampus this pathology appears cell-autonomous. However, it would be interesting to investigate if loss of microglial CYFIP1 had any effect on the density and/or morphology of dendritic spines. Microglial contact on dendrites during in early postnatal cortex initiates filipodia formation and microglial depletion during this time window decreases spine densities (Miyamoto et al., 2016). Microglial BDNF is also critical for learning-dependant synapse formation in the motor cortex (Parkhurst et al., 2013). Reduced surveillance could limit these microglial functions, impacting dendritic spine formation.

Numerous studies have shown microglia phagocytose synaptic material and that this is correlated with altered spine densities and/or functional connectivity (Paolicelli et al., 2011; Schafer et al., 2012; Zhang et al., 2014a). Phagocytosis involves a complex cascade of cytoskeletal changes during target recognition, cup formation and closure. Though poorly studied in microglia, studies in macrophages have shown the importance of Arp2/3 activity in C3-mediated phagocytosis (May et al., 2000; Rotty et al., 2017; Rougerie et al., 2013). Interestingly, Arp2/3 assembly does not require cdc42/WASP but is instead RhoA/ROCK dependent (Caron and Hall, 1998; Hall et al., 2006; May et al., 2000). Requirement of Rac1 activity is currently unclear, CR3-mediated phagocytosis is critically dependent on Rac1 activity in bone marrow-derived macrophages (BMMs), downstream of Vav GEFs, but dispensable in other systems (Caron and Hall, 1998; Hall et al., 2006). Additionally, Rac1 is also required for C5a-driven chemotaxis (Miller and Stella, 2009). Thus, loss of CYFIP1 could disrupt CR3-mediated phagocytosis via destabilisation of the WRC and perturbation of Rac signalling.

In this chapter, the role of the Rac1-CYFIP1-Arp2/3 actin remodelling pathway in microglial morphology and motility was investigated. Arp2/3 activity was found to have important roles in maintaining microglial process complexity and dynamics. Phenotypic similarity of Rac1 inhibition suggested that Arp2/3 activity is controlled in part by Rac1 signalling. Finally, a novel role for psychiatric disease-associated gene CYFIP1 was identified in regulating microglial morphology and surveillance behaviours. These results improve our understanding of the cytoskeletal machinery determinining microglial shape and motility and provide evidence for novel functions of CYFIP1 in a clinically relevant cell type.

Chapter 6

Final discussion

This thesis has focused on using novel transgenic mice to better understand what the neuropsychiatric disease-associated protein CYFIP1 is doing in the brain. The use of genetic models is a critical tool with which to research these conditions. Concretely, models aim to reproduce a subset of disease pathology in the hope of gaining mechanistic insight into molecular or cellular processes underlying such conditions. Examples of this include modelling the effect of deletion of a single associated gene in a complex disorder or replicating a genetic condition only in a single cell type. This approach can also be useful in overcoming barriers to studying proteins in simpler models, such as embryonic lethality of global knockouts.

In this thesis, these advantages have been fully utilised to gain novel insights into CYFIP1 function. Chapter 3 describes the generation of a cKO model in which CYFIP1 is deleted in principle cells of the hippocampus and neocortex. This model was shown to efficiently lead to the loss of CYFIP1 expression in neurons in embryonic development, facilitating its use as a neuronal knockout model *in vitro* and *in vivo*. The cKO did not alter the migration of neuronal progenitor cells through the cortex during embryogenesis, suggesting that the knockout was confined to post-mitotic differentiated neurons (Yoon et al., 2014). Next, the effects of CYFIP1 cKO on gross neuronal morphology were investigated. Both *in vitro* and *in vivo*,

the dendritic arbor of hippocampal neurons was reduced in total length, with a specific decrease in complexity of basal dendrites seen in the CA1 pyramidal cells. Interestingly, axon length in culture was increased in cKO neurons. These data suggest that loss of neuronal CYFIP1 has differential effects on axon and dendrite development.

Chapter 4 continued use of the NEX-CRE model in order to investigate changes in synaptic connectivity and transmission. Density and morphology of spines were found to be normal in mature hippocampal cultures but were longer in CA1 pyramidal cells from young adult mice, indicative of immaturity. Perinatal cKO mice had a hyperexcitation phenotype of increased VGLUT1 staining and increased frequency of mEPSCs. In contrast, inhibition was enhanced in the hippocampus of young adult cKO mice, as seen by increased gephyrin clusters, expression of inhibitory postsynaptic proteins and increased amplitude of mIPSCs. Excitatory signaling on the other hand appeared normal. Together these chapters further our understanding of the cell-autonomy and dosage effects of CYFIP1 expression in principle neurons *in vivo* and uncovered a novel role for CYFIP1 in the regulation of the inhibitory postsynapse.

Finally, a role for CYFIP1 in microglial morphology and motility was established in the chapter 5. A live imaging paradigm that enabled quantifications of surveillance, chemotaxis and cell morphology was established using acute slices of GFP-labelled microglia. In combination with drug treatments targeting actin remodeling pathways, we showed a critical requirement for actin polymerization and Arp2/3 activity in establishing normal microglial morphology and surveillance motility. An inducible conditional knockout system was then established to test the hypothesis that CYFIP1 could play a role in these actin dynamics. Indeed, loss of CYFIP1 decreased microglial complexity *in vivo* and led to reduced surveillance, thus uncovering a novel role for CYFIP1 in microglia.

6.1 Cell autonomy of neuronal defects

An outstanding question in the CYFIP1 literature is to what extent abnormalities reported in neuronal morphology and synaptic transmission of pyramidal cells of the hippocampus and neocortex represent cell autonomous effects (Bozdagi et al., 2012; Hsiao et al., 2016; Pathania et al., 2014). It is often under-appreciated that *in vivo* models of global genetic lesions could lead to altered function of neurons via several non-cell autonomous routes, including via precursor cells, other classes of neuron (e.g. inhibitory interneurons) and glia. Clarifying this is critical to linking cellular pathologies with molecular mechanisms, which are typically investigated in *in vitro* systems. This is because the relevant functions of a protein-of-interest may depend on the cellular context that protein is in. These points have been nicely highlighted in a group of studies on FMRP protein in astrocytes, that showed that altered astrocytic expression of GLT-1 transporters and neurotrophin-3 had indirect effects on dendrite and spine formation (Higashimori et al., 2016; Yang et al., 2012).

Several studies in mammalian systems have indicated that reduced CYFIP1 expression leads to decreased dendritic complexity and an increase in immature spines (de Rubeis et al., 2013; Pathania et al., 2014). The data presented in chapter 3 and 4 build on these studies and provide evidence that these defects can be explained by a cell autonomous effect in altered function of postmitotic neurons. A reduction in dendritic length and complexity of basal dendrites of cKO CA1 PCs and increased spine length along these dendrites were observed *in vivo*, consistent with these previous reports. The nature of the NEX-CRE cKO model also provides some useful insight into the developmental origin of these effects. Yoon et al. reported that knockdown of CYFIP1 in RGCs during development delayed cortical migration of neuronal progenitors (Yoon et al., 2014). Abnormal cortical migration of neurons has been associated with defects in dendritic morphology lasting into adulthood (Kimura et al., 2017; Li et al., 2018). The fact that progenitors migrate normally in the NEX-CRE system suggests that dendritic and spine defects are not a consequence of early developmental delay. Together, these data support the current consensus that

CYFIP1 functions in a cell-autonomous manner to alter dendritogenesis and spine maturation, though the precise mechanisms here remain poorly understood.

A consistent observation here is that the size of these effects is similar to those reported in the heterozygous model. This is surprising given that 1) haploinsufficiency of CYFIP1 is predicted to maintain some CYFIP1 functionality and therefore express a milder phenotype and 2) comparisons of haploinsufficient and OE of CYFIP1 suggest a dosage dependent effect on endpoints, such as dendritic morphology and mTOR activation (Abekhoukh et al., 2017; Oguro-Ando et al., 2015; Pathania et al., 2014). These discrepancies have many potential explanations, including compensation by CYFIP2 (discussed later) and mouse line differences. Interestingly, the CYFIP1 heterozygous mouse was generated in the substrain C57BL/6N that contains a CYFIP2 mutation shown to reduce protein stability (Kumar et al., 2013). Given that the substrain of the NEX-CRE line is not known, it is possible these animals do not carry the CYFIP2 mutation, which could have important implications for the effects of CYFIP1 reduction (Goebbels et al., 2006). It is also worth highlighting that other phenotypes do not show these dosage-dependent effects, such as spine immaturity which occurs in overexpression and haploinsuffiency/loss. This suggests these phenotypes are not driven by a simple loss or gain of function based on CYFIP1 dosage but rather altered activation of multiple upstream or downstream pathways. Indeed, there are many candidate signalling pathways that are implicated in the CYFIP1 literature, including mTOR, Rac1 and FMRP (discussed later).

It is worth highlighting that any Cre-driven recombination model is subject to a level of uncertainty about efficacy of recombination. Whilst clear reductions in CYFIP1 expression are observed in both brain lysates and primary neuron cultures, both still showed residual CYFIP1 expression. This is expected given the non-neuronal expression of CYFIP1 in other brain cells. However, residual CYFIP1 expression could also be due to variable efficiency of recombination in target cells (i.e. principle neurons) and would provide an alternative explanation for the subtle

effects observed in this model. To address this, analysis of single cell CYFIP1 expression, either via ICC/IHC of primary cultures/brain slices respectively with a antibody specifically against CYFIP1 would be required.

Some outstanding questions regarding the cellular origins of CYFIP1-associated pathologies remain. Accumulating evidence suggests that CYFIP1 positively regulates mTOR signalling (Abekhoukh et al., 2017; Oguro-Ando et al., 2015). However, *in vivo* evidence has come from patient or global expression mouse models, and so the neuronal origins of this effect remain to be proven (Hoeffer et al., 2012; Oguro-Ando et al., 2015). The NEX-CRE model represents a perfect system with which to do this. Additionally, a recent study showed that hyperactivation of microglial mTOR via conditional knockout of TSC lead to non-inflammatory, reactive-like phenotype in microglia that had increased phagocytic activity (Zhao et al., 2018). These changes led to reductions in both inhibitory and excitatory synapses and initiation of spontaneous recurrent seizures, recapitulating features seen in patients with TSC mutations. Given the initial evidence for CYFIP1 function in microglia, and the clinical associations between CYFIP proteins and epileptogenesis, it would be interesting to know if mTOR signalling was altered in the microglial cKO system also established here.

6.2 CYFIP1 in microglia: a new angle for disease association?

Data in chapter 5 points to a novel role for CYFIP1 in regulating microglial morphology and motility. Numerous studies over the last decade have shown that microglia have active roles in shaping neuronal connectivity, during development, healthy adulthood and in disease states (Neniskyte and Gross, 2017). Microglia do this via a range of interactions with neurons, including release of trophic factors, pruning of opsinised synapses, phagocytosis of whole cells and guidance of

migrating cells (Miyamoto et al., 2016; Paolicelli et al., 2011; Parkhurst et al., 2013). Given this, it is tempting to speculate whether these processes are disrupted by altered CYFIP1 expression.

A recent pre-publication report showed that CYFIP1 heterozygous mice have reduced apoptosis of newly born neurons in the dentate gyrus and suggested that this was due to altered release of secreted factors by microglia (Haan et al., 2018). This is the first evidence for a possible link between microglial CYFIP1 and neuronal function. However, cell-autonomy of these effects used an *in vitro* system. Microglia have been shown to undergo an extensive reprogramming when moved to culture, making interpretation of these results difficult (Bohlen et al., 2017).

Data presented in this thesis shows that CYFIP1 is required for normal microglial morphology and surveillance. Several studies have shown that microglia contact neurons during surveillance, with important functional implications. In the developing cortex contact promotes formation of dendritic filapodia and disruption of this reduces spine density (Miyamoto et al., 2016). In young adult mice, microglia regularly contact both presynaptic boutons and postsynaptic spines in an activity dependent manner (Sipe et al., 2016; Wake et al., 2009). A study in zebrafish larvae showed that contact was correlated with reduced response to evoked currents, suggesting another mechanism by which microglia shape network activity (Li et al., 2012). Thus, loss of microglial CYFIP1 could well impact neuronal function via disruption of these contacts, the functions of which are an emerging topic.

Additionally, the role of microglia in phagocytosis of synapses and cells is another appealing endpoint given that these processes involve dramatic remodelling of the cytoskeleton. Indeed, Arp2/3 activity is critical for CR3-mediated phagocytosis in macrophages, the process by which complement-tagged synapses are removed during development and neurodegeneration (Hong et al., 2016; Rotty et al., 2017; Schafer et al., 2012). The role of the WRC in this process is debated; WAVE2 is not required for Fcγ-mediated phagocytosis and a role for Rac1 in CR3-mediated phagocytosis is

unclear (Rougerie et al., 2013). A recent paper reported that a Parkinson's Disease mutant of LRRK2 phosphorylates WAVE2, protecting the protein from proteasomal degredation (Kim et al., 2018). Expressing this mutant in primary mouse microglia and human macrophages increased their phagocytic potential. Importantly, they show that this pathway is required for the loss of TH+ neurons and could be rescued by silencing of WAVE2. Thus, WRC-dependant phagocytosis could be important for microglial function.

The microglial WRC is composed primarily of WAVE2, CYFIP1, ABI3 and NAP1L. ABI3 is less well studied that ABI1/2 but is exclusively expressed by microglia in the brain and has come to attention recently due to its identification as a novel AD risk gene (Satoh et al., 2017; Sims et al., 2017; Zhang et al., 2014a). Interestingly, an MS screen for ABI3 interactors identified CYFIP1 but not CYFIP2, highlighting the importance of CYFIP1 in this context (Moraes et al., 2017). The effect of the AD-associated variant of ABI3 on WRC function is not currently known. However, a study in mouse fibroblasts showed that the ABI3-based WRC does not translocate to the PM or form lamellipodia in response to fibronectin but did stimulate invadopodia formation in response to Abl kinase inhibition (Sekino et al., 2015). This suggests that the microglial WRC may have unique functions related to its myeloid origins that distinguish it from the traditional views of WRC function. Interestingly, a GWAS study identified a nominal association between AD and duplication of the q11.2 locus (Ghani et al., 2012). Further, CYFIP1 was increased in hippocampus of late stage AD patients (Tiwari et al., 2016). This increase could represent microglial proliferation or increased microglial expression of CYFIP1 in response to neuronal death. Indeed, LPS treatment of microglia *in vitro* have been shown to increase CYFIP1 expression (Haan et al., 2018).

As discussed, microglia also actively prune synapses and phagocytose neurons during critical periods during development (Paolicelli et al., 2011; Sierra et al., 2010). These developmental periods coincide with the onset of neuropsychiatric diseases like ASD and SCZ, which typically present during early childhood and adolescence

respectively. Given the clinical associations between CYFIP1 and these conditions, it would be interesting to see if neuronal development was delayed or compromised in the microglia cKO mouse described here.

6.3 CYFIP protein redundancy

The effects of CYFIP1 loss in a particular cell type will depend on a host of factors, including expression levels of CYFIP2. This point was recently highlighted by the Holt lab that showed that differential expression of CYFIP1 and 2 in the zebrafish retina led to different phenotypes in axonal development (Cioni et al., 2018). The literature directly comparing the molecular functions of CYFIP1 and 2 is sparse, but suggests that CYFIP1 and 2 have high levels of redundancy. Both proteins have been reported as interacting with FMRP and critical WRC components, suggesting that they can function interchangeably in these two complexes (Eden et al., 2002; Schenck et al., 2003; Suetsugu et al., 2006). The only study to date comparing KD of individual CYFIPs with double KD showed that double knockdown have far more extreme defects and phenocopied loss of WAVE1 (Xu et al., 2016). Conversely, overexpression of CYFIP1 and CYFIP2 lead to similar increases in dendritic complexity (Pathania et al., 2014). These data support the functional redundancy of CYFIP proteins.

Given this, comparing studies of CYFIP1 and CYFIP2 haploinsufficient mice reveals some intriguing differences. A key phenotype of FMR1 KO mice is enhanced translation-independent, mGluR-dependent LTD. Interestingly, CYFIP1 haploinsufficient mice also display this enhancement whereas CYFIP2 haploinsufficient mice do not (Bozdagi et al., 2012; Gantois et al., 2017; Han et al., 2015). Further, CYFIP1 haploinsufficiency leads to increased length of spines in hippocampus with no change in density (cortical spines have not been reported). CYFIP2 haploinsufficient mice had normal hippocampal spines but increased density of mature spines in layer II/III of cortex (Han et al., 2015; Pathania et al.,

2014). An analysis of dendritic development in CYFIP2$^{+/-}$ mice has not been published, though it would be interesting to know if this phenocopied reduced complexity seen in the CYFIP1$^{+/-}$ (Pathania et al., 2014). These data suggest that CYFIP1 and 2 lead to different alterations in neuronal development and function *in vivo*.

What could explain these phenotypic disparities? Some differences between CYFIP functions have been suggested. The initial study by Schenck et al. showed that CYFIP2 had additional interactions with FXR1P and FXR2P, two closely related proteins to FMRP that CYFIP1 lacked (Schenck et al., 2001). FXR2P has roles in mRNA stabilisation and translation of excitatory postsynapse proteins and FXR1P overexpression in prefrontal cortex decreases GluA2 expression and leads to anxiety-like behaviours (Fernández et al., 2015; Guo et al., 2015; Khlghatyan et al., 2018). However, the relevance of CYFIP2 interaction with FXR1P and 2P in these functions is not known. A recent paper identified a phosphorylation site on CYFIP2 not present in CYFIP1 that effected spine morphology in hippocampus cultures Lee et al. (2017). Finally, CYFIP2 mRNA is also predicted to be a key target of FMRP-repression, coming ninth in a panel of 832 mRNA targets in which CYFIP1 was not identified (Darnell et al., 2011). Increased CYFIP2 expression has been seen in FXS patient lymphocytes, providing evidence that FMRP may indeed repress translation of CYFIP2, although CYFIP2 levels were normal in the CYFIP1 loss models presented here and elsewhere (Bozdagi et al., 2012; Hoeffer et al., 2012). These unique interactions go some way to explain these differences. However, a comparison of the CYFIP1 and CYFIP2 interactome would be extremely useful to begin teasing apart these differences rigorously.

Another possibility is that differences in expression of CYFIP1 and 2 determine the effect of their loss in the brain. Interestingly, multiple transcriptomic databases suggest that CYFIP2 is expressed much more than CYFIP1 in neurons specifically (Zeisel et al., 2018; Zhang et al., 2014a, 2016). Data from this thesis suggested that CYFIP1 and 2 were both expressed in neuronal cortical cultures, although

the presence of astrocytes in these cultures confounds this. The NEX-CRE model developed here represents an ideal system with which to test the cell-autonomous effects of loss of both CYFIP proteins *in vivo*, for instance via *in utero* electroporation of CYFIP2 shRNA.

6.4 WAVE complex specificity

As mentioned prior, both CYFIP1 and 2 interact with WRC components. There is evidence to suggest that CYFIP proteins may preferentially fall into two separate WRC compositions. Initial studies reconstituting the WRC identified different CYFIP paralogues. Three independent studies identified CYFIP2/Pir121 as the associated CYFIP in the WAVE1-containing WRC, in mammalian brain lysates and human cell lines (Eden et al., 2002; Kim et al., 2006; Kumar et al., 2013). One study also found that CYFIP2 was present in the reconstituted WAVE2-WRC in COS7 cells, which are derived from monkey kidney cells (Innocenti et al., 2004). CYFIP1 has more commonly been associated with the WAVE2-WRC; CYFIP1 pulled down both WAVE1 and WAVE2 in E14 brain lysates, was associated with the WAVE2-WRC in B16-F1 and MCF-10A cells, murine cancer and human epithelial cell lines respectively (Silva et al., 2009; Steffen et al., 2004). The reconstituted 'miniWRC' used by the Rosen lab for elucidation of the molecular structure of the WRC used a CYFIP1-WAVE1 based complex. However, this was prepared via viral overexpression of individual WRC components in the sf9 insect cell line, and thus does not represent an endogenous complex (Chen et al., 2010; Ismail et al., 2009). WAVE3-based complexes are less well-studied, although CYFIP1 is a critical constituent of the WAVE3-WRC in breast cancer cells (Teng et al., 2016).

Thus although both CYFIP proteins are likely capable of being incorporated into any WRC, CYFIP1 and 2 appear to have a preference for WAVE2/3- and WAVE1-based complexes respectively. This specificity could occur by 1) differential expression levels of CYFIP/WAVE variants in different cell/tissue types and/or

WRC component	Neurons	Astrocytes	OPCs	Microglia
CYFIP1	*	**	**	***
CYFIP2	**	*	**	*
WASF1	***	**	***	*
WASF2	*	*	*	***
WASF3	***	***	**	*
ABI1	**	***	**	**
ABI2	***	**	***	*
ABI3	*	*	*	***
NAP1	***	***	***	*
NAP1L	*	*	*	***
HSPC300	**	**	**	***

Fig. 6.1: Expression of mRNA transcripts of WRC components in neurons and glia Illustration of expression levels of different WRC components in neurons, astrocytes, oligodendrocyte precursor cells (OPCs) and microglia. * minimal expression, ** low-medium expression, *** high expression. Adapted from transcription data from (Zhang et al., 2014b).

2) different binding preferences of CYFIP and WAVE variants. Current evidence supports the former. Using the Barres lab transcriptome, a comparison of expression levels of WRC components in different brain cells is shown in Fig 6.1 (Zhang et al., 2014a, 2016). Neurons and OPCs have high levels of CYFIP2 and preferentially express WAVE1 and 3. Microglia, which preferentially express CYFIP1, almost exclusively express WAVE2. Of note, microglia also express unique variants of other WRC constituents, NAP1L and ABI3.

These differences may help explain the difference in lethality of CYFIP1 and CYFIP2 null mice. CYFIP1 mice die at E9 with severe defects in gastrulation similar to those observed in WAVE2 and NAP1 null mice (Rakeman and Anderson, 2006; Yan et al., 2003). In contrast, CYFIP2 null mice die hours after birth which is more reminiscent of the postnatal lethality of WAVE1 knockout mice, though other studies show WAVE1 mice can survive to adulthood (Dahl et al., 2003; Kumar et al., 2013; Soderling et al., 2007). These differences reflect expression patterns outside of the brain but illustrate the point that CYFIP1 and 2 are differentially associated with WAVE variants.

Several differences in WAVE1 and 2 complex function could be relevant for the interpretation of data in this thesis and publications. WAVE1 has a number of specific protein-binding partners that WAVE2 lacks, such as WRP, PKA and p47phox (Takenawa, 2007). Disrupting the WRP interaction has been shown to decrease spine density and increase filopodial spines, alongside increasing late-phase LTP (Soderling et al., 2007). WAVE2 and CYFIP1 both interact specifically with IRSp53, a protein that has been shown to be a critical component of the PSD: IRSp53 knockout mice have decreased spine density, enhanced NMDA function and social/cognitive deficits (Kang et al., 2016; Miki et al., 2000). In addition, WAVE1 and 2 activity is regulated by a number of kinases that phosphorylate unique residues.

6.5 Possible convergence on Rac1 signalling

Interpretation of current CYFIP literature, especially in neurons, has been made difficult by the multiple described functions of CYFIP1 in different protein complexes. The identification of functional mutations in CYFIP1 that impair association with either eIF4e or the WRC have enabled studies into the relative importance of these two features (Chen et al., 2010; Napoli et al., 2008). In the case of spine morphology, neither functional mutant was capable of rescuing increased spine length seen in CYFIP1 knockdown, suggesting that both functions are required for normal spine development (de Rubeis et al., 2013). This paper did suggest that BDNF-induced expression of Arc was dependant on the CYFIP1-eIF4E interaction specifically, whereas F-actin intensity required WRC interaction. Other phenotypes also appear to be specifically linked to impaired WRC function; only the eIF4E-binding mutant was able to rescue increased presynaptic puncta size in knockdown experiments in culture (Hsiao et al., 2016). In addition, defects in axonal pathfinding in CYFIP2 null Xenopus larvae were shown to depend of WAVE-complex activity (Cioni et al., 2018). It is worth noting that some of these experiments use a large truncation mutant to prevent WRC binding, which may well disturb as-yet unknown CYFIP1 interactions (Cioni et al., 2018; Hsiao et al., 2016).

One hypothesis to bring these two functions together is through perturbed Rac1 signalling (Fig 6.2). There is substantial evidence that CYFIP1 dosage inversely correlates with Rac1 activity. Inhibition of Rac1 rescues the increase in presynaptic puncta size seen with CYFIP1 knockdown in neuronal cultures (Hsiao et al., 2016). NSC23766 treatment also rescues Arc expression in cortical cultures with CYFIP1 KD and in fact reduced basal Arc levels in control neurons (de Rubeis et al., 2013). Further, the early characterisation of CYFIP1 in flies showed that overexpression (OE) of CYFIP1 could rescue misorganisation of the ommatidia (fly eye) expressing a constitutively active Rac1 mutation and that haploinsufficiency of CYFIP1 dramatically enhanced this defect and lead to aberrant midline crossing of CNS neurons (Schenck et al., 2003). One interpretation of these data is that loss of

CYFIP1 leads to hyperactivation of other Rac1-dependent pathways, such cofilin inactivation (via PAK), due to the freeing up of active Rac1 that would otherwise be complexed with CYFIP1 (Fig 6.2B).

Other phenotypes do not follow this trend. The decrease in dendritic complexity on CYFIP1 loss seen here and in published literature is more similar to phenotypes seen in loss of Rac1 signalling (Lee et al., 2003). Further, the increase in spine length seen in CYFIP1 loss observed in chapter 4 is similar to what has been seen in OE of dominant negative mutants of Rac1 *in vitro* and opposite to increased mushroom spine morphology of OE of constitutively active Rac1 (Tashiro and Yuste, 2004). However, a more recent paper looking at the Rac1-specific GAP, SRGAP2A, showed that knockdown of this protein (leading to increased Rac1 signalling) led to increased length and decreased head width of spines (Fossati et al., 2016). SRGAP2A binds to Homer and Gephyrin to locally inhibit Rac1 signalling at the postsynapse. The difference between these two studies highlights the importance of local regulation of Rac1 signalling to the downstream effects on spines.

A similar pattern is found with mTOR signalling. There is evidence that Rac1 can activate both mTORC1 and 2 in response to growth signalling (Saci et al., 2011). As reduced mTOR activity has already been associated with CYFIP1 loss, this further illustrates that effects of CYFIP1 loss cannot simply be seen as Rac1 overactivation (Abekhoukh et al., 2017). This also makes the interpretation of altered protein expression observed in any CYFIP1 loss models more difficult, as both mTORC1 activity and loss of FMRP function affect this.

In addition, there is growing evidence to suggest that Rac1 signalling is perturbed in Fragile X models. FMRP KO Drosophila have increased complexity of dendrites reminiscent of Rac1 OE and a recent study showed that memory deficits in these flies are due to an inability to activate Rac1-dependant synaptic plasticity, despite normal basal Rac1-GTP levels (Dong et al., 2016; Lee et al., 2003). Indeed, Rac1 mRNA is part of Fmr1-mRNP complexes *in vivo* and FMRP KO mice have increased Rac1-GTP levels and enhanced PAK-cofilin signalling downstream of Rac1 (Bongmba

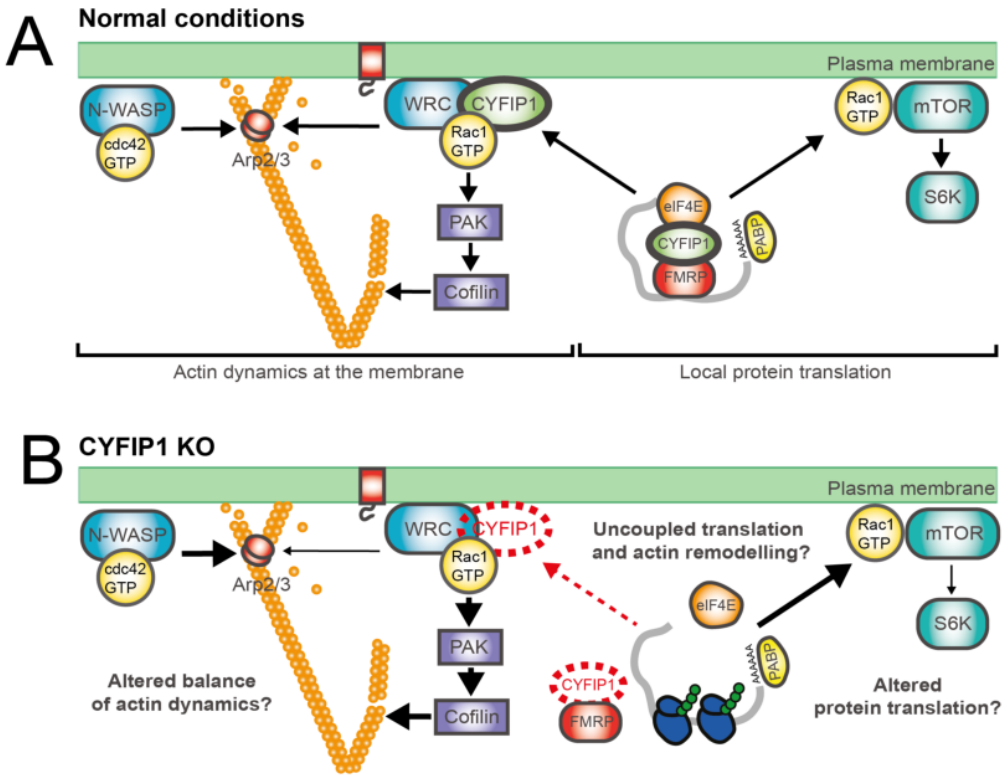

Fig. 6.2: Model for the effects of CYFIP1 loss on Rac1 signalling
A: Illustration of CYFIP1-dependent signalling under normal conditions. CYFIP1 couples actin remodelling to local protein translation in a Rac1-dependent manner. WRC activity at the membrane is in balance with actin remodelling pathways (both Arp2/3 and non-Arp2/3) to control cytoskeletal dynamics. mTOR signalling is also effected by activity of Rac1 and FMRP signalling. **B**: Loss of CYFIP1 disrupts multiple Rac1-dependent pathways, leading to altered actin dynamics and protein translation via imbalance of pathways mentioned.

et al., 2011; Pyronneau et al., 2017). Importantly, the enhanced mGluR-dependent LTD in FMRP KO can be rescued by inhibition of Rac1 (Bongmba et al., 2011). Here, Rac1 is likely to act directly via the established mechanism of LTD as basal and activity dependent Arc expression are both dependent of Rac1 signalling de Rubeis et al. (2013). The increase in Rac1 activity in FMRP KO mice could occur via enhanced translation of Rac1 protein (Bongmba et al., 2011). Whilst this is still possible in CYFIP1 loss, it is also probable that loss of CYFIP1 in isolated sub-structures like dendritic spines increases the pool of Rac1-GTP available to interact with other downstream binding partners.

Together, these studies suggest that when altering levels CYFIP1 and related proteins, perturbed Rac1 signalling is a common theme. In relation to work in this thesis, it suggests that this effect may be spatially localised to dendritic spines. Indeed, spines are compartmentalised signalling hubs enriched in Rac1 effectors and downstream targets. They are thus acutely sensitive to changes in the local pool of Rac1. In contrast, the effects of CYFIP1 loss on dendritic morphology likely reflect a more generic consequence of reduced coupling of Rac1 activity to actin remodelling via the WRC or mTOR dysfunction. This might also help explain the difference in effects between excitatory and inhibitory synapse function in the neuronal cKO, as inhibitory synapses are far less isolated. This hypothesis requires testing to assess its validity. For instance, it would be very interesting to know if increased Rac1-GTP signalling is specifically enhanced in postsynaptic compartments versus dendrites in models of CYFIP1 loss, and if other read outs of Rac1 activity, such as cofilin phosphorylation, are altered.

There are numerous potential consequences for enhanced Rac1 signalling at the postsynapse. Rac1 is part of a βPIX-GIT1-PAK pathway that regulates receptor stability and spine morphology (Smith et al., 2014; Zhang et al., 2005). This is partly via increasing local actin stabilisation through phosphorylation of cofilin. In addition, Rac1 state may have indirect effects on other RhoGTPases via altered interactions with the numerous shared GEFs and GAPs present in the spine, including kalarin-7

and SRGAP2. Given the evidence for Rac1 activity impinging on broader cellular processes, such as protein translation via mTOR activity, this could go some way to explaining the overall cell pathologies observed.

6.6 Comparing CYFIP1 in neurons and microglia

Chapter 5 suggested a novel role for CYFIP1 in microglia, the immune cells of the brain and an important glial cell type. Using a conditional knockout system, the loss of CYFIP1 expression specifically in microglia was shown to lead to a decrease in morphological complexity *in vivo*. This effect nicely parallels the established role of CYFIP1 in regulating dendritic morphology of neurons, and suggests that CYFIP1 has a general role in establishment of morphology in complex and polarised cell types. This is particularly interesting given the stark differences between the dynamics of microglia and neurons. The dendrites of neurons form gradually over the course of weeks *in vivo* by a process of slowly accumulating stable branches whilst the distal growth tips remain dynamic until a mature morphology is established. In contrast, live imaging assays of microglia performed in chapter 5 and in other published work show that the entire arbor of microglia is highly dynamic, with secondary processes turning over on a timescale of minutes and primary processes over minutes to hours. These data suggest that CYFIP1 is performing a similar function over different timescales in neurons and microglia.

The difference in process motility in the dynamic processes of dendrites and microglia likely originate from differences in stability of cytoskeletal structures. Growing dendrites are rapidly stabilised by microtubule complexes with a lower turnover rate than that of actin filaments. These MTs are bound by MAPs (e.g. MAP1a and MAP2) that stabilise filaments and protect them from severing proteins such as katanin, and are acetylated and detyrosinated to increase stability. Knockout of these MAPs leads to dramatic dendritic instability and reduced complexity (Szebenyi et al., 2005). In contrast, F-actin is largely excluded from the dendritic

shaft and concentrated at spines, growing tips of dendrites and axons. Whilst little is known about the microtubule organisation in microglia *in vivo*, one study suggested that acetylated MTs were only seen in a subset of primary processes and that this is inversely associated with motility in culture (Ilschner and Brandt, 1996). Data from chapter 5 highlights the critical importance of actin nucleation to maintain higher-order processes and dynamics. Thus, microglia appear to use actin-based structures for the generation and stabilisation of these processes, whereas MTs stabilise the primary branch structure.

Comparing data from chapter 3 and 5 could lend additional mechanistic insight into how CYFIP1 determines morphology. It is currently unclear to what extent CYFIP1 acts via FMRP or the WRC during dendritogenesis. Indeed, both FMRP and WRC activity have been implicated in this process (Bagni and Greenough, 2005; Xu et al., 2016). Part of the confusion here is that FMRP has well-established roles at the post-syanpse that could explain some of, if not all, its known associations in trafficking and stabilisation of dendritic mRNAs like MAP1B and CaMKII. Although not extensively studied, available data suggests that FMRP is absent in adult microglia in the hippocampus (Gholizadeh et al., 2015; Zhang et al., 2014a). Thus, it is unlikely that CYFIP1 is acting via it's 4E-BP role in microglia. In addition the drug treatment experiments performed in chapter 5 show that Rac1 and Arp2/3 signalling play a critical role in establishing normal microglial morphology and movement. This supports the hypothesis that effects of CYFIP1 loss could be fully explained by dysregulated activity of the WRC and associated signalling cascades.

6.7 Concluding remarks

The study of CYFIP proteins in relation to brain function is a fascinating and pertinant topic that bridges fundamental questions about how cells move, grow and interact with a need to understand the cellular origins of neuropsychiatric disorders. This

research has proven fruitful and important progress has been made in linking diverse intracellular processes into a common, dynamic system. However, several important questions still remain largely uncertain. How altered CYFIP levels effect the activity of signalling pathways upstream and downstream of it remains key. Additionally, this thesis has highlighted to importance of investigating the synapse-specific and cell-specific functions of CYFIP1, given its ubiquitous expression. As progress in this direction is made, it will be important to not lose sight of the end goal of understanding how altered CYFIP1 levels that arise clinically effect brain function. Moving towards a model for how cell-specific effects interact with each other to generate this overall pathology will be a critical and exciting area of research in the future.

References

Abbeduto, L., McDuffie, A., and Thurman, A. J. (2014). The fragile x syndrome-autism comorbidity: what do we really know? *Front Genet*, 5:355.

Abdelmoity, A. T., LePichon, J.-B., Nyp, S. S., Soden, S. E., Daniel, C. A., and Yu, S. (2012). 15q11.2 proximal imbalances associated with a diverse array of neuropsychiatric disorders and mild dysmorphic features. *J Dev Behav Pediatr*, 33(7):570–576.

Abekhoukh, S., Sahin, H. B., Grossi, M., Zongaro, S., Maurin, T., Madrigal, I., Kazue-Sugioka, D., Raas-Rothschild, A., Doulazmi, M., Carrera, P., Stachon, A., Scherer, S., Drula Do Nascimento, Maria Rita, Trembleau, A., Arroyo, I., Szatmari, P., Smith, I. M., Milà, M., Smith, A. C., Giangrande, A., Caillé, I., and Bardoni, B. (2017). New insights into the regulatory function of cyfip1 in the context of wave- and fmrp-containing complexes. *Dis Model Mech*, 10(4):463–474.

Abiega, O., Beccari, S., Diaz-Aparicio, I., Nadjar, A., Layé, S., Leyrolle, Q., Gómez-Nicola, D., Domercq, M., Pérez-Samartín, A., Sánchez-Zafra, V., Paris, I., Valero, J., Savage, J. C., Hui, C.-W., Tremblay, M.-È., Deudero, J. J. P., Brewster, A. L., Anderson, A. E., Zaldumbide, L., Galbarriatu, L., Marinas, A., Vivanco, M. d., Matute, C., Maletic-Savatic, M., Encinas, J. M., and Sierra, A. (2016). Neuronal hyperactivity disturbs atp microgradients, impairs microglial motility, and reduces phagocytic receptor expression triggering apoptosis/microglial phagocytosis uncoupling. *PLoS Biol*, 14(5):e1002466.

Abou-Kheir, W., Isaac, B., Yamaguchi, H., and Cox, D. (2008). Membrane targeting of wave2 is not sufficient for wave2-dependent actin polymerization: a role for irsp53 in mediating the interaction between rac and wave2. *J Cell Sci*, 121(Pt 3):379–390.

Agarwal, A., Dibaj, P., Kassmann, C. M., Goebbels, S., Nave, K.-A., and Schwab, M. H. (2012). In vivo imaging and noninvasive ablation of pyramidal neurons in adult nex-creert2 mice. *Cereb Cortex*, 22(7):1473–1486.

Al-Shammari, A. R., Bhardwaj, S. K., Musaelyan, K., Srivastava, L. K., and Szele, F. G. (2018). Schizophrenia-related dysbindin-1 gene is required for innate immune response and homeostasis in the developing subventricular zone. *NPJ Schizophr*, 4(1):15.

Alekhina, O., Burstein, E., and Billadeau, D. D. (2017). Cellular functions of wasp family proteins at a glance. *J Cell Sci*, 130(14):2235–2241.

Ali, A. J., Merzaban, J. S., and Abuelela, A. F. (2015). Cd44 and psgl-1 collaborate in controlling the migration of human activated t-cells. *Blood*.

Anitha, A., Nakamura, K., Yamada, K., Suda, S., Thanseem, I., Tsujii, M., Iwayama, Y., Hattori, E., Toyota, T., Miyachi, T., Iwata, Y., Suzuki, K., Matsuzaki, H., Kawai, M., Sekine, Y., Tsuchiya, K., Sugihara, G.-I., Ouchi, Y., Sugiyama, T., Koizumi, K., Higashida, H., Takei, N., Yoshikawa, T., and Mori, N. (2008). Genetic analyses of roundabout (robo) axon guidance receptors in autism. *Am J Med Genet B Neuropsychiatr Genet*, 147B(7):1019–1027.

Aoki, Y., Yoncheva, Y. N., Chen, B., Nath, T., Sharp, D., Lazar, M., Velasco, P., Milham, M. P., and Di Martino, A. (2017). Association of white matter structure with autism spectrum disorder and attention-deficit/hyperactivity disorder. *JAMA Psychiatry*, 74(11):1120–1128.

Arancibia-Cárcamo, I. L., Yuen, E. Y., Muir, J., Lumb, M. J., Michels, G., Saliba, R. S., Smart, T. G., Yan, Z., Kittler, J. T., and Moss, S. J. (2009). Ubiquitin-dependent lysosomal targeting of gaba(a) receptors regulates neuronal inhibition. *Proc Natl Acad Sci USA*, 106(41):17552–17557.

Ascano, M., Mukherjee, N., Bandaru, P., Miller, J. B., Nusbaum, J. D., Corcoran, D. L., Langlois, C., Munschauer, M., Dewell, S., Hafner, M., Williams, Z., Ohler, U., and Tuschl, T. (2012). Fmrp targets distinct mrna sequence elements to regulate protein expression. *Nature*, 492(7429):382–386.

Babbs, R. K., Kelliher, J. C., Scotellaro, J. L., Luttik, K. P., Mulligan, M. K., and Bryant, C. D. (2018). Genetic differences in the behavioral organization of binge eating, conditioned food reward, and compulsive-like eating in c57bl/6j and dba/2j strains. *Physiol Behav*.

Bagni, C. and Greenough, W. T. (2005). From mrnp trafficking to spine dysmorphogenesis: the roots of fragile x syndrome. *Nat Rev Neurosci*, 6(5):376–387.

Barcia, C., Ros, C. M., Annese, V., Carrillo-de Sauvage, M. A., Ros-Bernal, F., Gómez, A., Yuste, J. E., Campuzano, C. M., de Pablos, V., Fernandez-Villalba, E., and Herrero, M. T. (2012). Rock/cdc42-mediated microglial motility and gliapse formation lead to phagocytosis of degenerating dopaminergic neurons in vivo. *Sci Rep*, 2:809.

Barnes, A. P. and Polleux, F. (2009). Establishment of axon-dendrite polarity in developing neurons. *Annu Rev Neurosci*, 32:347–381.

Barres, B. A. (2008). The mystery and magic of glia: a perspective on their roles in health and disease. *Neuron*, 60(3):430–440.

Bassell, G. J. and Warren, S. T. (2008). Fragile x syndrome: loss of local mrna regulation alters synaptic development and function. *Neuron*, 60(2):201–214.

Basu, D., El-Assal, S. E.-D., Le, J., Mallery, E. L., and Szymanski, D. B. (2004). Interchangeable functions of arabidopsis pirogi and the human wave complex subunit sra1 during leaf epidermal development. *Development*, 131(17):4345–4355.

Bausen, M., Fuhrmann, J. C., Betz, H., and O'Sullivan, G. A. (2006). The state of the actin cytoskeleton determines its association with gephyrin: role of ena/vasp family members. *Mol Cell Neurosci*, 31(2):376–386.

Bergert, M., Chandradoss, S. D., Desai, R. A., and Paluch, E. (2012). Cell mechanics control rapid transitions between blebs and lamellipodia during migration. *Proc Natl Acad Sci USA*, 109(36):14434–14439.

Berry, K. P. and Nedivi, E. (2017). Spine dynamics: are they all the same? *Neuron*, 96(1):43–55.

Bialas, A. R. and Stevens, B. (2013). Tgf-\beta signaling regulates neuronal c1q expression and developmental synaptic refinement. *Nat Neurosci*, 16(12):1773–1782.

Bian, W.-J., Miao, W.-Y., He, S.-J., Qiu, Z., and Yu, X. (2015). Coordinated spine pruning and maturation mediated by inter-spine competition for cadherin/catenin complexes. *Cell*, 162(4):808–822.

Bittel, D. C., Kibiryeva, N., and Butler, M. G. (2006). Expression of 4 genes between chromosome 15 breakpoints 1 and 2 and behavioral outcomes in prader-willi syndrome. *Pediatrics*, 118(4):e1276–83.

Blanque, A., Repetto, D., Rohlmann, A., Brockhaus, J., Duning, K., Pavenstädt, H., Wolff, I., and Missler, M. (2015). Deletion of KIBRA, protein expressed in kidney and brain, increases filopodial-like long dendritic spines in neocortical and hippocampal neurons in vivo and in vitro. *Front Neuroanat*, 9:13.

Bliss, T. V. P., Collingridge, G. L., and Morris, R. G. M. (2014). Synaptic plasticity in health and disease: introduction and overview. *Philos Trans R Soc Lond, B, Biol Sci*, 369(1633):20130129.

Bockmann, J., Kreutz, M. R., Gundelfinger, E. D., and Böckers, T. M. (2002). Prosap/shank postsynaptic density proteins interact with insulin receptor tyrosine kinase substrate irsp53. *J Neurochem*, 83(4):1013–1017.

Bogdan, S., Grewe, O., Strunk, M., Mertens, A., and Klämbt, C. (2004). Sra-1 interacts with kette and wasp and is required for neuronal and bristle development in drosophila. *Development*, 131(16):3981–3989.

Bohlen, C. J., Bennett, F. C., Tucker, A. F., Collins, H. Y., Mulinyawe, S. B., and Barres, B. A. (2017). Diverse requirements for microglial survival, specification, and function revealed by defined-medium cultures. *Neuron*, 94(4):759–773.e8.

Bolton, P. F., Carcani-Rathwell, I., Hutton, J., Goode, S., Howlin, P., and Rutter, M. (2011). Epilepsy in autism: features and correlates. *Br J Psychiatry*, 198(4):289–294.

Bonaccorso, C. M., Spatuzza, M., Di Marco, B., Gloria, A., Barrancotto, G., Cupo, A., Musumeci, S. A., D'Antoni, S., Bardoni, B., and Catania, M. V. (2015). Fragile x mental retardation protein (fmrp) interacting proteins exhibit different expression patterns during development. *Int J Dev Neurosci*, 42:15–23.

Bongmba, O. Y. N., Martinez, L. A., Elhardt, M. E., Butler, K., and Tejada-Simon, M. V. (2011). Modulation of dendritic spines and synaptic function by rac1: a possible link to fragile x syndrome pathology. *Brain Res*, 1399:79–95.

Bopp, M. H. A., Zöllner, R., Jansen, A., Dietsche, B., Krug, A., and Kircher, T. T. J. (2017). White matter integrity and symptom dimensions of schizophrenia: A diffusion tensor imaging study. *Schizophr Res*, 184:59–68.

Bourne, J. N. and Harris, K. M. (2008). Balancing structure and function at hippocampal dendritic spines. *Annu Rev Neurosci*, 31:47–67.

Bovellan, M., Romeo, Y., Biro, M., Boden, A., Chugh, P., Yonis, A., Vaghela, M., Fritzsche, M., Moulding, D., Thorogate, R., Jégou, A., Thrasher, A. J., Romet-Lemonne, G., Roux, P. P., Paluch, E. K., and Charras, G. (2014). Cellular control of cortical actin nucleation. *Curr Biol*, 24(14):1628–1635.

Bozdagi, O., Sakurai, T., Dorr, N., Pilorge, M., Takahashi, N., and Buxbaum, J. D. (2012). Haploinsufficiency of cyfip1 produces fragile x-like phenotypes in mice. *PLoS ONE*, 7(8):e42422.

Braat, S., D'Hulst, C., Heulens, I., de Rubeis, S., Mientjes, E., Nelson, D. L., Willemsen, R., Bagni, C., van Dam, D., de Deyn, P. P., and Kooy, R. F. (2015). The gabaa receptor is an fmrp target with therapeutic potential in fragile x syndrome. *Cell Cycle*, 14(18):2985–2995.

Bravo-Cordero, J. J., Magalhaes, M. A. O., Eddy, R. J., Hodgson, L., and Condeelis, J. (2013). Functions of cofilin in cell locomotion and invasion. *Nat Rev Mol Cell Biol*, 14(7):405–415.

Breitsprecher, D. and Goode, B. L. (2013). Formins at a glance. *J Cell Sci*, 126(Pt 1):1–7.

Brennand, K. J., Simone, A., Jou, J., Gelboin-Burkhart, C., Tran, N., Sangar, S., Li, Y., Mu, Y., Chen, G., Yu, D., McCarthy, S., Sebat, J., and Gage, F. H. (2011). Modelling schizophrenia using human induced pluripotent stem cells. *Nature*, 473(7346):221–225.

Broadbelt, K., Byne, W., and Jones, L. B. (2002). Evidence for a decrease in basilar dendrites of pyramidal cells in schizophrenic medial prefrontal cortex. *Schizophr Res*, 58(1):75–81.

Brown, A. S., Begg, M. D., Gravenstein, S., Schaefer, C. A., Wyatt, R. J., Bresnahan, M., Babulas, V. P., and Susser, E. S. (2004). Serologic evidence of prenatal influenza in the etiology of schizophrenia. *Arch Gen Psychiatry*, 61(8):774–780.

Budreck, E. C. and Scheiffele, P. (2007). Neuroligin-3 is a neuronal adhesion protein at gabaergic and glutamatergic synapses. *Eur J Neurosci*, 26(7):1738–1748.

Burette, A. C., Park, H., and Weinberg, R. J. (2014). Postsynaptic distribution of irsp53 in spiny excitatory and inhibitory neurons. *J Comp Neurol*, 522(9):2164–2178.

C Yuen, R. K., Merico, D., Bookman, M., L Howe, J., Thiruvahindrapuram, B., Patel, R. V., Whitney, J., Deflaux, N., Bingham, J., Wang, Z., Pellecchia, G., Buchanan, J. A., Walker, S., Marshall, C. R., Uddin, M., Zarrei, M., Deneault, E., D'Abate, L., Chan, A. J. S., Koyanagi, S., Paton, T., Pereira, S. L., Hoang, N., Engchuan, W., Higginbotham, E. J., Ho, K., Lamoureux, S., Li, W., MacDonald, J. R., Nalpathamkalam, T., Sung, W. W. L., Tsoi, F. J., Wei, J., Xu, L., Tasse, A.-M., Kirby, E., Van Etten, W., Twigger, S., Roberts, W., Drmic, I., Jilderda, S., Modi, B. M., Kellam, B., Szego, M., Cytrynbaum, C., Weksberg, R., Zwaigenbaum, L., Woodbury-Smith, M., Brian, J., Senman, L., Iaboni, A., Doyle-Thomas, K., Thompson, A., Chrysler, C., Leef, J., Savion-Lemieux, T., Smith, I. M., Liu, X., Nicolson, R., Seifer, V., Fedele, A., Cook, E. H., Dager, S., Estes, A., Gallagher, L., Malow, B. A., Parr, J. R., Spence, S. J., Vorstman, J., Frey, B. J., Robinson, J. T., Strug, L. J., Fernandez, B. A., Elsabbagh, M., Carter, M. T., Hallmayer, J., Knoppers, B. M., Anagnostou, E., Szatmari, P., Ring, R. H., Glazer, D., Pletcher, M. T., and Scherer, S. W. (2017). Whole genome sequencing resource identifies 18 new candidate genes for autism spectrum disorder. *Nat Neurosci*, 20(4):602–611.

Campellone, K. G., Webb, N. J., Znameroski, E. A., and Welch, M. D. (2008). Whamm is an arp2/3 complex activator that binds microtubules and functions in er to golgi transport. *Cell*, 134(1):148–161.

Campellone, K. G. and Welch, M. D. (2010). A nucleator arms race: cellular control of actin assembly. *Nat Rev Mol Cell Biol*, 11(4):237–251.

Canali, G., Garcia, M., Hivert, B., Pinatel, D., Goullancourt, A., Oguievetskaia, K., Saint-Martin, M., Girault, J.-A., Faivre-Sarrailh, C., and Goutebroze, L. (2018). Genetic variants in autism-related cntnap2 impair axonal growth of cortical neurons. *Hum Mol Genet*, 27(11):1941–1954.

Capani, F., Ellisman, M. H., and Martone, M. E. (2001). Filamentous actin is concentrated in specific subpopulations of neuronal and glial structures in rat central nervous system. *Brain Res*, 923(1-2):1–11.

Careaga, M., Van de Water, J., and Ashwood, P. (2010). Immune dysfunction in autism: a pathway to treatment. *Neurotherapeutics*, 7(3):283–292.

Caron, E. and Hall, A. (1998). Identification of two distinct mechanisms of phagocytosis controlled by different rho gtpases. *Science*, 282(5394):1717–1721.

Case, L. B. and Waterman, C. M. (2015). Integration of actin dynamics and cell adhesion by a three-dimensional, mechanosensitive molecular clutch. *Nat Cell Biol*, 17(8):955–963.

Chai, J.-H., Locke, D. P., Greally, J. M., Knoll, J. H. M., Ohta, T., Dunai, J., Yavor, A., Eichler, E. E., and Nicholls, R. D. (2003). Identification of four highly conserved genes between breakpoint hotspots bp1 and bp2 of the prader-willi/angelman syndromes deletion region that have undergone evolutionary transposition mediated by flanking duplicons. *Am J Hum Genet*, 73(4):898–925.

Chanda, S., Hale, W. D., Zhang, B., Wernig, M., and Südhof, T. C. (2017). Unique versus redundant functions of neuroligin genes in shaping excitatory and inhibitory synapse properties. *J Neurosci*, 37(29):6816–6836.

Charych, E. I., Yu, W., Miralles, C. P., Serwanski, D. R., Li, X., Rubio, M., and de Blas, A. L. (2004). The brefeldin a-inhibited gdp/gtp exchange factor 2, a protein involved in vesicular trafficking, interacts with the beta subunits of the gaba receptors. *J Neurochem*, 90(1):173–189.

Chen, B., Brinkmann, K., Chen, Z., Pak, C. W., Liao, Y., Shi, S., Henry, L., Grishin, N. V., Bogdan, S., and Rosen, M. K. (2014a). The wave regulatory complex links diverse receptors to the actin cytoskeleton. *Cell*, 156(1-2):195–207.

Chen, B., Chou, H.-T., Brautigam, C. A., Xing, W., Yang, S., Henry, L., Doolittle, L. K., Walz, T., and Rosen, M. K. (2017). Rac1 gtpase activates the wave regulatory complex through two distinct binding sites. *elife*, 6.

Chen, C.-C., Lu, J., and Zuo, Y. (2014b). Spatiotemporal dynamics of dendritic spines in the living brain. *Front Neuroanat*, 8:28.

Chen, H. and Firestein, B. L. (2007). RhoA regulates dendrite branching in hippocampal neurons by decreasing cypin protein levels. *J Neurosci*, 27(31):8378–8386.

Chen, J. A., Peñagarikano, O., Belgard, T. G., Swarup, V., and Geschwind, D. H. (2015). The emerging picture of autism spectrum disorder: genetics and pathology. *Annu Rev Pathol*, 10:111–144.

Chen, X., Nelson, C. D., Li, X., Winters, C. A., Azzam, R., Sousa, A. A., Leapman, R. D., Gainer, H., Sheng, M., and Reese, T. S. (2011). Psd-95 is required to sustain the molecular organization of the postsynaptic density. *J Neurosci*, 31(17):6329–6338.

Chen, Z., Borek, D., Padrick, S. B., Gomez, T. S., Metlagel, Z., Ismail, A. M., Umetani, J., Billadeau, D. D., Otwinowski, Z., and Rosen, M. K. (2010). Structure and control of the actin regulatory wave complex. *Nature*, 468(7323):533–538.

Chesarone, M. A., DuPage, A. G., and Goode, B. L. (2010). Unleashing formins to remodel the actin and microtubule cytoskeletons. *Nat Rev Mol Cell Biol*, 11(1):62–74.

Choi, C. K., Vicente-Manzanares, M., Zareno, J., Whitmore, L. A., Mogilner, A., and Horwitz, A. R. (2008). Actin and alpha-actinin orchestrate the assembly and maturation of nascent adhesions in a myosin ii motor-independent manner. *Nat Cell Biol*, 10(9):1039–1050.

Cingolani, L. A. and Goda, Y. (2008). Actin in action: the interplay between the actin cytoskeleton and synaptic efficacy. *Nat Rev Neurosci*, 9(5):344–356.

Cioni, J.-M., Wong, H. H.-W., Bressan, D., Kodama, L., Harris, W. A., and Holt, C. E. (2018). Axon-axon interactions regulate topographic optic tract sorting via cyfip2-dependent wave complex function. *Neuron*, 97(5):1078–1093.e6.

Colonna, M. and Butovsky, O. (2017). Microglia function in the central nervous system during health and neurodegeneration. *Annu Rev Immunol*, 35:441–468.

Comery, T. A., Harris, J. B., Willems, P. J., Oostra, B. A., Irwin, S. A., Weiler, I. J., and Greenough, W. T. (1997). Abnormal dendritic spines in fragile x knockout mice: maturation and pruning deficits. *Proc Natl Acad Sci USA*, 94(10):5401–5404.

Cox, D. M. and Butler, M. G. (2015). The 15q11.2 bp1-bp2 microdeletion syndrome: a review. *Int J Mol Sci*, 16(2):4068–4082.

Crino, P. B. (2016). The mtor signalling cascade: paving new roads to cure neurological disease. *Nat Rev Neurol*, 12(7):379–392.

Cubelos, B., Sebastián-Serrano, A., Beccari, L., Calcagnotto, M. E., Cisneros, E., Kim, S., Dopazo, A., Alvarez-Dolado, M., Redondo, J. M., Bovolenta, P., Walsh, C. A., and Nieto, M. (2010). Cux1 and cux2 regulate dendritic branching, spine morphology, and synapses of the upper layer neurons of the cortex. *Neuron*, 66(4):523–535.

Cypher, C. and Letourneau, P. C. (1991). Identification of cytoskeletal, focal adhesion, and cell adhesion proteins in growth cone particles isolated from developing chick brain. *J Neurosci Res*, 30(1):259–265.

Dahl, J. P., Wang-Dunlop, J., Gonzales, C., Goad, M. E. P., Mark, R. J., and Kwak, S. P. (2003). Characterization of the wave1 knock-out mouse: implications for cns development. *J Neurosci*, 23(8):3343–3352.

Dailey, M. E. and Smith, S. J. (1996). The dynamics of dendritic structure in developing hippocampal slices. *J Neurosci*, 16(9):2983–2994.

Darnell, J. C., van Driesche, S. J., Zhang, C., Hung, K. Y. S., Mele, A., Fraser, C. E., Stone, E. F., Chen, C., Fak, J. J., Chi, S. W., Licatalosi, D. D., Richter, J. D., and Darnell, R. B. (2011). Fmrp stalls ribosomal translocation on mrnas linked to synaptic function and autism. *Cell*, 146(2):247–261.

Davalos, D., Grutzendler, J., Yang, G., Kim, J. V., Zuo, Y., Jung, S., Littman, D. R., Dustin, M. L., and Gan, W.-B. (2005). Atp mediates rapid microglial response to local brain injury in vivo. *Nat Neurosci*, 8(6):752–758.

Davalos, D., Ryu, J. K., Merlini, M., Baeten, K. M., Le Moan, N., Petersen, M. A., Deerinck, T. J., Smirnoff, D. S., Bedard, C., Hakozaki, H., Gonias Murray, S., Ling, J. B., Lassmann, H., Degen, J. L., Ellisman, M. H., and Akassoglou, K. (2012). Fibrinogen-induced perivascular microglial clustering is required for the development of axonal damage in neuroinflammation. *Nat Commun*, 3:1227.

Davenport, E. C., Szulc, B., Drew, J., Taylor, J., Morgan, T., Higgs, N. F., Lopez-Domenech, G., and Kittler, J. T. (2018). Correct cyfip1 dosage is essential for synaptic inhibition and the excitatory/inhibitory balance. *BioRxiv*.

de Kovel, Carolien G F, Trucks, H., Helbig, I., Mefford, H. C., Baker, C., Leu, C., Kluck, C., Muhle, H., von Spiczak, S., Ostertag, P., Obermeier, T., Kleefuss-Lie, A. A., Hallmann, K., Steffens, M., Gaus, V., Klein, K. M., Hamer, H. M., Rosenow, F., Brilstra, E. H., Trenité, D. K.-N., Swinkels, M. E. M., Weber, Y. G., Unterberger, I., Zimprich, F., Urak, L., Feucht, M., Fuchs, K., M\oller, R. S., Hjalgrim, H., de Jonghe, P., Suls, A., Rückert, I.-M., Wichmann, H.-E., Franke, A.,

Schreiber, S., Nürnberg, P., Elger, C. E., Lerche, H., Stephani, U., Koeleman, B. P. C., Lindhout, D., Eichler, E. E., and Sander, T. (2010). Recurrent microdeletions at 15q11.2 and 16p13.11 predispose to idiopathic generalized epilepsies. *Brain*, 133(Pt 1):23–32.

de Rubeis, S., He, X., Goldberg, A. P., Poultney, C. S., Samocha, K., Cicek, A. E., Kou, Y., Liu, L., Fromer, M., Walker, S., Singh, T., Klei, L., Kosmicki, J., Shih-Chen, F., Aleksic, B., Biscaldi, M., Bolton, P. F., Brownfeld, J. M., Cai, J., Campbell, N. G., Carracedo, A., Chahrour, M. H., Chiocchetti, A. G., Coon, H., Crawford, E. L., Curran, S. R., Dawson, G., Duketis, E., Fernandez, B. A., Gallagher, L., Geller, E., Guter, S. J., Hill, R. S., Ionita-Laza, J., Jimenz Gonzalez, P., Kilpinen, H., Klauck, S. M., Kolevzon, A., Lee, I., Lei, I., Lei, J., Lehtimäki, T., Lin, C.-F., Ma'ayan, A., Marshall, C. R., McInnes, A. L., Neale, B., Owen, M. J., Ozaki, N., Parellada, M., Parr, J. R., Purcell, S., Puura, K., Rajagopalan, D., Rehnström, K., Reichenberg, A., Sabo, A., Sachse, M., Sanders, S. J., Schafer, C., Schulte-Rüther, M., Skuse, D., Stevens, C., Szatmari, P., Tammimies, K., Valladares, O., Voran, A., Li-San, W., Weiss, L. A., Willsey, A. J., Yu, T. W., Yuen, R. K. C., DDD Study, Homozygosity Mapping Collaborative for Autism, UK10K Consortium, Cook, E. H., Freitag, C. M., Gill, M., Hultman, C. M., Lehner, T., Palotie, A., Schellenberg, G. D., Sklar, P., State, M. W., Sutcliffe, J. S., Walsh, C. A., Scherer, S. W., Zwick, M. E., Barett, J. C., Cutler, D. J., Roeder, K., Devlin, B., Daly, M. J., and Buxbaum, J. D. (2014). Synaptic, transcriptional and chromatin genes disrupted in autism. *Nature*, 515(7526):209–215.

de Rubeis, S., Pasciuto, E., Li, K. W., Fernández, E., Di Marino, D., Buzzi, A., Ostroff, L. E., Klann, E., Zwartkruis, F. J. T., Komiyama, N. H., Grant, S. G. N., Poujol, C., Choquet, D., Achsel, T., Posthuma, D., Smit, A. B., and Bagni, C. (2013). Cyfip1 coordinates mrna translation and cytoskeleton remodeling to ensure proper dendritic spine formation. *Neuron*, 79(6):1169–1182.

Dehmelt, L. and Halpain, S. (2005). The MAP2/tau family of microtubule-associated proteins. *Genome Biol*, 6(1):204.

Depienne, C., Moreno-De-Luca, D., Heron, D., Bouteiller, D., Gennetier, A., Delorme, R., Chaste, P., Siffroi, J.-P., Chantot-Bastaraud, S., Benyahia, B., Trouillard, O., Nygren, G., Kopp, S., Johansson, M., Rastam, M., Burglen, L., Leguern, E., Verloes, A., Leboyer, M., Brice, A., Gillberg, C., and Betancur, C. (2009). Screening for genomic rearrangements and methylation abnormalities of the 15q11-q13 region in autism spectrum disorders. *Biol Psychiatry*, 66(4):349–359.

Derry, J. M., Ochs, H. D., and Francke, U. (1994). Isolation of a novel gene mutated in wiskott-aldrich syndrome. *Cell*, 78(4):635–644.

Dhawale, A. and Bhalla, U. S. (2008). The network and the synapse: 100 years after cajal. *HFSP J*, 2(1):12–16.

D'Hulst, C., de Geest, N., Reeve, S. P., van Dam, D., de Deyn, P. P., Hassan, B. A., and Kooy, R. F. (2006). Decreased expression of the gabaa receptor in fragile x syndrome. *Brain Res*, 1121(1):238–245.

Di Marino, D., Chillemi, G., de Rubeis, S., Tramontano, A., Achsel, T., and Bagni, C. (2015). Md and docking studies reveal that the functional switch of cyfip1 is mediated by a butterfly-like motion. *J Chem Theory Comput*, 11(7):3401–3410.

Di Nardo, A., Cicchetti, G., Falet, H., Hartwig, J. H., Stossel, T. P., and Kwiatkowski, D. J. (2005). Arp2/3 complex-deficient mouse fibroblasts are viable and have normal leading-edge actin structure and function. *Proc. Natl. Acad. Sci. USA*, 102(45):16263–16268.

Dibaj, P., Nadrigny, F., Steffens, H., Scheller, A., Hirrlinger, J., Schomburg, E. D., Neusch, C., and Kirchhoff, F. (2010). No mediates microglial response to acute spinal cord injury under atp control in vivo. *Glia*, 58(9):1133–1144.

Dictenberg, J. B., Swanger, S. A., Antar, L. N., Singer, R. H., and Bassell, G. J. (2008). A direct role for fmrp in activity-dependent dendritic mrna transport links filopodial-spine morphogenesis to fragile x syndrome. *Dev Cell*, 14(6):926–939.

Dietz, D. M., Sun, H., Lobo, M. K., Cahill, M. E., Chadwick, B., Gao, V., Koo, J. W., Mazei-Robison, M. S., Dias, C., Maze, I., Damez-Werno, D., Dietz, K. C., Scobie, K. N., Ferguson, D., Christoffel, D., Ohnishi, Y., Hodes, G. E., Zheng, Y., Neve, R. L., Hahn, K. M., Russo, S. J., and Nestler, E. J. (2012). Rac1 is essential in cocaine-induced structural plasticity of nucleus accumbens neurons. *Nat Neurosci*, 15(6):891–896.

Ding, F., Li, H. H., Zhang, S., Solomon, N. M., Camper, S. A., Cohen, P., and Francke, U. (2008). Snorna snord116 (pwcr1/mbii-85) deletion causes growth deficiency and hyperphagia in mice. *PLoS ONE*, 3(3):e1709.

Dissing-Olesen, L., LeDue, J. M., Rungta, R. L., Hefendehl, J. K., Choi, H. B., and Macvicar, B. A. (2014). Activation of neuronal nmda receptors triggers transient atp-mediated microglial process outgrowth. *J Neurosci*, 34(32):10511–10527.

Dölen, G., Osterweil, E., Rao, B. S. S., Smith, G. B., Auerbach, B. D., Chattarji, S., and Bear, M. F. (2007). Correction of fragile x syndrome in mice. *Neuron*, 56(6):955–962.

Dominguez-Iturza, N., Shah, D., Vannelli, A., Lo, A. C., Armendariz, M., Li, K. W., Mercaldo, V., Trusel, M., Gastaldo, D., Mameli, M., Van der Linden, A., Smit, A. B., Achsel, T., and Bagni, C. (2018). The autism and schizophrenia-associated protein CYFIP1 regulates bilateral brain connectivity. *BioRxiv*.

Dong, T., He, J., Wang, S., Wang, L., Cheng, Y., and Zhong, Y. (2016). Inability to activate rac1-dependent forgetting contributes to behavioral inflexibility in mutants of multiple autism-risk genes. *Proc Natl Acad Sci USA*, 113(27):7644–7649.

Doornbos, M., Sikkema-Raddatz, B., Ruijvenkamp, C. A. L., Dijkhuizen, T., Bijlsma, E. K., Gijsbers, A. C. J., Hilhorst-Hofstee, Y., Hordijk, R., Verbruggen, K. T., Kerstjens-Frederikse, W. S. M., van Essen, T., Kok, K., van Silfhout, A. T., Breuning, M., and van Ravenswaaij-Arts, Conny M A (2009). Nine patients with a microdeletion 15q11.2 between breakpoints 1 and 2 of the prader-willi critical region, possibly associated with behavioural disturbances. *Eur J Med Genet*, 52(2-3):108–115.

Dziunycz, P. J., Neu, J., Lefort, K., Djerbi, N., Freiberger, S. N., Iotzova-Weiss, G., French, L. E., Dotto, G.-P., and Hofbauer, G. F. (2017). Cyfip1 is directly controlled by notch1 and down-regulated in cutaneous squamous cell carcinoma. *PLoS ONE*, 12(4):e0173000.

Eden, S., Rohatgi, R., Podtelejnikov, A. V., Mann, M., and Kirschner, M. W. (2002). Mechanism of regulation of wave1-induced actin nucleation by rac1 and nck. *Nature*, 418(6899):790–793.

Elmore, M. R. P., Najafi, A. R., Koike, M. A., Dagher, N. N., Spangenberg, E. E., Rice, R. A., Kitazawa, M., Matusow, B., Nguyen, H., West, B. L., and Green, K. N. (2014). Colony-stimulating factor 1 receptor signaling is necessary for microglia viability, unmasking a microglia progenitor cell in the adult brain. *Neuron*, 82(2):380–397.

Essrich, C., Lorez, M., Benson, J. A., Fritschy, J. M., and Lüscher, B. (1998). Postsynaptic clustering of major GABAA receptor subtypes requires the gamma 2 subunit and gephyrin. *Nat Neurosci*, 1(7):563–571.

Estes, M. L. and McAllister, A. K. (2015). Immune mediators in the brain and peripheral tissues in autism spectrum disorder. *Nat Rev Neurosci*, 16(8):469–486.

Eyo, U. B., Peng, J., Swiatkowski, P., Mukherjee, A., Bispo, A., and Wu, L.-J. (2014). Neuronal hyperactivity recruits microglial processes via neuronal nmda receptors and microglial p2y12 receptors after status epilepticus. *J Neurosci*, 34(32):10528–10540.

Fan, L., Lu, Y., Shen, X., Shao, H., Suo, L., and Wu, Q. (2018). Alpha protocadherins and pyk2 kinase regulate cortical neuron migration and cytoskeletal dynamics via rac1 gtpase and wave complex in mice. *elife*, 7.

Fanarraga, M. L., Villegas, J. C., Carranza, G., Castaño, R., and Zabala, J. C. (2009). Tubulin cofactor b regulates microtubule densities during microglia transition to the reactive states. *Exp Cell Res*, 315(3):535–541.

Faulkner, R. L., Low, L. K., and Cheng, H.-J. (2007). Axon pruning in the developing vertebrate hippocampus. *Dev Neurosci*, 29(1-2):6–13.

Feng, Y., Absher, D., Eberhart, D. E., Brown, V., Malter, H. E., and Warren, S. T. (1997). Fmrp associates with polyribosomes as an mrnp, and the i304n mutation of severe fragile x syndrome abolishes this association. *Mol Cell*, 1(1):109–118.

Fernández, E., Li, K. W., Rajan, N., de Rubeis, S., Fiers, M., Smit, A. B., Achsel, T., and Bagni, C. (2015). Fxr2p exerts a positive translational control and is required for the activity-dependent increase of psd95 expression. *J Neurosci*, 35(25):9402–9408.

Földy, C., Malenka, R. C., and Südhof, T. C. (2013). Autism-associated neuroligin-3 mutations commonly disrupt tonic endocannabinoid signaling. *Neuron*, 78(3):498–509.

Forrest, M. P., Parnell, E., and Penzes, P. (2018). Dendritic structural plasticity and neuropsychiatric disease. *Nat Rev Neurosci*, 19(4):215–234.

Fossati, M., Pizzarelli, R., Schmidt, E. R., Kupferman, J. V., Stroebel, D., Polleux, F., and Charrier, C. (2016). Srgap2 and its human-specific paralog co-regulate the development of excitatory and inhibitory synapses. *Neuron*, 91(2):356–369.

Galbraith, C. G., Yamada, K. M., and Galbraith, J. A. (2007). Polymerizing actin fibers position integrins primed to probe for adhesion sites. *Science*, 315(5814):992–995.

Gantois, I., Khoutorsky, A., Popic, J., Aguilar-Valles, A., Freemantle, E., Cao, R., Sharma, V., Pooters, T., Nagpal, A., Skalecka, A., Truong, V. T., Wiebe, S., Groves, I. A., Jafarnejad, S. M., Chapat, C., McCullagh, E. A., Gamache, K., Nader, K., Lacaille, J.-C., Gkogkas, C. G., and Sonenberg, N. (2017). Metformin ameliorates core deficits in a mouse model of fragile x syndrome. *Nat Med*, 23(6):674–677.

Geschwind, D. H. and Levitt, P. (2007). Autism spectrum disorders: developmental disconnection syndromes. *Curr Opin Neurobiol*, 17(1):103–111.

Ghani, M., Pinto, D., Lee, J. H., Grinberg, Y., Sato, C., Moreno, D., Scherer, S. W., Mayeux, R., St George-Hyslop, P., and Rogaeva, E. (2012). Genome-wide survey of large rare copy number variants in alzheimer's disease among caribbean hispanics. *G3 (Bethesda)*, 2(1):71–78.

Ghiretti, A. E. and Paradis, S. (2014). Molecular mechanisms of activity-dependent changes in dendritic morphology: role of RGK proteins. *Trends Neurosci*, 37(7):399–407.

Gholizadeh, S., Halder, S. K., and Hampson, D. R. (2015). Expression of fragile x mental retardation protein in neurons and glia of the developing and adult mouse brain. *Brain Res*, 1596:22–30.

Gibson, J. R., Huber, K. M., and Südhof, T. C. (2009). Neuroligin-2 deletion selectively decreases inhibitory synaptic transmission originating from fast-spiking but not from somatostatin-positive interneurons. *J Neurosci*, 29(44):13883–13897.

Ginhoux, F., Greter, M., Leboeuf, M., Nandi, S., See, P., Gokhan, S., Mehler, M. F., Conway, S. J., Ng, L. G., Stanley, E. R., Samokhvalov, I. M., and Merad, M. (2010). Fate mapping analysis reveals that adult microglia derive from primitive macrophages. *Science*, 330(6005):841–845.

Goebbels, S., Bormuth, I., Bode, U., Hermanson, O., Schwab, M. H., and Nave, K.-A. (2006). Genetic targeting of principal neurons in neocortex and hippocampus of nex-cre mice. *Genesis*, 44(12):611–621.

Goldmann, T., Wieghofer, P., Müller, P. F., Wolf, Y., Varol, D., Yona, S., Brendecke, S. M., Kierdorf, K., Staszewski, O., Datta, M., Luedde, T., Heikenwalder, M., Jung, S., and Prinz, M. (2013). A new type of microglia gene targeting shows tak1 to be pivotal in cns autoimmune inflammation. *Nat Neurosci*, 16(11):1618–1626.

Gomez, T. S., Gorman, J. A., de Narvajas, A. A.-M., Koenig, A. O., and Billadeau, D. D. (2012). Trafficking defects in wash-knockout fibroblasts originate from collapsed endosomal and lysosomal networks. *Mol Biol Cell*, 23(16):3215–3228.

Goode, B. L., Sweeney, M. O., and Eskin, J. A. (2018). Gmf as an actin network remodeling factor. *Trends Cell Biol*, 28(9):749–760.

Goodson, H. V. and Jonasson, E. M. (2018). Microtubules and microtubule-associated proteins. *Cold Spring Harb Perspect Biol*, 10(6).

Gordon, J., Amini, S., and White, M. K. (2013). General overview of neuronal cell culture. *Methods Mol Biol*, 1078:1–8.

Gorelik, R., Yang, C., Kameswaran, V., Dominguez, R., and Svitkina, T. (2011). Mechanisms of plasma membrane targeting of formin mdia2 through its amino terminal domains. *Mol Biol Cell*, 22(2):189–201.

Gray, E. G. (1959). Axo-somatic and axo-dendritic synapses of the cerebral cortex: an electron microscope study. *J Anat*, 93:420–433.

Greer, P. L., Hanayama, R., Bloodgood, B. L., Mardinly, A. R., Lipton, D. M., Flavell, S. W., Kim, T.-K., Griffith, E. C., Waldon, Z., Maehr, R., Ploegh, H. L., Chowdhury, S., Worley, P. F., Steen, J., and Greenberg, M. E. (2010). The angelman syndrome protein ube3a regulates synapse development by ubiquitinating arc. *Cell*, 140(5):704–716.

Griffin, A. L. (2015). Role of the thalamic nucleus reuniens in mediating interactions between the hippocampus and medial prefrontal cortex during spatial working memory. *Front Syst Neurosci*, 9:29.

Grove, M., Demyanenko, G., Echarri, A., Zipfel, P. A., Quiroz, M. E., Rodriguiz, R. M., Playford, M., Martensen, S. A., Robinson, M. R., Wetsel, W. C., Maness, P. F., and Pendergast, A. M. (2004). Abi2-deficient mice exhibit defective cell migration, aberrant dendritic spine morphogenesis, and deficits in learning and memory. *Mol Cell Biol*, 24(24):10905–10922.

Guo, J., Higginbotham, H., Li, J., Nichols, J., Hirt, J., Ghukasyan, V., and Anton, E. S. (2015). Developmental disruptions underlying brain abnormalities in ciliopathies. *Nat Commun*, 6:7857.

Haan, N., Carter, J., Westacott, L. J., Owen, M. J., Gray, W. P., Hall, J., and Wilkinson, L. S. (2018). Haploinsufficiency of the schizophrenia risk gene cyfip1 causes abnormal postnatal hippocampal neurogenesis through a novel microglia dependent mechanism. *BioRxiv*.

Hall, A. B., Gakidis, M. A. M., Glogauer, M., Wilsbacher, J. L., Gao, S., Swat, W., and Brugge, J. S. (2006). Requirements for vav guanine nucleotide exchange factors and rho gtpases in fcgammar- and complement-mediated phagocytosis. *Immunity*, 24(3):305–316.

Hammond, T. R., Dufort, C., Dissing-Olesen, L., Giera, S., Young, A., Wysoker, A., Walker, A. J., Gergits, F., Segel, M., Nemesh, J., Marsh, S. E., Saunders, A., Macosko, E., Ginhoux, F., Chen, J., Franklin, R. J. M., Piao, X., McCarroll, S. A., and Stevens, B. (2018). Single-cell RNA sequencing of microglia throughout the mouse lifespan and in the injured brain reveals complex cell-state changes. *Immunity*.

Han, K., Chen, H., Gennarino, V. A., Richman, R., Lu, H.-C., and Zoghbi, H. Y. (2015). Fragile x-like behaviors and abnormal cortical dendritic spines in cytoplasmic fmr1-interacting protein 2-mutant mice. *Hum Mol Genet*, 24(7):1813–1823.

Harburger, D. S. and Calderwood, D. A. (2009). Integrin signalling at a glance. *Journal of cell science*, 122(9):1472.

Harvey, K., Duguid, I. C., Alldred, M. J., Beatty, S. E., Ward, H., Keep, N. H., Lingenfelter, S. E., Pearce, B. R., Lundgren, J., Owen, M. J., Smart, T. G., Lüscher, B., Rees, M. I., and Harvey, R. J. (2004). The GDP-GTP exchange factor collybistin: an essential determinant of neuronal gephyrin clustering. *J Neurosci*, 24(25):5816–5826.

Harvey, R. J., Carta, E., Pearce, B. R., Chung, S.-K., Supplisson, S., Rees, M. I., and Harvey, K. (2008). A critical role for glycine transporters in hyperexcitability disorders. *Front Mol Neurosci*, 1:1.

Haynes, S. E., Hollopeter, G., Yang, G., Kurpius, D., Dailey, M. E., Gan, W.-B., and Julius, D. (2006). The p2y12 receptor regulates microglial activation by extracellular nucleotides. *Nat Neurosci*, 9(12):1512–1519.

Heasman, S. J. and Ridley, A. J. (2008). Mammalian rho gtpases: new insights into their functions from in vivo studies. *Nat Rev Mol Cell Biol*, 9(9):690–701.

Heimsath, E. G. and Higgs, H. N. (2012). The c terminus of formin fmnl3 accelerates actin polymerization and contains a wh2 domain-like sequence that binds both monomers and filament barbed ends. *J Biol Chem*, 287(5):3087–3098.

Henneberger, C., Papouin, T., Oliet, S. H. R., and Rusakov, D. A. (2010). Long-term potentiation depends on release of d-serine from astrocytes. *Nature*, 463(7278):232–236.

Herrmann, H., Bär, H., Kreplak, L., Strelkov, S. V., and Aebi, U. (2007). Intermediate filaments: from cell architecture to nanomechanics. *Nat Rev Mol Cell Biol*, 8(7):562–573.

Hetrick, B., Han, M. S., Helgeson, L. A., and Nolen, B. J. (2013). Small molecules ck-666 and ck-869 inhibit actin-related protein 2/3 complex by blocking an activating conformational change. *Chem Biol*, 20(5):701–712.

Higashimori, H., Morel, L., Huth, J., Lindemann, L., Dulla, C., Taylor, A., Freeman, M., and Yang, Y. (2013). Astroglial fmrp-dependent translational down-regulation of mglur5 underlies glutamate transporter glt1 dysregulation in the fragile x mouse. *Hum Mol Genet*, 22(10):2041–2054.

Higashimori, H., Schin, C. S., Chiang, M. S. R., Morel, L., Shoneye, T. A., Nelson, D. L., and Yang, Y. (2016). Selective deletion of astroglial fmrp dysregulates glutamate transporter glt1 and contributes to fragile x syndrome phenotypes in vivo. *J Neurosci*, 36(27):7079–7094.

Hilker, R., Helenius, D., Fagerlund, B., Skytthe, A., Christensen, K., Werge, T. M., Nordentoft, M., and Glenth\oj, B. (2018). Heritability of schizophrenia and schizophrenia spectrum based on the nationwide danish twin register. *Biol Psychiatry*, 83(6):492–498.

Hill, J. J., Hashimoto, T., and Lewis, D. A. (2006). Molecular mechanisms contributing to dendritic spine alterations in the prefrontal cortex of subjects with schizophrenia. *Mol Psychiatry*, 11(6):557–566.

Hines, D. J., Hines, R. M., Mulligan, S. J., and Macvicar, B. A. (2009). Microglia processes block the spread of damage in the brain and require functional chloride channels. *Glia*, 57(15):1610–1618.

Hinton, V. J., Brown, W. T., Wisniewski, K., and Rudelli, R. D. (1991). Analysis of neocortex in three males with the fragile x syndrome. *Am J Med Genet*, 41(3):289–294.

Hirasawa, T., Ohsawa, K., Imai, Y., Ondo, Y., Akazawa, C., Uchino, S., and Kohsaka, S. (2005). Visualization of microglia in living tissues using iba1-egfp transgenic mice. *J Neurosci Res*, 81(3):357–362.

Hirokawa, N., Noda, Y., Tanaka, Y., and Niwa, S. (2009). Kinesin superfamily motor proteins and intracellular transport. *Nat Rev Mol Cell Biol*, 10(10):682–696.

Hoeffer, C. A., Sanchez, E., Hagerman, R. J., Mu, Y., Nguyen, D. V., Wong, H., Whelan, A. M., Zukin, R. S., Klann, E., and Tassone, F. (2012). Altered mtor signaling and enhanced cyfip2 expression levels in subjects with fragile x syndrome. *Genes Brain Behav*, 11(3):332–341.

Holtmaat, A. and Svoboda, K. (2009). Experience-dependent structural synaptic plasticity in the mammalian brain. *Nat Rev Neurosci*, 10(9):647–658.

Hong, S., Beja-Glasser, V. F., Nfonoyim, B. M., Frouin, A., Li, S., Ramakrishnan, S., Merry, K. M., Shi, Q., Rosenthal, A., Barres, B. A., Lemere, C. A., Selkoe, D. J., and Stevens, B. (2016). Complement and microglia mediate early synapse loss in alzheimer mouse models. *Science*, 352(6286):712–716.

Hong, S. and Stevens, B. (2016). Microglia: phagocytosing to clear, sculpt, and eliminate. *Dev Cell*, 38(2):126–128.

Hotulainen, P. and Hoogenraad, C. C. (2010). Actin in dendritic spines: connecting dynamics to function. *J Cell Biol*, 189(4):619–629.

Hotulainen, P., Llano, O., Smirnov, S., Tanhuanpää, K., Faix, J., Rivera, C., and Lappalainen, P. (2009). Defining mechanisms of actin polymerization and depolymerization during dendritic spine morphogenesis. *J Cell Biol*, 185(2):323–339.

Hou, H., Chávez, A. E., Wang, C.-C., Yang, H., Gu, H., Siddoway, B. A., Hall, B. J., Castillo, P. E., and Xia, H. (2014). The rac1 inhibitor nsc23766 suppresses creb signaling by targeting nmda receptor function. *J Neurosci*, 34(42):14006–14012.

Hsiao, K., Harony-Nicolas, H., Buxbaum, J. D., Bozdagi-Gunal, O., and Benson, D. L. (2016). Cyfip1 regulates presynaptic activity during development. *The Journal of Neuroscience*.

Huang, Y. (2015). Up-regulated cytoplasmic fmrp-interacting protein 1 in intractable temporal lobe epilepsy patients and a rat model. *Int J Neurosci*, pages 1–10.

Hui, C. W., Zhang, Y., and Herrup, K. (2016). Non-neuronal cells are required to mediate the effects of neuroinflammation: Results from a neuron-enriched culture system. *PLoS ONE*, 11(1):e0147134.

Humeau, Y., Herry, C., Kemp, N., Shaban, H., Fourcaudot, E., Bissière, S., and Lüthi, A. (2005). Dendritic spine heterogeneity determines afferent-specific hebbian plasticity in the amygdala. *Neuron*, 45(1):119–131.

Hutsler, J. J. and Zhang, H. (2010). Increased dendritic spine densities on cortical projection neurons in autism spectrum disorders. *Brain Res*, 1309:83–94.

Ilić, D., Furuta, Y., Kanazawa, S., Takeda, N., Sobue, K., Nakatsuji, N., Nomura, S., Fujimoto, J., Okada, M., and Yamamoto, T. (1995). Reduced cell motility and enhanced focal adhesion contact formation in cells from FAK-deficient mice. *Nature*, 377(6549):539–544.

Ilschner, S. and Brandt, R. (1996). The transition of microglia to a ramified phenotype is associated with the formation of stable acetylated and detyrosinated microtubules. *Glia*.

Inagaki, N., Chihara, K., Arimura, N., Ménager, C., Kawano, Y., Matsuo, N., Nishimura, T., Amano, M., and Kaibuchi, K. (2001). CRMP-2 induces axons in cultured hippocampal neurons. *Nat Neurosci*, 4(8):781–782.

Ingason, A., Kirov, G., Giegling, I., Hansen, T., Isles, A. R., Jakobsen, K. D., Kristinsson, K. T., Le Roux, L., Gustafsson, O., Craddock, N., Möller, H.-J., McQuillin, A., Muglia, P., Cichon, S., Rietschel, M., Ophoff, R. A., Djurovic, S., Andreassen, O. A., Pietiläinen, O. P. H., Peltonen, L., Dempster, E., Collier, D. A., St Clair, D., Rasmussen, H. B., GlenthGROUP Investigators, Nöthen, M. M., Gurling, H., O'Donovan, M. C., Owen, M. J., Sigurdsson, E., Petursson, H., Stefansson, H., Rujescu, D., Stefansson, K., and Werge, T. (2011). Maternally derived microduplications at 15q11-q13: implication of imprinted genes in psychotic illness. *Am J Psychiatry*, 168(4):408–417.

Innocenti, M., Zucconi, A., Disanza, A., Frittoli, E., Areces, L. B., Steffen, A., Stradal, T. E. B., Di Fiore, P. P., Carlier, M.-F., and Scita, G. (2004). Abi1 is essential for the formation and activation of a wave2 signalling complex. *Nat Cell Biol*, 6(4):319–327.

Iossifov, I., Ronemus, M., Levy, D., Wang, Z., Hakker, I., Rosenbaum, J., Yamrom, B., Lee, Y.-H., Narzisi, G., Leotta, A., Kendall, J., Grabowska, E., Ma, B., Marks, S., Rodgers, L., Stepansky, A., Troge, J., Andrews, P., Bekritsky, M., Pradhan, K., Ghiban, E., Kramer, M., Parla, J., Demeter, R., Fulton, L. L., Fulton, R. S., Magrini, V. J., Ye, K., Darnell, J. C., Darnell, R. B., Mardis, E. R., Wilson, R. K., Schatz, M. C., McCombie, W. R., and Wigler, M. (2012). De novo gene disruptions in children on the autistic spectrum. *Neuron*, 74(2):285–299.

Irino, Y., Nakamura, Y., Inoue, K., Kohsaka, S., and Ohsawa, K. (2008). Akt activation is involved in p2y12 receptor-mediated chemotaxis of microglia. *J Neurosci Res*, 86(7):1511–1519.

Irwin, S. A., Galvez, R., and Greenough, W. T. (2000). Dendritic spine structural anomalies in fragile-x mental retardation syndrome. *Cereb Cortex*, 10(10):1038–1044.

Ishikawa, H., Bischoff, R., and Holtzer, H. (1969). Formation of arrowhead complexes with heavy meromyosin in a variety of cell types. *J Cell Biol*, 43(2):312–328.

Isles, A. R., Ingason, A., Lowther, C., Walters, J., Gawlick, M., Stöber, G., Rees, E., Martin, J., Little, R. B., Potter, H., Georgieva, L., Pizzo, L., Ozaki, N., Aleksic, B., Kushima, I., Ikeda, M., Iwata, N., Levinson, D. F., Gejman, P. V., Shi, J., Sanders, A. R., Duan, J., Willis, J., Sisodiya, S., Costain, G., Werge, T. M., Degenhardt, F., Giegling, I., Rujescu, D., Hreidarsson, S. J., Saemundsen, E., Ahn, J. W., Ogilvie, C., Girirajan, S. D., Stefansson, H., Stefansson, K., O'Donovan, M. C., Owen, M. J., Bassett, A., and Kirov, G. (2016). Parental origin of interstitial duplications at 15q11.2-q13.3 in schizophrenia and neurodevelopmental disorders. *PLoS Genet*, 12(5):e1005993.

Ismail, A. M., Padrick, S. B., Chen, B., Umetani, J., and Rosen, M. K. (2009). The wave regulatory complex is inhibited. *Nat Struct Mol Biol*, 16(5):561–563.

Ito, H., Morishita, R., Shinoda, T., Iwamoto, I., Sudo, K., Okamoto, K., and Nagata, K. (2010). Dysbindin-1, wave2 and abi-1 form a complex that regulates dendritic spine formation. *Mol Psychiatry*, 15(10):976–986.

Ivanov, A., Esclapez, M., Pellegrino, C., Shirao, T., and Ferhat, L. (2009). Drebrin a regulates dendritic spine plasticity and synaptic function in mature cultured hippocampal neurons. *J Cell Sci*, 122(Pt 4):524–534.

Jacinto, E., Loewith, R., Schmidt, A., Lin, S., Rüegg, M. A., Hall, A., and Hall, M. N. (2004). Mammalian tor complex 2 controls the actin cytoskeleton and is rapamycin insensitive. *Nat Cell Biol*, 6(11):1122–1128.

Jaffe, A. B. and Hall, A. (2005). Rho GTPases: biochemistry and biology. *Annu Rev Cell Dev Biol*, 21:247–269.

Jamain, S., Quach, H., Betancur, C., Råstam, M., Colineaux, C., Gillberg, I. C., Soderstrom, H., Giros, B., Leboyer, M., Gillberg, C., Bourgeron, T., and Paris Autism Research International Sibpair Study (2003). Mutations of the x-linked genes encoding neuroligins nlgn3 and nlgn4 are associated with autism. *Nat Genet*, 34(1):27–29.

Jan, Y.-N. and Jan, L. Y. (2010). Branching out: mechanisms of dendritic arborization. *Nat Rev Neurosci*, 11(5):316–328.

Janke, C. and Bulinski, J. C. (2011). Post-translational regulation of the microtubule cytoskeleton: mechanisms and functions. *Nat Rev Mol Cell Biol*, 12(12):773–786.

Jia, D., Gomez, T. S., Metlagel, Z., Umetani, J., Otwinowski, Z., Rosen, M. K., and Billadeau, D. D. (2010). Wash and wave actin regulators of the wiskott-aldrich syndrome protein (wasp) family are controlled by analogous structurally related complexes. *Proc Natl Acad Sci USA*, 107(23):10442–10447.

Jung, M.-Y., Lorenz, L., and Richter, J. D. (2006). Translational control by neuroguidin, a eukaryotic initiation factor 4E and CPEB binding protein. *Mol Cell Biol*, 26(11):4277–4287.

Kang, J., Park, H., and Kim, E. (2016). Irsp53/baiap2 in dendritic spine development, nmda receptor regulation, and psychiatric disorders. *Neuropharmacology*, 100:27–39.

Kast, D. J., Zajac, A. L., Holzbaur, E. L. F., Ostap, E. M., and Dominguez, R. (2015). WHAMM directs the arp2/3 complex to the ER for autophagosome biogenesis through an actin comet tail mechanism. *Curr Biol*, 25(13):1791–1797.

Kaufmann, W. E. and Moser, H. W. (2000). Dendritic anomalies in disorders associated with mental retardation. *Cereb Cortex*, 10(10):981–991.

Kawano, Y., Yoshimura, T., Tsuboi, D., Kawabata, S., Kaneko-Kawano, T., Shirataki, H., Takenawa, T., and Kaibuchi, K. (2005). Crmp-2 is involved in kinesin-1-dependent transport of the sra-1/wave1 complex and axon formation. *Mol Cell Biol*, 25(22):9920–9935.

Keeler, A. B., Molumby, M. J., and Weiner, J. A. (2015). Protocadherins branch out: Multiple roles in dendrite development. *Cell Adh Migr*, 9(3):214–226.

Kheir, W. A., Gevrey, J.-C., Yamaguchi, H., Isaac, B., and Cox, D. (2005). A wave2-abi1 complex mediates csf-1-induced f-actin-rich membrane protrusions and migration in macrophages. *J Cell Sci*, 118(Pt 22):5369–5379.

Khlghatyan, J., Evstratova, A., Chamberland, S., Marakhovskaia, A., Bahremand, A., Toth, K., and Beaulieu, J.-M. (2018). Mental illnesses-associated fxr1 and its negative regulator gsk3\beta are modulators of anxiety and glutamatergic neurotransmission. *Front Mol Neurosci*, 11:119.

Kierdorf, K., Erny, D., Goldmann, T., Sander, V., Schulz, C., Perdiguero, E. G., Wieghofer, P., Heinrich, A., Riemke, P., Hölscher, C., Müller, D. N., Luckow, B., Brocker, T., Debowski, K., Fritz, G., Opdenakker, G., Diefenbach, A., Biber, K., Heikenwalder, M., Geissmann, F., Rosenbauer, F., and Prinz, M. (2013). Microglia emerge from erythromyeloid precursors via pu.1- and irf8-dependent pathways. *Nat Neurosci*, 16(3):273–280.

Kim, C., Cho, E.-D., Kim, H.-K., You, S., Lee, H.-J., Hwang, D., and Lee, S.-J. (2014). \beta1-integrin-dependent migration of microglia in response to neuron-released \alpha-synuclein. *Exp Mol Med*, 46:e91.

Kim, K. S., Marcogliese, P. C., Yang, J., Callaghan, S. M., Resende, V., Abdel-Messih, E., Marras, C., Visanji, N. P., Huang, J., Schlossmacher, M. G., Trinkle-Mulcahy, L., Slack, R. S., Lang, A. E., in Inflammation Team (CLINT), C. L., and Park, D. S. (2018). Regulation of myeloid cell phagocytosis by LRRK2 via WAVE2 complex stabilization is altered in parkinson's disease. *Proc Natl Acad Sci USA*, 115(22):E5164–E5173.

Kim, Y., Sung, J. Y., Ceglia, I., Lee, K.-W., Ahn, J.-H., Halford, J. M., Kim, A. M., Kwak, S. P., Park, J. B., Ho Ryu, S., Schenck, A., Bardoni, B., Scott, J. D., Nairn, A. C., and Greengard, P. (2006). Phosphorylation of wave1 regulates actin polymerization and dendritic spine morphology. *Nature*, 442(7104):814–817.

Kimura, E., Kubo, K.-I., Endo, T., Ling, W., Nakajima, K., Kakeyama, M., and Tohyama, C. (2017). Impaired dendritic growth and positioning of cortical pyramidal neurons by activation of aryl hydrocarbon receptor signaling in the developing mouse. *PLoS ONE*, 12(8):e0183497.

Kirkpatrick, S. L., Goldberg, L. R., Yazdani, N., Babbs, R. K., Wu, J., Reed, E. R., Jenkins, D. F., Bolgioni, A. F., Landaverde, K. I., Luttik, K. P., Mitchell, K. S., Kumar, V., Johnson, W. E., Mulligan, M. K., Cottone, P., and Bryant, C. D. (2017). Cytoplasmic fmr1-interacting protein 2 is a major genetic factor underlying binge eating. *Biol Psychiatry*, 81(9):757–769.

Kirov, G., Pocklington, A. J., Holmans, P., Ivanov, D., Ikeda, M., Ruderfer, D., Moran, J., Chambert, K., Toncheva, D., Georgieva, L., Grozeva, D., Fjodorova, M., Wollerton, R., Rees, E., Nikolov, I., van de Lagemaat, L N, Bayés, A., Fernandez, E., Olason, P. I., Böttcher, Y., Komiyama, N. H., Collins, M. O., Choudhary, J., Stefansson, K., Stefansson, H., Grant, S. G. N., Purcell, S., Sklar, P., O'Donovan, M. C., and Owen, M. J. (2012). De novo cnv analysis implicates specific abnormalities of postsynaptic signalling complexes in the pathogenesis of schizophrenia. *Mol Psychiatry*, 17(2):142–153.

Knott, G. W., Holtmaat, A., Wilbrecht, L., Welker, E., and Svoboda, K. (2006). Spine growth precedes synapse formation in the adult neocortex in vivo. *Nat Neurosci*, 9(9):1117–1124.

Kobayashi, K., Kuroda, S., Fukata, M., Nakamura, T., Nagase, T., Nomura, N., Matsuura, Y., Yoshida-Kubomura, N., Iwamatsu, A., and Kaibuchi, K. (1998). p140sra-1 (specifically rac1-associated protein) is a novel specific target for rac1 small gtpase. *J Biol Chem*, 273(1):291–295.

Koleske, A. J. (2013). Molecular mechanisms of dendrite stability. *Nat Rev Neurosci*, 14(8):536–550.

Kolomeets, N. S., Orlovskaya, D. D., Rachmanova, V. I., and Uranova, N. A. (2005). Ultrastructural alterations in hippocampal mossy fiber synapses in schizophrenia: a postmortem morphometric study. *Synapse*, 57(1):47–55.

Konietzny, A., Bär, J., and Mikhaylova, M. (2017). Dendritic actin cytoskeleton: structure, functions, and regulations. *Front Cell Neurosci*, 11:147.

Korobova, F. and Svitkina, T. (2008). Arp2/3 complex is important for filopodia formation, growth cone motility, and neuritogenesis in neuronal cells. *Mol Biol Cell*, 19(4):1561–1574.

Korobova, F. and Svitkina, T. (2010). Molecular architecture of synaptic actin cytoskeleton in hippocampal neurons reveals a mechanism of dendritic spine morphogenesis. *Mol Biol Cell*, 21(1):165–176.

Koronakis, V., Hume, P. J., Humphreys, D., Liu, T., and HMcGhie, E. J. (2011). Wave regulatory complex activation by cooperating gtpases arf and rac1. *Proc Natl Acad Sci USA*, 108(35):14449–14454.

Krause, M. and Gautreau, A. (2014). Steering cell migration: lamellipodium dynamics and the regulation of directional persistence. *Nat Rev Mol Cell Biol*, 15(9):577–590.

Kulkarni, V. A. and Firestein, B. L. (2012). The dendritic tree and brain disorders. *Mol Cell Neurosci*, 50(1):10–20.

Kumar, V., Kim, K., Joseph, C., Kourrich, S., Yoo, S.-H., Huang, H. C., Vitaterna, M. H., de Villena, F. P.-M., Churchill, G., Bonci, A., and Takahashi, J. S. (2013). C57bl/6n mutation in cytoplasmic fmrp interacting protein 2 regulates cocaine response. *Science*, 342(6165):1508–1512.

Kunda, P., Craig, G., Dominguez, V., and Baum, B. (2003). Abi, sra1, and kette control the stability and localization of scar/wave to regulate the formation of actin-based protrusions. *Curr Biol*, 13(21):1867–1875.

Kurokawa, K., Itoh, R. E., Yoshizaki, H., Nakamura, Y. O. T., and Matsuda, M. (2004). Coactivation of rac1 and cdc42 at lamellipodia and membrane ruffles induced by epidermal growth factor. *Mol Biol Cell*, 15(3):1003–1010.

Lai, F. P. L., Szczodrak, M., Oelkers, J. M., Ladwein, M., Acconcia, F., Benesch, S., Auinger, S., Faix, J., Small, J. V., Polo, S., Stradal, T. E. B., and Rottner, K. (2009). Cortactin promotes migration and platelet-derived growth factor-induced actin reorganization by signaling to rho-gtpases. *Mol Biol Cell*, 20(14):3209–3223.

Lal, D., Ruppert, A.-K., Trucks, H., Schulz, H., de Kovel, C. G., Kasteleijn-Nolst Trenité, D., Sonsma, A. C. M., Koeleman, B. P., Lindhout, D., Weber, Y. G., Lerche, H., Kapser, C., Schankin, C. J., Kunz, W. S., Surges, R., Elger, C. E., Gaus, V., Schmitz, B., Helbig, I., Muhle, H., Stephani, U., Klein, K. M., Rosenow, F., Neubauer, B. A., Reinthaler, E. M., Zimprich, F., Feucht, M., MEPICURE Consortium, and Sander, T. (2015). Burden analysis of rare microdeletions suggests a strong impact of neurodevelopmental genes in genetic generalised epilepsies. *PLoS Genet*, 11(5):e1005226.

Lammers, M., Meyer, S., Kühlmann, D., and Wittinghofer, A. (2008). Specificity of interactions between mdia isoforms and rho proteins. *J Biol Chem*, 283(50):35236–35246.

Lawson, C. D. and Ridley, A. J. (2018). Rho gtpase signaling complexes in cell migration and invasion. *J Cell Biol*, 217(2):447–457.

Lebensohn, A. M. and Kirschner, M. W. (2009). Activation of the wave complex by coincident signals controls actin assembly. *Mol Cell*, 36(3):512–524.

Leblond, C. S., Heinrich, J., Delorme, R., Proepper, C., Betancur, C., Huguet, G., Konyukh, M., Chaste, P., Ey, E., Rastam, M., Anckarsäter, H., Nygren, G., Gillberg, I. C., Melke, J., Toro, R., Regnault, B., Fauchereau, F., Mercati, O., Lemière, N., Skuse, D., Poot, M., Holt, R., Monaco, A. P., Järvelä, I., Kantojärvi, K., Vanhala, R., Curran, S., Collier, D. A., Bolton, P., Chiocchetti, A., Klauck, S. M., Poustka, F., Freitag, C. M., Waltes, R., Kopp, M., Duketis, E., Bacchelli, E., Minopoli, F., Ruta, L., Battaglia, A., Mazzone, L., Maestrini, E., Sequeira, A. F., Oliveira, B., Vicente, A., Oliveira, G., Pinto, D., Scherer, S. W., Zelenika, D., Delepine, M., Lathrop, M., Bonneau, D., Guinchat, V., Devillard, F., Assouline, B., Mouren, M.-C., Leboyer, M., Gillberg, C., Boeckers, T. M., and Bourgeron, T. (2012). Genetic and functional analyses of shank2 mutations suggest a multiple hit model of autism spectrum disorders. *PLoS Genet*, 8(2):e1002521.

Lee, A., Li, W., Xu, K., Bogert, B. A., Su, K., and Gao, F.-B. (2003). Control of dendritic development by the drosophila fragile x-related gene involves the small gtpase rac1. *Development*, 130(22):5543–5552.

Lee, J. H., Kim, H. J., Yoon, J. M., Cheon, E. J., Lim, J. W., Ko, K. O., and Lee, G. M. (2016). Interstitial deletion of 5q33.3q35.1 in a boy with severe mental retardation. *Korean J Pediatr*, 59(Suppl 1):S19–S24.

Lee, J.-K. and Tansey, M. G. (2013). Microglia isolation from adult mouse brain. *Methods Mol Biol*, 1041:17–23.

Lee, S.-H., Hollingsworth, R., Kwon, H.-Y., Lee, N., and Chung, C. Y. (2012). Erk1/2 is required for adp-induced paxillin phosphorylation at ser(83) and microglia chemotaxis. *Glia*, 60(9):1366–1377.

Lee, Y., Kim, D., Ryu, J. R., Zhang, Y., Kim, S., Kim, Y., Lee, B., Sun, W., and Han, K. (2017). Phosphorylation of cyfip2, a component of the wave-regulatory complex, regulates dendritic spine density and neurite outgrowth in cultured hippocampal neurons potentially by affecting the complex assembly. *Neuroreport*, 28(12):749–754.

Lehrman, E. K., Wilton, D. K., Litvina, E. Y., Welsh, C. A., Chang, S. T., Frouin, A., Walker, A. J., Heller, M. D., Umemori, H., Chen, C., and Stevens, B. (2018). CD47 protects synapses from excess microglia-mediated pruning during development. *Neuron*, 100(1):120–134.e6.

Lenz, K. M., Nugent, B. M., Haliyur, R., and McCarthy, M. M. (2013). Microglia are essential to masculinization of brain and behavior. *J Neurosci*, 33(7):2761–2772.

Li, X., Han, X., Tu, X., Zhu, D., Feng, Y., Jiang, T., Yang, Y., Qu, J., and Chen, J.-G. (2018). An autism-related, nonsense foxp1 mutant induces autophagy and delays radial migration of the cortical neurons. *Cereb Cortex*.

Li, Y., Du, X.-F., Liu, C.-S., Wen, Z.-L., and Du, J.-L. (2012). Reciprocal regulation between resting microglial dynamics and neuronal activity in vivo. *Dev Cell*, 23(6):1189–1202.

Liang, K. J., Lee, J. E., Wang, Y. D., Ma, W., Fontainhas, A. M., Fariss, R. N., and Wong, W. T. (2009). Regulation of dynamic behavior of retinal microglia by cx3cr1 signaling. *Invest Ophthalmol Vis Sci*, 50(9):4444–4451.

Liao, L., Park, S. K., Xu, T., Vanderklish, P., and Yates, J. R. (2008). Quantitative proteomic analysis of primary neurons reveals diverse changes in synaptic protein content in fmr1 knockout mice. *Proc Natl Acad Sci USA*, 105(40):15281–15286.

Lim, K. B., Bu, W., Goh, W. I., Koh, E., Ong, S. H., Pawson, T., Sudhaharan, T., and Ahmed, S. (2008). The cdc42 effector irsp53 generates filopodia by coupling membrane protrusion with actin dynamics. *J Biol Chem*, 283(29):20454–20472.

Lim, S.-H., Park, E., You, B., Jung, Y., Park, A.-R., Park, S. G., and Lee, J.-R. (2013). Neuronal synapse formation induced by microglia and interleukin 10. *PLoS ONE*, 8(11):e81218.

Linder, S. (2007). The matrix corroded: podosomes and invadopodia in extracellular matrix degradation. *Trends Cell Biol*, 17(3):107–117.

Luo, L., Hensch, T. K., Ackerman, L., Barbel, S., Jan, L. Y., and Jan, Y. N. (1996). Differential effects of the rac gtpase on purkinje cell axons and dendritic trunks and spines. *Nature*, 379(6568):837–840.

Luscher, B., Fuchs, T., and Kilpatrick, C. L. (2011). Gabaa receptor trafficking-mediated plasticity of inhibitory synapses. *Neuron*, 70(3):385–409.

Machacek, M., Hodgson, L., Welch, C., Elliott, H., Pertz, O., Nalbant, P., Abell, A., Johnson, G. L., Hahn, K. M., and Danuser, G. (2009). Coordination of rho gtpase activities during cell protrusion. *Nature*, 461(7260):99–103.

Machesky, L. M., Atkinson, S. J., Ampe, C., Vandekerckhove, J., and Pollard, T. D. (1994). Purification of a cortical complex containing two unconventional actins from acanthamoeba by affinity chromatography on profilin-agarose. *J Cell Biol*, 127(1):107–115.

Madry, C., Arancibia-Cárcamo, I. L., Kyrargyri, V., Chan, V. T. T., Hamilton, N. B., and Attwell, D. (2018a). Effects of the ecto-atpase apyrase on microglial ramification and surveillance reflect cell depolarization, not atp depletion. *Proc Natl Acad Sci USA*, 115(7):E1608–E1617.

Madry, C. and Attwell, D. (2015). Receptors, ion channels, and signaling mechanisms underlying microglial dynamics. *J Biol Chem*, 290(20):12443–12450.

Madry, C., Kyrargyri, V., Arancibia-Cárcamo, I. L., Jolivet, R., Kohsaka, S., Bryan, R. M., and Attwell, D. (2018b). Microglial ramification, surveillance, and interleukin-1thik-1. *Neuron*, 97(2):299–312.e6.

Marini, C., Cecconi, A., Contini, E., Pantaleo, M., Metitieri, T., Guarducci, S., Giglio, S., Guerrini, R., and Genuardi, M. (2013). Clinical and genetic study of a family with a paternally inherited 15q11-q13 duplication. *Am J Med Genet A*, 161A(6):1459–1464.

Marshall, C. R., Howrigan, D. P., Merico, D., Thiruvahindrapuram, B., Wu, W., Greer, D. S., Antaki, D., Shetty, A., Holmans, P. A., Pinto, D., Gujral, M., Brandler, W. M., Malhotra, D., Wang, Z., Fajarado, K. V. F., Maile, M. S., Ripke, S., Agartz, I., Albus, M., Alexander, M., Amin, F., Atkins, J., Bacanu, S. A., Belliveau, R. A., Bergen, S. E., Bertalan, M., Bevilacqua, E., Bigdeli, T. B., Black, D. W., Bruggeman, R., Buccola, N. G., Buckner, R. L., Bulik-Sullivan, B., Byerley, W., Cahn, W., Cai, G., Cairns, M. J., Campion, D., Cantor, R. M., Carr, V. J., Carrera, N., Catts, S. V., Chambert, K. D., Cheng, W., Cloninger, C. R., Cohen, D., Cormican, P., Craddock, N., Crespo-Facorro, B., Crowley, J. J., Curtis, D., Davidson, M., Davis, K. L., Degenhardt, F., Del Favero, J., DeLisi, L. E., Dikeos, D., Dinan, T., Djurovic, S., Donohoe, G., Drapeau, E., Duan, J., Dudbridge, F., Eichhammer, P., Eriksson, J., Escott-Price, V., Essioux, L., Fanous, A. H., Farh, K.-H., Farrell, M. S., Frank, J., Franke, L., Freedman, R., Freimer, N. B., Friedman, J. I., Forstner, A. J., Fromer, M., Genovese, G., Georgieva, L., Gershon, E. S., Giegling, I., Giusti-Rodríguez, P., Godard, S., Goldstein, J. I., Gratten, J., de Haan, L., Hamshere, M. L., Hansen, M., Hansen, T., Haroutunian, V., Hartmann, A. M., Henskens, F. A., Herms, S., Hirschhorn, J. N., Hoffmann, P., Hofman, A., Huang, H., Ikeda, M., Joa, I., Kähler, A. K., Kahn, R. S., Kalaydjieva, L., Karjalainen, J., Kavanagh, D., Keller, M. C., Kelly, B. J., Kennedy, J. L., Kim, Y., Knowles,

J. A., Konte, B., Laurent, C., Lee, P., Lee, S. H., Legge, S. E., Lerer, B., Levy, D. L., Liang, K.-Y., Lieberman, J., Lönnqvist, J., Loughland, C. M., Magnusson, P. K. E., Maher, B. S., Maier, W., Mallet, J., Mattheisen, M., Mattingsdal, M., McCarley, R. W., McDonald, C., McIntosh, A. M., Meier, S., Meijer, C. J., Melle, I., Mesholam-Gately, R. I., Metspalu, A., Michie, P. T., Milani, L., Milanova, V., Mokrab, Y., Morris, D. W., Müller-Myhsok, B., Murphy, K. C., Murray, R. M., Myin-Germeys, I., Nenadic, I., Nertney, D. A., Nestadt, G., Nicodemus, K. K., Nisenbaum, L., Nordin, A., O'Callaghan, E., O'Dushlaine, C., Oh, S.-Y., Olincy, A., Olsen, L., O'Neill, F. A., van Os, J., Pantelis, C., Papadimitriou, G. N., Parkhomenko, E., Pato, M. T., Paunio, T., Psychosis Endophenotypes International Consortium, Perkins, D. O., Pers, T. H., Pietiläinen, O., Pimm, J., Pocklington, A. J., Powell, J., Price, A., Pulver, A. E., Purcell, S. M., Quested, D., Rasmussen, H. B., Reichenberg, A., Reimers, M. A., Richards, A. L., Roffman, J. L., Roussos, P., Ruderfer, D. M., Salomaa, V., Sanders, A. R., Savitz, A., Schall, U., Schulze, T. G., Schwab, S. G., Scolnick, E. M., Scott, R. J., Seidman, L. J., Shi, J., Silverman, J. M., Smoller, J. W., Söderman, E., Spencer, C. C. A., Stahl, E. A., Strengman, E., Strohmaier, J., Stroup, T. S., Suvisaari, J., Svrakic, D. M., Szatkiewicz, J. P., Thirumalai, S., Tooney, P. A., Veijola, J., Visscher, P. M., Waddington, J., Walsh, D., Webb, B. T., Weiser, M., Wildenauer, D. B., Williams, N. M., Williams, S., Witt, S. H., Wolen, A. R., Wormley, B. K., Wray, N. R., Wu, J. Q., Zai, C. C., Adolfsson, R., Andreassen, O. A., Blackwood, D. H. R., Bramon, E., Buxbaum, J. D., Cichon, S., Collier, D. A., Corvin, A., Daly, M. J., Darvasi, A., Domenici, E., Esko, T., Gejman, P. V., Gill, M., Gurling, H., Hultman, C. M., Iwata, N., Jablensky, A. V., Jönsson, E. G., Kendler, K. S., Kirov, G., Knight, J., Levinson, D. F., Li, Q. S., McCarroll, S. A., McQuillin, A., Moran, J. L., Mowry, B. J., Nöthen, M. M., Ophoff, R. A., Owen, M. J., Palotie, A., Pato, C. N., Petryshen, T. L., Posthuma, D., Rietschel, M., Riley, B. P., Rujescu, D., Sklar, P., St Clair, D., Walters, J. T. R., Werge, T., Sullivan, P. F., O'Donovan, M. C., Scherer, S. W., Neale, B. M., Sebat, J., CNV, and Schizophrenia Working Groups of the Psychiatric Genomics Consortium (2017). Contribution of copy number variants to schizophrenia from a genome-wide study of 41,321 subjects. *Nat Genet*, 49(1):27–35.

Mass, R. L., Zeller, R., Woychik, R. P., Vogt, T. F., and Leder, P. (1990). Disruption of formin-encoding transcripts in two mutant limb deformity alleles. *Nature*, 346(6287):853–855.

May, R. C., Caron, E., Hall, A., and Machesky, L. M. (2000). Involvement of the arp2/3 complex in phagocytosis mediated by fcgammar or cr3. *Nat Cell Biol*, 2(4):246–248.

Meguid, N., Fahim, C., Yoon, U., Nashaat, N. H., Ibrahim, A. S., Mancini-Marie, A., Brandner, C., and Evans, A. C. (2010). Brain morphology in autism and fragile x syndrome correlates with social iq: first report from the canadian-swiss-egyptian neurodevelopmental study. *J Child Neurol*, 25(5):599–608.

Mei, L. and Xiong, W.-C. (2008). Neuregulin 1 in neural development, synaptic plasticity and schizophrenia. *Nat Rev Neurosci*, 9(6):437–452.

Mendoza, M. C. (2013). Phosphoregulation of the wave regulatory complex and signal integration. *Semin Cell Dev Biol*, 24(4):272–279.

Miki, H., Yamaguchi, H., Suetsugu, S., and Takenawa, T. (2000). Irsp53 is an essential intermediate between rac and wave in the regulation of membrane ruffling. *Nature*, 408(6813):732–735.

Miller, A. M. and Stella, N. (2009). Microglial cell migration stimulated by atp and c5a involve distinct molecular mechanisms: quantification of migration by a novel near-infrared method. *Glia*, 57(8):875–883.

Milner, K. M., Craig, E. E., Thompson, R. J., Veltman, M. W. M., Thomas, N. S., Roberts, S., Bellamy, M., Curran, S. R., Sporikou, C. M. J., and Bolton, P. F. (2005). Prader-willi syndrome: intellectual abilities and behavioural features by genetic subtype. *J Child Psychol Psychiatry*, 46(10):1089–1096.

Mitra, S. K., Hanson, D. A., and Schlaepfer, D. D. (2005). Focal adhesion kinase: in command and control of cell motility. *Nat Rev Mol Cell Biol*, 6(1):56–68.

Miyamoto, A., Wake, H., Ishikawa, A. W., Eto, K., Shibata, K., Murakoshi, H., Koizumi, S., Moorhouse, A. J., Yoshimura, Y., and Nabekura, J. (2016). Microglia contact induces synapse formation in developing somatosensory cortex. *Nat Commun*, 7:12540.

Molumby, M. J., Anderson, R. M., Newbold, D. J., Koblesky, N. K., Garrett, A. M., Schreiner, D., Radley, J. J., and Weiner, J. A. (2017). \gamma-protocadherins interact with neuroligin-1 and negatively regulate dendritic spine morphogenesis. *Cell Rep*, 18(11):2702–2714.

Molumby, M. J., Keeler, A. B., and Weiner, J. A. (2016). Homophilic protocadherin cell-cell interactions promote dendrite complexity. *Cell Rep*, 15(5):1037–1050.

Monroy, B. Y., Sawyer, D. L., Ackermann, B. E., Borden, M. M., Tan, T. C., and Ori-McKenney, K. M. (2018). Competition between microtubule-associated proteins directs motor transport. *Nat Commun*, 9(1):1487.

Moraes, L., Zanchin, N. I. T., and Cerutti, J. M. (2017). Abi3, a component of the wave2 complex, is potentially regulated by pi3k/akt pathway. *Oncotarget*, 8(40):67769–67781.

Mostowy, S. and Cossart, P. (2012). Septins: the fourth component of the cytoskeleton. *Nat Rev Mol Cell Biol*, 13(3):183–194.

Moyer, C. E., Shelton, M. A., and Sweet, R. A. (2015). Dendritic spine alterations in schizophrenia. *Neurosci Lett*, 601:46–53.

Muhle, R., Trentacoste, S. V., and Rapin, I. (2004). The genetics of autism. *Pediatrics*, 113(5):e472–86.

Mukaetova-Ladinska, E. B., Arnold, H., Jaros, E., Perry, R., and Perry, E. (2004). Depletion of map2 expression and laminar cytoarchitectonic changes in dorsolateral prefrontal cortex in adult autistic individuals. *Neuropathol Appl Neurobiol*, 30(6):615–623.

Mukai, J., Tamura, M., Fénelon, K., Rosen, A. M., Spellman, T. J., Kang, R., MacDermott, A. B., Karayiorgou, M., Gordon, J. A., and Gogos, J. A. (2015). Molecular substrates of altered axonal growth and brain connectivity in a mouse model of schizophrenia. *Neuron*, 86(3):680–695.

Mullins, R. D., Heuser, J. A., and Pollard, T. D. (1998). The interaction of arp2/3 complex with actin: nucleation, high affinity pointed end capping, and formation of branching networks of filaments. *Proc Natl Acad Sci USA*, 95(11):6181–6186.

Murphy, D. A. and Courtneidge, S. A. (2011). The 'ins' and 'outs' of podosomes and invadopodia: characteristics, formation and function. *Nat Rev Mol Cell Biol*, 12(7):413–426.

Nakajima, K., Yin, X., Takei, Y., Seog, D.-H., Homma, N., and Hirokawa, N. (2012). Molecular motor kif5a is essential for gaba(a) receptor transport, and kif5a deletion causes epilepsy. *Neuron*, 76(5):945–961.

Nakashima, M., Kato, M., Aoto, K., Shiina, M., Belal, H., Mukaida, S., Kumada, S., Sato, A., Zerem, A., Lerman-Sagie, T., Lev, D., Leong, H. Y., Tsurusaki, Y., Mizuguchi, T., Miyatake, S., Miyake, N., Ogata, K., Saitsu, H., and Matsumoto, N. (2018). De novo hotspot variants in cyfip2 cause early-onset epileptic encephalopathy. *Ann Neurol*, 83(4):794–806.

Napoli, I., Mercaldo, V., Boyl, P. P., Eleuteri, B., Zalfa, F., de Rubeis, S., Di Marino, D., Mohr, E., Massimi, M., Falconi, M., Witke, W., Costa-Mattioli, M., Sonenberg, N., Achsel, T., and Bagni, C. (2008). The fragile x syndrome protein represses activity-dependent translation through cyfip1, a new 4e-bp. *Cell*, 134(6):1042–1054.

Nebel, R. A., Zhao, D., Pedrosa, E., Kirschen, J., Lachman, H. M., Zheng, D., and Abrahams, B. S. (2016). Reduced cyfip1 in human neural progenitors results in dysregulation of schizophrenia and epilepsy gene networks. *PLoS ONE*, 11(1):e0148039.

Needleman, L. A. and McAllister, A. K. (2012). The major histocompatibility complex and autism spectrum disorder. *Dev Neurobiol*, 72(10):1288–1301.

Neniskyte, U. and Gross, C. T. (2017). Errant gardeners: glial-cell-dependent synaptic pruning and neurodevelopmental disorders. *Nat Rev Neurosci*, 18(11):658–670.

Nezami, A., Poy, F., Toms, A., Zheng, W., and Eck, M. J. (2010). Crystal structure of a complex between amino and carboxy terminal fragments of mdia1: insights into autoinhibition of diaphanous-related formins. *PLoS ONE*, 5(9).

Nicolas, M., Wolfer, A., Raj, K., Kummer, J. A., Mill, P., van Noort, M., Hui, C.-c., Clevers, H., Dotto, G. P., and Radtke, F. (2003). Notch1 functions as a tumor suppressor in mouse skin. *Nat Genet*, 33(3):416–421.

Nimmerjahn, A., Kirchhoff, F., and Helmchen, F. (2005). Resting microglial cells are highly dynamic surveillants of brain parenchyma in vivo. *Science*, 308(5726):1314–1318.

Nishimura, Y., Martin, C. L., Vazquez-Lopez, A., Spence, S. J., Alvarez-Retuerto, A. I., Sigman, M., Steindler, C., Pellegrini, S., Schanen, N. C., Warren, S. T., and Geschwind, D. H. (2007). Genome-wide expression profiling of lymphoblastoid cell lines distinguishes different forms of autism and reveals shared pathways. *Hum Mol Genet*, 16(14):1682–1698.

Nithianandam, V. and Chien, C.-T. (2018). Actin blobs prefigure dendrite branching sites. *J Cell Biol*, 217(10):3731–3746.

Noroozi, R., Omrani, M. D., Sayad, A., Taheri, M., and Ghafouri-Fard, S. (2018). Cytoplasmic fmrp interacting protein 1/2 (cyfip1/2) expression analysis in autism. *Metab Brain Dis*.

Oguro-Ando, A., Rosensweig, C., Herman, E., Nishimura, Y., Werling, D., Bill, B. R., Berg, J. M., Gao, F., Coppola, G., Abrahams, B. S., and Geschwind, D. H. (2015). Increased cyfip1 dosage alters cellular and dendritic morphology and dysregulates mtor. *Mol Psychiatry*, 20(9):1069–1078.

Ohsawa, K., Irino, Y., Nakamura, Y., Akazawa, C., Inoue, K., and Kohsaka, S. (2007). Involvement of p2x4 and p2y12 receptors in atp-induced microglial chemotaxis. *Glia*, 55(6):604–616.

Ohsawa, K., Irino, Y., Sanagi, T., Nakamura, Y., Suzuki, E., Inoue, K., and Kohsaka, S. (2010). P2y12 receptor-mediated integrin-beta1 activation regulates microglial process extension induced by atp. *Glia*, 58(7):790–801.

Oikawa, T., Yamaguchi, H., Itoh, T., Kato, M., Ijuin, T., Yamazaki, D., Suetsugu, S., and Takenawa, T. (2004). Ptdins(3,4,5)p3 binding is necessary for wave2-induced formation of lamellipodia. *Nat Cell Biol*, 6(5):420–426.

Okamoto, K.-I., Nagai, T., Miyawaki, A., and Hayashi, Y. (2004). Rapid and persistent modulation of actin dynamics regulates postsynaptic reorganization underlying bidirectional plasticity. *Nat Neurosci*, 7(10):1104–1112.

Pagani, F., Paolicelli, R. C., Murana, E., Cortese, B., Di Angelantonio, S., Zurolo, E., Guiducci, E., Ferreira, T. A., Garofalo, S., Catalano, M., D'Alessandro, G., Porzia, A., Peruzzi, G., Mainiero, F., Limatola, C., Gross, C. T., and Ragozzino, D. (2015). Defective microglial development in the hippocampus of cx3cr1 deficient mice. *Front Cell Neurosci*, 9:111.

Palazzo, A. F., Cook, T. A., Alberts, A. S., and Gundersen, G. G. (2001). mDia mediates rho-regulated formation and orientation of stable microtubules. *Nat Cell Biol*, 3(8):723–729.

Paluch, E. K. and Raz, E. (2013). The role and regulation of blebs in cell migration. *Curr Opin Cell Biol*, 25(5):582–590.

Paolicelli, R. C., Bisht, K., and Tremblay, M.-È. (2014). Fractalkine regulation of microglial physiology and consequences on the brain and behavior. *Front Cell Neurosci*, 8:129.

Paolicelli, R. C., Bolasco, G., Pagani, F., Maggi, L., Scianni, M., Panzanelli, P., Giustetto, M., Ferreira, T. A., Guiducci, E., Dumas, L., Ragozzino, D., and Gross, C. T. (2011). Synaptic pruning by microglia is necessary for normal brain development. *Science*, 333(6048):1456–1458.

Papadopoulos, T., Korte, M., Eulenburg, V., Kubota, H., Retiounskaia, M., Harvey, R. J., Harvey, K., O'Sullivan, G. A., Laube, B., Hülsmann, S., Geiger, J. R. P., and Betz, H. (2007). Impaired gabaergic transmission and altered hippocampal synaptic plasticity in collybistin-deficient mice. *EMBO J*, 26(17):3888–3899.

Park, H., Chan, M. M., and Iritani, B. M. (2010). Hem-1: putting the "wave" into actin polymerization during an immune response. *FEBS Lett*, 584(24):4923–4932.

Parkhurst, C. N., Yang, G., Ninan, I., Savas, J. N., Yates, J. R., Lafaille, J. J., Hempstead, B. L., Littman, D. R., and Gan, W.-B. (2013). Microglia promote learning-dependent synapse formation through brain-derived neurotrophic factor. *Cell*, 155(7):1596–1609.

Pathania, M., Davenport, E. C., Muir, J., Sheehan, D. F., López-Doménech, G., and Kittler, J. T. (2014). The autism and schizophrenia associated gene cyfip1 is critical for the maintenance of dendritic complexity and the stabilization of mature spines. *Transl Psychiatry*, 4:e374.

Penagarikano, O., Mulle, J. G., and Warren, S. T. (2007). The pathophysiology of fragile x syndrome. *Annu Rev Genomics Hum Genet*, 8:109–129.

Peng, H., Bria, A., Zhou, Z., Iannello, G., and Long, F. (2014). Extensible visualization and analysis for multidimensional images using vaa3d. *Nat Protoc*, 9(1):193–208.

Peng, J., Wallar, B. J., Flanders, A., Swiatek, P. J., and Alberts, A. S. (2003). Disruption of the diaphanous-related formin drf1 gene encoding mdia1 reveals a role for drf3 as an effector for cdc42. *Curr Biol*, 13(7):534–545.

Penzes, P., Cahill, M. E., Jones, K. A., VanLeeuwen, J.-E., and Woolfrey, K. M. (2011). Dendritic spine pathology in neuropsychiatric disorders. *Nat Neurosci*, 14(3):285–293.

Peris, L., Wagenbach, M., Lafanechère, L., Brocard, J., Moore, A. T., Kozielski, F., Job, D., Wordeman, L., and Andrieux, A. (2009). Motor-dependent microtubule disassembly driven by tubulin tyrosination. *J Cell Biol*, 185(7):1159–1166.

Peykov, S., Berkel, S., Schoen, M., Weiss, K., Degenhardt, F., Strohmaier, J., Weiss, B., Proepper, C., Schratt, G., Nöthen, M. M., Boeckers, T. M., Rietschel, M., and Rappold, G. A. (2015). Identification and functional characterization of rare shank2 variants in schizophrenia. *Mol Psychiatry*, 20(12).

Pfeiffer, T., Avignone, E., and Nägerl, U. V. (2016). Induction of hippocampal long-term potentiation increases the morphological dynamics of microglial processes and prolongs their contacts with dendritic spines. *Sci Rep*, 6(1):32422.

Pinto, D., Delaby, E., Merico, D., Barbosa, M., Merikangas, A., Klei, L., Thiruvahindrapuram, B., Xu, X., Ziman, R., Wang, Z., Vorstman, J. A. S., Thompson, A., Regan, R., Pilorge, M., Pellecchia, G., Pagnamenta, A. T., Oliveira, B., Marshall, C. R., Magalhaes, T. R., Lowe, J. K., Howe, J. L., Griswold, A. J., Gilbert, J., Duketis, E., Dombroski, B. A., de Jonge, M. V., Cuccaro, M., Crawford, E. L., Correia, C. T., Conroy, J., Conceição, I. C., Chiocchetti, A. G., Casey, J. P., Cai, G., Cabrol, C., Bolshakova, N., Bacchelli, E., Anney, R., Gallinger, S., Cotterchio, M., Casey, G., Zwaigenbaum, L., Wittemeyer, K., Wing, K., Wallace, S., van Engeland, H., Tryfon, A., Thomson, S., Soorya, L., Rogé, B., Roberts, W., Poustka, F., Mouga, S., Minshew, N., McInnes, L. A., McGrew, S. G., Lord, C., Leboyer, M., Le Couteur, A. S., Kolevzon, A., Jiménez González, P., Jacob, S., Holt, R., Guter, S., Green, J., Green, A., Gillberg, C., Fernandez, B. A., Duque, F.,

Delorme, R., Dawson, G., Chaste, P., Café, C., Brennan, S., Bourgeron, T., Bolton, P. F., Bölte, S., Bernier, R., Baird, G., Bailey, A. J., Anagnostou, E., Almeida, J., Wijsman, E. M., Vieland, V. J., Vicente, A. M., Schellenberg, G. D., Pericak-Vance, M., Paterson, A. D., Parr, J. R., Oliveira, G., Nurnberger, J. I., Monaco, A. P., Maestrini, E., Klauck, S. M., Hakonarson, H., Haines, J. L., Geschwind, D. H., Freitag, C. M., Folstein, S. E., Ennis, S., Coon, H., Battaglia, A., Szatmari, P., Sutcliffe, J. S., Hallmayer, J., Gill, M., Cook, E. H., Buxbaum, J. D., Devlin, B., Gallagher, L., Betancur, C., and Scherer, S. W. (2014). Convergence of genes and cellular pathways dysregulated in autism spectrum disorders. *Am J Hum Genet*, 94(5):677–694.

Pinyol, R., Haeckel, A., Ritter, A., Qualmann, B., and Kessels, M. M. (2007). Regulation of n-wasp and the arp2/3 complex by abp1 controls neuronal morphology. *PLoS ONE*, 2(5):e400.

Pittman, A. J., Gaynes, J. A., and Chien, C.-B. (2010). nev (cyfip2) is required for retinal lamination and axon guidance in the zebrafish retinotectal system. *Dev Biol*, 344(2):784–794.

Pollard, T. D. and Cooper, J. A. (2009). Actin, a central player in cell shape and movement. *Science*, 326(5957):1208–1212.

Pont-Lezica, L., Beumer, W., Colasse, S., Drexhage, H., Versnel, M., and Bessis, A. (2014). Microglia shape corpus callosum axon tract fasciculation: functional impact of prenatal inflammation. *Eur J Neurosci*, 39(10):1551–1557.

Portera-Cailliau, C., Pan, D. T., and Yuste, R. (2003). Activity-regulated dynamic behavior of early dendritic protrusions: evidence for different types of dendritic filopodia. *J Neurosci*, 23(18):7129–7142.

Potkin, S. G., Turner, J. A., Guffanti, G., Lakatos, A., Fallon, J. H., Nguyen, D. D., Mathalon, D., Ford, J., Lauriello, J., Macciardi, F., and FBIRN (2009). A genome-wide association study of schizophrenia using brain activation as a quantitative phenotype. *Schizophr Bull*, 35(1):96–108.

Pozner, A., Xu, B., Palumbos, S., Gee, J. M., Tvrdik, P., and Capecchi, M. R. (2015). Intracellular calcium dynamics in cortical microglia responding to focal laser injury in the pc::g5-tdt reporter mouse. *Front Mol Neurosci*, 8:12.

Presumey, J., Bialas, A. R., and Carroll, M. C. (2017). Complement system in neural synapse elimination in development and disease. *Adv Immunol*, 135:53–79.

Prinz, M. and Priller, J. (2014). Microglia and brain macrophages in the molecular age: from origin to neuropsychiatric disease. *Nat Rev Neurosci*, 15(5):300–312.

Purcell, S. M., Moran, J. L., Fromer, M., Ruderfer, D., Solovieff, N., Roussos, P., O'Dushlaine, C., Chambert, K., Bergen, S. E., Kähler, A., Duncan, L., Stahl, E., Genovese, G., Fernández, E., Collins, M. O., Komiyama, N. H., Choudhary, J. S., Magnusson, P. K. E., Banks, E., Shakir, K., Garimella, K., Fennell, T., DePristo, M., Grant, S. G. N., Haggarty, S. J., Gabriel, S., Scolnick, E. M., Lander, E. S., Hultman, C. M., Sullivan, P. F., McCarroll, S. A., and Sklar, P. (2014). A polygenic burden of rare disruptive mutations in schizophrenia. *Nature*, 506(7487):185–190.

Pyronneau, A., He, Q., Hwang, J.-Y., Porch, M., Contractor, A., and Zukin, R. S. (2017). Aberrant rac1-cofilin signaling mediates defects in dendritic spines, synaptic function, and sensory perception in fragile x syndrome. *Sci Signal*, 10(504).

Quinlan, M. E., Heuser, J. E., Kerkhoff, E., and Mullins, R. D. (2005). Drosophila spire is an actin nucleation factor. *Nature*, 433(7024):382–388.

Radtke, F. A., Chapman, G., Hall, J., and Syed, Y. A. (2017). Modulating neuroinflammation to treat neuropsychiatric disorders. *Biomed Res Int*, 2017:5071786.

Radyushkin, K., Hammerschmidt, K., Boretius, S., Varoqueaux, F., El-Kordi, A., Ronnenberg, A., Winter, D., Frahm, J., Fischer, J., Brose, N., and Ehrenreich, H. (2009). Neuroligin-3-deficient mice: model of a monogenic heritable form of autism with an olfactory deficit. *Genes Brain Behav*, 8(4):416–425.

Rakeman, A. S. and Anderson, K. V. (2006). Axis specification and morphogenesis in the mouse embryo require nap1, a regulator of wave-mediated actin branching. *Development*, 133(16):3075–3083.

Rangaraju, V., Tom Dieck, S., and Schuman, E. M. (2017). Local translation in neuronal compartments: how local is local? *EMBO Rep*, 18(5):693–711.

Rashid, M., Belmont, J., Carpenter, D., Turner, C. E., and Olson, E. C. (2017). Neural-specific deletion of the focal adhesion adaptor protein paxillin slows migration speed and delays cortical layer formation. *Development*, 144(21):4002–4014.

Raymond, G. V., Bauman, M. L., and Kemper, T. L. (1996). Hippocampus in autism: a golgi analysis. *Acta Neuropathol*, 91(1):117–119.

Rees, E., O\textquoterightDonovan, M. C., and Owen, M. J. (2015). Genetics of schizophrenia. *Curr Opin Behav Sci*, 2:8–14.

Rees, E., Walters, J. T. R., Georgieva, L., Isles, A. R., Chambert, K. D., Richards, A. L., Mahoney-Davies, G., Legge, S. E., Moran, J. L., McCarroll, S. A., O'Donovan, M. C., Owen, M. J., and Kirov, G. (2014). Analysis of copy number variations at 15 schizophrenia-associated loci. *Br J Psychiatry*, 204(2):108–114.

Réu, P., Khosravi, A., Bernard, S., Mold, J. E., Salehpour, M., Alkass, K., Perl, S., Tisdale, J., Possnert, G., Druid, H., and Frisén, J. (2017). The lifespan and turnover of microglia in the human brain. *Cell Reports*.

Richter, J. D. and Sonenberg, N. (2005). Regulation of cap-dependent translation by eIF4E inhibitory proteins. *Nature*, 433(7025):477–480.

Ridley, A. J. (2011). Life at the leading edge. *Cell*, 145(7):1012–1022.

Risher, W. C., Ustunkaya, T., Singh Alvarado, J., and Eroglu, C. (2014). Rapid golgi analysis method for efficient and unbiased classification of dendritic spines. *PLoS ONE*, 9(9):e107591.

Roh-Johnson, M. and Goldstein, B. (2009). In vivo roles for arp2/3 in cortical actin organization during c. elegans gastrulation. *J Cell Sci*, 122(Pt 21):3983–3993.

Rothwell, P. E., Fuccillo, M. V., Maxeiner, S., Hayton, S. J., Gokce, O., Lim, B. K., Fowler, S. C., Malenka, R. C., and Südhof, T. C. (2014). Autism-associated neuroligin-3 mutations commonly impair striatal circuits to boost repetitive behaviors. *Cell*, 158(1):198–212.

Rotty, J. D., Brighton, H. E., Craig, S. L., Asokan, S. B., Cheng, N., Ting, J. P., and Bear, J. E. (2017). Arp2/3 complex is required for macrophage integrin functions but is dispensable for fcr phagocytosis and in vivo motility. *Dev Cell*, 42(5):498–513.e6.

Rougerie, P., Miskolci, V., and Cox, D. (2013). Generation of membrane structures during phagocytosis and chemotaxis of macrophages: role and regulation of the actin cytoskeleton. *Immunol Rev*, 256(1):222–239.

Rouiller, I., Xu, X.-P., Amann, K. J., Egile, C., Nickell, S., Nicastro, D., Li, R., Pollard, T. D., Volkmann, N., and Hanein, D. (2008). The structural basis of actin filament branching by the arp2/3 complex. *J Cell Biol*, 180(5):887–895.

Roy, B. C., Kakinuma, N., and Kiyama, R. (2009). Kank attenuates actin remodeling by preventing interaction between irsp53 and rac1. *J Cell Biol*, 184(2):253–267.

Rudolph, U. and Möhler, H. (2014). Gabaa receptor subtypes: Therapeutic potential in down syndrome, affective disorders, schizophrenia, and autism. *Annu Rev Pharmacol Toxicol*, 54:483–507.

Russell, T. A., Blizinsky, K. D., Cobia, D. J., Cahill, M. E., Xie, Z., Sweet, R. A., Duan, J., Gejman, P. V., Wang, L., Csernansky, J. G., and Penzes, P. (2014). A sequence variant in human kalrn impairs protein function and coincides with reduced cortical thickness. *Nat Commun*, 5:4858.

Saci, A., Cantley, L. C., and Carpenter, C. L. (2011). Rac1 regulates the activity of mTORC1 and mTORC2 and controls cellular size. *Mol Cell*, 42(1):50–61.

Saetre, P., Emilsson, L., Axelsson, E., Kreuger, J., Lindholm, E., and Jazin, E. (2007). Inflammation-related genes up-regulated in schizophrenia brains. *BMC Psychiatry*, 7:46.

Sala, C. and Segal, M. (2014). Dendritic spines: the locus of structural and functional plasticity. *Physiol Rev*, 94(1):141–188.

Salter, M. W. and Stevens, B. (2017). Microglia emerge as central players in brain disease. *Nat Med*, 23(9):1018–1027.

San Miguel-Ruiz, J. E. and Letourneau, P. C. (2014). The role of arp2/3 in growth cone actin dynamics and guidance is substrate dependent. *J Neurosci*, 34(17):5895–5908.

Sarkar, K., Sadhukhan, S., Han, S.-S., and Vyas, Y. M. (2015). SUMOylation-disrupting WAS mutation converts WASp from a transcriptional activator to a repressor of nf-kappab response genes in t cells. *Blood*, 126(14):1670–1682.

Satoh, J.-I., Kino, Y., Yanaizu, M., Tosaki, Y., Sakai, K., Ishida, T., and Saito, Y. (2017). Microglia express abi3 in the brains of alzheimer's disease and nasu-hakola disease. *Intractable Rare Dis Res*, 6(4):262–268.

Sauer, B. (1998). Inducible gene targeting in mice using the cre/lox system. *Methods*, 14(4):381–392.

Saunders, A., Macosko, E. Z., Wysoker, A., Goldman, M., Krienen, F. M., de Rivera, H., Bien, E., Baum, M., Bortolin, L., Wang, S., Goeva, A., Nemesh, J., Kamitaki, N., Brumbaugh, S., Kulp, D., and McCarroll, S. A. (2018). Molecular diversity and specializations among the cells of the adult mouse brain. *Cell*, 174(4):1015–1030.e16.

Sayad, A., Ranjbaran, F., Ghafouri-Fard, S., Arsang-Jang, S., and Taheri, M. (2018). Expression analysis of cyfip1 and camkk2 genes in the blood of epileptic and schizophrenic patients. *J Mol Neurosci*, 65(3):336–342.

Schafer, D. P., Lehrman, E. K., Kautzman, A. G., Koyama, R., Mardinly, A. R., Yamasaki, R., Ransohoff, R. M., Greenberg, M. E., Barres, B. A., and Stevens, B. (2012). Microglia sculpt postnatal neural circuits in an activity and complement-dependent manner. *Neuron*, 74(4):691–705.

Schenck, A., Bardoni, B., Langmann, C., Harden, N., Mandel, J. L., and Giangrande, A. (2003). Cyfip/sra-1 controls neuronal connectivity in drosophila and links the rac1 gtpase pathway to the fragile x protein. *Neuron*, 38(6):887–898.

Schenck, A., Bardoni, B., Moro, A., Bagni, C., and Mandel, J. L. (2001). A highly conserved protein family interacting with the fragile x mental retardation protein (fmrp) and displaying selective interactions with fmrp-related proteins fxr1p and fxr2p. *Proc Natl Acad Sci USA*, 98(15):8844–8849.

Schenck, A., Qurashi, A., Carrera, P., Bardoni, B., Diebold, C., Schejter, E., Mandel, J.-L., and Giangrande, A. (2004). Wave/scar, a multifunctional complex coordinating different aspects of neuronal connectivity. *Dev Biol*, 274(2):260–270.

Schirenbeck, A., Arasada, R., Bretschneider, T., Stradal, T. E. B., Schleicher, M., and Faix, J. (2006). The bundling activity of vasodilator-stimulated phosphoprotein is required for filopodium formation. *Proc. Natl. Acad. Sci. USA*, 103(20):7694–7699.

Schizophrenia Working Group of the Psychiatric Genomics Consortium (2014). Biological insights from 108 schizophrenia-associated genetic loci. *Nature*, 511(7510):421–427.

Sekar, A., Bialas, A. R., de Rivera, H., Davis, A., Hammond, T. R., Kamitaki, N., Tooley, K., Presumey, J., Baum, M., van Doren, V., Genovese, G., Rose, S. A., Handsaker, R. E., Schizophrenia Working Group of the Psychiatric Genomics Consortium, Daly, M. J., Carroll, M. C., Stevens, B., and McCarroll, S. A. (2016). Schizophrenia risk from complex variation of complement component 4. *Nature*, 530(7589):177–183.

Sekino, S., Kashiwagi, Y., Kanazawa, H., Takada, K., Baba, T., Sato, S., Inoue, H., Kojima, M., and Tani, K. (2015). The nesh/abi-3-based wave2 complex is functionally distinct from the abi-1-based wave2 complex. *Cell Commun Signal*, 13:41.

Selemon, L. D., Rajkowska, G., and Goldman-Rakic, P. S. (1998). Elevated neuronal density in prefrontal area 46 in brains from schizophrenic patients: application of a three-dimensional, stereologic counting method. *J Comp Neurol*, 392(3):402–412.

Selten, M., van Bokhoven, H., and Nadif Kasri, N. (2018). Inhibitory control of the excitatory/inhibitory balance in psychiatric disorders. *F1000Res*, 7:23.

Sharma, A., Hoeffer, C. A., Takayasu, Y., Miyawaki, T., McBride, S. M., Klann, E., and Zukin, R. S. (2010). Dysregulation of mtor signaling in fragile x syndrome. *J Neurosci*, 30(2):694–702.

Sheng, M. and Kim, E. (2011). The postsynaptic organization of synapses. *Cold Spring Harb Perspect Biol*, 3(12).

Sidani, M., Wessels, D., Mouneimne, G., Ghosh, M., Goswami, S., Sarmiento, C., Wang, W., Kuhl, S., El-Sibai, M., Backer, J. M., Eddy, R., Soll, D., and Condeelis, J. (2007). Cofilin determines the migration behavior and turning frequency of metastatic cancer cells. *J Cell Biol*, 179(4):777–791.

Siddiqui, T. A., Lively, S., Vincent, C., and Schlichter, L. C. (2012). Regulation of podosome formation, microglial migration and invasion by ca(2+)-signaling molecules expressed in podosomes. *J Neuroinflammation*, 9:250.

Sierra, A., Encinas, J. M., Deudero, J. J. P., Chancey, J. H., Enikolopov, G., Overstreet-Wadiche, L. S., Tsirka, S. E., and Maletic-Savatic, M. (2010). Microglia shape adult hippocampal neurogenesis through apoptosis-coupled phagocytosis. *Cell Stem Cell*, 7(4):483–495.

Silva, A. I., Haddon, J. E., Trent, S., Syed, Y. A., Lin, T.-C. E., Patel, Y., Carter, J., Haan, N., Honey, R. C., Humby, T., Assaf, Y., Linden, D. E., Owen, M. J., Hall, J., and Wilkinson, L. (2018). Cyfip1 haploinsufficiency is associated with white matter changes, myelin thinning, reduction of mature oligodendrocytes and behavioural inflexibility:. *BioRxiv*.

Silva, J. M., Ezhkova, E., Silva, J., Heart, S., Castillo, M., Campos, Y., Castro, V., Bonilla, F., Cordon-Cardo, C., Muthuswamy, S. K., Powers, S., Fuchs, E., and Hannon, G. J. (2009). Cyfip1 is a putative invasion suppressor in epithelial cancers. *Cell*, 137(6):1047–1061.

Sims, R., van der Lee, Sven J, Naj, A. C., Bellenguez, C., Badarinarayan, N., Jakobsdottir, J., Kunkle, B. W., Boland, A., Raybould, R., Bis, J. C., Martin, E. R., Grenier-Boley, B., Heilmann-Heimbach, S., Chouraki, V., Kuzma, A. B., Sleegers, K., Vronskaya, M., Ruiz, A., Graham, R. R., Olaso, R., Hoffmann, P., Grove, M. L., Vardarajan, B. N., Hiltunen, M., Nöthen, M. M., White, C. C., Hamilton-Nelson, K. L., Epelbaum, J., Maier, W., Choi, S.-H., Beecham, G. W., Dulary, C., Herms, S., Smith, A. V., Funk, C. C., Derbois, C., Forstner, A. J., Ahmad, S., Li, H., Bacq, D., Harold, D., Satizabal, C. L., Valladares, O., Squassina, A., Thomas, R., Brody, J. A., Qu, L., Sánchez-Juan, P., Morgan, T., Wolters, F. J., Zhao, Y., Garcia, F. S., Denning, N., Fornage, M., Malamon, J., Naranjo, M. C. D., Majounie, E., Mosley, T. H., Dombroski, B., Wallon, D., Lupton, M. K., Dupuis, J., Whitehead, P., Fratiglioni, L., Medway, C., Jian, X., Mukherjee, S., Keller, L., Brown, K., Lin, H., Cantwell, L. B., Panza, F., McGuinness, B., Moreno-Grau, S., Burgess, J. D., Solfrizzi, V., Proitsi, P., Adams, H. H., Allen, M., Seripa, D.,

Pastor, P., Cupples, L. A., Price, N. D., Hannequin, D., Frank-García, A., Levy, D., Chakrabarty, P., Caffarra, P., Giegling, I., Beiser, A. S., Giedraitis, V., Hampel, H., Garcia, M. E., Wang, X., Lannfelt, L., Mecocci, P., Eiriksdottir, G., Crane, P. K., Pasquier, F., Boccardi, V., Henández, I., Barber, R. C., Scherer, M., Tarraga, L., Adams, P. M., Leber, M., Chen, Y., Albert, M. S., Riedel-Heller, S., Emilsson, V., Beekly, D., Braae, A., Schmidt, R., Blacker, D., Masullo, C., Schmidt, H., Doody, R. S., Spalletta, G., Longstreth, W. T., Fairchild, T. J., Bossù, P., Lopez, O. L., Frosch, M. P., Sacchinelli, E., Ghetti, B., Yang, Q., Huebinger, R. M., Jessen, F., Li, S., Kamboh, M. I., Morris, J., Sotolongo-Grau, O., Katz, M. J., Corcoran, C., Dunstan, M., Braddel, A., Thomas, C., Meggy, A., Marshall, R., Gerrish, A., Chapman, J., Aguilar, M., Taylor, S., Hill, M., Fairén, M. D., Hodges, A., Vellas, B., Soininen, H., Kloszewska, I., Daniilidou, M., Uphill, J., Patel, Y., Hughes, J. T., Lord, J., Turton, J., Hartmann, A. M., Cecchetti, R., Fenoglio, C., Serpente, M., Arcaro, M., Caltagirone, C., Orfei, M. D., Ciaramella, A., Pichler, S., Mayhaus, M., Gu, W., Lleó, A., Fortea, J., Blesa, R., Barber, I. S., Brookes, K., Cupidi, C., Maletta, R. G., Carrell, D., Sorbi, S., Moebus, S., Urbano, M., Pilotto, A., Kornhuber, J., Bosco, P., Todd, S., Craig, D., Johnston, J., Gill, M., Lawlor, B., Lynch, A., Fox, N. C., Hardy, J., ARUK Consortium, Albin, R. L., Apostolova, L. G., Arnold, S. E., Asthana, S., Atwood, C. S., Baldwin, C. T., Barnes, L. L., Barral, S., Beach, T. G., Becker, J. T., Bigio, E. H., Bird, T. D., Boeve, B. F., Bowen, J. D., Boxer, A., Burke, J. R., Burns, J. M., Buxbaum, J. D., Cairns, N. J., Cao, C., Carlson, C. S., Carlsson, C. M., Carney, R. M., Carrasquillo, M. M., Carroll, S. L., Diaz, C. C., Chui, H. C., Clark, D. G., Cribbs, D. H., Crocco, E. A., DeCarli, C., Dick, M., Duara, R., Evans, D. A., Faber, K. M., Fallon, K. B., Fardo, D. W., Farlow, M. R., Ferris, S., Foroud, T. M., Galasko, D. R., Gearing, M., Geschwind, D. H., Gilbert, J. R., Graff-Radford, N. R., Green, R. C., Growdon, J. H., Hamilton, R. L., Harrell, L. E., Honig, L. S., Huentelman, M. J., Hulette, C. M., Hyman, B. T., Jarvik, G. P., Abner, E., Jin, L.-W., Jun, G., Karydas, A., Kaye, J. A., Kim, R., Kowall, N. W., Kramer, J. H., LaFerla, F. M., Lah, J. J., Leverenz, J. B., Levey, A. I., Li, G., Lieberman, A. P., Lunetta, K. L., Lyketsos, C. G., Marson, D. C., Martiniuk, F., Mash, D. C., Masliah, E., McCormick, W. C., McCurry, S. M., McDavid, A. N., McKee, A. C., Mesulam, M., Miller, B. L., Miller, C. A., Miller, J. W., Morris, J. C., Murrell, J. R., Myers, A. J., O'Bryant, S., Olichney, J. M., Pankratz, V. S., Parisi, J. E., Paulson, H. L., Perry, W., Peskind, E., Pierce, A., Poon, W. W., Potter, H., Quinn, J. F., Raj, A., Raskind, M., Reisberg, B., Reitz, C., Ringman, J. M., Roberson, E. D., Rogaeva, E., Rosen, H. J., Rosenberg, R. N., Sager, M. A., Saykin, A. J., Schneider, J. A., Schneider, L. S., Seeley, W. W., Smith, A. G., Sonnen, J. A., Spina, S., Stern, R. A., Swerdlow, R. H., Tanzi, R. E., Thornton-Wells, T. A., Trojanowski, J. Q., Troncoso, J. C., van Deerlin, V. M., van Eldik, L. J., Vinters, H. V., Vonsattel, J. P., Weintraub, S., Welsh-Bohmer, K. A., Wilhelmsen, K. C., Williamson, J., Wingo, T. S., Woltjer, R. L., Wright, C. B., Yu, C.-E., Yu, L., Garzia, F., Golamaully, F., Septier, G., Engelborghs, S., Vandenberghe, R., de Deyn, P. P., Fernadez, C. M., Benito, Y. A., Thonberg, H., Forsell, C., Lilius, L., Kinhult-Stählbom, A., Kilander, L., Brundin, R., Concari, L., Helisalmi, S., Koivisto, A. M., Haapasalo, A., Dermecourt, V., Fievet, N., Hanon, O., Dufouil, C., Brice, A., Ritchie, K., Dubois, B., Himali, J. J., Keene, C. D., Tschanz, J., Fitzpatrick, A. L., Kukull (2017). Rare coding variants in plcg2, abi3, and trem2 implicate microglial-mediated innate immunity in alzheimer's disease. *Nat Genet*, 49(9):1373–1384.

Sipe, G. O., Lowery, R. L., Tremblay, M.-È., Kelly, E. A., Lamantia, C. E., and Majewska, A. K. (2016). Microglial p2y12 is necessary for synaptic plasticity in mouse visual cortex. *Nat Commun*, 7:10905.

Smith, K. R., Davenport, E. C., Wei, J., Li, X., Pathania, M., Vaccaro, V., Yan, Z., and Kittler, J. T. (2014). Git1 and gaba(a) receptor synaptic stability and inhibitory neurotransmission. *Cell Rep*, 9(1):298–310.

Snapper, S. B., Takeshima, F., Antón, I., Liu, C. H., Thomas, S. M., Nguyen, D., Dudley, D., Fraser, H., Purich, D., Lopez-Ilasaca, M., Klein, C., Davidson, L., Bronson, R., Mulligan, R. C., Southwick, F., Geha, R., Goldberg, M. B., Rosen, F. S., Hartwig, J. H., and Alt, F. W. (2001). N-wasp deficiency reveals distinct pathways for cell surface projections and microbial actin-based motility. *Nat Cell Biol*, 3(10):897–904.

Soderling, S. H., Guire, E. S., Kaech, S., White, J., Zhang, F., Schutz, K., Langeberg, L. K., Banker, G., Raber, J., and Scott, J. D. (2007). A wave-1 and wrp signaling complex regulates spine density, synaptic plasticity, and memory. *J Neurosci*, 27(2):355–365.

Sossey-Alaoui, K., Li, X., and Cowell, J. K. (2007). c-abl-mediated phosphorylation of wave3 is required for lamellipodia formation and cell migration. *J Biol Chem*, 282(36):26257–26265.

Soto, M. C., Qadota, H., Kasuya, K., Inoue, M., Tsuboi, D., Mello, C. C., and Kaibuchi, K. (2002). The gex-2 and gex-3 proteins are required for tissue morphogenesis and cell migrations in c. elegans. *Genes Dev*, 16(5):620–632.

Sousa, C., Golebiewska, A., Poovathingal, S. K., Kaoma, T., Pires-Afonso, Y., Martina, S., Coowar, D., Azuaje, F., Skupin, A., Balling, R., Biber, K., Niclou, S. P., and Michelucci, A. (2018). Single-cell transcriptomics reveals distinct inflammation-induced microglia signatures. *EMBO Rep*.

Spence, E. F., Kanak, D. J., Carlson, B. R., and Soderling, S. H. (2016). The arp2/3 complex is essential for distinct stages of spine synapse maturation, including synapse unsilencing. *J Neurosci*, 36(37):9696–9709.

Spranger, S., Rommel, B., Jauch, A., Bodammer, R., Mehl, B., and Bullerdiek, J. (2000). Interstitial deletion of 5q33.3q35.1 in a girl with mild mental retardation. *Am. J. Med. Genet.*, 93(2):107–109.

Squarzoni, P., Oller, G., Hoeffel, G., Pont-Lezica, L., Rostaing, P., Low, D., Bessis, A., Ginhoux, F., and Garel, S. (2014). Microglia modulate wiring of the embryonic forebrain. *Cell Rep*, 8(5):1271–1279.

Stefansson, H., Meyer-Lindenberg, A., Steinberg, S., Magnusdottir, B., Morgen, K., Arnarsdottir, S., Bjornsdottir, G., Walters, G. B., Jonsdottir, G. A., Doyle, O. M., Tost, H., Grimm, O., Kristjansdottir, S., Snorrason, H., Davidsdottir, S. R., Gudmundsson, L. J., Jonsson, G. F., Stefansdottir, B., Helgadottir, I., Haraldsson, M., Jonsdottir, B., Thygesen, J. H., Schwarz, A. J., Didriksen, M., Stensb\ol, T. B., Brammer, M., Kapur, S., Halldorsson, J. G., Hreidarsson, S., Saemundsen, E., Sigurdsson, E., and Stefansson, K. (2014). Cnvs conferring risk of autism or schizophrenia affect cognition in controls. *Nature*, 505(7483):361–366.

Stefansson, H., Rujescu, D., Cichon, S., Pietiläinen, O. P. H., Ingason, A., Steinberg, S., Fossdal, R., Sigurdsson, E., Sigmundsson, T., Buizer-Voskamp, J. E., Hansen, T., Jakobsen, K. D., Muglia, P., Francks, C., Matthews, P. M., Gylfason, A., Halldorsson, B. V., Gudbjartsson, D., Thorgeirsson, T. E., Sigurdsson, A., Jonasdottir, A., Jonasdottir, A., Bjornsson, A., Mattiasdottir, S., Blondal, T., Haraldsson, M., Magnusdottir, B. B., Giegling, I., Möller, H.-J., Hartmann, A., Shianna, K. V., Ge, D., Need, A. C., Crombie, C., Fraser, G., Walker, N., Lonnqvist, J., Suvisaari, J., Tuulio-Henriksson, A., Paunio, T., Toulopoulou, T., Bramon, E., Di Forti, M., Murray, R., Ruggeri, M., Vassos, E., Tosato, S., Walshe, M., Li, T., Vasilescu, C., Mühleisen, T. W., Wang, A. G., Ullum, H., Djurovic, S., Melle, I., Olesen, J., Kiemeney, L. A., Franke, B., GROUP, Sabatti, C., Freimer, N. B., Gulcher, J. R., Thorsteinsdottir, U., Kong, A., Andreassen, O. A., Ophoff, R. A., Georgi, A., Rietschel, M., Werge, T., Petursson, H., Goldstein, D. B., Nöthen, M. M., Peltonen, L., Collier, D. A., St Clair, D., and Stefansson, K. (2008). Large recurrent microdeletions associated with schizophrenia. *Nature*, 455(7210):232–236.

Steffen, A., Faix, J., Resch, G. P., Linkner, J., Wehland, J., Small, J. V., Rottner, K., and Stradal, T. E. B. (2006). Filopodia formation in the absence of functional wave- and arp2/3-complexes. *Mol Biol Cell*, 17(6):2581–2591.

Steffen, A., Rottner, K., Ehinger, J., Innocenti, M., Scita, G., Wehland, J., and Stradal, T. E. B. (2004). Sra-1 and nap1 link rac to actin assembly driving lamellipodia formation. *EMBO J*, 23(4):749–759.

Stein, V., House, D. R. C., Bredt, D. S., and Nicoll, R. A. (2003). Postsynaptic density-95 mimics and occludes hippocampal long-term potentiation and enhances long-term depression. *J Neurosci*, 23(13):5503–5506.

Strasser, G. A., Rahim, N. A., VanderWaal, K. E., Gertler, F. B., and Lanier, L. M. (2004). Arp2/3 is a negative regulator of growth cone translocation. *Neuron*, 43(1):81–94.

Streit, W. J., Graeber, M. B., and Kreutzberg, G. W. (1988). Functional plasticity of microglia: a review. *Glia*, 1(5):301–307.

Stuart, M. J., Corrigan, F., and Baune, B. T. (2014). Knockout of cxcr5 increases the population of immature neural cells and decreases proliferation in the hippocampal dentate gyrus. *J Neuroinflammation*, 11:31.

Südhof, T. C. (2008). Neuroligins and neurexins link synaptic function to cognitive disease. *Nature*, 455(7215):903–911.

Suetsugu, S., Kurisu, S., Oikawa, T., Yamazaki, D., Oda, A., and Takenawa, T. (2006). Optimization of wave2 complex-induced actin polymerization by membrane-bound irsp53, pip(3), and rac. *J Cell Biol*, 173(4):571–585.

Suo, L., Lu, H., Ying, G., Capecchi, M. R., and Wu, Q. (2012). Protocadherin clusters and cell adhesion kinase regulate dendrite complexity through rho GTPase. *J Mol Cell Biol*, 4(6):362–376.

Svitkina, T. M. and Borisy, G. G. (1999). Arp2/3 complex and actin depolymerizing factor/cofilin in dendritic organization and treadmilling of actin filament array in lamellipodia. *J Cell Biol*, 145(5):1009–1026.

Svitkina, T. M., Bulanova, E. A., Chaga, O. Y., Vignjevic, D. M., Kojima, S.-i., Vasiliev, J. M., and Borisy, G. G. (2003). Mechanism of filopodia initiation by reorganization of a dendritic network. *J Cell Biol*, 160(3):409–421.

Swann, J. W., Al-Noori, S., Jiang, M., and Lee, C. L. (2000). Spine loss and other dendritic abnormalities in epilepsy. *Hippocampus*, 10(5):617–625.

Sweet, R. A., Henteleff, R. A., Zhang, W., Sampson, A. R., and Lewis, D. A. (2009). Reduced dendritic spine density in auditory cortex of subjects with schizophrenia. *Neuropsychopharmacology*, 34(2):374–389.

Szebenyi, G., Bollati, F., Bisbal, M., Sheridan, S., Faas, L., Wray, R., Haferkamp, S., Nguyen, S., Caceres, A., and Brady, S. T. (2005). Activity-driven dendritic remodeling requires microtubule-associated protein 1a. *Curr Biol*, 15(20):1820–1826.

Tabuchi, K., Blundell, J., Etherton, M. R., Hammer, R. E., Liu, X., Powell, C. M., and Südhof, T. C. (2007). A neuroligin-3 mutation implicated in autism increases inhibitory synaptic transmission in mice. *Science*, 318(5847):71–76.

Tahirovic, S., Hellal, F., Neukirchen, D., Hindges, R., Garvalov, B. K., Flynn, K. C., Stradal, T. E., Chrostek-Grashoff, A., Brakebusch, C., and Bradke, F. (2010). Rac1 regulates neuronal polarization through the wave complex. *J Neurosci*, 30(20):6930–6943.

Takahashi, H., Katayama, K.-I., Sohya, K., Miyamoto, H., Prasad, T., Matsumoto, Y., Ota, M., Yasuda, H., Tsumoto, T., Aruga, J., and Craig, A. M. (2012). Selective control of inhibitory synapse development by slitrk3-ptp\delta trans-synaptic interaction. *Nat Neurosci*, 15(3):389–98, S1.

Takenawa, T. (2007). The wasp-wave protein network: connecting the membrane to the cytoskeleton. *Nat Rev Mol Cell Biol*, 8:37.

Tam, G. W. C., van de Lagemaat, Louie N, Redon, R., Strathdee, K. E., Croning, M. D. R., Malloy, M. P., Muir, W. J., Pickard, B. S., Deary, I. J., Blackwood, D. H. R., Carter, N. P., and Grant, S. G. N. (2010). Confirmed rare copy number variants implicate novel genes in schizophrenia. *Biochem Soc Trans*, 38(2):445–451.

Tang, G., Gudsnuk, K., Kuo, S.-H., Cotrina, M. L., Rosoklija, G., Sosunov, A., Sonders, M. S., Kanter, E., Castagna, C., Yamamoto, A., Yue, Z., Arancio, O., Peterson, B. S., Champagne, F., Dwork, A. J., Goldman, J., and Sulzer, D. (2014). Loss of mtor-dependent macroautophagy causes autistic-like synaptic pruning deficits. *Neuron*, 83(5):1131–1143.

Tashiro, A. and Yuste, R. (2004). Regulation of dendritic spine motility and stability by rac1 and rho kinase: evidence for two forms of spine motility. *Mol Cell Neurosci*, 26(3):429–440.

Tatavarty, V., Das, S., and Yu, J. (2012). Polarization of actin cytoskeleton is reduced in dendritic protrusions during early spine development in hippocampal neuron. *Mol Biol Cell*, 23(16):3167–3177.

Tay, T. L., Mai, D., Dautzenberg, J., Fernández-Klett, F., Lin, G., Sagar, Datta, M., Drougard, A., Stempfl, T., Ardura-Fabregat, A., Staszewski, O., Margineanu, A., Sporbert, A., Steinmetz, L. M., Pospisilik, J. A., Jung, S., Priller, J., Grün, D., Ronneberger, O., and Prinz, M. (2017). A new fate mapping system reveals context-dependent random or clonal expansion of microglia. *Nat Neurosci*, 20(6):793–803.

Teixeira, C. M., Rosen, Z. B., Suri, D., Sun, Q., Hersh, M., Sargin, D., Dincheva, I., Morgan, A. A., Spivack, S., Krok, A. C., Hirschfeld-Stoler, T., Lambe, E. K., Siegelbaum, S. A., and Ansorge, M. S. (2018). Hippocampal 5-ht input regulates memory formation and schaffer collateral excitation. *Neuron*, 98(5):992–1004.e4.

Teng, Y., Pi, W., Wang, Y., and Cowell, J. K. (2016). Wasf3 provides the conduit to facilitate invasion and metastasis in breast cancer cells through her2/her3 signaling. *Oncogene*, 35(35):4633–4640.

Thobe, K., Sers, C., and Siebert, H. (2017). Unraveling the regulation of mtorc2 using logical modeling. *Cell Commun Signal*, 15(1):6.

Thomas, A. M., Bui, N., Graham, D., Perkins, J. R., Yuva-Paylor, L. A., and Paylor, R. (2011). Genetic reduction of group 1 metabotropic glutamate receptors alters select behaviors in a mouse model for fragile x syndrome. *Behav Brain Res*, 223(2):310–321.

Thrasher, A. J. and Burns, S. O. (2010). Wasp: a key immunological multitasker. *Nat Rev Immunol*, 10(3):182–192.

Tiwari, S. S., Mizuno, K., Ghosh, A., Aziz, W., Troakes, C., Daoud, J., Golash, V., Noble, W., Hortobágyi, T., and Giese, K. P. (2016). Alzheimer-related decrease in cyfip2 links amyloid production to tau hyperphosphorylation and memory loss. *Brain*, 139(Pt 10):2751–2765.

Toma, C., Torrico, B., Hervás, A., Valdés-Mas, R., Tristán-Noguero, A., Padillo, V., Maristany, M., Salgado, M., Arenas, C., Puente, X. S., Bayés, M., and Cormand, B. (2014). Exome sequencing in multiplex autism families suggests a major role for heterozygous truncating mutations. *Mol Psychiatry*, 19(7):784–790.

Truett, G. E., Heeger, P., Mynatt, R. L., Truett, A. A., Walker, J. A., and Warman, M. L. (2000). Preparation of pcr-quality mouse genomic dna with hot sodium hydroxide and tris (hotshot). *BioTechniques*, 29(1):52–54.

Tsai, P. T., Hull, C., Chu, Y., Greene-Colozzi, E., Sadowski, A. R., Leech, J. M., Steinberg, J., Crawley, J. N., Regehr, W. G., and Sahin, M. (2012). Autistic-like behaviour and cerebellar dysfunction in purkinje cell tsc1 mutant mice. *Nature*, 488(7413):647–651.

Tu, J. C., Xiao, B., Naisbitt, S., Yuan, J. P., Petralia, R. S., Brakeman, P., Doan, A., Aakalu, V. K., Lanahan, A. A., Sheng, M., and Worley, P. F. (1999). Coupling of mGluR/homer and PSD-95 complexes by the shank family of postsynaptic density proteins. *Neuron*, 23(3):583–592.

Twelvetrees, A. E., Yuen, E. Y., Arancibia-Carcamo, I. L., MacAskill, A. F., Rostaing, P., Lumb, M. J., Humbert, S., Triller, A., Saudou, F., Yan, Z., and Kittler, J. T. (2010). Delivery of gabaars to synapses is mediated by hap1-kif5 and disrupted by mutant huntingtin. *Neuron*, 65(1):53–65.

Tyagarajan, S. K. and Fritschy, J.-M. (2014). Gephyrin: a master regulator of neuronal function? *Nat Rev Neurosci*, 15(3):141–156.

Ueno, M., Fujita, Y., Tanaka, T., Nakamura, Y., Kikuta, J., Ishii, M., and Yamashita, T. (2013). Layer v cortical neurons require microglial support for survival during postnatal development. *Nat Neurosci*, 16(5):543–551.

Uezu, A., Kanak, D. J., Bradshaw, T. W. A., Soderblom, E. J., Catavero, C. M., Burette, A. C., Weinberg, R. J., and Soderling, S. H. (2016). Identification of an elaborate complex mediating postsynaptic inhibition. *Science*, 353(6304):1123–1129.

Urban, E., Jacob, S., Nemethova, M., Resch, G. P., and Small, J. V. (2010). Electron tomography reveals unbranched networks of actin filaments in lamellipodia. *Nat Cell Biol*, 12(5):429–435.

Valente, K. D., Varela, M. C., Koiffmann, C. P., Andrade, J. Q., Grossmann, R., Kok, F., and Marques-Dias, M. J. (2013). Angelman syndrome caused by deletion: a genotype-phenotype correlation determined by breakpoint. *Epilepsy Res*, 105(1-2):234–239.

van der Zwaag, B., Staal, W. G., Hochstenbach, R., Poot, M., Spierenburg, H. A., de Jonge, M. V., Verbeek, N. E., van 't Slot, R., van Es, M. A., Staal, F. J., Freitag, C. M., Buizer-Voskamp, J. E., Nelen, M. R., van den Berg, Leonard H, van Amstel, Hans K Ploos, van Engeland, H., and Burbach, J. P. H. (2010). A co-segregating microduplication of chromosome 15q11.2 pinpoints two risk genes for autism spectrum disorder. *Am J Med Genet B Neuropsychiatr Genet*, 153B(4):960–966.

Varela, M. C., Kok, F., Setian, N., Kim, C. A., and Koiffmann, C. P. (2005). Impact of molecular mechanisms, including deletion size, on prader-willi syndrome phenotype: study of 75 patients. *Clin Genet*, 67(1):47–52.

Varga, E. A., Pastore, M., Prior, T., Herman, G. E., and McBride, K. L. (2009). The prevalence of pten mutations in a clinical pediatric cohort with autism spectrum disorders, developmental delay, and macrocephaly. *Genet Med*, 11(2):111–117.

Varoqueaux, F., Aramuni, G., Rawson, R. L., Mohrmann, R., Missler, M., Gottmann, K., Zhang, W., Südhof, T. C., and Brose, N. (2006). Neuroligins determine synapse maturation and function. *Neuron*, 51(6):741–754.

Veltman, D. M. and Insall, R. H. (2010). WASP family proteins: their evolution and its physiological implications. *Mol Biol Cell*, 21(16):2880–2893.

Vignjevic, D., Kojima, S.-i., Aratyn, Y., Danciu, O., Svitkina, T., and Borisy, G. G. (2006). Role of fascin in filopodial protrusion. *J Cell Biol*, 174(6):863–875.

Vincent, C., Siddiqui, T. A., and Schlichter, L. C. (2012). Podosomes in migrating microglia: components and matrix degradation. *J Neuroinflammation*, 9:190.

Vogan, V. M., Morgan, B. R., Leung, R. C., Anagnostou, E., Doyle-Thomas, K., and Taylor, M. J. (2016). Widespread white matter differences in children and adolescents with autism spectrum disorder. *J Autism Dev Disord*, 46(6):2138–2147.

Wake, H., Moorhouse, A. J., Jinno, S., Kohsaka, S., and Nabekura, J. (2009). Resting microglia directly monitor the functional state of synapses in vivo and determine the fate of ischemic terminals. *J Neurosci*, 29(13):3974–3980.

Wall, M. J. and Corrêa, S. A. L. (2018). The mechanistic link between arc/arg3.1 expression and AMPA receptor endocytosis. *Semin Cell Dev Biol*, 77:17–24.

Waltes, R., Duketis, E., Knapp, M., Anney, R. J. L., Huguet, G., Schlitt, S., Jarczok, T. A., Sachse, M., Kämpfer, L. M., Kleinböck, T., Poustka, F., Bölte, S., Schmötzer, G., Voran, A., Huy, E., Meyer, J., Bourgeron, T., Klauck, S. M., Freitag, C. M., and Chiocchetti, A. G. (2014). Common variants in genes of the postsynaptic fmrp signalling pathway are risk factors for autism spectrum disorders. *Hum Genet*, 133(6):781–792.

Wang, J., Wegener, J. E., Huang, T.-W., Sripathy, S., de Jesus-Cortes, H., Xu, P., Tran, S., Knobbe, W., Leko, V., Britt, J., Starwalt, R., McDaniel, L., Ward, C. S., Parra, D., Newcomb, B., Lao, U., Nourigat, C., Flowers, D. A., Cullen, S., Jorstad, N. L., Yang, Y., Glaskova, L., Vingeau, S., Kozlitina, J., Yetman, M. J., Jankowsky, J. L., Reichardt, S. D., Reichardt, H. M., Gärtner, J., Bartolomei, M. S., Fang, M., Loeb, K., Keene, C. D., Bernstein, I., Goodell, M., Brat, D. J., Huppke, P., Neul, J. L., Bedalov, A., and Pieper, A. A. (2015). Wild-type microglia do not reverse pathology in mouse models of rett syndrome. *Nature*, 521(7552):E1–4.

Wang, T., Guo, H., Xiong, B., Stessman, H. A. F., Wu, H., Coe, B. P., Turner, T. N., Liu, Y., Zhao, W., Hoekzema, K., Vives, L., Xia, L., Tang, M., Ou, J., Chen, B., Shen, Y., Xun, G., Long, M., Lin, J., Kronenberg, Z. N., Peng, Y., Bai, T., Li, H., Ke, X., Hu, Z., Zhao, J., Zou, X., Xia, K., and Eichler, E. E. (2016). De novo genic mutations among a chinese autism spectrum disorder cohort. *Nat Commun*, 7:13316.

Wang, W., Ju, Y.-Y., Zhou, Q.-X., Tang, J.-X., Li, M., Zhang, L., Kang, S., Chen, Z.-G., Wang, Y.-J., Ji, H., Ding, Y.-Q., Xu, L., and Liu, J.-G. (2017). The small gtpase rac1 contributes to extinction of aversive memories of drug withdrawal by facilitating gabaa receptor endocytosis in the vmpfc. *J Neurosci*, 37(30):7096–7110.

Weinhard, L., Di Bartolomei, G., Bolasco, G., Machado, P., Schieber, N. L., Neniskyte, U., Exiga, M., Vadisiute, A., Raggioli, A., Schertel, A., Schwab, Y., and Gross, C. T. (2018). Microglia remodel synapses by presynaptic trogocytosis and spine head filopodia induction. *Nat Commun*, 9(1):1228.

Wheeler, A. P., Wells, C. M., Smith, S. D., Vega, F. M., Henderson, R. B., Tybulewicz, V. L., and Ridley, A. J. (2006). Rac1 and rac2 regulate macrophage morphology but are not essential for migration. *J Cell Sci*, 119(Pt 13):2749–2757.

Williams, D. A., Tao, W., Yang, F., Kim, C., Gu, Y., Mansfield, P., Levine, J. E., Petryniak, B., Derrow, C. W., Harris, C., Jia, B., Zheng, Y., Ambruso, D. R., Lowe, J. B., Atkinson, S. J., Dinauer, M. C., and Boxer, L. (2000). Dominant negative mutation of the hematopoietic-specific rho gtpase, rac2, is associated with a human phagocyte immunodeficiency. *Blood*, 96(5):1646–1654.

Wiśniowiecka-Kowalnik, B., Kastory-Bronowska, M., Bartnik, M., Derwińska, K., Dymczak-Domini, W., Szumbarska, D., Ziemka, E., Szczałuba, K., Sykulski, M.,

Gambin, T., Gambin, A., Shaw, C. A., Mazurczak, T., Obersztyn, E., Bocian, E., and Stankiewicz, P. (2013). Application of custom-designed oligonucleotide array cgh in 145 patients with autistic spectrum disorders. *Eur J Hum Genet*, 21(6):620–625.

Woo, J., Kwon, S.-K., Nam, J., Choi, S., Takahashi, H., Krueger, D., Park, J., Lee, Y., Bae, J. Y., Lee, D., Ko, J., Kim, H., Kim, M.-H., Bae, Y. C., Chang, S., Craig, A. M., and Kim, E. (2013). The adhesion protein igsf9b is coupled to neuroligin 2 via s-scam to promote inhibitory synapse development. *J Cell Biol*, 201(6):929–944.

Wu, C., Asokan, S. B., Berginski, M. E., Haynes, E. M., Sharpless, N. E., Griffith, J. D., Gomez, S. M., and Bear, J. E. (2012). Arp2/3 is critical for lamellipodia and response to extracellular matrix cues but is dispensable for chemotaxis. *Cell*, 148(5):973–987.

Xing, G., Li, M., Sun, Y., Rui, M., Zhuang, Y., Lv, H., Han, J., Jia, Z., and Xie, W. (2018). Neurexin-neuroligin 1 regulates synaptic morphology and functions via the wave regulatory complex in drosophila neuromuscular junction. *elife*, 7.

Xu, B., Zang, K., Ruff, N. L., Zhang, Y. A., McConnell, S. K., Stryker, M. P., and Reichardt, L. F. (2000). Cortical degeneration in the absence of neurotrophin signaling: dendritic retraction and neuronal loss after removal of the receptor TrkB. *Neuron*, 26(1):233–245.

Xu, C., Fu, X., Zhu, S., and Liu, J.-J. (2016). Retrolinkin recruits the wave1 protein complex to facilitate bdnf-induced trkb endocytosis and dendrite outgrowth. *Mol Biol Cell*.

Xu, K., Zhong, G., and Zhuang, X. (2013). Actin, spectrin, and associated proteins form a periodic cytoskeletal structure in axons. *Science*, 339(6118):452–456.

Xue, G. and Hemmings, B. A. (2013). Pkb/akt-dependent regulation of cell motility. *J Natl Cancer Inst*, 105(6):393–404.

Yamaguchi, H., Lorenz, M., Kempiak, S., Sarmiento, C., Coniglio, S., Symons, M., Segall, J., Eddy, R., Miki, H., Takenawa, T., and Condeelis, J. (2005). Molecular mechanisms of invadopodium formation: the role of the n-wasp-arp2/3 complex pathway and cofilin. *J Cell Biol*, 168(3):441–452.

Yan, C., Martinez-Quiles, N., Eden, S., Shibata, T., Takeshima, F., Shinkura, R., Fujiwara, Y., Bronson, R., Snapper, S. B., Kirschner, M. W., Geha, R., Rosen, F. S., and Alt, F. W. (2003). Wave2 deficiency reveals distinct roles in embryogenesis and rac-mediated actin-based motility. *EMBO J*, 22(14):3602–3612.

Yang, N., Higuchi, O., Ohashi, K., Nagata, K., Wada, A., Kangawa, K., Nishida, E., and Mizuno, K. (1998). Cofilin phosphorylation by lim-kinase 1 and its role in rac-mediated actin reorganization. *Nature*, 393(6687):809–812.

Yang, Q., Feng, B., Zhang, K., Guo, Y.-y., Liu, S.-b., Wu, Y.-m., Li, X.-q., and Zhao, M.-g. (2012). Excessive astrocyte-derived neurotrophin-3 contributes to the abnormal neuronal dendritic development in a mouse model of fragile x syndrome. *PLoS Genet*, 8(12):e1003172.

Ydenberg, C. A., Padrick, S. B., Sweeney, M. O., Gandhi, M., Sokolova, O., and Goode, B. L. (2013). Gmf severs actin-arp2/3 complex branch junctions by a cofilin-like mechanism. *Curr Biol*, 23(12):1037–1045.

Yi, F., Danko, T., Botelho, S. C., Patzke, C., Pak, C., Wernig, M., and Südhof, T. C. (2016). Autism-associated shank3 haploinsufficiency causes ih channelopathy in human neurons. *Science*, 352(6286):aaf2669.

Yona, S., Kim, K.-W., Wolf, Y., Mildner, A., Varol, D., Breker, M., Strauss-Ayali, D., Viukov, S., Guilliams, M., Misharin, A., Hume, D. A., Perlman, H., Malissen, B., Zelzer, E., and Jung, S. (2013). Fate mapping reveals origins and dynamics of monocytes and tissue macrophages under homeostasis. *Immunity*, 38(1):79–91.

Yoon, K.-J., Nguyen, H. N., Ursini, G., Zhang, F., Kim, N.-S., Wen, Z., Makri, G., Nauen, D., Shin, J. H., Park, Y., Chung, R., Pekle, E., Zhang, C., Towe, M., Hussaini, S. M. Q., Lee, Y., Rujescu, D., St Clair, D., Kleinman, J. E., Hyde, T. M., Krauss, G., Christian, K. M., Rapoport, J. L., Weinberger, D. R., Song, H., and Ming, G.-L. (2014). Modeling a genetic risk for schizophrenia in ipscs and mice reveals neural stem cell deficits associated with adherens junctions and polarity. *Cell Stem Cell*, 15(1):79–91.

Yoshida, T., McCarley, R. W., Nakamura, M., Lee, K., Koo, M.-S., Bouix, S., Salisbury, D. F., Morra, L., Shenton, M. E., and Niznikiewicz, M. A. (2009). A prospective longitudinal volumetric mri study of superior temporal gyrus gray matter and amygdala-hippocampal complex in chronic schizophrenia. *Schizophr Res*, 113(1):84–94.

Yu, X. and Malenka, R. C. (2003). Beta-catenin is critical for dendritic morphogenesis. *Nat Neurosci*, 6(11):1169–1177.

Yu, X., Wang, G., Gilmore, A., Yee, A. X., Li, X., Xu, T., Smith, S. J., Chen, L., and Zuo, Y. (2013). Accelerated experience-dependent pruning of cortical synapses in ephrin-a2 knockout mice. *Neuron*, 80(1):64–71.

Zalfa, F., Giorgi, M., Primerano, B., Moro, A., Di Penta, A., Reis, S., Oostra, B., and Bagni, C. (2003). The fragile x syndrome protein fmrp associates with bc1 rna and regulates the translation of specific mrnas at synapses. *Cell*, 112(3):317–327.

Zeisel, A., Hochgerner, H., Lönnerberg, P., Johnsson, A., Memic, F., van der Zwan, J., Häring, M., Braun, E., Borm, L. E., La Manno, G., Codeluppi, S., Furlan, A., Lee, K., Skene, N., Harris, K. D., Hjerling-Leffler, J., Arenas, E., Ernfors, P., Marklund, U., and Linnarsson, S. (2018). Molecular architecture of the mouse nervous system. *Cell*, 174(4):999–1014.e22.

Zhang, H., Webb, D. J., Asmussen, H., Niu, S., and Horwitz, A. F. (2005). A git1/pix/rac/pak signaling module regulates spine morphogenesis and synapse formation through mlc. *J Neurosci*, 25(13):3379–3388.

Zhang, J., Malik, A., Choi, H. B., Ko, R. W. Y., Dissing-Olesen, L., and Macvicar, B. A. (2014a). Microglial cr3 activation triggers long-term synaptic depression in the hippocampus via nadph oxidase. *Neuron*, 82(1):195–207.

Zhang, Y., Chen, K., Sloan, S. A., Bennett, M. L., Scholze, A. R., O'Keeffe, S., Phatnani, H. P., Guarnieri, P., Caneda, C., Ruderisch, N., Deng, S., Liddelow, S. A., Zhang, C., Daneman, R., Maniatis, T., Barres, B. A., and Wu, J. Q. (2014b). An rna-sequencing transcriptome and splicing database of glia, neurons, and vascular cells of the cerebral cortex. *J Neurosci*, 34(36):11929–11947.

Zhang, Y., Sloan, S. A., Clarke, L. E., Caneda, C., Plaza, C. A., Blumenthal, P. D., Vogel, H., Steinberg, G. K., Edwards, M. S. B., Li, G., Duncan, J. A., Cheshier, S. H., Shuer, L. M., Chang, E. F., Grant, G. A., Gephart, M. G. H., and Barres, B. A. (2016). Purification and characterization of progenitor and mature human astrocytes reveals transcriptional and functional differences with mouse. *Neuron*, 89(1):37–53.

Zhao, L., Wang, D., Wang, Q., Rodal, A. A., and Zhang, Y. Q. (2013). Drosophila cyfip regulates synaptic development and endocytosis by suppressing filamentous actin assembly. *PLoS Genet*, 9(4):e1003450.

Zhao, X., Liao, Y., Morgan, S., Mathur, R., Feustel, P., Mazurkiewicz, J., Qian, J., Chang, J., Mathern, G. W., Adamo, M. A., Ritaccio, A. L., Gruenthal, M., Zhu, X., and Huang, Y. (2018). Noninflammatory changes of microglia are sufficient to cause epilepsy. *Cell Rep*, 22(8):2080–2093.

Zuchero, J. B., Belin, B., and Mullins, R. D. (2012). Actin binding to wh2 domains regulates nuclear import of the multifunctional actin regulator jmy. *Mol Biol Cell*, 23(5):853–863.

Zuchero, J. B., Coutts, A. S., Quinlan, M. E., La Thangue, N. B., and Mullins, R. D. (2009). p53-cofactor jmy is a multifunctional actin nucleation factor. *Nat Cell Biol*, 11(4):451–459.

Appendix A

Dissemination of work

Alongside this thesis, data presented here contributed to the following publication(s) and conference/meeting abstracts:

Publications

Davenport et al., Autism and Schizophrenia-Associated CYFIP1 Regulates the Balance of Synaptic Excitation and Inhibition, Cell Reports (2019), https://doi.org/10.1016/j.celrep.2019.01.092

Meeting abstracts

EMBO Microglia Workshop 2018, poster 68, https://www.embl.de/training/events/2018/GLI18-01/Poster-numbers-Microglia-2018.pdf